



Technische Universität München

TECHNISCHE UNIVERSITÄT MÜNCHEN

TUM School of Life Sciences

Microwave-assisted vacuum and freeze drying of sensitive biomolecules incorporated into an aerated matrix

Peter Kubbutat

Vollständiger Abdruck der von der TUM School of Life Sciences der Technischen Universität München zur Erlangung des akademischen Grades eines
Doktors der Ingenieurwissenschaften
genehmigten Dissertation.

Vorsitzende: apl. Prof. Dr.-Ing. habil. Petra Först

Prüfer der Dissertation: 1. Prof. Dr.-Ing. Ulrich Kulozik
2. Prof. Dr. Wilfried Schwab
3. Priv.-Doz. Dr. Volker Gaukel

Die Dissertation wurde am 30.08.2021 bei der Technischen Universität München eingereicht und durch die TUM School of Life Sciences am 07.03.2022 angenommen.

Für meine Familie

Acknowledgment

This work resulted from the Chair of Food and Bioprocess Engineering of the Technical University of Munich between April 2016 and September 2021.

My special thanks go to Prof. Dr. Ing. Ulrich Kulozik. He granted me the maximum of scientific freedom and trust and supported the research by supplying excellent facilities and staff to perform the experiments. I appreciate his continuous support, discussion, and motivation. Apart from that, he supported my personal and educational development.

I want to thank my office colleagues of E.14, Evelyn Dachmann, Oliver Gmach, Isabel Kalinke, Heidi Wohlschläger, Dr. Somayeh Taghian Dinani and Takashi Tanizawa for giving me personal balance, interesting discussions, and constant support.

Further, I want to deeply thank all members of the institute who supported my project. I want to emphasize the internal workshop's team, Christian Ederer, Franz Fraunhofer, and Erich Schneider, who have continuously helped me with their knowledge and modifying facilities and experimental setups. Apart from them, I would like to thank the laboratory staff for giving experimental support and analysis. Among them, Martin Hiliz, Christine Haas, Heidi Wohlschläger, Claudia Hengst, and Annette Brümmer-Rolf are especially thanked. Friederike Schöpflin, Sabine Becker and Sabine Grabbe are thanked for their administrative and IT support.

Furthermore, I would like to thank my students, Katrin Wegmayer, Thomas Cummings, Elena Fellenberger, Johanna Wellenhofer, Patrick Mancenka, Annika Tauchnitz, Phillip Sochatzky, Christoph Paschen, Laura Lüthje, Thomas Bickel-Haase, Katharina Hinrichs, Luísa Leitão, Isabel Kalinke and Sebastian Picker, whose theoretical and practical work significantly contributed to this thesis.

In addition, I want to thank all other colleagues, in particular Dr. Jannika Dombrowski, Isabel Kalinke, and Dr. Sabine Ambros pleasant atmosphere and deep discussions.

Besides, I want to thank Prof. Petra Först for giving me access to the freeze drying microscope and Dr. Michael Gebhard for giving me the opportunity to use the scanning electron microscope.

I want to thank my friends and family for giving me tireless support and motivation for this work. Finally, I want to thank my wife Marianne for giving me personal balance and accompany me during ups and downs during this interesting and challenging period of my life.

Contents

1	Summary/Zusammenfassung	9
1.1	Summary.....	9
1.2	Zusammenfassung.....	14
2	General introduction	21
2.1	Common drying methods in the food and pharmaceutical industry.....	21
2.2	Characteristics of protein- and surfactant stabilized foams.....	29
2.3	Microwave-supported vacuum- and freeze drying	40
3	Objective and outline	47
4	Results	49
4.1	Interactions of sugar alcohol, di-saccharides and polysaccharides with polysorbate 80 as surfactant in the stabilization of foams.....	49
4.2	Thermal and mechanical stability of dialyzed β -galactosidase from <i>Kluyveromyces lactis</i>	73
4.3	Water vapor pathways during freeze drying of foamed product matrices stabilized by maltodextrin at different concentrations.....	78
4.4	Foam structure preservation during microwave-assisted vacuum drying: Significance of interfacial and dielectric properties of the bulk phase of foams from polysorbate 80-maltodextrin dispersions.....	95
4.5	Influence of interfacial characteristics and dielectric properties on foam structure preservation during microwave-assisted vacuum drying of whey protein isolate-maltodextrin dispersions.....	111
4.6	Stability of foams in vacuum drying processes. Effects of interactions between sugars, proteins, and surfactants on foam stability and dried foam properties	128
4.7	Influence foam properties and excipients on the residual stability of β -galactosidase after microwave-assisted freeze drying	151
4.8	Influence of microwave power input and product temperature on the residual activity of β -galactosidase in microwave-assisted vacuum and freeze drying.....	159
4.9	Up-Scaling of microwave-assisted freeze drying by generating small spherical foamy samples	166
5	Overall discussion and main findings.....	175

5.1	Influence of saccharides on the properties of surfactant or protein stabilized foams...	175
5.2	Foam stability during microwave-assisted vacuum drying	176
5.3	Influence of foam structures on the microwave-assisted freeze drying process....	179
5.4	Influence of process parameters on the product quality of microwave-assisted vacuum and freeze drying of aerated product matrices	180
5.5	Up-scaling of microwave-assisted drying processes.....	181
5.6	Overall conclusion and perspectives	182
6	References	187
7	Appendix.....	Fehler! Textmarke nicht definiert.

Abbreviations

Latin symbols

Abbreviation	Description	Unit
A	absorbance	Au
A ₀	initial surface area	m ²
A ₂	second virial coefficient	mol·dm ³ ·g ⁻²
BSA	bovine serum albumin	-
c	gas solubility	mol·l ⁻¹
c	speed of light in vacuum	m·s ⁻¹
c	moisture content	-
CFD	conventional freeze drying	-
c _{max}	maximal used concentration	mol·l ⁻¹
CMC	critical micelle concentration	mol·l ⁻¹
CVD	conventional vacuum drying	-
d ₂₅	25-percentile of the diameters	m
d ₅₀	mean diameter	m
d ₇₅	75-percentile of the diameters	m
DE	dextrose equivalent	-
D _{eff,gas}	effective diffusivity of a gaseous phase	m ² ·s ⁻¹
D _{eff,liq.}	effective diffusivity of a liquid phase	m ² ·s ⁻¹
E	electric field	V·m ⁻¹
E	complex viscoelastic modulus	N·m ⁻¹
E'	surface elasticity modulus	N·m ⁻¹
E'	surface dilatational elasticity	N·m ⁻¹
E''	surface dilatational viscosity	N·m ⁻¹
ETSI	European Telecommunication Standards Institute	-
f	frequency	s ⁻¹

Abbreviation	Description	Unit
FCC	Federal Communication Commission	-
FD	freeze drying	-
fps	frames per second	s ⁻¹
f _{res}	resonant frequency	s ⁻¹
h	thickness of lamella	m
H	magnetic field	A·m ⁻¹
HLB	hydrophilia-lipophilia balance	-
HPLC	high-pressure liquid chromatography	
IQR	interquartile range	m
ISM	Industrial, scientific, and medical frequency band	-
ITU	International Telecommunication Union	-
j	imaginary proportion	-
K	slope of the logarithmic moisture decrease rate	s ⁻¹
K _H	Henry coefficient	-
L	product thickness	m
L _{eff}	effective thickness of a foam	m
L _{foam}	foam thickness	m
L _{Gas}	accumulated thickness of gaseous phase within a foam	m
L _{liq.}	thickness of a liquid sample	m
L _{liq.,foam}	accumulated thickness of liquid layers within a foam	m
MC ₀	initial moisture content	-
MC _e	moisture content in equilibrium	-
MC _x	moisture content at the time t	-
mDSC	modulated differential scanning calorimetry	-
MDX	maltodextrin	-
m _{empty}	mass of an empty sample cup	kg

Abbreviation	Description	Unit
m_F	foam mass	kg
MR	moisture ratio	-
M_{mass}	molar mass	$\text{g}\cdot\text{mol}^{-1}$
m_S	mass of sample solution	kg
$m_{t=0\text{min}}$	the initial mass of a cup of sample	kg
$m_{t=45\text{min}}$	mass of a cup of a sample after 45 min	kg
MTO	maltose	-
MWCO	mean weight cut off	Da
MWFD	microwave-assisted freeze drying	
MWVD	microwave-assisted vacuum drying	
ONPG	o-nitrophenyl- β -D-galactopyranosid	-
P	volumetric absorption of microwave energy	$\text{W}\cdot\text{m}^{-3}$
p_1	pressure in the liquid film	Pa
p_2	pressure in the bubble	Pa
p_3	pressure in the plateau border	Pa
p_c	capillary pressure	Pa
p_d	internal bubble pressure	Pa
PD	penetration depth	m
PDI	polydispersity index	
PDM	pendent drop measurement	
PEO	polyethylene oxide	-
p_l	external pressure	Pa
PPO	polypropylene oxide	-
PS80	polysorbate 80	-
r	radius	m
r	bubble radius	m

Abbreviation	Description	Unit
r_1, r_2	radii of curvature	m
R_{hor}	radius of a circular horizontal film	m
S_{11}	complex reflection coefficient	dB
SEM	scanning electron microscopy	-
SLS	static light scattering	
SOB	sorbitol	-
SUC	sucrose	-
t	time	s
T'_g	glass transition temperature of a maximally concentrated amorphous phase	K
T_C	crystallization temperature	K
T_D	denaturation temperature	K
T_G	glass transition temperature	K
T_{gW}	glass transition temperature of water	K
T_U	eutectic point	K
V_{cup}	volume of the used cups	m^3
VD	vacuum drying	-
v_{Re}	Reynolds velocity	$m \cdot s^{-1}$
WPI	whey protein isolate	-
x	length of diffusion pathway	m
ΔA	change in surface area	m^2
Δp	Laplace pressure	Pa
w/w	weight by weight	-
w/v	weight by volume	-

Greek symbols

Abbreviation	Description	Unit
$\tan(\delta)$	dielectric loss tangent	-
α -la	α -lactalbumin	-
β -Gal	β -galactosidase	-
β -lg	β -lactoglobulin	-
$\Delta\sigma$	changes in surface tension during oscillation	$\text{N}\cdot\text{m}^{-1}$
ϵ^*	complex dielectric constant	-
ϵ'	dielectric constant	-
ϵ''	dielectric loss	-
ϵ''_d	dipole rotation contributing to dielectric loss	-
ϵ''_σ	ionic conduction contributing to dielectric loss	-
ϵ_0	permittivity of free space in the vacuum	$\text{A}\cdot\text{s}\cdot\text{V}^{-1}\cdot\text{m}^{-1}$
η_{dyn}	dynamic viscosity	$\text{Pa}\cdot\text{s}$
λ	wavelength	m
π	surface pressure	$\text{N}\cdot\text{m}^{-1}$
Π	disjoining pressure	$\text{N}\cdot\text{m}^{-1}$
Π_{elec}	electrostatic interactions contributing to disjoining pressure	$\text{N}\cdot\text{m}^{-1}$
Π_{steric}	steric interactions contributing to disjoining pressure	$\text{N}\cdot\text{m}^{-1}$
Π_{vdW}	van der Waals interactions contributing to disjoining pressure	$\text{N}\cdot\text{m}^{-1}$
ρ_{solution}	density of solution	$\text{kg}\cdot\text{m}^{-3}$
σ	surface tension	$\text{N}\cdot\text{m}^{-1}$
$\sigma_{\text{s+s}}$	surface tension of surfactant combined with saccharides	$\text{N}\cdot\text{m}^{-1}$
σ_{solvent}	surface tension of the solvent	$\text{N}\cdot\text{m}^{-1}$
φ	phase angle	$^\circ$
Φ	volume fraction of gas	-
ω	angular frequency	s^{-1}

1 Summary/Zusammenfassung

1.1 Summary

Many food and pharmaceutical products are heat-sensitive or perish within a short period. Therefore, such often highly-valuable products are dried to have a possibility to store or distribute them without losing too much value or pharmaceutical activity. The most gentle and, therefore, common drying process for the preservation of biological substances is freeze drying. However, freeze drying is a highly energy-consuming process. In addition, the process requires a long drying time, whereby the drying process becomes more and more the bottleneck in the production of biological pharmaceuticals. Hence, there is continuous development in drying technology searching for faster drying processes, which are able to provide high product quality. A possible alternative for the drying of sensitive biologicals is vacuum drying. This drying type requires less drying time and can also be applied for freeze-sensitive products, but the concentration of the product during the drying process can be problematic. However, it is widely used for bacteria or food, and high-quality samples can be obtained.

Nonetheless, freeze drying and vacuum drying still take several hours or days. This can be mainly attributed to slow heat conduction within the product because samples can be only efficiently heated using product shelves at the bottom or top. A possible way to overcome this problem is the application of microwaves to heat the product. Microwaves, in principle, heat up the product volumetrically, and therefore, the influence of heat conduction on the drying speed is low. However, microwaves are not heating the product entirely uniformly, which can be observed by the formation of hot and cold spots. Further, thermal runaway can occur if geometrical or product-based issues are present. Hence, the use of microwave-assisted drying for heat-sensitive products is challenging.

Therefore, the described issues of microwave-assisted vacuum or freeze drying should be solved in this work by using an aerated product instead of a highly-dense liquid product structure. Foams provide a higher surface area, which further accelerates the drying process. Additionally, the open-pored system benefits the water vapor transport within the product. Thereby, the sample structures do not collapse that easily, and the drying process gains on repeatability. In addition, the grindability and solubility can be improved by using a foamy product structure. As a model substance for sensitive biomolecules, β -galactosidase from *Kluyveromyces lactis* was used due to its low denaturation temperature. Thereby, it was assumed to detect unfavorable conditions during the drying process, even for low or moderate overheating of the sample. Besides the successful drying of sensitive biomolecules, the study aimed to understand the influence of the foam matrix on the drying process and determine relevant foam properties to design suitable formulations regarding microwave-assisted foam vacuum and

freeze drying. Therefore, this work was split into three sections. The first part corresponds to the determination of suitable foam matrices and how ingredients influence their suitability for the investigated drying processes. The second section corresponds to how the foam matrix influences the drying kinetic and how a good product quality can be obtained. Further, different process parameters are tested to determine limiting product properties. The last section covers the upscale the microwave-assisted drying process while maintaining the same product quality.

In a first step, the influence of saccharides, which are typical excipients in the food and pharmaceutical industry, on foams, stabilized by nonionic surfactants, was investigated. The hypothesis was that different types of sugars differ in their ability to form hydrogen bonds and that, thereby, foam properties are influenced. It was shown that depending on the type of saccharide, foam properties like drainage and overrun differed. Since this was observed as an effect not only depending on the bulk viscosity, but also on the concentration of the saccharides, this was attributed to structural differences between saccharide types and macromolecular crowding.

In a second step, the investigated surfactant-stabilized foam matrices utilizing maltodextrin (MDX) as foam thickener were investigated in their ability to withstand the mechanical and thermal stress during vacuum drying. It was found that for conventional vacuum drying, only formulations with 30% MDX were stable throughout the process. In microwave-assisted vacuum drying (MWVD), no formulation retained its structure. An explanation for the collapse of the foam during the conventional vacuum drying was the low elasticity of the air-water interface. Thereby, the foam could collapse due to the foam expansion in the vacuum and the fast evaporation. Since these effects were even more pronounced in MWVD, the foam could not be sufficiently stabilized, even at the highest possible MDX concentration of 40%. Another explanation for the decay during MWVD was the resonant frequency of polysorbate 80 within the microwave plant's operating frequency. Thereby, a partial overheating of the interface could occur, which would also explain the observed foam collapse.

This was a problematic aspect due to the fact that the foam stability during the drying process is essential for the repeatability of the process and the grindability of the final product. Further, the drying speed decreases significantly because the surface area of the product decreases. Therefore, foams stabilized with whey protein isolate were investigated regarding their suitability for CVD and MWVD. It was shown that WPI-stabilized foams withstand the harsh conditions during the drying much better, and nearly all investigated formulations showed a foamy structure throughout the drying process. In contrast to polysorbate 80 stabilized foams, the surface elasticity of the investigated formulations was much higher, which was attributed to

more pronounced interactions between proteins at the interface. Further, the dielectric properties of the investigated formulations were investigated, and an increasing heat conversion potential with increasing saccharides concentration was detected.

As only maltodextrin was investigated as a thickener in the previous two steps, surfactant and protein-stabilized foams were investigated on their stability utilizing different saccharides. Besides the comparison of interfacial properties, the molecular interactions between foaming agents and excipients were examined. It was shown that the repulsion between surfactant micelles was less pronounced than that of proteins in the presence of saccharides. This was attributed to the preferential exclusion due to the presence of saccharides, which stabilize the protein in their most favorable conformation. Since the conformation is dependent on whether it is inside the liquid or at the interface, saccharides showed different abilities to influence the surface rheology and surface elasticity. However, these interactions were not present to the same extent for polysorbate stabilized foams. Therefore, most of those foams collapsed during CVD or MWVD. Nonetheless, the study showed that the interactions between foaming agents and saccharides have an influence on the dilational surface rheology and, therefore, foam stability during the drying process.

One question, which arose working with foams in microwave-assisted freeze drying (MWFD), was how the water vapor leaves the product since the product is frozen. Hence, the freeze drying process was examined utilizing a freeze drying microscope and the observed drying compared with the drying kinetics of microwave-assisted freeze drying. One finding from this study was that dependent on the foam properties, the water vapor pathway and the drying behavior differed significantly. For foams with an overrun below about 200%, foam acted like a liquid and showed only a single sublimation front during the drying process, running from the outside to the inside. In contrast, multiple sublimation fronts were observed for foams with higher overrun. Those were showing up around the bubbles and merging within the lamellae. In MWFD, foams with high overrun were much more stable in terms of collapse or melting compared to foams with low overrun. One explanation for this was that due to the merging sublimation fronts in high overrun foams, the water vapor could leave the sample much easier compared to the "liquid-like" drying of foams with low overrun. Therefore, one conclusion of this study was that in MWFD, foams should be used with an overrun above 200% to accelerate the process and minimize the damage of heat-sensitive target substances.

Since the investigations in a freeze drying microscope were only performed for a limited amount of samples and without a sensitive biomolecule, the influence of foam properties and stabilizing excipients was investigated in MWFD in detail. Glycerin was chosen as a typical excipient, and its influence on the drying process was investigated. It was observed that due

to the higher evaporation temperature, glycerin was able to be heated in even water-free sections of the sample. Thereby, the drying process was accelerated, but a negative impact on the residual enzyme activity was observed, especially for samples with high overrun. This was attributed to the delayed temperature measurement because, in microwave-assisted drying, the only surface temperature can be measured in combination with a turntable system. One conclusion was, therefore, that for the formulation design in MWFD, excipients that are able to be dielectrically heated and have higher evaporation temperature than water should be used in only small amounts or even avoided. Besides the influence of glycerin, the influence of foam properties on the residual enzyme activity was investigated. It was observed that independent of the used saccharide or foaming agent, the highest residual enzyme activity was obtained for high overrun values. Since the overrun is an indication for the thickness of the lamellae, which has a massive influence on the internal water vapor resistance, one can conclude that due to even low or moderate pressure differences inside the product, overheating and subsequent damage to the enzyme occurs. However, the drying time increases with increasing overrun, and therefore, there is the need to find the best compromise between product quality and drying speed in MWFD.

Process parameters and different product sizes were investigated to find the limitations of the MWFD and MWVD. In MWFD, it was shown that with increasing sample thickness, the overheating became more pronounced, cracks and melting occurred. This was also observed for a power input value above $1.7 \text{ W}\cdot\text{g}^{-1}$. As a result of the overheating, significant damage to the enzyme was observed. Besides, the probability of plasma formation increased, and the process became unstable. In MWVD, much higher power input can be applied since plasma formation becomes less probable with higher pressure. Furthermore, the product can boil, resulting in less overheating. Best drying results in terms of product quality were obtained at $5.7 \text{ W}\cdot\text{g}^{-1}$ since this power input represents the best compromise between the speed of passing unfavorable drying conditions and local overheating.

Finally, upscale experiments were performed. In MWFD, upscale experiments were conducted utilizing two different strategies. The first strategy should find a way to change the amount of product without losing product quality to adjust production on demand. It was found that equal product quality can be achieved by using a negative relationship between microwave power input and sample weight. The required drying time scaled linearly with the amount of sample between 80 and 140 g. Above that sample weight, a much higher increase in required drying time was observed. For the second strategy, the sample structure was changed to spherical foam droplets to improve the external surface area and minimize the sample's inner water vapor resistance. It was shown that even non-foamed samples could be quickly and easily dried in MWFD utilizing this product shape. Further, an amount of 600 g was successfully dried

within 10 h at only slightly lower residual enzyme activity than that of smaller samples. This was explained by overdrying, as the required drying time could only be predetermined due to no connection between the used drum and the plant's scale. Overall, one conclusion from the upscaling experiments was that the product as well as the drying plant show limitations. For samples dried with MWFD, the water vapor transfer resistance was the limiting key factor, which was improved by using spherical foam droplets. However, if the drying process was accelerated, the drying plant showed limitations in water transfer between the product and condenser chamber, which resulted in unstable process conditions. For MWVD, no upscaling experiments could be carried out since the product chamber was too small for the expanding volume of the foam.

Overall, it was shown that microwave-assisted vacuum and freeze drying is suited to dry sensitive biomolecules within a short period. Using aerated product matrices significantly decreased the water transfer resistance, and thereby, higher microwave power input could be applied without damaging the product. However, plasma formation during the drying process still remains a problem, which could be presumably solved by adjusting the microwave frequency, as applicable in solid-state systems. Furthermore, the use of solid-state microwave systems would allow to change the microwave field mode, resulting in more uniform heating of the product.

1.2 Zusammenfassung

Viele Lebensmittel und pharmazeutische Produkte sind hitzeempfindlich oder verderben innerhalb eines kurzen Zeitraums. Daher werden viele empfindliche und hochwertige Produkte getrocknet, um sie ohne zu großen Wert- oder pharmazeutischen Aktivitätsverlust lagern oder vertreiben zu können. Das schonendste und daher gängigste Trocknungsverfahren zur Konservierung von biologischen Substanzen ist die Gefriertrocknung. Dabei wird Wasser im gefrorenen Zustand unter Ausschluss des flüssigen Zustands entfernt (Sublimationstrocknung). Allerdings ist die Gefriertrocknung ein sehr energieaufwändiger Prozess und benötigt eine lange Trocknungszeit. Dadurch wird der Trocknungsprozess mehr und mehr zum Engpass bei der Herstellung von biologischen Arzneimitteln. Daher wird in der Trocknungstechnik kontinuierlich nach schnelleren Trocknungsprozessen gesucht, die eine hohe Produktqualität gewährleisten. Eine mögliche Alternative für die Trocknung von sensitiven Biomolekülen stellt die Vakuumtrocknung dar. Diese ermöglicht deutlich kürzere Trocknungszeiten und ist auch für Produkte geeignet, welche empfindlich gegenüber Gefrierprozessen sind. Daher wird die Vakuumtrocknung häufig als Alternative zur Gefriertrocknung beispielsweise zur Trocknung von Starterkulturen oder hochqualitativen Lebensmitteln verwendet.

Trotz aller Entwicklungen in den letzten Jahren benötigt sowohl die Gefriertrocknung als auch die Vakuumtrocknung mehrere Stunden oder Tage, bis die Trocknung abgeschlossen ist. Hauptursache hierfür ist die geringe Wärmeleitfähigkeit innerhalb des Produktes, da dieses in der Regel auf einer Stellfläche erwärmt werden. Somit muss die für die Sublimation notwendige Energie zunächst vom Produktboden bis zu der Stelle geleitet werden, an der das Wasser sublimieren werden soll, was den Prozess verlangsamt. Eine Möglichkeit, dieses Problem zu beheben, ist die Verwendung von Mikrowellen zur Erhitzung des Produkts anstelle der Stellflächen. Mit Mikrowellen kann das Produkt volumetrisch erhitzt werden, wodurch die geringe Wärmeleitfähigkeit des gefrorenen Produkts weniger stark ins Gewicht fällt. Allerdings ist die Erhitzung mit Mikrowellen nicht komplett gleichmäßig, wodurch sich Hot- und Coldspots bilden können. Außerdem kann es zu sehr starken Überhitzungen kommen, wenn das Produkt aufgrund seiner Form oder unpassende Inhaltsstoffen nicht zur Trocknung mit Hilfe von Mikrowellen geeignet ist. Insgesamt kann es daher leicht zur Überhitzung des Produkts kommen, wodurch die Trocknung von hitzesensitiven Stoffen eine große Herausforderung für den industriellen Einsatz darstellt.

Um die bei der Verwendung von Mikrowellen entstehenden Probleme zu lösen, soll in dieser Arbeit anstelle einer normalen flüssigen oder gefrorenen Probe ein geschäumtes Produkt eingesetzt werden. Schäume haben eine große Oberfläche, wodurch der Trocknungsprozess weiter beschleunigt werden kann. Außerdem kann der entstehende Wasserdampf das Produkt besser durch das offenporige System verlassen. Dadurch treten seltener Überhitzungen auf,

was wiederum auch den Trocknungsprozess stabilisiert. Des Weiteren kann das poröse Endprodukt einfacher weiterverarbeitet und vermahlen werden.

Um Überhitzungsphänomene einfach und zuverlässig zu detektieren, wurde ein Modellenzym eingesetzt. Hierfür würde das Enzym β -Galactosidase verwendet, welches sich aufgrund seiner niedrigen Denaturierungstemperatur von etwa 45 °C besonders gut eignete. Durch den Einsatz der β -Galactosidase sollten daher auch relativ geringe Überhitzungen detektierbar sein, welche rein optisch nicht zu analysieren wären. Ein Ziel dieser Studie war es daher, eine schnelle und zuverlässige Trocknungsmethode zur Konservierung von sensitiven Biomolekülen zu entwickeln. Zusätzlich war es Ziel der Arbeit, den Einfluss der Schaummatrix auf den Trocknungsprozess zu ermitteln. Dabei sollten die für die Trocknung relevanten Schaumeigenschaften ermittelt und die Möglichkeit geschaffen werden, Grundeigenschaften für Produkte zu definieren, welche für die Trocknung mittels mikrowellenunterstützten Verfahren geeignet sind.

Die Arbeit kann in drei Abschnitte untergliedert werden: Im ersten Abschnitt wurden potentiell geeignete Schaummatrizen untersucht und wie sich deren Eigenschaften mit Hilfe von Sacchariden beeinflussen lassen. Der zweite Abschnitt beschäftigte sich mit der der Trocknung von ausgewählten Schaummatrizen und versuchte die Schaum- mit den Trocknungseigenschaften zu korrelieren. Außerdem sollten Formulierungen gefunden werden, mit denen sich das Modelenzym gut konservieren lässt. Diese Formulierungen sollten auf mögliche Einschränkungen seitens Prozess- oder Produktparameter genauer beleuchtet werden. Im letzten Abschnitt wurde der Upscale der am besten geeignetsten Formulierungen durchgeführt und versucht, mehr Produktmenge bei gleichbleibender Qualität zu trocknen.

Im ersten Schritt wurde der Einfluss von häufig in der Lebensmittel- oder pharmazeutischen Industrie eingesetzten Hilfsstoffen auf die Eigenschaften von tensidstabilisierten Schäumen untersucht. Es wurde angenommen, dass die unterschiedlichen Arten von eingesetzten Zuckern auch unterschiedliche Eigenschaften hinsichtlich der Bildung von Wasserstoffbrückenbindungen besitzen und darüber Einfluss auf die Eigenschaften von Schäumen ausüben können. Es konnte gezeigt werden, dass Schaumeigenschaften wie der Overrun oder die Drainage Unterschiede aufgrund des Einsatzes verschiedener Zucker aufwiesen. Da der Einfluss der Viskosität der flüssigen Phase des Schaums mitberücksichtigt wurde, konnte der Schluss gezogen werden, dass es sich neben dem Einfluss verschiedener Zuckertypen auch um konzentrationsabhängige Unterschiede handelt. Dabei wurde angenommen, dass sowohl besondere strukturelle Unterschiede zwischen den Zuckertypen als auch so genanntes „macro-molecular crowding“, welche erst ab einer systemabhängigen Kohlenhydratkonzentration zum Tragen kommen, für die Abweichungen in den Schaumeigenschaften verantwortlich sind.

Anschließend wurde der Einfluss von tensidstabilisierten Schäumen, welche mit Maltodextrin angedickt wurden, auf ihre Stabilität während der Vakuumtrocknung untersucht. Dabei wurde beobachtet, dass nur Formulierungen mit mehr als 30% Maltodextrin während der konventionellen Vakuumtrocknung stabil blieben. Zudem war keine der untersuchten Formulierungen stabil genug um den mikrowellenunterstützten Trocknungsprozess zu überstehen. Eine Erklärung hierfür war die geringe Oberflächenelastizität, die die Proben aufwiesen. Dadurch kollabierten Schäume während der des Anlegens des Vakuums aufgrund von mechanischer Beanspruchung in Form des expandierenden Volumens. Da die Belastung in mikrowellenunterstützten Prozessen aufgrund der größer ausgelegten Pheripherie noch stärker ausfällt, würde dies auch erklären, wieso hier keine der untersuchten Formulierungen stabil geblieben ist. Eine andere Erklärung, wieso während der MWVD keine Probe stabil blieb, wären die dielektrischen Eigenschaften des Schaumbildners. Die Resonanzfrequenz des Schaumbildners befand sich innerhalb des Frequenzbandes der Mikrowellenanlage. Daher könnte es zu einer Resonanzkatastrophe an der Grenzfläche oder zumindest einer lokalen Überhitzung dieser gekommen sein. Auch dies würde ein Kollabieren der Schaumstruktur erklären.

Da die Schaumstabilität für die Wiederholbarkeit und Produkteigenschaften von essentieller Bedeutung ist, wurden molkenproteinisolatstabilisierte Schäume, welche auch mit Maltodextrin versetzt waren, hinsichtlich ihrer Eignung zur Vakuum- oder mikrowellenunterstützten Vakuumtrocknung untersucht. Es wurde gezeigt, dass die untersuchten Schäume die rauen Bedingungen während der Trocknung deutlich besser überstanden und dass nahezu alle Formulierungen ihre Schaumstruktur behielten. Im Gegensatz zu tensidstabilisierten Schäumen war die Oberflächenelastizität deutlich höher, was den stärker ausgebildeten Interaktionen von Proteinen an der Grenzfläche zugeschrieben wurde. Außerdem wurden die dielektrischen Eigenschaften der Formulierungen untersucht und eine mit zunehmenden Maltodextrinanteil steigende Effizienz der Wärmeumwandlung aus elektromagnetischen Wellen festgestellt.

Nachdem bis jetzt nur Maltodextrin als Kohlenhydrat in den Formulierungen für die (mikrowellenunterstützten) Vakuumtrocknungen eingesetzt worden ist, wurden zusätzliche Versuche mit strukturell anderen Kohlenhydraten (Sorbitol, Saccharose und Maltose) untersucht. Zudem wurde statt des Molkenproteinisolates reines β -Lactoglobulin verwendet, um Interaktionen zwischen Schaumbildner und Zucker auf molekularer Ebene untersuchen zu können. Dabei konnte gezeigt werden, dass in Anwesenheit von Kohlenhydraten die repulsiven Kräfte zwischen Tensidmizellen deutlich schwächer waren als die von Proteinen. Erklärt wurde dies mit der „preferential exclusion“, bei der durch die Anwesenheit von Kohlenhydraten die thermodynamisch stabilsten Konformationen von Proteinen begünstigt werden. Da es in einem Schaum sowohl eine flüssige Phase als auch die Luft-Wasser-Grenzschichten oder Oberflächenschichten gibt, in der sich Proteine ansammeln, unterscheiden sich auch die Konformationen, welche

unterstützt werden. Es wurde daher angenommen, dass die eingesetzten Zucker auch die Grenzfläche stabilisierten, was sich in einer erhöhten Grenzflächenelastizität widerspiegelte. Allerdings trat dieser Effekt nicht bei tensidstabilisierten Schäumen auf, was durch schwächere Interaktionen zwischen den nichtionischen Tensiden an der Grenzfläche erklärt wurde. Daher kollabierten die meisten Formulierungen der tensidstabilisierten Schäume sowohl in der konventionellen als auch in der mikrowellenunterstützten Vakuumtrocknung. Bei proteinstabilisierten Schäumen zeigten mit Maltodextrin versetzte Formulierungen die höchste Stabilität. Daher konnte mit der Studie gezeigt werden, wie die auftretenden Interaktionen auf molekularer Ebene Einfluss auf die Grenzfläche und somit auf die Stabilität während der Trocknung ausüben und welche Rolle dabei Zucker einnehmen können.

Eine Frage, die sich bei der Arbeit mit Schäumen in der mikrowellenunterstützten Gefriertrocknung stellte, war, wie der Wasserdampf das gefrorene Produkt verlässt. Zu diesem Zweck wurde der Gefriertrocknungsprozess mit Hilfe eines Gefriertrocknungsmikroskops untersucht und die Ergebnisse mit der Trocknungskinetik einer mikrowellenunterstützten Gefriertrocknung verglichen. Eine daraus gewonnene Erkenntnis war, dass sich in Abhängigkeit der Schaumeigenschaften der Weg des Wasserdampfs und somit das Trocknungsverhalten deutlich unterschieden. Bei Schäumen mit einem Overrun unter ca. 200 % verhielt sich der Schaum eher wie eine gefrorene Flüssigkeit und zeigte während des Trocknungsprozesses nur eine einzige Sublimationsfront auf, die von außen nach innen verlief. Im Gegensatz dazu wurden bei Schäumen mit höherem Overrun mehrere Sublimationsfronten beobachtet. Diese traten um die Blasen herum auf und verschmolzen über den Trocknungsprozess hinweg innerhalb der Lamellen. In der MWFD waren Schäume mit hohem Overrun im Vergleich zu Schäumen mit niedrigem Overrun wesentlich stabiler in Bezug auf einen Produktkollaps oder das Anschmelzen des Produkts. Eine Erklärung dafür war, dass aufgrund der zusammenlaufenden Sublimationsfronten in Schäumen mit hohem Overrun der Wasserdampf die Probe, verglichen mit der "flüssigkeitsähnlichen" Trocknung von Schäumen mit niedrigem Overrun, viel leichter verlassen konnte. Ein Ergebnis dieser Studie war daher die Schlussfolgerung, dass bei der MWFD ein Schaum mit einem Overrun über 200 % verwendet werden sollte, um den Prozess zu beschleunigen und die Schädigung wärmeempfindlicher Zielsubstanzen zu minimieren.

Da die Untersuchungen im Gefriertrocknungsmikroskop nur für eine begrenzte Menge an Proben und ohne ein sensitives Biomolekül durchgeführt wurden, wurde der Einfluss von Schaumeigenschaften und stabilisierenden Hilfsstoffen für die MWFD untersucht. Als häufig genutzter und typischer Hilfsstoff wurde Glycerin gewählt und dessen Einfluss auf den Trocknungsprozess untersucht. Es wurde beobachtet, dass sich Glycerin aufgrund der höheren Verdampfungstemperatur auch in wasserfreien Bereichen der Probe erwärmen konnte. Dadurch wurde der Trocknungsprozess zwar beschleunigt, jedoch wurde ein negativer Einfluss auf die

verbleibende Enzymaktivität beobachtet, insbesondere bei Proben mit hohem Overrun. Dies wurde auf die verzögerte Temperaturmessung zurückgeführt, da bei Mikrowellen in Kombination mit einem Drehtischsystem nur die Oberflächentemperatur gemessen werden konnte. Eine Schlussfolgerung war daher, dass für die Entwicklung von Formulierungen für die MWFD, Hilfsstoffe, die dielektrisch erwärmt werden können und eine höhere Verdampfungstemperatur als Wasser haben, nur in geringen Mengen verwendet oder sogar vermieden werden sollten. Neben dem Einfluss von Glycerin wurde auch der Einfluss der Schaumeigenschaften auf die verbleibende Enzymaktivität untersucht. Es wurde festgestellt, dass unabhängig vom verwendeten Saccharid oder Schaumbildner die höchste Restenzymaktivität bei hohen Overrunwerten erreicht wurde. Da der Overrun auch einen Hinweis auf die Lamellendicke gibt, die wiederum den inneren Wasserdampf Widerstand massiv beeinflusst, kann daraus geschlossen werden, dass bereits bei geringen oder moderaten Druckunterschieden im Produktinneren eine Überhitzung und damit eine Schädigung des Enzyms auftritt. Die Trocknungszeit verlängerte sich mit zunehmendem Overrun, so dass bei der MWFD ein Kompromiss zwischen Produktqualität und Trocknungsgeschwindigkeit gefunden werden muss.

Zusätzlich wurden Prozessparameter und verschiedene Produktgrößen untersucht, um die Einschränkungen und Grenzen der MWFD und MWVD zu finden. Bei der MWFD zeigte sich, dass mit zunehmender Probendicke die Überhitzung stärker ausgeprägt war. Dies äußerte sich zudem durch das Anschmelzen des Produkts sowie das Auftreten von Rissen. Neben einer zu großen Produktdicke wurde dies auch bei einem Leistungseintragswert über $1,7 \text{ W}\cdot\text{g}^{-1}$ beobachtet. Zudem wurde als Folge der Überhitzung eine signifikante Schädigung des Enzyms beobachtet. Außerdem stieg die Wahrscheinlichkeit der Plasmabildung, wodurch sowohl der Trocknungsprozess instabil als auch das Produkt geschädigt wurde. Bei der MWVD konnte im Vergleich zur MWFD eine höhere Mikrowellenleistung eingesetzt werden, da die Plasmabildung bei höherem Druck weniger wahrscheinlich wird. Außerdem kann das Produkt siedend und sich somit selbst mischen, was zu einer geringeren Überhitzung führt. Die besten Trocknungsergebnisse in Bezug auf die Produktqualität wurden bei $5,7 \text{ W}\cdot\text{g}^{-1}$ erzielt, da diese Leistungsaufnahme den besten Kompromiss zwischen der Geschwindigkeit des Passierens unter ungünstigen Trocknungsbedingungen und der lokalen Überhitzung darstellte.

Abschließend wurden Upscale Experimente durchgeführt. Für MWVD konnten allerdings keine Upscale-Experimente durchgeführt werden, da die Produktkammer zu klein für das expandierende Volumen des Schaums war. Die Upscale-Experimente für MWFD wurden mit zwei verschiedenen Strategien durchgeführt. In der Ersten sollte ein Weg gefunden werden, die Produktmenge zu verändern, ohne die Produktqualität zu verlieren und somit die Produktion an den Bedarf flexibel nach oben und unten anpassen zu können. Es wurde gezeigt, dass durch

die Verwendung einer negativen linearen Beziehung zwischen Mikrowelleneintrag und Probengewicht eine gleiche Produktqualität erreicht werden kann. Auch die benötigte Trocknungszeit skalierte linear bei Verwendung einer Probenmenge zwischen 80 und 140 g. Oberhalb von 140 g wurde ein deutlich höherer Anstieg der benötigten Trocknungszeit beobachtet. Bei der zweiten Strategie wurde die Probenstruktur von einem zylindrischen geschäumten Produktkuchen in kugelförmige Schaumtröpfchen geändert, um die äußere Oberfläche zu vergrößern und den Wasserdampf Widerstand innerhalb der Probe durch die Schaumstruktur zu minimieren. Es wurde gezeigt, dass auch nicht geschäumte Proben mit dieser Produktform erfolgreich mittels MWFD getrocknet werden können, was bei der Verwendung eines Probenkuchens schwierig war. Zudem wurde eine Menge von 600 g innerhalb von 10 h getrocknet, wobei die verbleibende Enzymaktivität nur geringfügig niedriger war als bei kleineren Proben. Dies wurde mit einer Über Trocknung erklärt, da die benötigte Trocknungszeit aufgrund der fehlenden Verbindung zwischen der verwendeten Trommel und der Waage der Anlage nur manuell vorgegeben und der Prozess nicht über eine Waage gesteuert werden konnte. Eine Schlussfolgerung aus den Upscaling Versuchen war, dass sowohl beim Produkt als auch bei der Trocknungsanlage die prozesstechnischen Grenzen der MWFD erreicht wurden. Bei den mit MWFD getrockneten Proben war der produktinterne Wasserdampf Widerstand der limitierende Faktor für den Einsatz von höheren Mikrowellenleistungen und damit schnelleren Trocknungsprozessen. Durch den Einsatz von sphärischen Schaumtröpfchen konnte diese Grenze erfolgreich erweitert und der Prozess beschleunigt werden. Die Beschleunigung des Trocknungsprozesses zeigte die Limitierung der Trocknungsanlage in ihrer Möglichkeit auf, sublimiertes Wasser aus der Produktkammer in die Kondensatorkammer zu befördern. Dadurch verringerte sich die Prozessstabilität.

Insgesamt konnte gezeigt werden, dass die mikrowellenunterstützte Vakuum- und Gefrier-trocknung für die Trocknung sensitiver Biomoleküle gut geeignet ist. Durch die Verwendung von Schaummatrizen verringerte sich der innere Wassertransportwiderstand erheblich. Dadurch war es möglich eine höhere Mikrowellenleistung einzusetzen, ohne das Produkt zu schädigen. Die Bildung von Plasma während des Trocknungsprozesses stellt jedoch nach wie vor ein Problem dar. Dieses könnte durch eine Frequenz- bzw. Modenänderung in einem halbleiterbasierten Mikrowellentrockner gelöst werden. Außerdem könnte das Produkt dadurch gleichmäßiger erhitzt werden, als es im hier verwendeten Magnetronsystem der Fall war.

2 General introduction

2.1 Common drying methods in the food and pharmaceutical industry

To increase the shelf life of heat-sensitive products like biopharmaceuticals, probiotics, or high-value food components and improve their handling and distribution, they are often preserved by drying. Secondary targets can be a reduction of weight and volume and hence, minimized packaging, storage, and transport costs (Falade and Solademi 2010; Fumagalli and Silveira 2005).

Next to the product quality, cost and time effort are important for industrial application (Karim and Wai 1999). The most expensive and time-consuming drying process is freeze drying if the costs are defined by the costs per kg evaporated water (Santivarangkna et al. 2007b; Roser 1991). Nevertheless, the higher the product's value, the higher the costs of a particular damaged product, which might be the reason for commonly used freeze drying (Walters et al. 2014). However, the increased demand for freeze drying capacity can result in a bottleneck of entire production chains in the pharmaceutical industry (Schmitt 2012).

The most commonly used processes are spray drying, vacuum drying, foam-mat drying, or freeze drying. They differ in their mechanism of dehydration (Fig. 2.1.1), and each drying process has specific advantages and disadvantages, well documented in the literature (2014; Ratti 2008; Sankat and Castaigne 2004). Therefore, for each product, the drying process should be chosen with care, finding the best match between product and process properties. However, for biomolecules like proteins or vaccines, freeze drying is the most common drying technique (Walters et al. 2014; Pikal 1990b).

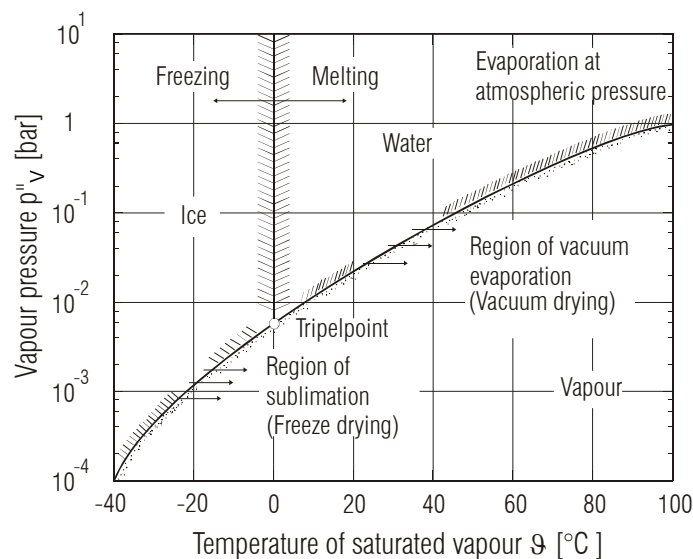


Fig. 2.1.1 Phase diagram of water, ice, and vapor in dependency of water vapor pressure and temperature of saturated vapor in relation to important drying processes according to Kessler (2006).

Vacuum drying, convective drying, or foam-mat drying are more common for food products, as their costs are lower (Roser 1991). Next to those conventional drying techniques, combinations of techniques like foam vacuum drying or microwave-supported processes are more and more used to solve specific disadvantages of single drying techniques and to optimize the product quality (Ambros et al. 2019b; Ozcelik et al. 2019b; Qadri and Srivastava 2017; Raharitisfa and Ratti 2010).

Stabilization of proteins during drying processes and storage

The preservation of functional properties of biomolecules or taste of food over a long storage time is one of the main goals of drying in the food and pharmaceutical industry and can be improved by the product's formulation due to the addition of excipients like saccharides, polyols, or polymers. Thereby, the stability can be enhanced during the drying process as well as during storage time through the inhibition of degradation mechanisms. In general, those mechanisms can be split into chemical processes, like oxidation, deamination, or Maillard reaction, and physical processes, like precipitation, crystallization, or non-covalent aggregation (Mensink et al. 2017; Köpf and Frieß 2016; Simon et al. 2011).

As the products' state changes throughout the drying process from liquid to dry and within freeze drying processes from a frozen state, different preservation mechanisms are important to stabilize the product. In order to remain within one representative system, the following stabilization mechanisms are described for protein or peptide-based products. Primarily, two stabilization mechanisms are reported in the literature, the glass dynamics or vitrification and the water replacement theory (Chang and Pikal 2009; Chang et al. 2005).

Most degradation mechanisms can be minimized by the incorporation of functional substances into a glassy matrix. Glass itself is a highly viscous, amorphous state, which can cover, e.g., proteins or probiotics and stabilize them via hydrogen bonds (Carpenter and Crowe 1989). Thereby, sensitive substances are protected against aggregation or chemical degradation, as even in the appearance of problematic substances, like oxygen, the diffusion is slowed down.

The ability of excipients to stabilize proteins within a glassy matrix differs strongly. For example, the molecular size and the flexibility of sugars can strongly influence the stabilization of freeze-dried proteins, as shown by Tonniss et al. (2015). The sugar molecules should be able to fit the substance's surface closely and thus to cover it to obtain the most suitable interactions (Grasmeijer et al. 2013). With higher molecular weight and lower flexibility of the saccharides, their ability to interact with the proteins and cover their surface is lower compared to small or flexible saccharides, resulting in faster degradation of proteins during their storage (Allison et al. 1999). Therefore, most commonly, small sugars are used like the disaccharides trehalose or sucrose (Carpenter et al. 1992; Timasheff 1992; Arakawa et al. 1991).

However, glasses are thermodynamically instable and tend to change to the so-called rubbery state. The rubbery state is much less viscous than the glassy state, whereby the stabilization of, e.g. proteins is also less effective. With lower viscosity, glass-forming substances can move faster, which results in crystallization. As the straightly ordered structure of crystals cannot closely cover the protein's surface or embed the proteins into an amorphous matrix, the crystallization of drug-containing formulations is unwanted. The temperature at which a system leaves the glassy state is called glass transition temperature T_G , whereas T_C corresponds to the crystallization temperature. As the glass transition temperature is of particular interest for the drug stability, it should be much higher than the storage temperature (Alhalaweh et al. 2015; Hancock et al. 1995). However, in some cases, physical degradation of pharmaceuticals of foods was even detected below T_G (Chung and Lim 2006; Noel et al. 2005; Hancock et al. 1995).

The glass transition is usually not spontaneously happening at a single temperature point. It is a transition, which consists of on-set, mid-point, and end temperature and therefore occurs within a specific temperature range, as shown in Fig. 2.1.2 (Thomas 2017). The value of T_G and the temperature range are strongly dependent on the used excipients and the water content of the formulation (Alvino Granados et al. 2019; Dereymaker and van den Mooter 2015; Abiad et al. 2009). In the case of different excipients, the glass transition temperature can be easily influenced by combining substances with different molecular weights (Legucha-Balteseros et al. 2002; Yu et al. 1994). Another way to increase T_G is the addition of phosphates, which are often present in buffer solutions (Ohtake et al. 2004). However, as already discussed, the glass transition temperature itself is not the only parameter for the stabilization inside an amorphous matrix. Therefore, interactions between proteins and excipients should also receive attention.

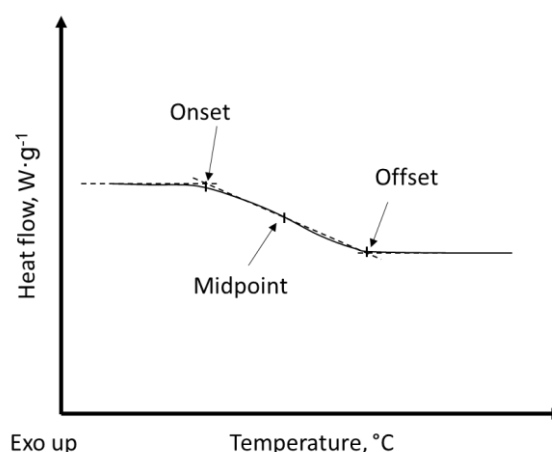


Fig. 2.1.2: Typical glass transition of amorphous materials measured with dynamic scanning calorimetry (DSC), with extrapolated onset, midpoint, and offset temperature according to Thomas (2017).

The stabilizing interactions between sugars and proteins during dehydration can be explained best by hydrogen bonds. In liquid phase, the water interacts *via* hydrogen bonds with proteins resulting in the solubility of proteins inside the aqueous phase. However, during drying, water is removed, and the protein would tend to aggregate due to increasing protein concentration in the residual liquid. As sugars can form H-bonds with the proteins, they can replace the water molecules at the protein and, therefore, stabilize the native structure. This is mainly referred to as the “water replacement theory” (Arakawa et al. 1991; Carpenter and Crowe 1989), which is strongly dependent on the ability of sugars to cover the protein's surface.

Therefore, the stabilization of proteins during drying and storage depends mainly on vitrification and water replacement. Recently, it was not possible to explain the stabilization of proteins just by one of those mechanisms, and therefore, both need to be considered during drug development (Mensink et al. 2017). However, it was stated that the predominant mechanism is dependent on the storage temperature, as below T_G the water replacement will be the critical property, while above T_G the vitrification will be the limiting property (Grasmeijer et al. 2013).

2.1.1 Freeze drying

The most common drying method for the preservation of sensitive material is freeze drying. It is performed at a pressure below the Triple point (Fig. 2.1.1), and therefore, the water is sublimating and not boiling. Thereby, the free water evaporates without being liquid throughout the drying process, providing several advantages. One of them is that the sample will not concentrate during the drying process as it occurs during hot-air drying or vacuum drying. Further, low pressure during the sublimation phase results in a low presence of oxygen during the drying, effectively decreasing product oxidation, in combination with low temperatures. Hence, chemical degradation of products and solubility problems can be avoided by freeze drying, resulting in the gentlest available drying process for the most sensitive materials (Walters et al. 2014).

Freeze drying consists of three main steps, freezing (fast or slow), primary drying, the so-called sublimation phase, and secondary drying, which is also called desorption phase (Köpf and Frieß 2016).

A simplified sketch of how the freezing rate influences the drying speed and crystal size is shown in Fig. 2.1.3. During the freezing step, a concentration of ingredients might occur, combined with a pH-shift of buffered solutions, affecting the quality of the product (Kolhe et al. 2010; Gómez et al. 2001). Therefore, the freezing rate is usually as high as possible for the case of protein drying. However, the higher the freezing rate, the smaller the crystal size. This results in higher water vapor resistance inside the product and causes slower drying rates compared to samples with larger ice crystals (Patapoff and Overcashier 2002). Therefore, a so-called “annealing” step can be performed, where the product temperature is cycled between

the ice melting temperature and the glass transition temperature of the freeze concentrate (Searles et al. 2001; Lu and Pikal 2004). Thereby, the product partially crystallizes and the crystals grow because of ‘Ostwald ripening’ (see section 2.2.), which stabilize the product against collapse (Wang and Pikal 2012). Thereby, uniformity of ice-crystals and drying speed can be significantly increased by storing the product for a defined time at temperatures above the glass transition temperature of the maximally freeze-concentrated amorphous phase, T'_g , as shown by Searles et al. (2001) or Fonte et al. (2016).

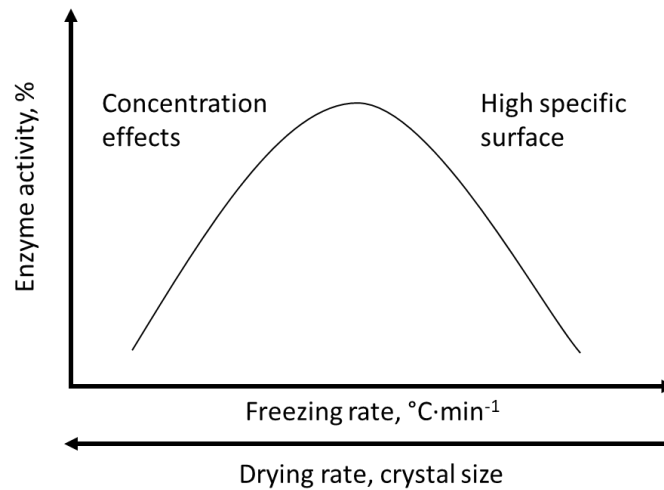


Fig. 2.1.3: Simplified sketch on the influence of freezing rate on the crystal size and enzyme degradation mechanisms.

However, it should be noted that not all water can be frozen, as some water will be bound by hydrated molecules and remains, therefore, unfrozen. In Fig. 2.1.4, different possible states of sample matrices are schematically shown in dependency of temperature and saccharide concentration. It is clearly shown that above a certain sugar concentration, a supersaturated solution will always be present. Furthermore, the dependency of the glassy state on temperature and sugar concentration is shown. To obtain a glassy product is of particular interest in the drying technology of enzymes or probiotics, as the products are stabilized *via* so-called vitrification, as already discussed in the previous chapters.

Besides the glass transition temperature, the collapse temperature can be used to estimate the boundary conditions for the freeze drying process. Above the collapse temperature, which is usually 1–3 K higher than T_G , the product gets able to flow, and therefore, the product loses its structure and ‘pharmaceutical elegance’ (Schersch et al. 2010; Nail and Akers 2002; Pikal 1990a). However, the structure loss is not only relevant for the optical acceptance of consumers. A decreased sublimation rate was observed due to the structural collapse and consequently blocking of pores. Furthermore, secondary drying takes longer, as the structure is more compact, decreasing the effective diffusivity and drying speed (Wang et al. 2004; Carpenter et al. 1997; Bellows and King 1972). Further, reconstitution time will be longer for products that

collapsed compared to those of non-collapsed products due to a lower specific surface (Adams and Irons 1993; Tsourouflis et al. 1976).

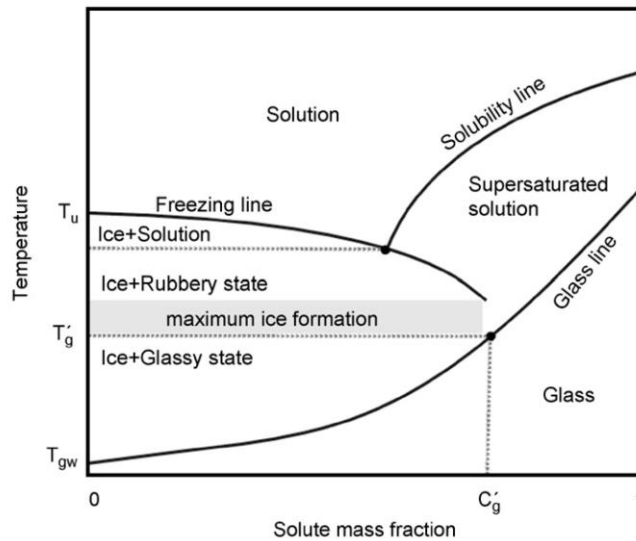


Fig. 2.1.4: State diagram showing different regions and states of sugar at different concentrations with T_u as eutectic point, T_g as glass transition temperature of the freeze-concentrated amorphous matrix, and T_{gw} , the glass transition temperature of water. The shaded area shows the temperature range for the maximum ice formation at the sugar concentration C'_g , while the glass line corresponds to the glass transition temperature at various sugar concentrations (Santivarangkna et al. 2008).

For the residual activity of the target protein, the reported results differ. Some researchers reported less activity after drying or consecutive storage as a result of collapsed products (Pascot et al. 2007; Fonseca et al. 2004; Lueckel et al. 1998), whereas other studies showed an equal or even improved activity directly after drying as long as parts remained amorphous (Schersch et al. 2012; Schersch et al. 2010; Chatterjee et al. 2005; Wang et al. 2004).

Further, the water distribution in the dried product will vary if the drying process is applied above the collapse temperature, as a result of promoted crystallization and the fact that crystal structure remains lower water content compared to amorphous structures (Chatterjee et al. 2005). Furthermore, due to the slower secondary drying, the total water content might be higher than for non-collapsed samples, resulting in lower product quality (Adams and Irons 1993). Therefore, a collapse of the product structure must not be detrimental for the stability of protein products and should be investigated case-by-case. Nonetheless, if optimized drying speed is targeted, the collapse of the glassy matrix should be prevented.

2.1.2 Vacuum drying

Vacuum drying uses low pressure to decrease the evaporation temperature of water. In comparison to freeze drying, the applied pressure is above the Triple point, and therefore, the product remains liquid during the drying process, and the water evaporates, while during freeze

drying, the water is sublimating. Thereby, due to better heat transfer and water mobility, the drying speed is higher than that of freeze drying (King and Su 1993). However, the drying times are still long compared to other drying processes, and therefore, conventional vacuum drying cannot be stated as a fast process.

Vacuum drying can be used for heat and freezing-sensitive products and for products that are sensitive to oxidation. Therefore, vacuum drying seems to be a good alternative for freeze drying (Bauer et al. 2012; King et al. 1989). However, it should be mentioned that predominantly liquid products tend to shrink during vacuum drying, which slows down the drying speed and results in poor grindability and rehydration properties (King and Su 1993). Therefore, it is often used only for products where the physical structure is not of significant interest, like pastes or products, which are often post-processed into powders.

2.1.3 Conventional foam-mat drying

Conventional foam-mat drying can be defined as the drying of a liquid or semi-liquid fluid, which is whipped to a stable foam, spread out as a thin layer, and followed by a dehydration step, most often *via* convection and hot air (Karim and Wai 1999; Brygidyr et al. 1977). Nonetheless, many food systems already contain proteins or surface-active substances, their concentration is often too low, and therefore, foaming agents have to be added (Sankat and Castaigne 2004). Foam-mat drying provides the user a possibility to dry heat-sensitive, highly viscous or sticky, as well as other hard-to-dry products, like tomato juice (Kadam and Balasubramanian 2011; Brygidyr et al. 1977; Hertzendorf et al. 1970), starfruits (Karim and Wai 1999), passion fruits (Khamjae and Rojanakorn 2018) or mango pastes (Lobo et al. 2017). Further, the dried products are easier to grind than non-foamed hot-air dried products due to the open-pored structure. In addition, foam-mat drying can be used to save up to 80% of energy consumption compared to the drying of non-foamed products, as calculated for foamed apple juice by Kudra and Ratti (2006).

One of the most important advantages of foam-mat drying compared to the drying of non-foamed samples is the acceleration in drying speed. The acceleration of drying can be attributed to the higher inner surface and the lamellae, which can act as capillaries that pump the water to the product's surface (Rajkumar et al. 2007). However, the drying process is an interrelationship between heat transfer and mass transfer, and therefore, the foam does not provide only advantages. For example, air has a lower ability to conduct heat compared to liquids. Thus, the heat transfer into the product will be slower than for non-foamed products, and therefore, the drying rate might decrease with increasing product thickness. A common way to handle this problem is using products in thin layers (Hertzendorf et al. 1970).

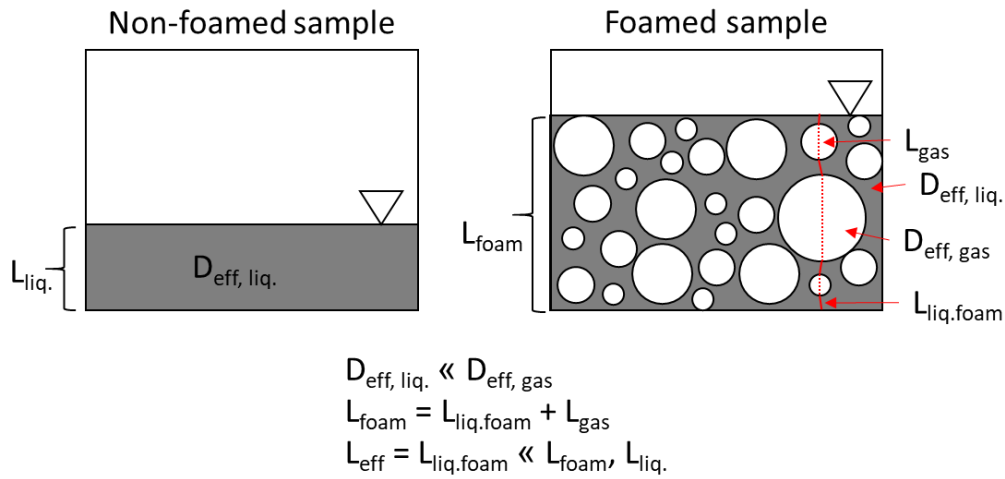


Fig. 2.1.5: Comparison of the drying of non-foamed and foamed products with regard to the products' density, with $L_{\text{liq.}}$ as the thickness of the non-foamed product, $D_{\text{eff, liq.}}$ as the effective diffusivity of the liquid, $D_{\text{eff, gas}}$ as the effective diffusivity of the gas inside the bubbles, $L_{\text{liq, foam}}$ as the thickness of the solution inside a foam, L_{gas} as the thickness of bubbles and L_{eff} as the effective thickness of the foam.

In contrast, the mass transfer rate and effective diffusivity will be enhanced by a less dense product, e.g., due to higher overrun values (Thuwapanichayanan et al. 2012). In Fig. 2.1.5, the difference between non-foamed and foamed products concerning the foam density is shown. While the height of the foamed product L_{foam} is much higher than for the non-foamed sample $L_{\text{liq.}}$, the effective diffusivity $D_{\text{eff, gas}}$ inside the void is also higher compared to that of the non-foamed sample $D_{\text{eff, liq.}}$. Hence, it can be assumed that the effective length, which the water has to pass L_{eff} is inside the foam predominantly influenced by the length of the liquid $L_{\text{liq, foam}}$, which has to be passed by the evaporated water. Thereby, the overall effective diffusion of the foam will be much higher than that of a non-foamed product. Therefore, the interplay between heat transfer and mass transfer in foam-mat drying plays a significant role in optimizing the process.

Next to the drying characteristics, the foam density has an impact on the product characteristics. Products with lower foam density showed smaller hardness and lower crispiness than products with high foam density (Thuwapanichayanan et al. 2012). Next to the layer thickness and the density of the foam, the bubble size influences the foam-mat drying. It appears that foams are most suitable for foam mat drying if their bubbles are as small as possible and of uniform size distribution (Ratti and Kudra 2006b). However, due to a high amount of pores inside the product, the apparent color intensity can be reduced.

As the drying speed depends on the higher inner surface and the lamellae, the foam must be stable throughout the drying process. Therefore, it is stated in the literature that a foam should be stable for at least one hour (Ratti and Kudra 2006a; Brygidyr et al. 1977). If the foam collapses during the drying, the drying speed will be reduced, and advantages like good rehydration, color, texture, or nutritional value might be lost (Ratti and Kudra 2006a; Sankat and

Castaigne 2004). Hence, most food systems are thickened by an additive or concentrated to increase their viscosity for a stable foam (Hertendorf et al. 1970).

Overall, foam mat drying provides a fast process combined with high product quality. However, it is strongly dependent on the properties of the used foam. Therefore, the most relevant foam properties and stabilization mechanisms of foams will be shown in the following chapters.

2.2 Characteristics of protein- and surfactant stabilized foams

2.2.1 General characteristics of foams

Foam is known as a dispersion of gas in a liquid and can be divided into “liquid” and “solid” foams (Weaire and Hutzler 2001; Walstra 1989). Due to the effort of an immiscible two-phase system to minimize its surface area, foams are thermodynamically unstable. During foam formation, the continuous phase is usually liquid and directly influences the structure of the foam. After foam formation, the liquid phase can change into a solid phase, e.g., due to gelation, and the foam turns into a “solid” foam. The volume fraction of gas Φ of foam is usually between 0.5 and 0.97, and the shape of bubbles changes with increasing Φ : For $0.52 < \Phi < 0.74$, bubbles exhibit relatively spherical, while for $\Phi > 0.74$ bubbles are deforming neighbored bubbles into a polyhedral shape (Walstra 1989). Besides, foams can be characterized by their bubble structure into “wet” and “dry” foams, as shown in Fig. 2.2.1 (Weaire and Hutzler 2001).

Further, in Fig. 2.2.1, the bubbles are separated by liquid films (or lamellae), which is important for the stability of foams. Additionally, the areas, at which three liquid films meet are called plateau border. In the particular case of perfect polyhedral foam, the angle between the connected liquid films will be 120° . Both liquid films and plateau borders have a high impact on foam decay, which will be discussed in chapter 2.2.2.

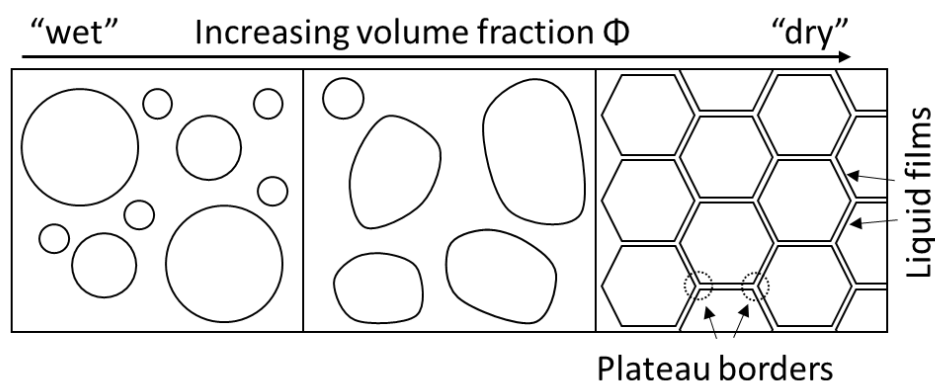


Fig. 2.2.1: Changes of foam structure in dependency of the gas volume fraction Φ . Modified according to Walstra (1989).

Foams can be characterized by their foaming behavior and the time-dependent change of foam properties (e.g., foamability, foam capacity, density and overrun, foam stability, foam

drainage, bubble size distribution). Foam stability is commonly used in terms of the main characteristics like foam volume, density or liquid volume fraction, and bubble size distribution. Nevertheless, foam stability differs in the literature due to the experimental design of each study, as not every potential property is investigated, especially since it is difficult to differentiate between destabilization mechanisms in complex systems. Therefore, it is more common for complex systems to discuss the foam properties in terms of general stabilization than concentration on a single parameter.

Therefore, foam stability can be interpreted as overall stability, which is important for the successful and repeatable drying of foams, as previously discussed in chapter 2.1. As already mentioned, the thickness of lamellae or liquid film is crucial for the stability of foams. One aspect are differences in pressure between the internal pressure of the gas (p_d) inside the bubble and the external pressure, which can be attributed to the continuous phase (p_l). This pressure difference is also known as Laplace pressure, Δp , or capillary pressure, p_c , and can be calculated according to Equation 2.2.1 (Stubenrauch and Klitzing 2003),

$$\Delta p = p_c = p_d - p_l = \frac{2\sigma}{r} \quad (2.2.1)$$

where σ corresponds to the surface tension of the continuous phase and r to the radius of dispersed bubbles, respectively.

Besides the thickness of liquid films, interactions between converging surface films, also called disjoining pressure, Π , are important for the foams' stability. Without surface-active substances, like proteins or surfactants, the disjoining pressure is negligible, and film rupture instantly occurs. The disjoining pressure acts perpendicular to the bubble surface and counteracts capillary pressure and thus drainage (Stubenrauch and Klitzing 2003). Further, Π stabilizes the thickness of the liquid film and therefore prevents its thinning, which would result in foam destabilization (Damodaran 2005). The influence of disjoining pressure on foam stability is dependent on the interactions between surface-active molecules. The disjoining pressure can be summed up (Equation 2.2.2), based on the most common interactions like long-range repulsive electrostatic (Π_{elec}), short-range repulsive (Π_{steric}), and short-range attractive van der Waals (Π_{vdW}) (Stubenrauch and Klitzing 2003; Bergeron 1999). It is worth noting that the contribution of van der Waals forces to the disjoining pressure is always negative, while Π_{elec} and Π_{steric} are always positive (Damodaran 2005).

$$\Pi = \Pi_{elec} + \Pi_{steric} + \Pi_{vdW} + \dots \quad (2.2.2)$$

In addition to the disjoining pressure, the viscoelasticity of surface films is reported to be of high relevance for the stability of foams. Viscoelastic surfaces can be explained by interactions between surface-active components, which are promoted by the adsorption at the interface.

Hence, intermolecular interactions, like ionic interactions or covalent disulfide bonds, resulting in aggregation or linkage between surface-active molecules (Bos and van Vliet 2001). These interactions differ based on the used surface-active substance and the environmental conditions, like pH value, salt content, or temperature, which directly influences the mechanical properties of the formed foam and is more present for proteins than for surfactants (Dombrowski et al. 2018; Dombrowski et al. 2017; Dickinson 1989). Although all surface-active substances adsorb at the interface, not all of them can easily detach. For example, pure protein samples are very unlikely to detach from a surface, while small surfactants are known to detach very easily (Fainerman and Miller 2005). Besides, proteins can be stretched during a surface expansion, while surfactants cannot. To prevent gaps in the interface, which can occur during stretching a surface (e.g., due to drainage), surfactant molecules have to adsorb from bulk phase or/and *via* lateral diffusion along with the surface film. Since this is only effective for fast desorption/adsorption processes, it is commonly discussed in conjunction with surfactants and is named the “Gibbs-Marangoni” effect (Wilde et al. 2004; Clark et al. 1989).

2.2.2 Foam decay mechanisms

As already mentioned in the previous chapter, foams are thermodynamically unstable. Destabilization mechanisms are occurring simultaneously and may affect each other, which leads to a reorganization of foam structure and may cause instability of foams (Wilson 1989). However, disproportionation (Ostwald ripening), coalescence, and foam drainage are separately discussed as they are the main physical destabilization mechanisms for food- and pharmaceutical foams.

Disproportionation

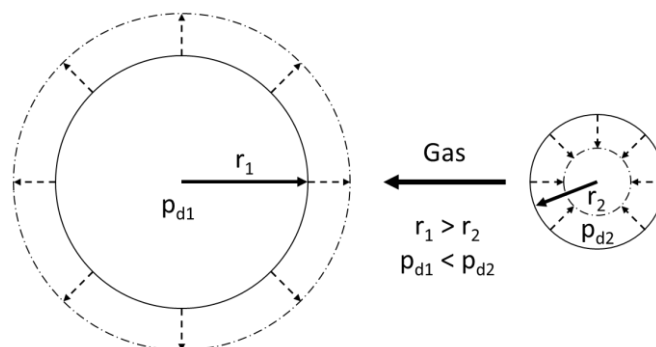


Fig. 2.2.2: Disproportionation or Ostwald ripening of gas bubbles inside a liquid with r as bubble radius and p_d as partial gas pressure inside the bubble.

Disproportionation or “Ostwald ripening” describes the mechanism of diffusional gas transport through the liquid films according to the Laplace pressure Δp (Equation 2.2.1) and is schematically shown in Fig. 2.2.2. As Δp is dependent on the radius of the bubbles (the smaller r , the higher Δp), the gas from smaller bubbles diffuses into bigger ones. Further, gas solubility c

increases with increasing pressure, and therefore, gas will be solved faster near to small than large bubbles. This induces a gas concentration gradient between the surfaces of the smaller and larger bubbles. This relationship can be described by Henry's law, where K_H is the Henry coefficients, which corresponds to the nature of the gas and liquid phase (Equation 2.2.3).

$$c = \frac{p_d}{K_H} \quad (2.2.3)$$

Thereby, smaller bubbles shrink through gas diffusion from small to large bubbles until they are eventually totally dissolved, whereas bigger bubbles grow (Cantat et al. 2013; Damodaran 2005; Wilson 1989). In this context, Lucassen (1981) found that the bubble shrinkage is connected to the interfacial dilatational properties and proposed that disproportionation would not occur for purely elastic surfaces and higher surface elasticity E' above the Gibbs stability criterion according to Equation 2.2.4.

$$E' \geq \frac{\sigma}{2} \quad (2.2.4)$$

However, protein and surfactant stabilized surfaces are viscoelastic, and therefore, disproportionation cannot be totally prevented. Another possibility to prevent coarsening would be an ideal monodisperse polyhedral foam. However, for food- and pharmaceutical applications, this seems neither practical nor achievable.

Foam drainage

The passage of liquid through the foam is commonly called drainage. It can be divided into two distinct mechanisms: Hydrodynamic drainage, which happens due to gravity in wet foams, and film drainage, which considers the pressure difference within foam structures in dry foams (Fig. 2.2.3) (Cantat et al. 2013).

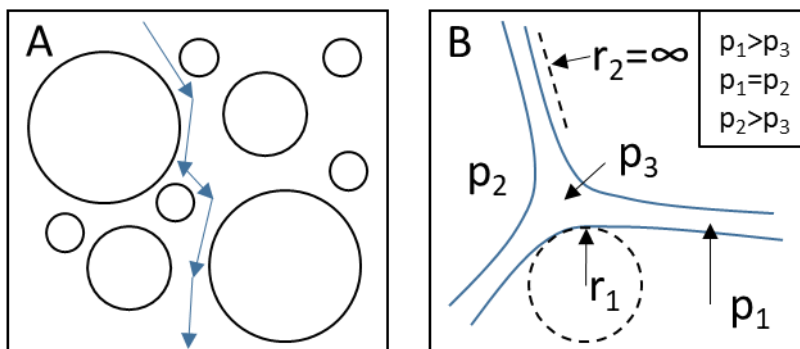


Fig. 2.2.3: (A) Gravimetric drainage inside a foam with spherical bubbles and (B) for liquid drainage responsible pressure conditions within lamellae, modified according to Walstra (1989) where r_1 and r_2 represent the radii of curvature, p_1 , p_2 , and p_3 the pressures within the liquid film, the bubble, and the plateau border, respectively.

Usually, both drainage mechanisms are present, while at first gravitational drainage occurs instantaneously after foam formation and as long as the bubbles are spherical. As drainage progresses, the liquid volume fraction (see chapter 2.2.1) decreases, and bubbles are deforming and consequently getting more and more polyhedral. Thereby, the drainage mechanism changes towards film drainage, and the capillary pressure becomes relevant. Generally, drainage occurs until the hydrostatic pressure is not in equilibrium with the capillary pressure. However, the foam might be completely collapsed even before getting into a polyhedral bubble shape.

The film drainage can be expressed by an imbalance between the Laplace pressure and the pressure induced by gravitation. While the gravitational pressure is independent of the bubble size and foam structure, the Laplace pressure is dependent on liquid film thickness (see chapter 2.2.1) and the bubble size. Because the pressure inside the liquid film is bigger than in the plateau border, the liquid flows into the plateau border (Walstra 1989). As a result of antagonistic and promoting effects, the drainage becomes very complex. A simple model determining the rate of film drainage and film thinning is the Reynolds velocity (v_{Re}), which can be expressed by the thickness of lamella (h), the pressure difference between capillary pressure (p_c), the disjoining pressure (Π), the dynamic viscosity (η_{dyn}) of the bulk phase, and the radius of a circular horizontal film (R_{hor}) (Equation 2.2.5) (Cantat et al. 2013):

$$v_{Re} = 2h^3 \frac{(p_c - \Pi)}{3\eta_{dyn}R_{hor}^2} \quad (2.2.5)$$

However, as the Reynolds viscosity assumes that interfaces are parallel, flat, and horizontal, this expression can be only used as an approximation to real systems and only valid for high interfacial mobility and the coupling of liquid flow at the surface and within the liquid film (Cantat et al. 2013). Nonetheless, Equation 2.2.5 is helpful to understand that because p_c is always bigger than the disjoining pressure, film drainage is generally not preventable. However, it could be slowed down by increasing the disjoining pressure or the solution's viscosity (Damodaran 2005).

Coalescence

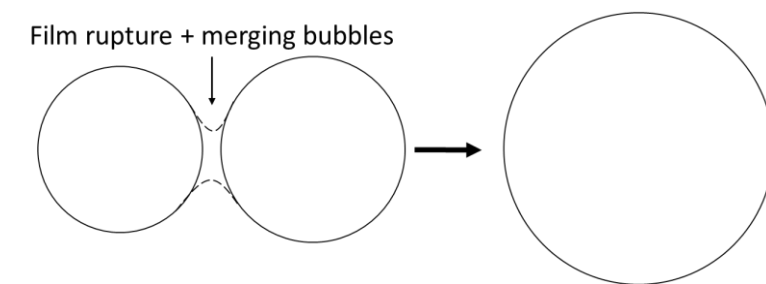


Fig. 2.2.4: Schematically mechanism of coalescence.

The merging of bubbles inside a foam is commonly called coalescence (Fig. 2.2.4). Thereby, the surface film between two bubbles breaks, and two bubbles are connecting into one bigger bubble, and consequently, the number of bubbles decreases (Hupperts 2010). For coalescence, the stability of liquid films between two bubbles is of particular interest, as it needs to break the liquid film in order to merge two bubbles. Therefore, the interface's chemical composition and viscoelasticity have a strong influence on the rate of coalescence (Cantat et al. 2013; Walstra 1989). Further, the distance between two bubbles plays an important role, which will be promoted by, e.g., drainage. Thereby, film thinning occurs first, followed by film rupture, which results in bubble fusion (Damodaran 2005). This will be spontaneously and for film thicknesses of a few times 10 nm (Walstra 1989). A way to slow down coalescence is to slow down the drainage, e.g., by increasing the viscosity of the bulk phase.

2.2.3 Foaming agents, foam thickener, and biological marker

In this work, several combinations of foaming agents and thickening agents were used. As already mentioned in chapter 2.1. the drying performance, as well as the activity of sensitive molecules, can be improved by the addition of different sugar types or surface-active substances. Besides, these ingredients may directly or indirectly influence the foam properties due to interactions between foaming agents and thickening agents and the increase of the solution's viscosity.

A brief description of each used substance will be given here, as the specific interactions between foaming agents and thickeners will be presented in the results and discussion.

Foaming agents

Foaming agents can be divided into two main groups, the non-ionic and the ionic foaming agents. Besides, they can be distinguished by organic foaming agents like proteins and synthetic ones like surfactants. In the following paragraphs, the foaming agents, which were used in this study, are introduced.

Whey protein isolate and β -lactoglobulin: The main components of whey protein isolate (WPI) are β -lactoglobulin, α -lactalbumin, and bovine serum albumin (BSA). Further, some minor fractions like immunoglobulins are present (Töpel 2016). Whey proteins are globular proteins and, in comparison to the used sensitive biological indicators, heat stable. As whey protein isolate is often used in industry, it is frequently used for foam formation and well-studied.

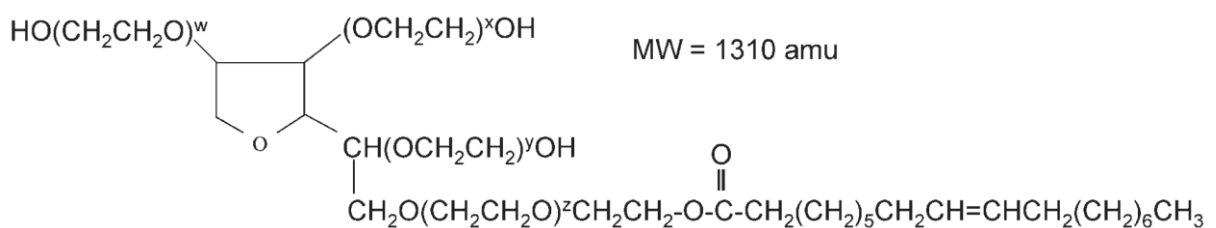
The biggest fraction of whey protein isolate is β -lactoglobulin (β -lg), with about 50% of whey protein and 3.2 g kg^{-1} in milk (Walstra 1999). Its molecular weight is 18.4 kDa, and several genetic variants are known, of which variants A and B are the most often (Sawyer et al. 1999). Further, β -lg is stabilized by hydrophobic and electrostatic interactions, H-bonds, and two in-

tramolecular disulfide bridges, which in sum results in comparable high heat stability (Denaturation temperature T_D above 70 °C) (Loveday 2016). A free cysteine group is buried inside the tertiary structure of β -lg and, therefore, not accessible in the native protein state for potential crosslinking between proteins.

The second considerable fraction of whey proteins is α -lactalbumin (α -la). In milk, the concentration is about 1.2 g kg⁻¹ (Walstra 1999). Its molecular size is 14,2 kDa and slightly smaller than β -lg, and two predominant genetic versions are known (McKenzie 1971). The globular structure of α -la is stabilized by four disulfide bridges. However, α -la has no free thiol group, and therefore, structural changes are reported to be reversible (Permyakov et al. 1985).

However, it is worth noting that the foaming properties are strongly dependent on environmental conditions like pH, ionic strength, and temperature (Permyakov et al. 1985; McKenzie 1970). Therefore, in this work, the environmental conditions for samples and foaming were kept equal, and whey protein isolate was purchased from one single supplier with a high degree of protein nativity.

Polysorbate 80: Polyoxyethylene sorbitan monooleate, Polysorbate 80, or Tween 80[®] is a synthetic and non-ionic surfactant. It is assembled of 20 ethylene oxide units, one sorbitol, and one oleic acid (Fig. 2.2.5), which results in a molecular weight of 1.31 kDa and critical micelle concentration (CMC) of 12 – 14 mg·l⁻¹ (Kerwin 2008; Merck & Co. 1989; Wan and Lee 1974). Its comparatively high monomer solubility results in a fast rate of adsorption to the interface, combined with a good ability to lower the surface tension, results in the formation of multiple small bubbles or good emulsification properties (Bezalgues et al. 2008). Therefore, polysorbates are widely used as surfactant and solubilization enhancing agents in the food, cosmetic, and pharmaceutical industries (Chou et al. 2005; Coors et al. 2005).



Polysorbate 80 (Tween 80): polyoxyethylene sorbitan monooleate

Fig. 2.2.5: Chemical structure of polysorbate 80, $w+x+y+z$ represents the total number of oxyethylene subunits on each surfactant molecule and may not exceed 20 (Kerwin 2008).

Poloxamer: Poloxamers are non-ionic block-copolymers with a lipophilic polypropylene oxide chain (PPO) in the center and two hydrophilic polyethylene oxide chains (PEO) in the flanks (Fig. 2.2.6). By changing the ratio between PEO and PPO, the hydrophilia–lipophilia balance (HLB) can be changed, which provides the opportunity to widely use poloxamers as solving

agents (Chaudhari and Dugar 2017; Santander-Ortega et al. 2006). For example, the poloxamer Pluronic F68 consists of 68 PEO units and 30 PPO units, resulting in a molecular weight of 8.5 kDa (Santander-Ortega et al. 2006).

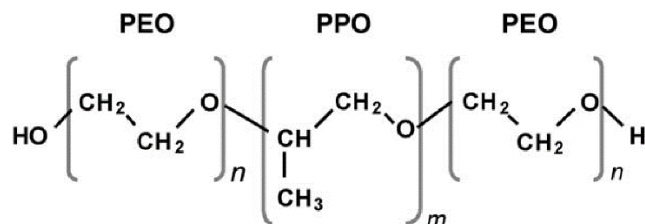


Fig. 2.2.6: Typical chemical structure of a poloxamer, where the central PPO represents the hydrophobic polypropylene oxide chain, while PEO represents identical hydrophilic polyethylene oxide chains at both sides.

Saccharides

Saccharides are often added to food or pharmaceutical formulations as a protective or thickening agent. Further, they influence the physical properties of the dried product, as already mentioned in chapter 2.1, or influence the morphology of foams (chapter 2.2.1 and 2.2.2). Therefore, the saccharides used in this study are briefly introduced in the following sections.

Sorbitol: Sorbitol is a six-carbon sugar alcohol with a molar mass of $182.2 \text{ g}\cdot\text{mol}^{-1}$ (Fig. 2.2.7). Besides the natural appearance in plants and fruits (Reif 1934), sorbitol can be synthesized at high heat from other saccharides or bacterial fermentation (Ortiz et al. 2013). Sorbitol has a low glycemic index, a reduced caloric value, and a sweetness of about 60% compared to sucrose (Dash et al. 2019; Grembecka 2018). Further, sorbitol is highly water soluble ($2350 \text{ g}\cdot\text{l}^{-1}$) and highly hygroscopic (Grembecka 2018). In addition, sorbitol has a cooling effect when solved in water and is free from any possible carcinogenic effects (Dash et al. 2019; Basedow et al. 2008). Sorbitol is used in the food and pharmaceutical industry as a sweetener and anti-crystallization agent (Mortensen 2016). Further, sorbitol is in contrast to sucrose, not cariogenic, and therefore used in, e.g., toothpaste (Nabors 2001). Furthermore, it is widely used as stabilizing excipient in liquid or freeze-dried parenteral protein formulations (Bakaltcheva et al. 2007).

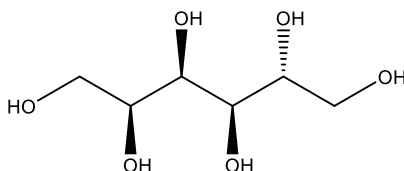


Fig. 2.2.7: Chemical structure of D-sorbitol.

Sucrose: Sucrose is the most commonly known disaccharide, which is widely occurring in nature. It is composed of the two monosaccharides glucose and fructose, which are connected

by a glycosidic (1→2) linkage (Fig. 2.2.8). Since it does not contain anomeric hydroxyl groups, sucrose is a non-reducing saccharide. It has a molar mass of 342 g·mol⁻¹ and is soluble at room temperature up to 2039 g·l⁻¹ (Browne 1912).

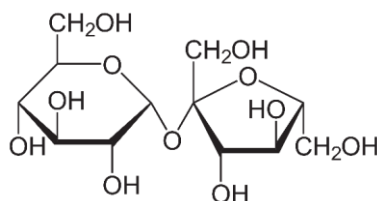


Fig. 2.2.8: Chemical structure of sucrose.

Besides the commonly known use of sucrose in the food industry as a sweetener and thickening agent, sucrose is widely used in pharmaceutical formulations as an excipient (Yang and Foegeding 2010; Lee and Timasheff 1981).

Maltose: Maltose is a disaccharide, consisting of two glucose molecules, linked with an α 1→4 glycosidic bond (Fig. 2.2.9). The molar mass weight of maltose is, like for sucrose, 342 g·mol⁻¹. However, the solubility of maltose in water is 1080 g·l⁻¹ and, therefore, much lower compared to that of sucrose (Lide et al. 2019). The sweetness of maltose is about 90% compared to sucrose (BeMiller 2019).

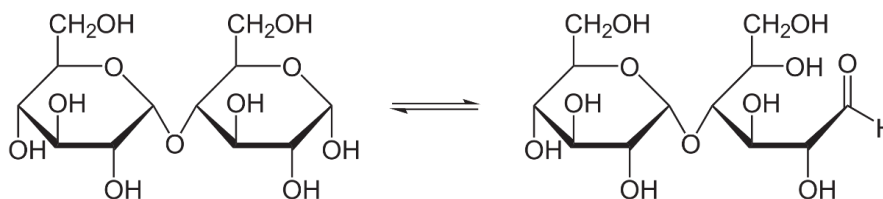


Fig. 2.2.9: Chemical structure of maltose in cyclic (left) and open (right) conformation.

Since only one anomeric carbon is involved in the ether bond, maltose can partly convert to an open-chain form, whereby it is commonly classified as a reducing sugar (Klein 2012).

Maltodextrin: Maltodextrin describes polysaccharides resulting from acid hydrolysis or enzymatic digestion of starch and thus contain amylose and branched amylopectin as degradation products. Thus, maltodextrins are considered as D-glucose polymers in which the individual units are linked by α 1→4 glycosidic bonds (Fig. 2.2.10). In order to characterize polysaccharides produced from starches, the dextrose equivalent (DE) is used. The DE value represents the total reducing power of all sugars present relative to glucose as 100 and can be expressed on a dry mass basis (Chronakis 1998a). Hence, highly degraded starch has high DE values, while high molecular products have comparable low DE. Maltodextrins are defined as hydrolyzed starch with a DE lower than 20, while products with higher DE values are defined as dextrans (Dokic-Baucal et al. 2004). Besides the DE, the origin of starch impacts the functionality of maltodextrin since the ratio between amylose and branched amylopectin is dependent

on the starch source. This makes it difficult to compare or substitute maltodextrin with the same DE value, but from different plants (Chronakis 1998a).

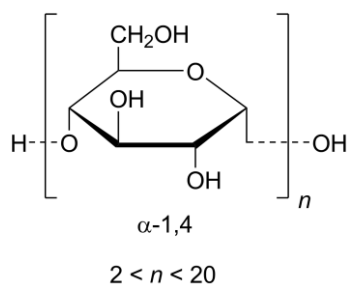


Fig. 2.2.10: Chemical structure of maltodextrin, with n the number of glucose units.

Maltodextrin with high DE is sweet and well soluble in water. In contrast, maltodextrin with low DE has nearly no sweetening function but has high water capability and can work well as a thickening agent. Therefore, they have been used as a constituent for fat in calorie-reduced food (Chronakis 1998a). Further, maltodextrins have several functions and functional properties like bulking, gelling, thickening, the promotion of dispersibility, freezing control, crystallization prevention, the binding of flavor, pigments, and fat (Blanchard and Katz 2006). Further, the properties of product structures like foams or emulsions can be effectively influenced by the addition of maltodextrins (Pycia et al. 2016; Dokic-Baucal et al. 2004).

β -galactosidase as a model for sensitive biomolecule

The enzyme β -galactosidase (β -Gal), commonly known as lactase, cleaves the disaccharide by hydrolysis of lactose into galactose and glucose (Saqib et al. 2017). Further, β -galactosidase can convert lactose into allolactose and other di- and polysaccharides and can therefore be used for the production of galactooligosaccharides (Fig. 2.2.11) (Juers et al. 2001; Tanaka et al. 1975). The yield of galactooligosaccharides varies between 1 and 45% and depends on the source of the enzyme and the total amount and type of saccharides (Juers et al. 2001; Boon et al. 2000). Besides, β -Gal can be used for the treatment of whey in order to make it suitable for the production of bioprocess intermediates (Domingues et al. 2005) or substrate for cell cultivation (Parashar et al. 2016). Further, β -Gal can be utilized to improve the production of ethanol or sweet syrup (Saqib et al. 2017). Furthermore, β -Gal is widely used to decrease the amount of lactose in food or pharmaceutical products to make it more suitable for lactose-sensitive or intolerant consumers (Rao and Dutta 1978). In addition, β -Gal is used in medicines, which can be consumed before eating milk products (Francesconi et al. 2016). For this, fungal-derived β -Gal is often used because it is more stable at low pH and can therefore allow the proper functioning in the stomach (Francesconi et al. 2016; Panesar et al. 2007).

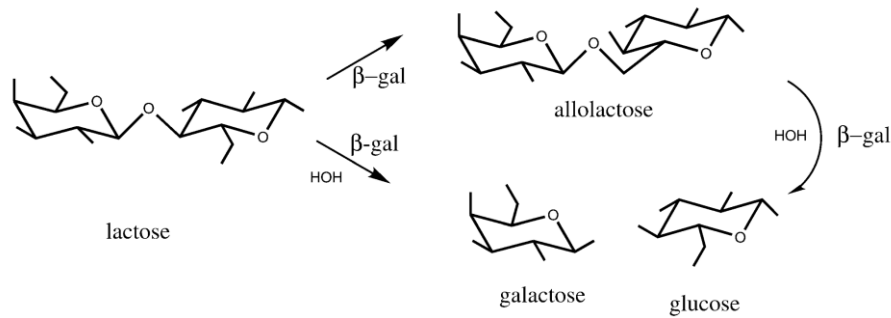


Fig. 2.2.11: General scheme for the action of β -galactosidase on lactose with hydrolysis (lower path) or transglycosylation (upper path) according to Juers et al. (2001).

Structurally, β -Gal is a tetramer with a molecular weight of 464.9 kDa, consisting of four identical polypeptide chains with a molecular weight of 116.2 kDa (Fowler and Zabin 1977). Each chain has five domains (Fig. 2.2.12), where the central domain is catalytically active (Saqib et al. 2017). β -Gal is produced in industrial amounts with bacteria or fungi. *Bifidobacterium sp.*, *Escherichia sp.*, *Aspergillus sp.* and *Kluyveromyces sp.* are most commonly used to produce β -Gal (Saqib et al. 2017; Zhou and Chen 2001). Although the physical properties of subunits depend strongly on the origin, the active side of β -Gal always remains the same (Zhou and Chen 2001). However, the enzyme activity has, in general, for *Aspergillus*-derived β -Gal a pH optimum between 2.5–5.4, whereas it is for yeast-derived β -Gal between 6.0–7.0, respectively (Panesar et al. 2007; Zhou and Chen 2001; Borglum and Sternberg 1972).

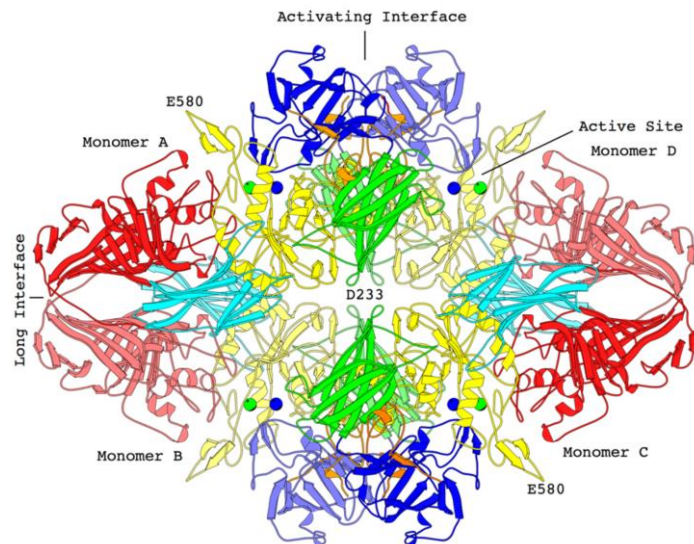


Fig. 2.2.12: Tetrameric backbone structure of β -galactosidase consisting of domain 1 (blue), domain 2 (green), domain 3 (yellow), domain 4 (cyan), and domain 5 (red). Lighter and darker shading is used to differentiate equivalent domains in different subunits. Metal ions are shown as spheres, Na^+ , green; Mg^{++} (Juers et al. 2012).

The denaturation temperature of β -Gal varies from 39 °C to 63 °C dependent on the source and can be further improved by the modification of disulfide bonds, the addition of salts, or the pH-value (Klein et al. 2018; Rico-Díaz et al. 2017; Kishore et al. 2012; Edwards et al. 1990). Due to the low denaturation temperatures, β -Gal seems suitable for the investigation of thermal stress during the development of processes, e.g., in the pharmaceutical industry, and is therefore also used in this study as a model to study the processing effects on losses of activity.

2.3 Microwave-supported vacuum- and freeze drying

2.3.1 General introduction to microwaves

Microwaves are defined as electromagnetic waves within the frequency f of 300 MHz and 300 GHz, corresponding to a wavelength λ from 1 mm to 1 m according to Equation 2.3.1, where c is the speed of light in a vacuum (Regier et al. 2016).

$$\lambda = \frac{c}{f} \quad (2.3.1)$$

In order to prevent disturbance of wireless communication, like mobile phones, radar, or television, microwave heating applications are only allowed within released frequency bands authorized by the International Telecommunication Unions (ITU). Those frequency bands are between 13 MHz and 22125 MHz and for industrial, scientific, and medical (ISM) use. For microwaves, the frequencies are within the ISM at 433, 915, 2450, and 5800 MHz (Regier et al. 2016). Therefore, most microwave ovens are working at 2450 ± 50 MHz (worldwide available) or 915 ± 13 MHz (only available in the United Kingdom or the United States of America) (Mullin 1995). However, the responsibility of frequency bands is governed by local administrations like the Federal Communication Commission (FCC) in the United States of America or the European Telecommunications Standards Institute (ETSI) in Europe.

As microwaves are electromagnetic waves, they are coupled electric and magnetic waves, whose correlation between electric (E) and magnetic (H) field can be described by the Maxwell's equations. Microwaves can be reflected, transmitted, or adsorbed by matter. Conductors like metals almost completely reflect microwaves, whereas insulators like glass, ceramics, some plastics, or papers transmit microwaves. Polar and ionic materials, like many food systems, are absorbing microwaves, whereby the amplitude of microwaves decreases by passing the dielectric (Fig. 2.3.1). (Mullin 1995)

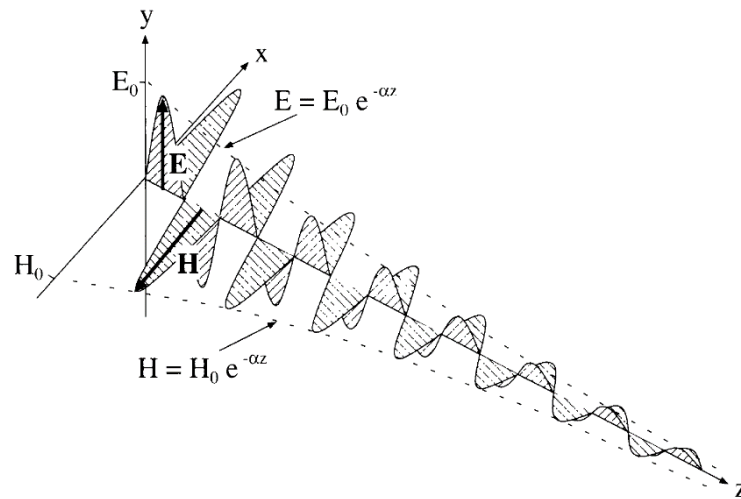


Fig. 2.3.1: Travelling wave in a lossy dielectric medium (Dibben 2001).

2.3.2 Heating of products with microwave energy

The heating of products due to electromagnetic waves can be explained by two basic molecular mechanisms, dipole rotation and ionic polarization, where the first one contributed to mobile dipoles and the second one to mobile ions (Fig. 2.3.2).

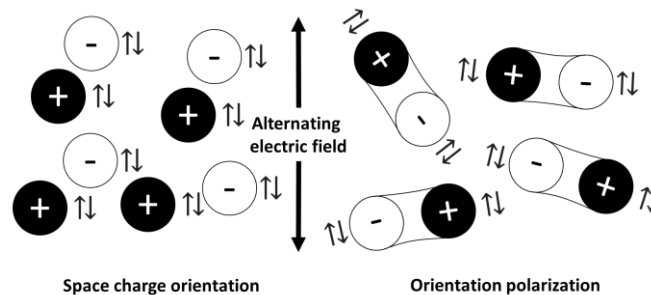


Fig. 2.3.2: Ionic and polar orientation in an alternating electronic field according to Mullin (1995).

However, in both cases, the molecules only interact with the electric field and not with the magnetic field (Yam and Lai 2004). Wang et al. (2003) described that the influence of ionic conduction increases with increasing temperature, while the influence of dipole rotation decreases (Fig. 2.3.3).

In ionic conduction, charged molecules, like dissociated salts, get accelerated in the opposite direction to their polarity by the electric field. As the electric field is not static, the movement occurs for microwaves many million times per second, and the molecules start vibrating (Mullin 1995). The same will appear for polar substances or dipoles like water, and due to collision with other molecules, the energy will be converted into frictional heat (Ratti 2008).

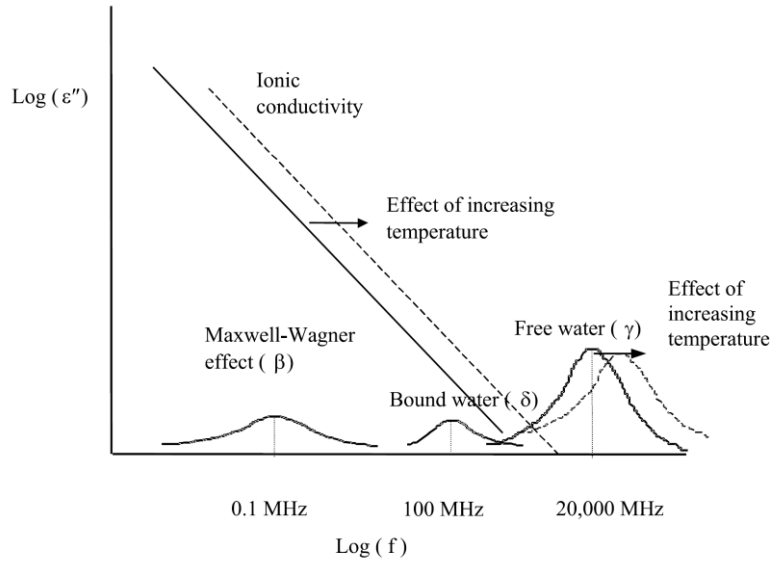


Fig. 2.3.3: Influence of temperature and frequency on the dielectric loss of high moisture samples (Tang et al. 2002).

Despite the heating of products, microwaves belong to non-ionizing radiation and cannot break up chemical bonds as they contain too little energy (Durance and Yaghmaee 2011). However, as valid for all heating processes, massive overheating and especially burning of the product might cause the occurrence of harmful ingredients. Therefore, it is of special interest to prevent overheating and burnings inside products.

The heating of products can be described by the dielectric properties. The complex dielectric constant ϵ^* or permittivity can be described by its real part, termed as dielectric constant ϵ' and the imaginary part, termed as the dielectric loss ϵ'' (Equation 2.3.2), where j is an imaginary proportion ($\sqrt{-1}$). The real part signifies the ability to store electric energy, while the imaginary part signifies the ability to convert electric energy into heat. (Chandrasekaran et al. 2013; Sosa-Morales et al. 2010)

$$\epsilon^* = \epsilon' - j\epsilon'' \quad (2.3.2)$$

Mechanisms, which can contribute to the loss factor are dipole, ionic, electronic, and Maxwell-Wagner mechanisms (Metaxas and Meredith 1988). However, for radio and microwave frequency, the predominant mechanisms are dipole rotation and ionic conduction, and the loss factor can be expressed as Equation 2.3.3 (Tang et al. 2002),

$$\epsilon'' = \epsilon_d'' + \epsilon_\sigma'' = \epsilon_d'' + \frac{\sigma}{\epsilon_0\omega}, \quad (2.3.3)$$

where ω contributes to the angular frequency, ϵ_d'' to the dielectric loss dependent on dipole rotation and ϵ_σ'' to the ionic conduction, respectively. ϵ_0 corresponds to the permittivity of free space or vacuum ($8.854 \cdot 10^{-12} \text{ F} \cdot \text{m}^{-1}$).

The dissipation factor or dielectric loss tangent, $\tan(\delta)$, describes the ability of a material to convert electromagnetic energy into thermal heat at a given temperature and frequency and can be expressed by the relation of dielectric loss factor and dielectric constant, Equation 2.3.4 (Bart 2005):

$$\tan(\delta) = \frac{\epsilon''}{\epsilon'} \quad (2.3.4)$$

The energy converted into heat inside the product related to the volume, or the volumetric absorption of microwave energy, P , can be described as Equation 2.3.5 and is dependent on the electrical field strength E and the frequency f .

$$P = 2\pi E^2 f \epsilon_0 \epsilon'' \quad (2.3.5)$$

The penetration depth PD is defined by the distance at which the power density remains $1/e$ (Euler's number $e=2.718$) from its value at the surface. D_P can be expressed (Equation 2.3.6) as a relationship between the wavelength λ and the dielectric properties (ϵ' and ϵ'') (Schiffmann 2016; Metaxas and Meredith 1988)

$$PD = \frac{\lambda \sqrt{\epsilon'}}{2\pi \epsilon''} \quad (2.3.6)$$

Therefore, the penetration depth is about 2.7 times deeper for 915 MHz than for 2450 MHz. Due to a more uniform heating and a deeper penetration, 915 MHz is often preferred in industrial applications (Scaman et al. 2015).

However, the dielectric properties are related to several factors, like microwave frequency, temperature, water content, salt content, density, or the phase state of the sample, such as gaseous, liquid, or solid (Durance and Yaghmaee 2011; Sosa-Morales et al. 2010; Yaghmaee and Durance 2002; Kaatze 1997).

The influence of water content on the dielectric properties of white bread was investigated by Liu et al. (Liu et al. 2009) using different temperatures and frequencies. It was shown that the dielectric constant and loss factor increased with increasing water content and temperature. Further, it was shown that the higher the frequency, the lower the impact of water content and temperature on the dielectric properties.

An overview of the different dielectric properties of food systems at different microwave frequencies can be found in a work by Sosa-Molares et al. (2010).

2.3.3 Microwave-assisted drying processes

Due to the combination of microwave and foam drying, it is possible to overcome one of the biggest disadvantages of foam drying: the low heat conduction through the product. As the heating of microwaves is volumetric, the heat will be applied throughout the product, and as a

result, the drying speed is accelerated immensely. Further, this combination suits well for drying, where vacuum is applied, like vacuum foam drying or freeze drying. Therefore, the following paragraphs will be about microwave-assisted vacuum drying (MWVD) and microwave-assisted freeze drying (MWFD).

During the drying process, the heating of water is of great importance. As already discussed in the previous chapter, the heating properties of products will change throughout the process due to the high dependency of dielectric properties on temperature, water content, and physical state of the polar substances. Further, the temperature measurement is challenging, as no metallic sensor can be used inside the product due to the microwave application. Therefore, pyrometer or thermographic cameras are often used for process control. However, they are limited to local temperature measurement or surface temperature measurement. Therefore, independent of vacuum or freeze drying, further investigations on microwave field distribution, changes of dielectric properties of the product during the process, and development of easy-to-apply models are necessary to get microwave-assisted drying technology ready for industrial application (Fan et al. 2019).

Microwave-assisted vacuum drying

The microwave-assisted vacuum drying provides a fast and gentle process for sensitive and oxygen-sensitive products, like probiotics, enzymes, or fruits. Functional food components like phenols, antioxidants anthocyanins can be preserved in equal or even better compared to conventional vacuum drying or even freeze drying (Wojdyło et al. 2014). This has also been found for the sensory attributes in the case of banana or carrot slices, which was attributed to the fast, efficient heating and the lack of oxygen during the vacuum drying process (Drouzas et al. 1999; Lin et al. 1998). The drying speed can be shortened by about 50–90% of the necessary drying time in conventional drying methods (Mayer-Miebach et al. 2005; Drouzas and Schubert 1996). In general, the drying speed could be improved by reducing the pressure in the product chamber and higher applied microwave power values (Song et al. 2009; Hu et al. 2006; Mayer-Miebach et al. 2005). However, with higher applied microwave power, the chance for plasma formation or arcing increases, which results in overheating of the product and off-flavor (Hu et al. 2006). A typical plasma during microwave-assisted vacuum drying is shown in Fig. 2.3.4.

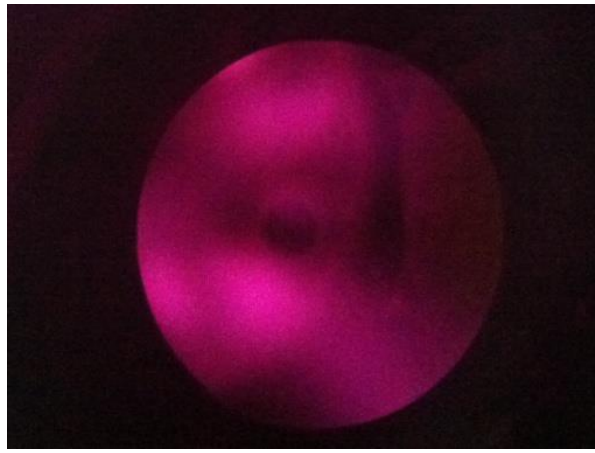


Fig. 2.3.4: Plasma formation during microwave-assisted vacuum drying.

Besides the microwave-assisted vacuum drying of fruits, the microwave-assisted drying of foams was focused the last few years (Qadri and Srivastava 2017; Zhang et al. 2015; Zheng et al. 2011), only a few studies about microwave-assisted foam vacuum drying are known (Ambros et al. 2019a, 2019b). Compared to microwave-assisted vacuum drying of liquids, the MWVD of foams provides advantages of foam structure (chapter 2.1.2) and even a decrease in required process time (Ambros et al. 2019b). As already discussed, it is necessary to preserve the foamy structure during the drying process to obtain a good product quality. Because of the harsher drying conditions in microwave-assisted vacuum drying (higher drying rate and more frequent pressure regulation), foams often collapse during the drying process. However, the overall stability of foams during microwave-assisted vacuum drying and the key properties responsible for the foam decay during MWVD are not investigated yet, which represents a crucial lack of knowledge.

Microwave-assisted freeze drying

Microwave-assisted freeze drying is a suitable way to reduce the necessary drying time, while the product quality remains equal to that of conventional freeze drying (Duan et al. 2012; Wang et al. 2009; Duan et al. 2007). This can be attributed to the volumetric heating of the product, which is much faster compared to the heat transduction through the frozen product (Duan et al. 2010a; Zhang et al. 2006). However, as already discussed in chapter 2.1, drying processes are always a combination of mass and heat transfer. Since the mass transfer rate of a frozen liquid is low, products can be foamed up before the freezing step. Thereby, the advantages of foam can also be used in MWFD.

The heating of frozen products with microwaves might be challenging because the dielectric properties of ice are low. However, if the product is melting at a single spot, thermal runaway might occur, as liquids have much higher dielectric loss factors, as already mentioned before. Thereby, thermal damage and the loss of the original product structure might occur (Jiang et

al. 2010; Wang et al. 2009). In general, the heating of food or pharmaceutical products is easier than pure ice because they usually contain saccharides, which have a higher loss factor than water in a frozen state (Chandrasekaran et al. 2013).

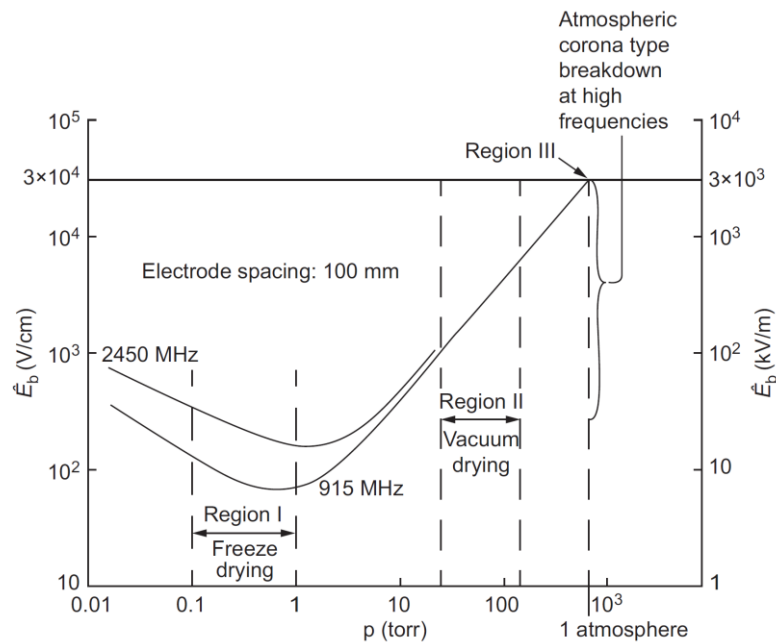


Fig. 2.3.5: Electric field strength versus pressure profile showing critical values leading to arcs and plasma formation during different microwave-assisted drying methods (Metaxas and Meredith 1988).

As the microwaves enter the product cavity at so-called ports, the microwave power density is very high within a small area next to the port. Thereby, cold plasma can be formed, which is unsuitable for the product quality, as it causes off-taste and burning of the product (Wang et al. 2009; Metaxas and Meredith 1988). The plasma formation occurs with high probability within a range of pressure and above a specific field strength (Fig. 2.3.5). Therefore, it can be controlled by, e.g., cycling the pressure (Chandrasekaran et al. 2013). Another way to prevent plasma formation is to lower microwave power input in the secondary drying or when the moisture content is low (Duan et al. 2010b). However, together with difficulties in temperature measurement, microwave-assisted freeze drying is a complex control problem, and it is necessary to investigate particular phenomena such as hotspots, thermal runaway, and plasma discharge to get from lab-scale into pilot or production scale (Fan et al. 2019; Zhang et al. 2006)

About microwave-assisted freeze drying of foams, only a few publications are known. However, it was shown that due to the foamy structure, benefits in drying speed, flavor preservation, or viability of microorganisms are achievable (Ozcelik et al. 2019a; Ozcelik et al. 2019b; Ambros et al. 2018). Therefore, microwave-assisted freeze drying of foams seems a good way to overcome problems like slow mass transfer or too high power density inside the products. However, it is still an open question how frozen foams influence the drying kinetic and which foam properties fit best in microwave-assisted foam freeze drying.

3 Objective and outline

As already stated in the previous chapter, the drying process increasingly represents the bottleneck of production of sensitive, biological products as the demand for vaccines and protein-based pharmaceutical products increases due to the growing world population and its average age. As a result, products like vaccines or drugs have to be distributed in liquid or frozen state, which needs high investments in cooling devices and quality control mechanisms. Further, a well-working infrastructure is necessary for the worldwide distribution and safe application, which is challenging the handling of worldwide occurring diseases. In addition, new products or products adapted to new situations are needed within even shorter development times, as can be well observed with the current pandemic of Covid-19 or the annual influenza protection vaccination. In view of the global situation, it is therefore essential to improve the downstream and drying processes in order to be able to distribute life-essential products equally and safely to the world.

However, the preparation of the products is crucial for the success of the subsequent drying. To stabilize sensitive biomolecules against the freezing, surface, or thermal stress, excipients such as saccharides or surfactants are added to the formulation. Further, salts are added to buffer the liquid solution at a certain pH value. Besides the stabilization of the biomolecules, these excipients directly influence the morphology of the product, the structural stability of the product, or the drying performance. In the case of foam drying, the excipients may also affect the foam properties or the interaction between surface-active components and biomolecules. Hence, the formulation of products is quite complex when all these potential crosslinks are mentioned. Furthermore, by introducing microwave technology to the drying process, the dielectric properties of the formulation or single components may have an influence on the drying success and the drug stability. Interestingly, most of the available studies investigate the influence of sugars and salts on, e.g., the foaming properties of proteins or the thermal stability of sensitive substances, but not the interactions of commonly used small non-surfactants and their influence on the foam properties. In addition, interactions between foaming agents and used excipients are rarely related to the foam drying process. Further, formulations in the food industry are often very complex, so that the specific investigation of the influence of different saccharides on foam stability during drying is still missing. In addition, the impact of various excipients on the stability of foams during microwave-assisted drying processes has not been investigated, so far, which represents a knowledge gap.

Therefore, this thesis aimed to systematically and comprehensively investigate the impact of different excipients on foam properties, drying success, and suitability for the preservation of sensitive biomolecules. To this end, the influence of sugars on the properties of surfactant-

stabilized foams was investigated. Based on previous findings, it was hypothesized that different sugars have different abilities to interact with nonionic foaming agents as well, due to their varying ability to form H-bridges. This, in addition to the influence of viscosity, would lead to different foam properties. The information obtained was used for the investigation of water vapor transport during freeze drying and microwave-assisted freeze drying. For this, different concentrations of maltodextrin were added to a polysorbate-stabilized foam, and the freeze drying process was initially investigated using a freeze drying microscope. After that, the results from freeze drying microscopy were correlated with the drying kinetics and drying behavior of samples processed with microwave-assisted freeze drying. The hypothesis was that the water vapor pathway changes due to different foam structures, which result in higher or lower water transfer resistance within the product. Moreover, the influence of interactions between sugar and foaming agent and their dielectric properties on foam stability during conventional and microwave-assisted vacuum drying was investigated. It was assumed that the stability of foams during drying can be related to the different dielectric, bulk and foam properties of the samples. Therefore, the dielectric constant, the loss factor, and the resonant frequency were determined. Furthermore, the surface tension and dilatational rheology were measured and correlated with the foam stability during the drying process.

In the next step, the results from freeze drying and vacuum drying were used to find suitable foam matrices for drying of sensitive biomolecules. For this purpose, the model enzyme β -galactosidase was used and added to samples with different saccharide types and concentrations, resulting in different foam matrices. The residual activity of the enzyme was studied and correlated with the previously obtained results. Then, different process parameters such as microwave power input and surface temperature were varied in order to find suitable process conditions. Finally, scale-up experiments on microwave-assisted freeze drying were performed. The hypothesis was that the drying rate can be increased by increasing the surface area and minimizing the effective height of the product. Consequently, more product can be processed within a batch while maintaining the same product quality. For this, foamed samples were dripped into liquid nitrogen and compared to the drying behavior of product cakes at different microwave-power input – sample height combinations. Thereby, product as well as plant dependent limitations of the drying process should be observable.

4 Results

The following chapters are combined with published and unpublished results. The chapters 4.2, 4.7, 4.8, and 4.9 are so far unpublished, whereas chapters 4.1, 4.3, 4.4, 4.5, and 4.6 are based on publications in peer-reviewed journals.

4.1 Interactions of sugar alcohol, di-saccharides and polysaccharides with polysorbate 80 as surfactant in the stabilization of foams

Summary and contribution of the doctoral candidate

Saccharides are highly used in the food and pharmaceutical industry to sweeten or thicken a product, as well as excipient during drying processes. Further, they are used for the stabilization of foams as a result of increased viscosity. However, saccharides are known to form H-bonds, which may also impact the surfactant interactions at the air-water interface of foams. Nevertheless, no study investigated the impact of different types of saccharides like sugar-alcohols, di-saccharides, and polysaccharides on the foaming properties of surfactants. Therefore, this study aimed to examine the impact of saccharides on non-ionic surfactants at the air-water interface and to determine the impact on the macroscopic foam properties like drainage, overrun, the bubble size distribution of firmness.

This study hypothesized that the interactions of surfactants at the air-water interface are influenced by different strengths due to chemical and structural differences between the saccharides. This means that the foam properties are changing depending on the used saccharide and not only by the increase in bulks viscosity.

It was shown that the used saccharide has a massive influence on the foam properties depending on the type of sugar. Foam stability was most improved by the addition of maltodextrin, while sorbitol stabilized the bubble size the best. Further, the results allow choosing the correct formulation with a different amount of added sugar with regard to the same overrun. Thereby, it is possible to compare different formulations with equal product density, which is important for foam-mat drying.

The substantial contribution of the doctoral candidate was the conception and design of the experiments. Further, he was substantially involved in the performance of experiments, acquired parts of the data for the manuscript, and interpreted the data set. Furthermore, the critical literature review and writing of the manuscript were done by the candidate. Co-authors contributed to the discussion of the results and provided input to the drafted manuscript before and during submission.

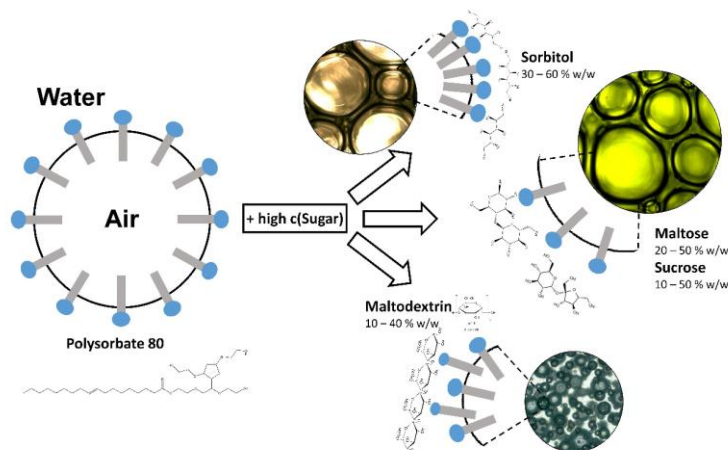
Interactions of sugar alcohol, di-saccharides and polysaccharides with polysorbate 80 as surfactant in the stabilization of foams¹

Peter Kubbutat * and Ulrich Kulozik

Chair of Food and Bioprocess Engineering, TUM School of Life Sciences, Technical University of Munich, 85354 Freising, Germany

* Correspondence: peter.kubbutat@tum.de

Received: 10 December 2020; Revised 10 February 2021; Accepted: 15 February 2021; Published: 18 February 2021



Abstract:

The interaction of different sugars with polysorbate 80 as a surfactant at foam bubble interfaces was investigated with regard to the creation of stable foams. Sorbitol, maltose, sucrose and maltodextrin DE6 were applied at concentrations of 10 to 60% w/w. Added sugars generally resulted in a lower foam overrun, but a narrower bubble size distribution and less drainage, especially at higher viscosities. The specific overrun, however, was found to strongly depend on the type of sugar used. Sorbitol enhanced the properties of polysorbate 80 as surfactant in terms of achievable overrun. Except for sucrose, higher sugar contents close to saturation were able to minimize detectable drainage after foaming. This effect was found to depend on interactions between polysorbate 80 as surfactant with sucrose or maltodextrin as viscosity builder, which could be indirectly assessed by comparing macroscopic foam property data. Sorbitol and maltodextrin led to the most homogeneous bubble size distribution and thus, helped to create the most stable foams. According to our findings, the functions of increasing viscosity by sugars and the interfacial activity of polysorbate 80 seem to overlap or to partially compete. This knowledge is of relevance for formulating foams with the highest level of robustness, e.g. for drying processes like foam-mat or vacuum drying.

Keywords: Foaming, Surface active substances, Surfactant, Sugars, Excipient, Foam properties

¹ Original publication: Kubbutat, P.; Kulozik, U. (2021) Interactions of sugar alcohol, di-saccharides and polysaccharides with polysorbate 80 as surfactant in the stabilization of foams. *Colloids Surf. A*, 616: 126349 <https://doi.org/10.1016/j.colsurfa.2021.126349>. Adapted original manuscript. Adaptions of the manuscript refer to enumeration, citation style, spelling, notation of units and format. Permission for reuse of article is granted by Elsevier Ltd.

References of all chapters are merged at the end of the dissertation.

4.1.1 Introduction

Foams are thermodynamically instable and their properties start changing immediately after foam formation. Depending on the practical application, the required foam stability varies from seconds to months. The most common way to preserve foam properties is the addition of thickening agents. Thickening agents such as saccharides or polysaccharides increase the viscosity of the liquid phase by water binding up to the point of gel formation and stabilize the foam against foam destabilizing effects like drainage, Ostwald ripening and coalescence, thus preventing foam destruction in too short time frames (Weaire and Hutzler 2001; Dickinson 1989; Walstra 1989).

While various studies in food research exist on the properties of protein-stabilized foams in combination with saccharides (Dachmann et al. 2018; Thuwapanichayanan et al. 2012; Sankat and Castaigne 2004; Bals and Kulozik 2003; Lee and Timasheff 1981; Kinsella 1981), only few studies are reported combining sugars with small non-ionic surfactants like polysorbate 80, an often used interfacially-active component in pharmaceutical applications.

The application of foams in the pharmaceutical industry, on the other side, is not as common as in the food industry, and therefore, less research has been conducted in this area so far. The specification of the used excipients in the formulation largely differs from components used in food applications. For instance, protein isolates are mainly used as foaming agents in the food industry. Through the use of proteins or their peptides in addition of salts and sugars as well as the shift of pH, the properties of the surface-active components will change significantly (Manassero et al. 2018; Dombrowski et al. 2018; Sadahira et al. 2018; Karamoko et al. 2013). However, these complex ingredients are rarely used or even not allowed in pharmaceutical applications at the same level of purity. According to pharmaceutical handbooks, synthetic, well defined surfactants like polyoxyethylene sorbitan fatty acid esters or poloxamers are more common (Rowe et al. 2009). Semenova et al. (2003) investigated the impact of maltodextrin on the surface activity of three different small molecule surfactants. These authors reported that hydrophobic interactions as well as hydrogen bonds between maltodextrin in the bulk and the surfactants have an impact on the surface activity of small molecule surfactants. Based on these results, it could be expected that other sugars will also interact with small surfactants and that these interactions will have an impact on the properties of a foam. Surprisingly, however, no study was found reporting on the interactions of polysorbate 80 and different sugars related to foam formation and foam properties as applied or required particularly in pharmaceutical treatment concepts.

The background of this study is therefore to enhance the manufacture of pharmaceutical products during downstream operations like drying of therapeutic heat-sensitive agents, e.g. by foam mat drying (Abdul-Fattah et al. 2007a; Abdul-Fattah et al. 2007b). Comparable studies

on food systems with a similar purpose of preserving quality or function of ingredients or nutrients have been reported (Kardum et al. 2001). Conventional vacuum foam drying (VFD) is often performed as a combination of steps where foaming naturally results from creating the vacuum and simultaneous drying. As Walter et al. (2014) state, insufficient efforts are invested in research on the generation of foams with high process stability, and therefore, some issues like uncontrolled foaming and rapid foam decay occur, e.g. during vacuum foam drying. This study is based on the idea to first produce a stable foam from solutions composed such that pharmaceutical applications of foam drying can be targeted at. At first sight, it might be argued that under the influence of vacuum during drying foams naturally occur by evaporation of water and the water vapor creating bubbles in the liquid solution. Most solutions to be dried form in fact foams under the influence of the vacuum during drying, but they mostly do not have the necessary composition required for a stable foam. Therefore, the formulation of a composition comprised of foam-forming and foam-stabilizing agents combined with a dedicated whipping or foaming process prior to and separately from vacuum drying should yield the desired foam properties independent from the conditions applied in the drying stage. However, there is a lack of information about the interactions of protective sugars, especially sorbitol, maltose and maltodextrin with non-ionic surfactants like polysorbate 80. This would be important knowledge for the creation of a stable and controllable foam drying process (Ambros et al. 2019a) as well as for preserving the function of a therapeutic protein. Previous studies show that next to the viscosity other parameters like interfacial elasticity or surface pressure have an impact on the properties of the foam system (Lexis and Willenbacher 2014; Yang and Foegeding 2010; Ruiz-Henestrosa et al. 2008; Lau and Dickinson 2005).

This study, covering a range of different sugar types at concentration levels not investigated so far in combination with a small non-ionic surfactant that will provide a detailed view on how sugars can influence the characteristics of foams built by surfactants. In contrast to existing studies, which investigated single sugar-surfactant combinations on molecular level and low concentrations in order to determine changes of the critical micelle concentrations (Sharma and Rakshit 2004), this work will provide information on the macroscopic foam properties with relatively high sugar concentrations and variable type of sugar. Synergistic and antagonistic effects might result from these conditions. Examples for these effects are e.g. macromolecular crowding which describes interactions of molecules at high concentrations (Laurent 1995) or as results of particle formation, i.e. the well-known Pickering effect (Pickering 1907). Further, the used sugars differ in their hydrophilic character (Sharma and Rakshit 2004; Galema and Hoeiland 1991): sorbitol and sucrose are very hydrophilic, whereas maltose and maltodextrin are comparatively less hydrophilic. This can be attributed to different saccharide structures like the type of integrated monomers or the conformation of the saccharide (Aumann et al. 2010) and was also proven by hydrophilic interaction chromatography (Grumbach and Fountain

2010). The hypothesis is that the foam properties and foam stability will differ in dependence on the composition of the small surfactant polysorbate 80 and the type of sugar due to different interactions mechanisms between the different molecules. Of special interest are the high concentrations of the sugars close to their solubility limits. Thereby, the possibility of selecting or creating formulations yielding foams with certain overrun, drainage, firmness and bubble size distribution will enable the design of the foam drying processes with consciously selected processing conditions required to create special target product properties. By closing the knowledge gap of the interactions between nonionic surfactants and sugars, this study will provide the basis for further investigations on foam-based drying processes, where the product to be dried is exposed to high mechanical stress levels.

4.1.2 Materials and methods

4.1.2.1 Materials

Polysorbate 80 as surfactant, the sugar alcohol d-sorbitol (SOB; molecular mass (M_{mass}) = 182.17 g·mol⁻¹) and d-maltose (MTO; M_{mass} = 342.3 g·mol⁻¹) as thickening agents were obtained from Gerbu Biotechnik GmbH (Heidelberg, Germany). Furthermore, two other thickening agents, sucrose (SUC, M_{mass} = 342.3 g·mol⁻¹) and maltodextrin DE6 (MDX; M_{mass} = 2879 g·mol⁻¹, calculated by Castro et al. (2016) were purchased from Carl Roth GmbH (Karlsruhe, Germany) and Nutricia GmbH (Erlangen, Germany), respectively. All reagents were of analytical grade.

The CMC of polysorbate 80 was given by the manufacturer with 13–15 mg·l⁻¹ or 0.012 mM (20–25 °C) (Merck KGaA 2020) and is therefore much lower than the used concentration within the paper (3% w/w).

4.1.2.2 Sample preparation

Sample solutions of 200 g each were prepared by mixing and dissolving 3% (w/w) polysorbate 80 with different amounts of carbohydrate (i.e., sucrose 10, 20, 30, 40, 50 and 60% (w/w)) in demineralized water. To ensure full dissolution, the sample solutions were gently stirred by a magnet stirrer (Maxi Direct, Fisher Scientific GmbH, Schwerte, Germany) at 200 rpm for 12 h at 4 °C. Prior to the experiments, the sample solutions were tempered at 20 °C inside a water bath (F3, Fisher Scientific GmbH, Schwerte, Germany). All sugars, even at the highest concentration levels, were completely dissolved, no sediment was observed. However, some cloudiness was observed for maltodextrin solutions, which is not unusual for polysaccharides (Zeeb et al. 2019).

4.1.2.3 Determination of solution properties

4.1.2.3.1 Density

Density of the sample solutions was determined with the Density Meter DMA 4100M (Anton Paar GmbH, Graz, Austria) at 20 °C.

4.1.2.3.2 Solution viscosity

For determination of viscosity of the various solutions, the Modular Compact Rheometer MCR 302 (Anton Paar GmbH, Graz, Austria) was used. Measurements were performed with a concentric cylinder (CC27, Anton Paar GmbH, Graz, Austria) at 20 °C and a sample amount of 12 ml. The applied procedure started with a pre-shearing of the sample solutions at 20 s⁻¹ for 30 s, which was followed by a waiting phase of 60 s at shear rate of 0 s⁻¹. Afterwards, the shear rate was increased linearly from 0 s⁻¹ to 100 s⁻¹ within 120 s. During the holding phase, it was kept constant at a shear rate of 100 s⁻¹ for 60 s. Finally, the shear rate was decreased linearly from 100 s⁻¹ to 0 s⁻¹ within 120 s. The average apparent viscosity was measured at the holding phase with the shear rate of 100 s⁻¹. The obtained data for the investigated solutions are summarized in Supplementary 4.1-1.

4.1.2.3.3 Determination of surface pressure

The surface tension (σ) of the investigated sugar solutions without and with polysorbate 80 were measured against air with a drop volume tensiometer Lauda TVT 2 (LAUDA-Scientific GmbH, Lauda-Königshofen, Germany) at 20 °C. The surface pressure (π) was calculated by the difference of surface tension of the pure sugar solutions (see Supplementary 4.1-2) $\sigma_{solvent}$ (sugar solution without surfactant) in equilibrium and the surfactant containing solution, σ_{s+s} (sugar + surfactant solution) at the time t (Equation 4.1.1):

$$\pi(t) = \sigma_{solvent} - \sigma(t)_{s+s} \quad (4.1.1)$$

By calculating the surface pressure, changes of the behavior of polysorbate 80 at the air-liquid interface due to the addition of saccharides were detectable.

4.1.2.4 Foam formation

For foam formation, 150 g of sample solution was whipped with a commercial planetary mixer (KitchenAid ARTISAN, 5KSM150PS, Whirlpool Corp., Greenville, United States of America) for 15 min at 220 rpm and 20 °C. The mixer was equipped with a wire whisk geometry (K45WW, Whirlpool Corp., Greenville, United States of America).

4.1.2.5 Determination of foam properties

As foams without added saccharide collapsed within the time of analysis, only foams with added saccharides were investigated according the methods in the following chapters.

4.1.2.5.1 Overrun

The overrun is a parameter, which indicates the samples' volume increase due to the incorporation of gas bubbles into the liquid, sometimes in literature also referred to as foamability. In order to determine the incorporated gas volume of foam, the overrun was measured according to the method of Kreuß et al. (2009) and was calculated using equation (4.1.2) (Phillips et al. 1987):

$$\text{Overrun, \%} = \frac{(\rho_{\text{Solution}} \times V_{\text{Cup}}) - (m_{\text{F}})}{(m_{\text{F}})} \times 100 \quad (4.1.2)$$

Where ρ_{Solution} is the density of the investigated solution at a temperature of 20 °C. In addition, V_{Cup} is the volume of the used cup and m_{F} the mass of the foam in the cup.

4.1.2.5.2 Bubble size distribution

The size of the bubbles in the foam was measured 15 min after foam formation. Foam was gently spread out across an object slide in a thin layer with a spatula and placed under an Axiovert 135 microscope, an AxioCam ICc 1 with the AxioVision software (Version 4.8.2.0) (all from Carl Zeiss AG, Oberkochen, Germany). Photos were taken with a 10-fold magnification. The bubble size of at least 300 bubbles was taken for each sample. The bubble size distribution contains the following values relating to the bubble diameter: the 1-, 10-, 25-, 50-, 75-, 90-, and 99-percentiles, where e.g. the 25-percentile d_{25} represents the diameter of bubbles below which 25% of all bubbles investigated. In order to better estimate the wideness of each bubble size distribution, the interquartile range (IQR) was calculated using the following equation (4.1.3)

$$\text{IQR, } \mu\text{m} = d_{75} - d_{25} \quad (4.1.3)$$

Where d_{75} is the 75% percentile and d_{25} is the 25% percentile. The IQR was chosen, because it is more robust against outliers compared to SPAN-value or polydispersity index. This seems to be more suitable to compare foams, of which properties are changing a lot within the investigated saccharide concentration.

4.1.2.5.3 Firmness of the foam

Two filled cups were used to measure the firmness of the foam with a texture analyzer (TA.XT.plus, Stable Micro Systems Ltd., Godalming, UK). The test was performed with a foam-filled cup 20 min after foam formation at 20 °C. The texture of the foam was defined by the

maximum force, which is necessary to get into the foam with a reticle shaped fixture with a diameter of 32 mm at a speed of $1 \text{ mm}\cdot\text{s}^{-1}$ for 10 s.

4.1.2.5.4 Drainage

The drainage relevant masses were measured 45 min after foam formation and computed according equation (4.1.4).

$$\text{Drainage, \%} = \frac{m_{t=0\text{min}} - m_{t=45\text{min}}}{m_{t=0\text{min}} - m_{\text{empty}}} \quad (4.1.4)$$

Where, $m_{t=0\text{min}}$ is mass of sample after foam formation, $m_{t=45\text{min}}$ is the mass of the cup after decanting the drained liquid with an age of 45 min, and m_{empty} is the mass of the empty cup.

4.1.2.6 Statistical analysis

For surface pressure, each formulation was replicated twice and analyzed in triplicate. For foam properties, each formulation was replicated three times and analyzed twice. Therefore, in total six values per sample were obtained. Mean values are presented, the error bars indicate the standard deviation and lines are guide to the eye.

4.1.3 Results and discussion

4.1.3.1 Surface pressure of sugar-surfactant solutions

The results of surface pressure of the investigated solutions are shown in Fig. 4.1.1. The plot of surface pressure at $80 \pm 9 \text{ s}$ over saccharide concentration is shown in Supplementary 4.1-3. We decided to plot the surface pressure over the time, as the first seconds are the most relevant for the formation of foam (Boos et al. 2013) and equilibrium might be never reached in a fragile real foam systems. It can be observed that the surface pressure for different solutions increased sharply due to the adsorption of the surfactant during the first 20 s before the curves asymptotically levelled off towards an almost constant final value for all investigated sugars and concentrations. A higher level of surface pressure with higher content of sugar indicates a higher ability of polysorbate 80 to decrease the surface tension at the air-water interface. A constant value with different concentrations of sugars shows instead that there is no influence on the surface tension lowering properties. Furthermore, it can be seen that the different concentrations of maltose and sucrose showed nearly no impact on the surface pressure (Fig. 4.1.1a and b), while varying the concentration of sorbitol and maltodextrin (Fig. 4.1.1c and d) resulted in different levels of surface pressure. However, the error bars for the samples containing 60% of sorbitol were high and therefore these samples were not taken into consideration for the discussion. By comparison with the surfactant-free solution for the calculation of

the surface pressure, it can be stated that both, sorbitol and maltodextrin, seem to be interacting with polysorbate 80, while sucrose might interact at high concentrations and maltose not at all, independently of the sugar concentration.

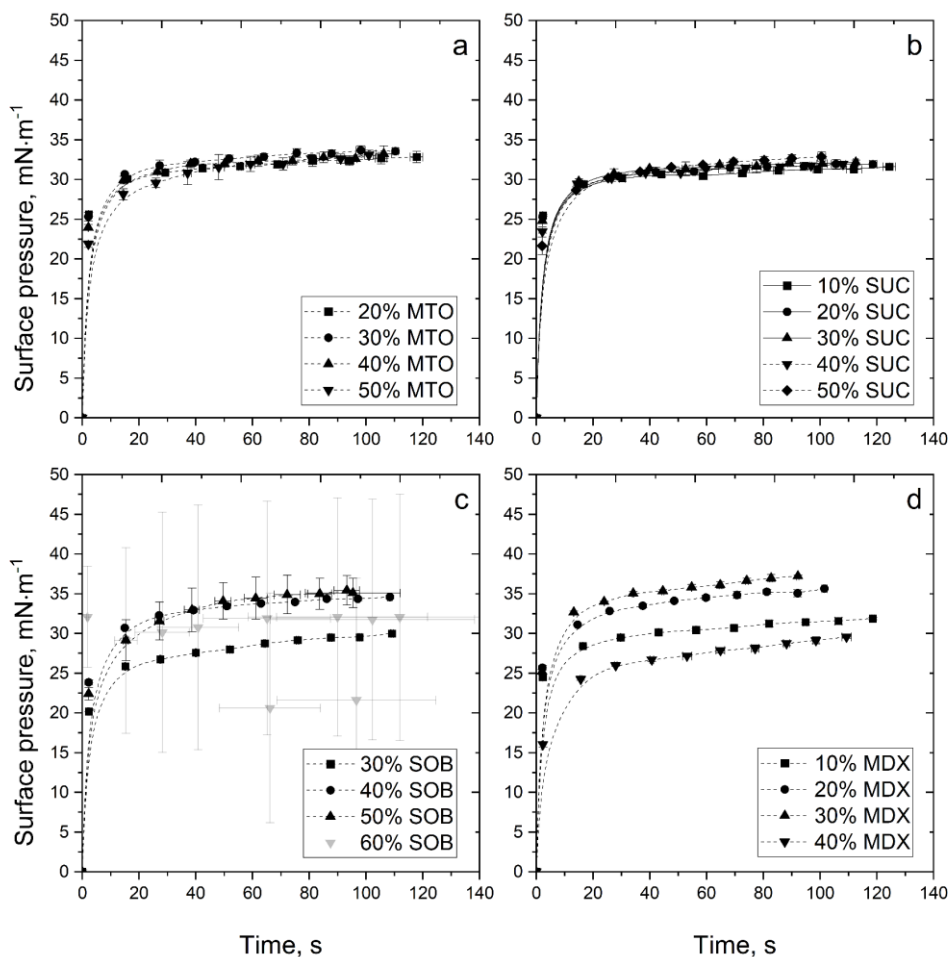


Fig. 4.1.1: Surface pressure of 3% polysorbate 80 solutions with (a) maltose (MTO), (b) sucrose (SUC), (c) sorbitol (SOB) and (d) maltodextrin (MDX) at 20 °C.

It was expected that sorbitol would interact with the ethylene oxide groups of the surfactant via hydrogen bonds. Due to this interaction, the ethylene oxide group will change its conformation and the sorbitol might extend the surfactant chain length. Strong indications for this interaction and mechanism were found by Staples et al. (1996), who investigated the influence of sorbitol on the adsorption of monododecyl hexaethylene glycol, n-dodecyl triethylene glycol and sodium dodecyl sulfate at the air-water interface, however, only at one single concentration (300 g·l⁻¹). The interaction resulted in a lower surface tension compared to the sorbitol-free solution. Our results are in accordance with these findings, and we therefore conclude that this

mechanism seems to be valid for polysorbate 80, too. The interaction between sorbitol and polysorbate leads to a higher surface pressure, and thus, supports foam formation. We think that this effect can be attributed to a more concentrated surfactant at the air-water surface. This phenomenon could also possibly be explained by a chemical potential of the surfactant, when present in form of micelles. Complementary to the results of Staples et al. (1996) regarding surfactant additive interactions, changes in surfactant surface concentration were published by Xu et al. (2013) and Chauhan et al. (2013) for other combinations of surfactants and additives. This appears to support our argumentation regarding higher surfactant surface concentrations induced by the interaction with saccharides. Above a concentration of 50% sorbitol, however, the properties of polysorbate 80 in lowering the surface tension are negatively affected, which might be due to macromolecular crowding.

The addition of sucrose and maltose has only a slight impact on the surface pressure. While both molecules are relatively small, we assume that the interactions between the disaccharides and polysorbate can be explained by the formation of hydrogen bonds between OH-groups of the saccharides and OH- groups of the ethylene-oxide head of polysorbate. However, there is a difference between sucrose and maltose. Sucrose shows the higher impact compared to maltose, especially at high concentrations. This can be attributed to the more hydrophilic character of sucrose (Galema and Hoeiland 1991), macromolecular crowding (Yadav 2013) and the related expected change in surface pressure (Claesson et al. 2006). As we used mass weight based concentration and not molar ratio for the experimental setup, we cannot directly state that the number of hydrogen bonds per saccharide molecule is the predominant reason for the observed differences. However, as we observed differences between maltose and sucrose, where the number of molecules is the same, we assume that the number of hydrogen bonds per saccharide molecule is not the predominant factor. Nonetheless, it should be mentioned that the number of hydrogen bonds is not directly correlating with the number of functional groups, as they can be sterically hindered as a result of size and structure of the investigated saccharide (Ali et al. 2019).

Next, we compared sorbitol with maltodextrin as an added sugar. Previous studies on the impact of maltodextrin on the surface activity showed that the addition of low concentrations of maltodextrin (0.5% w/w) results in a higher surface tension than without polysaccharide addition (Semenova et al. 2003). In the study of Semenova et al. (2003), maltodextrin lowered the surface activity and increased the surface tension of low concentrated ($2 - 6 \text{ mg}\cdot\text{dm}^{-3}$) sodium salt of stearyl-lactoyl lactic acid (SSL(Na^+)) and polyglycerol ester solutions, as well. The authors postulated that strong hydrogen bonds between the sugar and the surfactant lead to an incorporation into sugar molecules. We prefer to characterize this as adhesion of the surfactant molecules at the sugar molecule surface, which results in a decrease of effective surfactant

concentration. In contrast, our study applies significantly higher concentration of surfactant (3% w/w) and MDX (10–40% w/w) in order to stabilize the foams such that they will be able to withstand the rough conditions in vacuum drying processes, which are planned to be investigated in continuation of this work. The addition of maltodextrin resulted in a higher surface pressure, and therefore, in a lower surface tension. Reason for this might be a denser surfactant layer due to size differences between polysorbate 80 and maltodextrin. The polysorbate covers the surface first, however, leaving gaps between the hydrophilic ethylene oxide head groups due to steric repulsion. These gaps can be assumed to be filled by sugars associated with surfactant molecules, having a different hydrophobic and hydrophilic character and which might work as a co-surfactant. This in turn increases the surfactant concentration at the interface. Comparable synergistic effects were also described for the combination Tween 80 and Span 20 by Posocco et al. (2016) as a result of different molecular sizes and head group repulsion. Another possibility to explain how the surface concentration increases would be by strong hydrogen bonds between sugar and polysorbate, as described previously. The hydrogen bonds, interacting directly or mediated by water, are able to increase the packaging density within the surfactant monolayer as also suggested Claesson et al. (2006). Further to that, for high concentrations of maltodextrin and surfactant, no negative impact on the surfactant's surface properties was detected. Only at a MDX concentration of 40%, the high apparent viscosity of the bulk phase hinders the polysorbate 80 to diffuse to the air-solution interface. Further, with high concentrations, the adhesion of polysorbate to maltodextrin can be a limiting factor for lowering the surface tension.

In addition, the shape of polysorbate 80 micelles might change in presence of co-solvents, as described in literature e.g. for water–1,4-dioxane mixtures with different concentrations (Aizawa 2009). However, polysorbate 80 forms in water most probably spherical micelles (Karjiban et al. 2012; Kerwin 2008). As we do not know about the change of micelles morphology in presence of sugars, we assume that the micellar shape was spherical throughout the experiments.

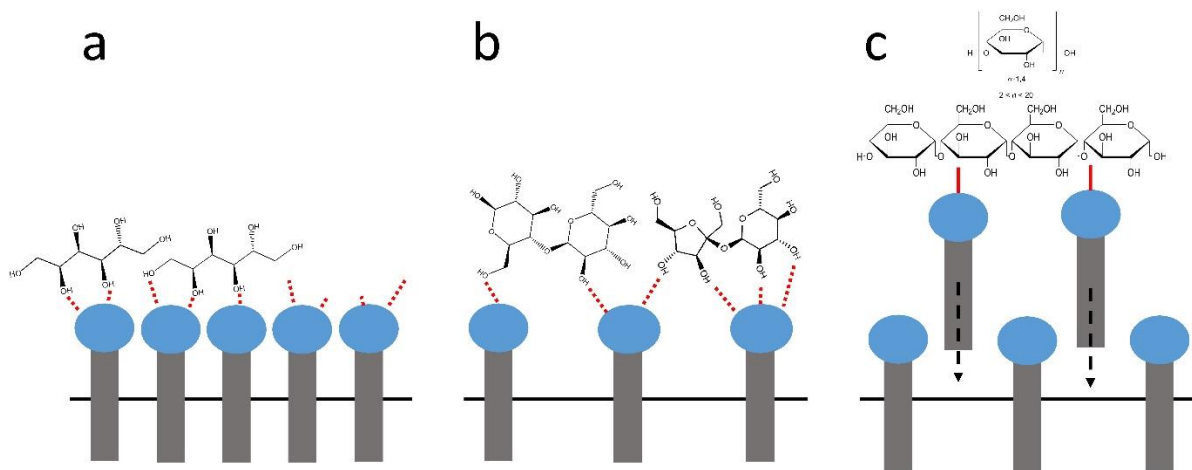


Fig. 4.1.2: Scheme of different surfactant concentration at the air-water interface as a result of interactions between saccharides and polysorbate 80 with (a) sorbitol, (b) sucrose or maltose and (c) maltodextrin.

A scheme of how the authors image the above discussed interactions of saccharides and polysorbate at the surface is shown in Fig. 4.1.2. Fig. 4.1.2a corresponds to small sugar-alcohols, Fig. 4.1.2b disaccharides and Fig. 4.1.2c polysaccharides, respectively.

The impact of how the surfactant lowers the surface tension, and therefore, better foamability was investigated by assessing the overrun in the following chapter.

4.1.3.2 Overrun of sugar containing polysorbate 80 foams

The foam overrun was determined and plotted over the sugar content as displayed in Fig. 4.1.3a. For all types of sugars, a decreasing overrun with increasing sugar concentration can be observed. Samples with an MDX concentration of 40% had the lowest overrun (41%), while an overrun of 683% was measured for foams with 50% sucrose. One reason for the differences in the overrun values at high sugar concentration can obviously be the different viscosities. The foam overrun plotted against the apparent viscosity is presented in Fig. 4.1.3b. Samples with 40% maltodextrin exhibited a viscosity of 1.706 Pa·s. Samples with 50% sucrose and 3% polysorbate 80 remained at a much lower viscosity (0.025 Pa·s). This resulted in a higher overrun because of the lower resistance of the solution against the incorporation of air. The increasing viscosity of the liquid phase hinders the incorporation of air into the liquid phase, as well as the diffusion of the surfactants to the air-water interface. Differences in viscosity between samples with the same mass content of saccharide can be attributed to different number of H-bonds between sugar and sugar, polysorbate and sugar or sugar and water molecules as well as different steric hindrance due to differences in molecules sizes as also stated for viscosity differences between saccharides by Ali et al. (2019).

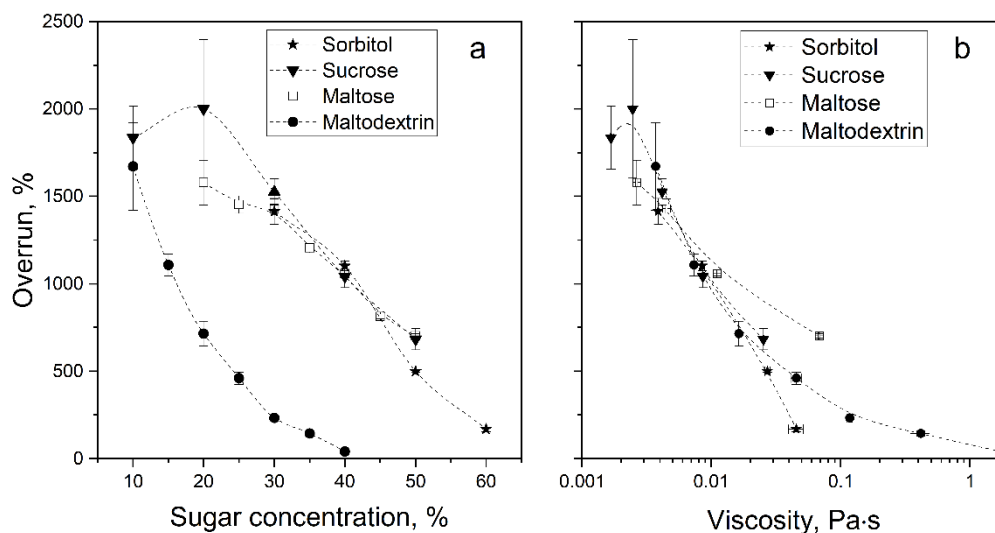


Fig. 4.1.3: Overrun of 3% polysorbate 80 foams as function of (a) the sugar concentration with maltodextrin, sorbitol, sucrose and maltose and (b) the viscosity of their solutions at 20 °C, respectively.

Furthermore, a clear difference in overrun between the sugar types was observed. Foams, where sorbitol was added had a much lower overrun than maltose foams, even when the apparent viscosity of sorbitol solutions was lower than for maltose solutions. For example, a sample with 50% sorbitol and a viscosity of 0.0272 Pa·s yielded an overrun of 500%, while for samples with 50% maltose and a viscosity of 0.068 Pa·s an overrun of 700% was obtained. This clearly shows that factors other than viscosity of the solution contribute to foam formation.

A possible explanation for this difference is a competition of the sugars with polysorbate 80 at the interface of the bubbles. The air bubbles' surfaces obviously interact with both sorbitol and polysorbate 80 as can be seen in Supplementary 4.1-2. Therefore, polysorbate 80 does not seem to be able to reach the water-air interface as quickly and as completely as without competition with sorbitol, which results in a lower foamability of the sorbitol solution. According to Blanchard et al. (1977), the competition between sorbitol and polysorbate 80 in covering hydrophilic particles is low. Therefore, we think that we can apply this observation also to hydrophobic gas bubble interfaces. The competitive behavior at the water phase between polysorbate 80 and sorbitol could not be considered as a factor influencing overrun. In contrast to that, a study of Staples et al. (1996) on the interfacial behavior of sorbitol combined with different low concentrated nonionic surfactants ($c_{max} = 10^{-4}$ M) at the air-liquid interface showed that sorbitol is able to interact with non-ionic surfactants and seems to render it more surface active. This would lower the surface tension more efficiently, leading to smaller bubbles and a narrower bubble size distribution, as assumed from Fig. 4.1.1, and as shown later in Fig. 4.1.7d. However, as described in chapter 4.1.3.1, it is not necessarily given that the decrease of surface tension results in a higher overrun. This also appears to be dependent on the sugar type.

When we compare the effects of maltose and sorbitol, it can be observed (Fig. 4.1.3b) that foams with high maltose content result in high overrun values, whereas samples with sorbitol showed only low overruns. In order to explain this effect, the differences in hydrophobicity between maltose and sucrose as a result of slight differences in conformation and chemical structure can be taken into account. This was also stated by Aumann et al. (2010). Thus, a less effective decrease of the surface tension due to a competitive surface occupation of maltose and polysorbate 80 may result in a quicker bubble formation, and consequently, in higher overrun values but in a more brittle foam compared to other sugar-stabilized foams. The samples containing sucrose display an inverse trend. The reason for this might be an increased surface tension at the air-liquid interface due to the high sucrose content and the highly hydrophilic character of sucrose as stated by Aumann et al. (2010) for pure sucrose solution in addition with macromolecular crowding effects (Yadav 2013).

As can be seen from the results presented above the various sugars have different effects on the overrun. In comparison to published works, we observe a different behavior and unknown interactions between polysorbate 80 as surfactant and the sugars, which seems to result from the high sugar concentrations applied in this study.

In order to understand how the sugars are able to change the solution properties at the air-liquid interface under the conditions applied in this study, further experiments on liquid loss from the foam (drainage) and bubble size distribution as relevant macroscopic properties of the foams were conducted.

Since the surface pressure does not correlate well with the variables chosen, we studied other macroscopic foam properties to indirectly identify sugar surfactant interactions at or in vicinity to bubble surfaces to explain the observed differences in foam overrun.

4.1.3.3 Drainage of sugar containing polysorbate 80 foams

The influence of the sugar concentration on the drainage is shown in Fig. 4.1.4a. The drainage was observed as total liquid loss of the foam within 45 min and presumably mainly driven by the liquid loss in the center of lamellae. For low sugar contents, the drainage remained at high levels, and then reached a maximum depending on the type of sugar, before steeply decreasing to very low levels.

This behavior could be observed for all foams, where different sugar were applied. However, for concentrations of 50% maltose, 60% sorbitol, and 30% maltodextrin no drainage was detectable. Sucrose, in contrast, could not completely prevent drainage within the time frame investigated.

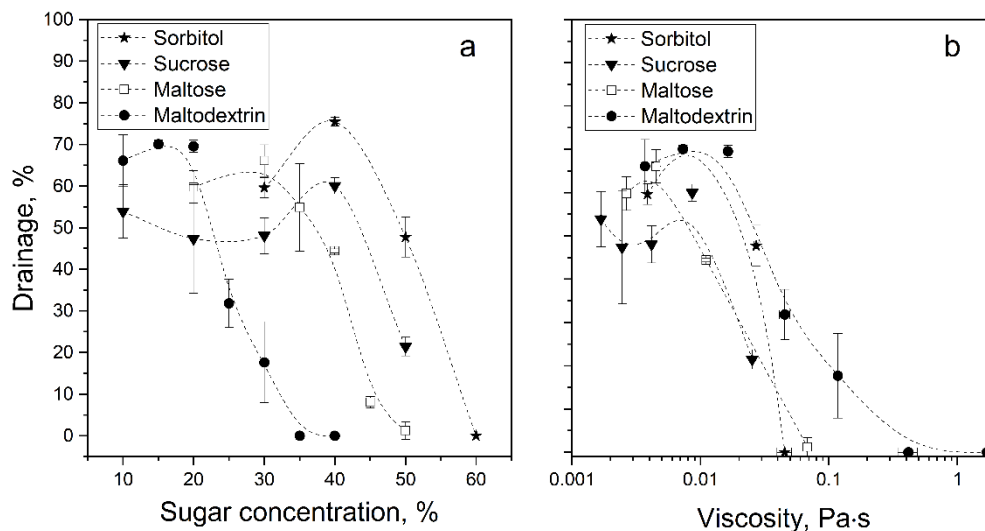


Fig. 4.1.4: Drainage of 3% polysorbate 80 foams as function of (a) the sugar concentration with maltodextrin, sorbitol, sucrose and maltose and (b) the viscosity of their solutions at 20 °C, respectively.

Even at a sucrose concentration of 50%, a serum loss of 21% was obtained. The correlation of viscosity and drainage is plotted in Fig. 4.1.4b. The observed trend is similar to the one shown in Fig. 4.1.4a for the effect of concentration on drainage. The only difference is that sucrose foams show less drainage at low viscosity compared to maltose or sorbitol foams. With higher viscosities of sorbitol, maltose and maltodextrin solutions, no observable drainage within the investigated time scale (45 min) occurred. The foam with the lowest viscosity and no drainage was best stabilized by sorbitol (0.045 Pa·s), then by maltose at 0.068 Pa·s, and finally by maltodextrin at 0.416 Pa·s.

We explain the change of the drainage values by the change of the foam structure from a polyhedral foam to a spherical foam, as shown in Fig. 4.1.5. In polyhedral foams, capillary effects decrease the drainage value. With increasing viscosity, the bubble size decreases as later described and discussed in chapter 4.1.3.4. and as long as the viscosity of the bulk phase is too low to prevent drainage or the separation of bubbles and bulk phase. Beyond this point, the viscosity of the bulk phase hinders the separation and the drainage is reduced until no drainage was observable during the time frame of interest. However, it should be mentioned that the pictures were taken 15 min after foam formation. For samples with low saccharide content, drainage might have already occurred during the first minutes, influencing shape and size of bubbles before taking the foam pictures. Nonetheless, the chosen time is a good compromise with regard on the ability to use the obtained data it in later industrial applications, where the foam will be not processed immediately.

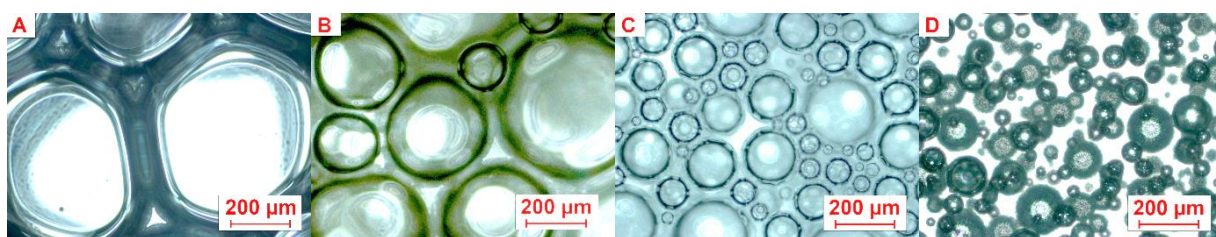


Fig. 4.1.5: Microscopic images of 3% polysorbate 80 foams (10-fold magnification) with (A) 10% MDX, (B) 20% MDX, (C) 30% MDX and (D) 40% MDX, 15 min after foam formation.

Another effect, which we also considered as an explanation, was that at high viscosity, particle-like crystals or micellar foaming agent might have been able to block the lamella. This could be assumed for all sugar types due to the observed higher levels of cloudiness at concentrations near the solubility limit. In case the sugars were not well dissolved, it would be expected that residues of sugar particles would be observable by light microscopy, comparable to the crystals observed by Lau et al. (2007) during their study on the effect of crystallized sucrose on the stability of foams. However, particles smaller than detectable can cause turbidity. Those small particles might also play a role as surface-stabilizing agents as shown by Pickering (1907) as one of the first scientists. A particle-supported system may lead to a long-time stability of the foams, as it would be necessary for further process steps like drying or pumping the foam. However, particles according to Pickering-theory are mainly hydrophobic or amphiphilic, as they tend to adsorb at the air-water surface (Fameau and Salonen 2014), while saccharides are highly hydrophilic and should therefore stay in the solution. Nonetheless, Ellis et al. (2017) could reach a shelf-life time of six days due to the addition of agar-gel particles to Tween 20 foams. This shows that small particles, which are nominally not acting as surfactants or foaming agents, are a useful tool to decrease drainage and to stabilize the foam. In contrast to other studies, where added particles were used to create these effects (Ellis et al. 2017; Guignot et al. 2010), we think that we could achieve this effect just by increasing the sugar content to near the solubility limit such that local super-saturation leads to a loss in sugar solubility, followed by formation of microscopic saccharide crystals.

In addition to surface pressure, overrun and drainage, the bubble size distribution can provide information about the interactions between polysorbate 80 and sugar molecules. It is expected that sorbitol and maltodextrin formulations result in smaller bubble sizes than sucrose and maltose due to the increased surface concentration of polysorbate 80 in presence of sorbitol or maltodextrin. Further, it is expected that interactions in the bulk are strongly dependent on the concentration of the sugar and will have influence on the coalescence resulting e.g. for MDX in smaller bubble size and narrower bubble size distribution.

4.1.3.4 Bubble size distribution

The bubble size distribution for samples with different sugar concentrations is shown in Fig. 4.1.6a – d. For higher concentration of sugar, the bubble size is decreasing. One effect is the higher viscosity with increasing sugar content and can be observed for all investigated used sugars. Sorbitol shows good properties to generate a small and narrow bubble size distribution at high concentrations.

The d_{50} decreased from 330 μm with 30% to 33 μm at 60% sorbitol. Maltose shows even larger differences with 421 μm at 20% compared to 11 μm at 50% maltose. Maltodextrin shows a similar behavior like sorbitol.

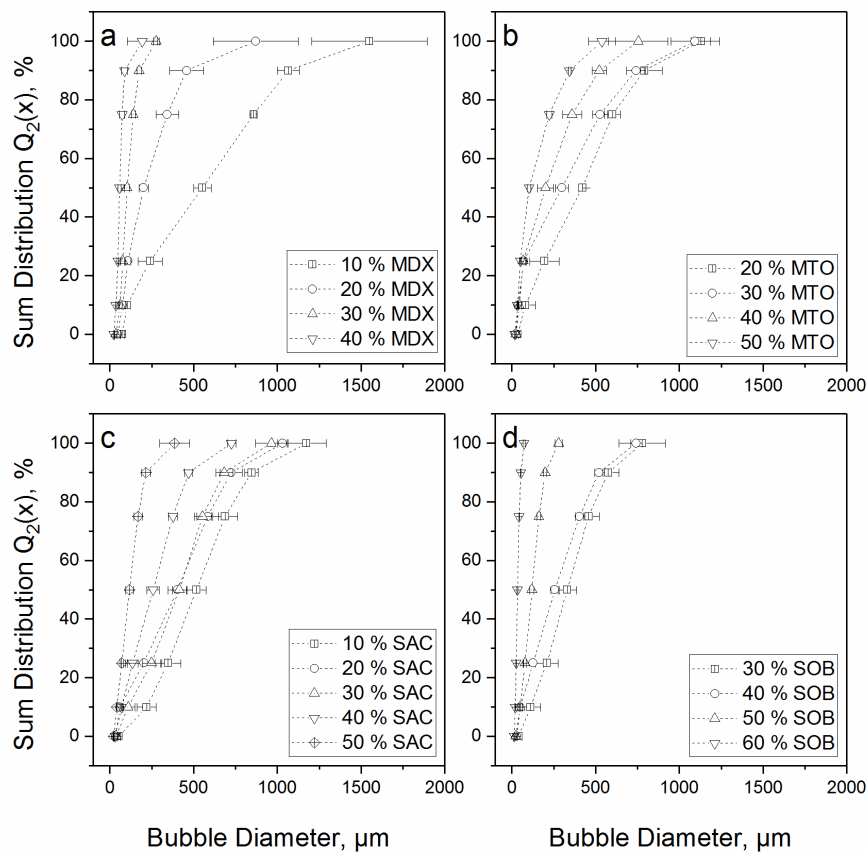


Fig. 4.1.6: Bubble size distribution of 3% polysorbate 80 foams with added (a) maltodextrin, (b) maltose, (c) sucrose and (d) sorbitol.

The impact on the bubble diameter with the addition of sucrose to the foams was much weaker ($d_{50} = 516 \mu\text{m}$ at 10% compared to $d_{50} = 117 \mu\text{m}$ at 50% sucrose). As stated by Samanta et al. (2011), pure polysorbate 80 water solutions at high surfactant concentration even above the CMC are not able to prevent coalescence over a period of 10 s due to a relative low surface

concentration. The fast foam decay of foams without added saccharides was also observed in our study, as already mentioned in 'Materials and methods'. With regard to this fast foam decay of polysorbate 80 foams without sugar, changes in bubbles size distribution are assumed to be directly related to the used concentration and type of sugar. Samples with sorbitol were able to form the smallest bubbles, which appears to be the increased polysorbate 80 concentration at the interface in presence of sorbitol as discussed in chapter 4.1.3.1.

Apart from that, the presence of very small sugar particles resulting from sugar concentrations near the supersaturation level might have an impact on the properties of the foam (see chapter 4.1.3.4). Next to the prevention of drainage, interactions between bubbles are sterically hindered, resulting in less coalescence, and therefore, smaller bubbles at the time of interest. This results in a better stabilization of the bubble size at high sugar concentrations. For maltodextrin, the same effect occurs, but the bubbles are larger compared to maltose or sucrose-containing foams. This is attributed to the larger and more inhomogeneous molecular structure of maltodextrin, which, despite its surface activity, is not able to cover the bubbles with a homogeneous layer in comparison to smaller sugars because of its molecular size. In addition, maltodextrin binds polysorbate, which results in higher surface pressure as discussed in chapter 4.1.3.1. The high sugar concentration results in very high viscosity and possibly very rigid interface, which upon shear stress induces a lower strain as compared to lower sugar concentrations. This induces bubble coalescence and would explain why the bubbles are growing faster and becoming bigger than in maltose-stabilized foams at low sugar concentrations. In contrast, the maltodextrin solutions with higher concentration and thus, with high viscosities, hinder the bubbles to grow, which under these conditions remain as small and stable as observed for other sugar types.

The interquartile range (IQR) of the bubble diameter gives a value for the width of the distribution and is shown in Fig. 4.1.7a and b and is more robust against outliers compared to SPAN or PDI value. The smaller the IQR the narrower the distribution, the bigger the IQR the wider, respectively. With rising sugar concentration as well as rising viscosity, the IQR decreased for all used sugars. For sorbitol and sucrose-stabilized foams, the IQR was minimized even at low viscosity (0.025 – 0.045 Pa·s).

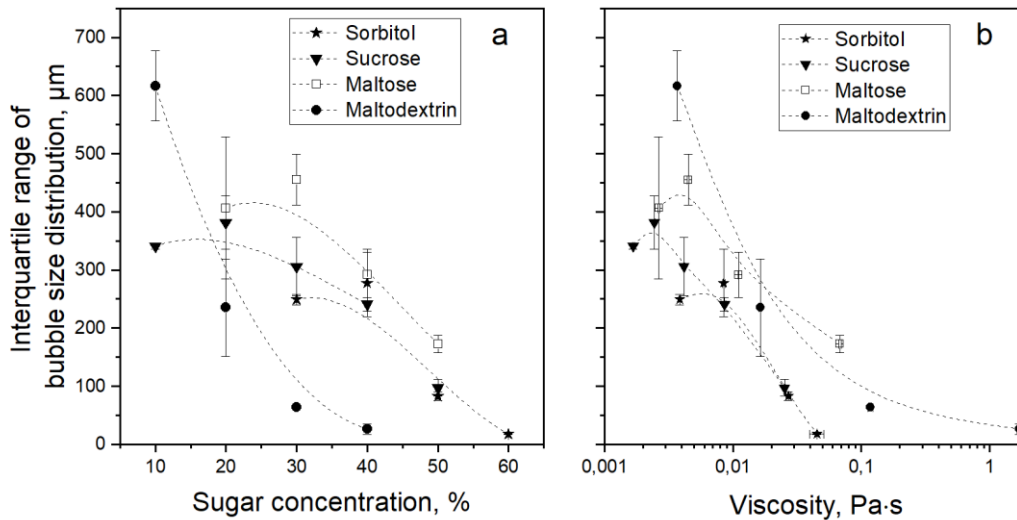


Fig. 4.1.7: Interquartile range of 3% polysorbate 80 foams as a function of (a) the sugar concentration with maltodextrin, sorbitol, sucrose and maltose and (b) the viscosity of their solutions at 20 °C, respectively.

Maltodextrin-stabilized foams could reach a small IQR, but only for samples with a high viscosity (1.7 Pa·s). Maltose-stabilized foams could not reach an IQR below 172 µm, which is a result of the weak interactions between maltose and polysorbate 80. In other words, retention of the bubble size is weak and growth of the bubbles occurs due to coalescence. The IQR-values show that the width of the bubble size distribution is directly dependent on the used sugar type, which provides an option to formulate the solution in a targeted manner.

Overall, the bubble size distribution results are in accordance with the overrun, drainage and surface pressure. They show that the addition of sugars not only affects the viscosity of the continuous phase, but also influence the interactions with the surfactant at the interface. Sugars therefore can affect bubble size by increasing viscosity and by additional effects unrelated to viscosity. The intermolecular interactions in the bulk and between surfactant and sugar also seem to have a large effect on the macroscopic behavior of the foam. This was also concluded by Briceño-Ahumada & Langevin (2017) for the influence of surfactant mixtures on the coarsening rate of foams.

For vacuum drying, the foam should be firm to withstand the mechanical stress until a certain level of water removal has been reached to keep the shape of the product. To assess under which condition this can be achieved, the impact of the different sugar types on the foam firmness will be shown in the next chapter.

4.1.3.5 Foam firmness

Foam firmness was measured by pushing a reticule into a foam at a known rate and measuring force (see chapter 4.1.2.5.3). The foam firmness can be influenced by the liquid content, which also separate the foam into a dry (high yield stress) or wet (low yield stress) state (Marze et al. 2009; Weaire and Hutzler 2001). Therefore, the liquid fraction was calculated by dividing the mass of a cup filled with foam through the mass of a cup completely filled with sample solution and plotted versus foam firmness (Supplementary 4.1-4). Thereby, we could prove that all investigated foams had a liquid content above 5%, which indicates that the foam can be considered to be wet (Drenckhan and Hutzler 2015), although this value is not a hard figure, but an established criterion in foam literature. Further, the plot showed comparable trends to that of the plot versus the viscosity (Fig. 4.1.8b). Bals et al. (2003) stated for protein foams that the increasing viscosity of the lamellae will increase the foam firmness. This was expected, as the liquid fraction in this experimental setup is directly linked to the overrun value, which follows the trend of viscosity.

The influence of the sugar concentration on the foam texture is shown in Fig. 4.1.8a. For sucrose and maltodextrin samples, a linearly increasing maximum force could be detected with increasing sugar concentrations. Maltodextrin samples show a little higher maximal firmness than sucrose foams. For sorbitol and maltose, the influence of the sugar concentration on the firmness seems to be negligible. The solution properties show more impact on the firmness of the foam with increasing sugar concentration due to a decreased bubble size, which results from the higher fluid viscosity. Therefore, it can be stated that maltose and sorbitol do not embed the bubbles into a firm structure. If mechanical stress pushes the foam, the bubbles can move independently, if the foams are wet. Therefore, the firmness remains low and seems to be independent of the bubble size or sugar concentration. Further, this behavior can be an effect of non-elastic properties of the bubbles. A shear-induced collapse by the probe geometry during the measurement could lead to a constant and low firmness value while a rising value due to the higher solution viscosity would be expected. However, both mechanisms, bubble rearrangement and bubble collapse could explain the low firmness values.

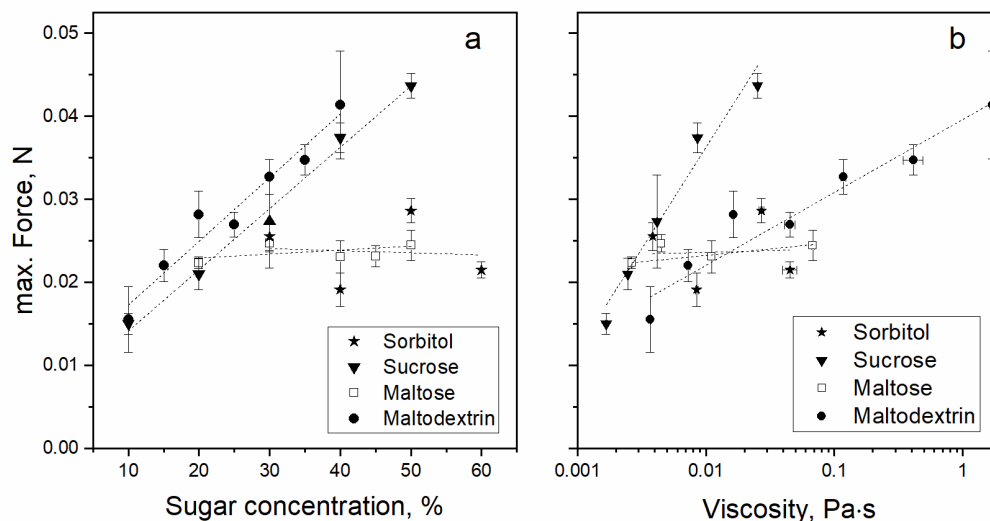


Fig. 4.1.8: Firmness of 3% polysorbate 80 foams as a function of (a) the sugar concentration with maltodextrin, sorbitol, sucrose and maltose and (b) the viscosity of their solutions at 20 °C, respectively.

Sugars in general are known to bind hydrate water, thus increasing viscosity. However, the firmness increase of the foams produced with the various sugars is quite different (Fig. 4.1.8a). The different potentials for sugar-sugar interactions are an explanation for the higher firmness of sucrose and maltodextrin foams. Sucrose molecules can interact with themselves in solution (Bock and Lemieux 1982). This results in a firmer texture and a higher firmness even at low viscosity (Fig. 4.1.8b). The higher firmness of maltodextrin-stabilized foams with higher MDX content can be explained by interactions between maltodextrin molecules themselves, which lead to higher viscosity of the bulk phase. These interactions can be explained by the interactions of the non-polar glucose units of two maltodextrin molecules as also stated by Duan et al. (2001). Further, the molecules of incorporated polysorbate 80 and maltodextrin at the interface are sterically hindering the movement of the bubbles and thus, increase the firmness of the foam. With increasing sugar concentration, both mechanisms become more pronounced resulting in a higher texture value.

4.1.4 Conclusion

Foams produced with polysorbate 80 as surface-active agent and with different sugar types at various concentration levels were analyzed. Overruns between 1800% and 41% could be obtained by the use of different sugar concentrations. Maltose can lead to foams with high overrun and low drainage. Foam formulations with sorbitol show a more uniform bubble size distribution. Maltodextrin can modify foams such that a stable, homogenous and firm matrix is obtained, which should be able to withstand mechanical processing stress conditions. The firmness of the foams was found to be at the highest levels for sucrose and maltodextrin. Maltose

and sorbitol did not show a dependency of sugar concentration or viscosity on the foam firmness. The usage of sugar concentrations near the solubility limit provides an option to prevent drainage. The surface pressure results show that sorbitol and maltodextrin improve the surfactants properties the most due to interactions with the surfactant, while for sucrose only slight changes were detectable and maltose did not change the properties of polysorbate 80. We believe that these findings will be very helpful for the development of vacuum drying processes using stable foams with targeted properties preserved across the whole processes stage.

It was shown that interactions between components like incorporation of surfactants or interactions between residuals of molecules have a massive impact on the foam properties. Each studied sugar showed specific behavior due interactions between sugar and polysorbate 80 related to the individual molecular characteristics of maltose and sucrose as short sugars, sorbitol as sugar alcohol and maltodextrin as longer sugar chain. The study shows that the type of sugar has a major influence on the foam properties and foam stability. This could be of relevance for creating foams, which have to withstand processing stress conditions, e.g. in foam mat drying processes or during pumping and can be combined with other e.g. the use of non- or low soluble gas mixtures to prevent foam decay (Bey et al. 2017).

Further, this study shows that interactions of non-ionic surfactants and in pharmaceutical industry often used excipients occur. This is of special relevance for aerated pharmaceuticals, which provide advantages as a better skin feeling, easier and more gentle application to injured areas, less residuals, and better removal compared to conventionally used ointments (Purdon et al. 2003). However, nonionic surfactants are added in conventional formulations, too, and therefore the interactions should be taken into consideration for the design of all formulations using surfactants in combination with saccharides.

Acknowledgments: This research project was supported by the German Ministry of Economics and Energy (via AiF) and the FEI (Forschungskreis der Ernährungsindustrie e.V., Bonn), Project AiF 18819N. The authors would like to thank Thomas Cummings and Elena Fellenberger for helping with the experimental data collection.

Author contributions: Peter Kubbutat planned and performed experiments and drafted the manuscript. Ulrich Kulozik initiated the study, discussed the results with Peter Kubbutat and contributed to the editing of the text.

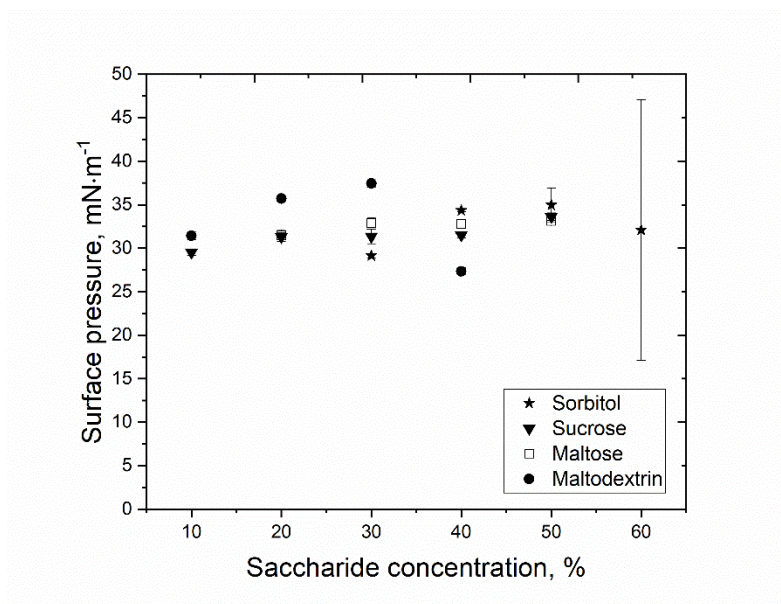
4.1.5 Supplementary

Supplementary 4.1-1: Apparent viscosity of 3% polysorbate 80 solutions with different type and concentration of saccharides at 100 s⁻¹ and 20 °C.

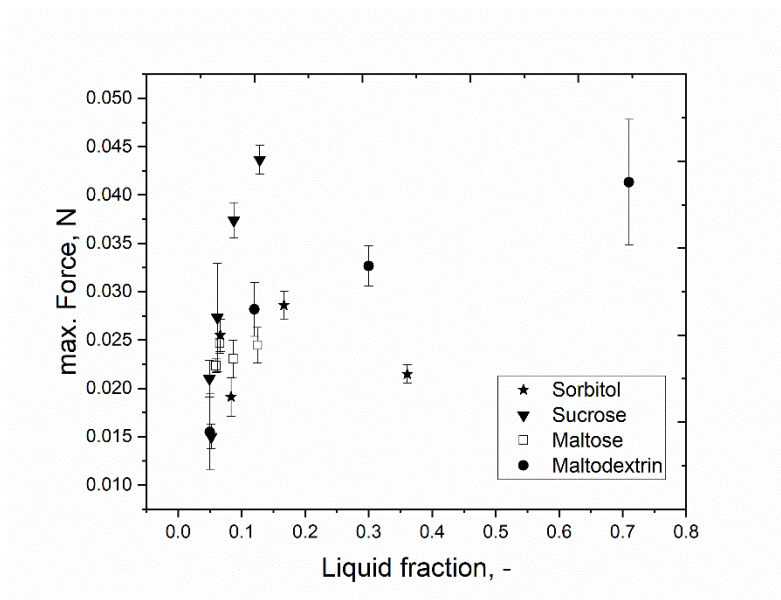
Apparent viscosity, Pa·s				
Concentration, % w/w	Sorbitol	Sucrose	Maltose	Maltodextrin
10		0.0017		0.0037
20		0.0025	0.0027	0.0163
30	0.0039	0.0042	0.0045	0.1177
40	0.0085	0.0086	0.0111	1.7067
50	0.0272	0.0253	0.0682	
60	0.0454			

Supplementary 4.1-2: Surface tension of sugar solutions without surfactant at 20 °C.

Surface tension, mN·m ⁻¹				
Concentration, % w/w	Sorbitol	Sucrose	Maltose	Maltodextrin
10		72.1		72.2
20		73.4	73.5	72.5
30	69.5	73.4	74.0	72.5
40	75.8	73.6	74.9	71.2
50	76.8	75.3	74.9	
60	78.4			



Supplementary 4.1-3: Surface pressure of sorbitol, sucrose, maltose and maltodextrin at variable concentrations at 80 ± 9 s and 20 °C.



Supplementary 4.1-4: Firmness of 3% polysorbate 80 foams with added sorbitol, sucrose, maltose and maltodextrin in different concentration as a function of the obtained liquid fraction of the foams.

4.2 Thermal and mechanical stability of dialyzed β -galactosidase from *Kluyveromyces lactis*

4.2.1 Introduction

In order to investigate the influence of process conditions and different product matrices on the product quality after microwave-assisted vacuum and freeze drying, β -galactosidase (β -Gal) from *Kluyveromyces lactis* in liquid formulation (Opti-lactase LX2, Optiferm GmbH, Oy-Mittelberg, Germany) was used as a biological marker. However, one open question was if the biological marker, change its activity during the sample preparation, since this would make the evaluation of the obtained data very difficult. The hypothesis therefore was that β -Gal retain its enzymatic conversion rate due to its flexible tertiary structure and that no side-effects occur. Therefore, the stability of β -Gal against whipping, freezing, and long-term stirring was examined, which was essential to exclude side-effects during sample preparation.

Besides the aqueous buffer solution and β -Gal, glycerin was used to stabilize the formulation. However, the evaporation temperature of glycerin is much higher than that of water, which may cause problems during the drying process and reduce the residual activity of β -Gal as a result of overheating. Therefore, samples with and without glycerin were investigated to examine, if glycerin is required to prevent side-effects during the sample preparation.

4.2.2 Methods

4.2.2.1 Dialysis of β -galactosidase

A dialysis step was performed to decrease the liquid formulation's glycerin content and exchange it with formulation buffer. For dialysis, 20 ml of glycerin containing β -Gal solution was transferred into dialysis tubes (Art. Nr. 2-9025, MWCO: 12–14 kDa, neoLab GmbH, Heidelberg, Germany) with a length of 16 cm and put into a beaker with 5 l phosphate buffer (pH 7.5). Thereafter, the sample was stirred at 100 rpm at 4 °C. For investigating the dialysis kinetic, the dialysis was stopped at 1, 2, 4, 6, 8, 14, 16, 24, and 48 h. For each investigated time, three independent runs were performed, and the concentration of glycerin and β -Gal, as well as the denaturation temperature of β -Gal, determined.

4.2.2.2 Determination of protein content, glycerin content, and enzyme activity of dialyzed samples

The concentration of β -Gal and glycerin was measured using high-pressure liquid chromatography (HPLC, Agilent 1100 Series, Agilent Technologies Inc., Santa Clara, USA). For the determination of glycerin, a PLRP-S 8 μ 300 Å column (Agilent Technologies Inc.; Santa Clara, USA) was used, whereas for the determination of β -Gal concentration, a Bio-Rad Aminex HPX-87H 300 x 7,8 mm (Bio-Rad Laboratories GmbH, Feldkirchen, Germany) was used.

The total protein content was measured with a VarioMaxCube (Elementar Analysensysteme GmbH, Langenselbold, Germany), which measures the nitrogen content in a sample with thermal combustion according to the method of Dumas (1831). The protein content was calculated by the correlation of nitrogen content and the use of a protein-specific conversion factor (β -Gal = 6.045). For calculating the conversion factor, the protein sequence (Uniprot 2021) was used. The weight of amino acids was divided through the weight of amino acid nitrogen (Owusu-Apenten 2002; Sosulski and Imafidon 1990; Boisen et al. 1987).

The denaturation temperature was measured using two methods: The first method used a modulated dynamic scanning calorimetry, mDSC, (Q1000, TA Instruments Inc., New Castle, USA). For this, a temperature modulation of $0.5\text{ }^{\circ}\text{C}\cdot\text{min}^{-1}$ and a temperature slope of $2.0\text{ }^{\circ}\text{C}\cdot\text{min}^{-1}$ was used to examine the melting temperature of the dialyzed samples.

Further, the denaturation temperature was determined by a photometric enzyme assay. The assay uses the lactose analog o-nitrophenyl- β -D-galactopyranosid (ONPG), which is cleaved by β -Gal into β -D-Galactose and o-nitrophenol. The o-nitrophenol is yellow and can be measured at 420 nm, whereby the enzyme activity can be measured by the change of absorption over reaction time. Before starting the test, the temperature of the solutions was adjusted to $24\text{ }^{\circ}\text{C}$. The reaction was started by mixing 2.5 ml ONPG solution with 0.1 ml in phosphate buffer solved sample inside a cuvette. Directly after, the cuvette was transferred into a photometer (T80 UV/VIS Spectrometer, PG Instruments Ltd., Leicestershire, UK), and the measurement started. The absorption A was recorded with a time resolution of 2 s. For the calculation of enzyme activity, the slope of the first 5–30 s after mixing was chosen to be in the linear region of reaction. Samples were analyzed in duplicate, and three individual runs of each test were performed. Therefore, six values for each sample were obtained.

4.2.3 Results

4.2.3.1 Influence of dialysis on the glycerin and enzyme content of β -Gal and examination of change in denaturation temperature

In Fig. 4.2.1A, the decreasing concentration of β -Gal and glycerin over the dialysis time is shown. It can be observed that within 8 h, an equilibrium was reached at about $15\text{ mg}\cdot\text{ml}^{-1}$ β -Gal and a glycerin content $<1\%$. The low glycerin concentration in the dialyzed β -Gal solution seemed suitable for microwave-assisted drying. Therefore, a dialysis time between 8 and 16 h was chosen for the subsequent preparation of drying samples. Further, the change in denaturation temperature, measured with mDSC, is shown in Fig. 4.2.1B. The denaturation temperature decreased with increasing dialysis time, which shows how effective the glycerin was in stabilizing β -Gal.

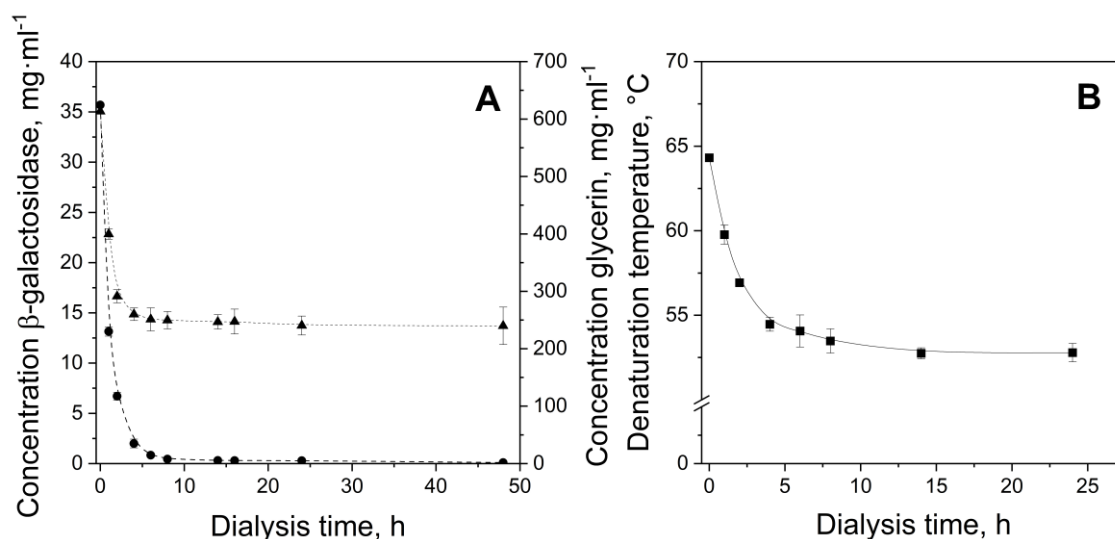


Fig. 4.2.1: Time-dependent concentration of β -galactosidase (▲) and glycerin (●) during dialysis of β -galactosidase raw solution (A) and resulting denaturation temperature, measured with mDSC (B).

The decreasing concentration of β -Gal during the dialysis can be explained by the diffusion of water into the dialysis tubes, which resulted in a dilution. This was optically validated because the dialysis tube was tighter and thicker after the dialysis than before. The lower glycerin content can explain the decrease in denaturation temperature. Glycerin, as a polyol, is known to stabilize proteins very effectively by the preservation of the hydration shell of the protein (preferential hydration) or direct replacement of water in the hydration shell (neutral solvation) (Hirai et al. 2018; Gekko and Timasheff 1981). Both mechanisms are strongly dependent on the glycerin concentration. It was found that preferential exclusion occurs below a concentration of 40% glycerin, whereas above 50% partial replacement by glycerin proceeds within the framework of the neutral solvation model (Hirai et al. 2018). However, the final denaturation temperature of about 50–55 $^{\circ}\text{C}$ appears slightly higher than comparable temperatures from literature, which is about 45–50 $^{\circ}\text{C}$ (Zhou and Chen 2001). This was attributed to the different methods of measuring the denaturation temperature. In the study of Zhou and Chen, the denaturation temperature was measured by an ONPG enzyme assay, whereas in this study, mDSC was used. In mDSC, the melting point is used as denaturation temperature. This melting point is strongly affected by the slope of increasing temperature, which affects that with fast temperature ramps, the melting point will be at a higher temperature detected as it would be suspected. Therefore, a second test was performed, using the ONPG enzyme assay and 5 min temperature holding time, which resulted in a denaturation temperature of about 40–45 $^{\circ}\text{C}$ (Fig. 4.2.2). This seems to agree with the determined denaturation temperatures of Zhou and Chen (2001). Therefore, it can be now assumed that at least 40 $^{\circ}\text{C}$ was reached within a sample if denaturation of enzymes is recorded after the drying process.

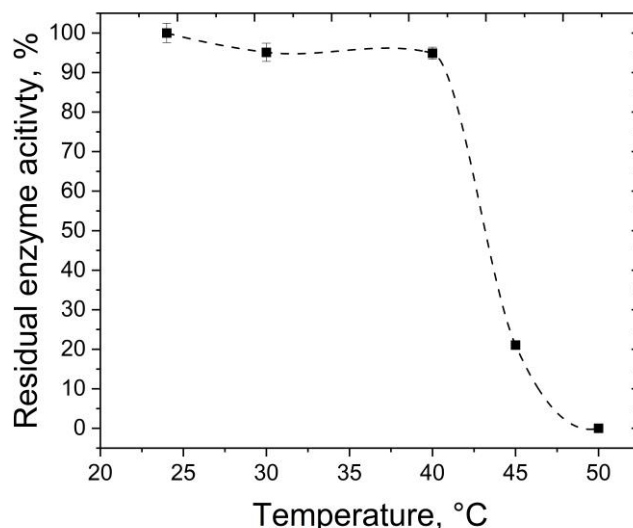


Fig. 4.2.2: Residual enzyme activity of β -galactosidase after 5 min holding time at a different temperature, measured with ONPG enzyme assay at 24 °C.

4.2.3.2 Influence of freezing, whipping and drying on the activity of β -galactosidase in a maltodextrin formulation

The influence of sample preparation, e.g., whipping, stirring overnight at 4 °C, foaming agent, and freezing was examined to exclude uncontrollable effects on the enzyme activity before starting the drying process. It was expected that the freezing and the whipping would damage the enzyme due to mechanical stress and surface denaturation because β -Gal has a high molecular weight and is only functional within its native tetrameric structure (Juers et al. 2012; Manning et al. 2010).

In Fig. 4.2.3A, the influence of stirring, freezing, and whipping on the enzyme activity is shown. It is clearly observable that neither stirring nor freezing or whipping influenced the activity of β -Gal. This can be explained by the ingredients of the formulation, which protect the enzyme against surface denaturation and concentration during freezing. Firstly, the phosphate buffer can stabilize β -Gal during freeze-thawing cycles due to preferential exclusion comparable to the explanation of Timasheff (1992) for the protective properties of saccharides in protein solutions. This was also assumed by Jiang and Nail (1998) in a study about the influence of process conditions on the residual activity of enzymes. Further, the small and non-ionic surfactant polysorbate 80 is highly surface-active and might have prevented β -Gal from reaching the surface. Polysorbates are widely used in the pharmaceutical industry as a protective agent against surface degradation (Manning et al. 2010; Charman et al. 1993). Besides the formation of air-water interfaces during the whipping, the surface area, which is formed during the freezing process in the form of ice crystals, correlates with the extent of protein damage (Hillgren et

al. 2002). We assume, therefore, that the used amount of PS80 was able to protect proteins also during the freezing process.

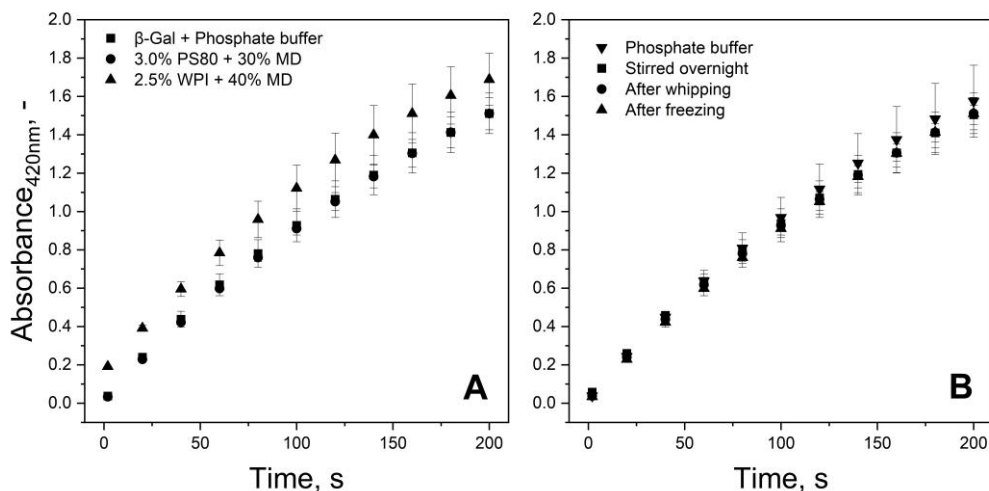


Fig. 4.2.3: (A) Influence of stirring, whipping, or freezing on the change of absorbance due to cleavage of ONPG by β -gal with 30%MDX, 3% PS80 in comparison to an untreated enzyme in buffer solution, and (B) absorbance of samples over time for β -galactosidase containing samples with 2.5% WPI and 40%MDX (\blacktriangle), 3% PS80 and 30% MDX (\bullet) and β -galactosidase in phosphate buffer (\blacksquare) at 24 °C.

The influence of different formulations is shown in Fig. 4.2.3B. It can be observed that the slope is equal for the investigated samples, while the initial absorbance differed. This can be explained by formulation-dependent turbidity, which was higher at 40% MDX compared to samples with 30% MDX concentration. This effect was also determined for other sample formulations containing WPI, maltose, sorbitol, or sucrose (data not shown). However, this was declared not to be a problem since no differences in slope were observable.

4.2.4 Conclusion

Overall, in chapter 4.2.3.2 it was shown that the investigated β -galactosidase formulations were stable during the preparation steps before the conventional or microwave-assisted drying process. Therefore, no degradation of β -Gal due to the sample preparation is expected, and hence, denaturation effects can be attributed to the drying process. Further, the different foaming agents and sugar types did not influence the enzyme activity of β -Gal, even at high concentrations. Furthermore, it was shown that the denaturation temperature of dialyzed β -Gal is between 40 and 50 °C. However, it is worth to note that for subsequent drying experiments, different saccharide types are investigated. Concerning Timasheff's (1992) results, it can be assumed that the improvement of thermal stability due to the addition of saccharides will also be dependent on the type of saccharide. Nonetheless, the used saccharide concentrations are generally high (>10%), and therefore, the set-up should be suitable to compare results within one saccharide type.

4.3 Water vapor pathways during freeze drying of foamed product matrices stabilized by maltodextrin at different concentrations

Summary and contribution of the doctoral candidate

An open question for the freeze drying of foamed matrices was why foamed matrices are drying faster compared to non-foamed samples. Further, different behavior of drying kinetics between different foamed products was reported by other research groups but just explained and not investigated in detail.

Therefore, this study was based on the hypothesis that the different drying behavior can be attributed to the foam properties and that due to a change of foam properties, the drying behavior can be changed from a “non-foamed-like” to a “foamed-like” drying behavior. It was assumed that this effect would appear due to the change of internal mass transfer or water-vapor transfer. Therefore, the water vapor pathway was investigated during freeze drying and correlated with the conditions during microwave-assisted freeze drying of foams. For this, the drying process was investigated inside a freeze drying microscope for samples with different bubble-size distribution, overrun, and concentration of thickening agent (maltodextrin). The findings from the microscope were correlated with the drying results from microwave-assisted freeze drying. An important aspect was that the heating of the sample was volumetric during the microscope as well as during the drying experiments. Thereby, it was expected that a good correlation between microscopic and macroscopic experiments would be achievable.

It was shown that foams with high overrun have higher water diffusion coefficients compared to high-density foams. However, the drying time of high-density samples was shorter, as the total amount of water to sublimate was less compared to low-density samples. Further, it was observed that samples with low density sublimate throughout the product, whereas products with high density form a single drying front. This results in a more “liquid-like” drying behavior compared to low-density foams. Hence, it was assumed that the change in drying behavior has only an impact on the quality of the dried product, as foam drying provides several advantages compared to the drying of non-foamed materials.

The substantial contribution of the doctoral candidate was the conception and design of the experiments. Further, he was substantially involved in the performance of experiments, acquired parts of the data for the manuscript, and interpreted the data set. Furthermore, the critical literature review and chiefly writing of the manuscript were done by the candidate. Co-authors contributed to the experimental part and/or in the discussion of the results and provided input to the drafted manuscript prior to and during submission.

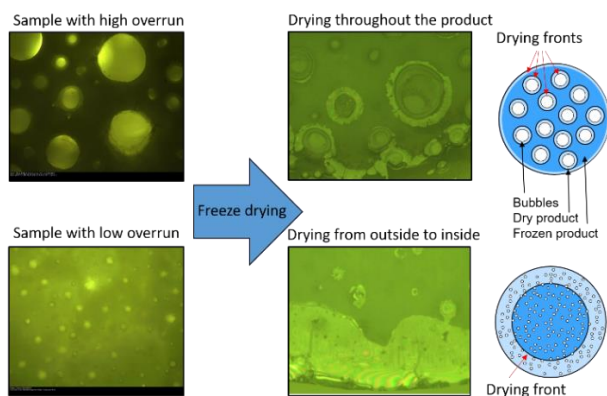
Water Vapor Pathways during Freeze drying of Foamed Product Matrices Stabilized by Maltodextrin at Different Concentrations²

Peter Kubbutat *, Annika Tauchnitz and Ulrich Kulozik

Chair of Food and Bioprocess Engineering, TUM School of Life Sciences, Technical University of Munich, 85354 Freising, Germany; annika.tauchnitz@tum.de(A.T.); ulrich.kulozik@tum.de(U.K.)

* Correspondence: peter.kubbutat@tum.de

Received: 15 October 2020; Revised 10 November 2020; Accepted: 11 November 2020; Published: 15 November 2020



Abstract:

This study aimed to identify the water-vapor transport mechanisms through an aerated matrix during microwave freeze drying. Due to the larger surface area and lower water vapor transport resistance of an aerated product compared to the solution, foam structures dry faster. Different foam structures were produced with different maltodextrin (MDX) concentrations (10–40%) as a foam-stabilizing agent. Depending on the initial viscosity of the solution prior to foaming, the samples differed in overrun (41–1671%) and pore size ($d_{50} = 58\text{--}553\ \mu\text{m}$). Experiments were partially performed in a freeze drying chamber of a light microscope to visualize structural changes in-situ. Different mechanisms were identified explaining the accelerated drying of foams, depending on the MDX concentration, above or below 30%. At lower MDX concentration, high overruns could be produced prior to freezing with big bubbles and thin lamellae with short diffusion pathway length. At 40% MDX concentration, the viscosity was too high to integrate much air into the product. Therefore, the foam overrun was low and the bubble size small. Under these conditions, the water vapor generates high pressure, resulting in the formation of channels between bubbles, thus creating the pathways with low resistance for a very fast water vapor mass transfer. In addition, microwave freeze drying experiments using a pilot plant unit were conducted to validate the findings of the freeze drying microscope. A reduction of the drying time from 150 min (10% MDX) to 78 min (40% MDX) was achieved.

Keywords: foam drying; freeze drying; channel formation; maltodextrin; process acceleration; cracks

² Original publication: Kubbutat, P.; Tauchnitz, A.; Kulozik, U. (2021) Water Vapor Pathways during Freeze-Drying of Foamed Product Matrices Stabilized by Maltodextrin at Different Concentrations, *Processes*, 8, 1463. <https://doi.org/10.3390/pr8111463> Adapted original manuscript. Adaptions of the manuscript refer to enumeration, citation style, spelling, notation of units and format. Permission for reuse of article is granted by MDPI and authors.

References of all chapters are merged at the end of the dissertation.

4.3.1 Introduction

To increase the shelf life of biogenic substances of relevance in the food and pharmaceutical industries such as proteins, antibodies, immunoglobulins or microorganisms and to improve their handling, biomolecules are often preserved by freeze drying (FD), which mainly uses sugar as protectants (Pikal 1990a, 1990b). FD has been well established as a very gentle process, which maintains high physiological activity of the substrates (Flickinger 2013). However, FD is a highly time- and energy-consuming process, and thus often presents the main capacity bottleneck in the entire production chain for biotechnological applications (Schmitt 2012).

To accelerate the drying process, energy can be introduced using microwave technology, which allows a more effective and more uniform volumetric energy input (Ambros et al. 2019b), and by foaming the product before drying. This will increase the surface area of the product and lower the water vapor transfer resistance (Huang et al. 2015). Several studies have shown that foam drying results in high-quality products and shorter drying processes (Ozcelik et al. 2019a; Thuwapanichayanan et al. 2012; Hajare et al. 2006; Ratti and Kudra 2006b). In addition, foam drying can possibly be used to process products that are difficult to dry, such as sticky tomato (Kadam and Balasubramanian 2011; Ratti and Kudra 2006a), raspberry (Ozcelik et al. 2019b) or mango pastes (Lobo et al. 2017).

One advantage of drying liquid foam is that the lamellae act as capillaries, pumping water to the surface (Rajkumar et al. 2007). This accelerates the drying process, whereas the lower heat-transfer rate appears to be non-dominant (Ratti and Kudra 2006a). However, because of the natural instability of foam, it tends to collapse before being dried (Walters et al. 2014). To stabilize the foam, sugar and other polymers are used to increase the viscosity of the bulk phase before the drying starts. Thus, producing kinetically stable foam becomes possible, which allows it to withstand foam decay until stabilization due to solidification when subjected to the drying process (Ambros et al. 2019b).

Freezing of foam yields another possibility of preserving the foam characteristics over the entire drying process, which enables the development of drying models similar to that used by Sochanski et al. (1990) for the microwave-supported freeze drying (MWFD) of aerated milk. These authors stated that the water vapor leaves the frozen foam through air voids, creating an open porous structure where gas can pass through the structure without resistance. In their study, they concluded that their model appeared to be valid, however the water vapor pathway has yet to be identified by further experiments. As shown in a study by Wang et al. (Wang et al. 2015), who investigated the foam freeze drying of a mannitol, skim milk and sodium carboxymethylcellulose containing formulation the drying speed and vapor transport can be positively influenced by the use of initially foamed samples. Further, they assumed that the drying will take place throughout the sample. Nonetheless, they assumed this only by temperature

measurement inside their sample mold, but did not validate this experimentally by microscopic analysis. While the background of foam freeze drying has not yet been fully understood, industry is already using this technology, e.g., for pharmaceutical forms of delivery (Davies), the drying of coffee (Wertheim and Mishkin), apple juice (Raharitisfa and Ratti 2010) or egg white concentrates (Muthukumaran et al. 2008).

The approach in the present study was therefore the investigation of the drying behavior of foam with different properties to identify the not fully understood drying mechanisms of frozen foam. Different concentrations of the polysaccharide maltodextrin were used in combination with surfactant polysorbate 80. This process resulted in different foam properties such as volume increase (overrun) and bubble size and gave the possibility of examining the water vapor pathway of different product structures. Regarding freeze drying of bulk solid materials, some studies investigated the effect of pore size on the drying kinetics. While small pores (<20 μm) resulted in a single, sharp sublimation front starting from the top (Liapis and Bruttini 2009), particles of a few hundred micrometers dry with two sublimation fronts starting from the bottom and the top simultaneously (Chitu et al. 2015). For particles of several millimeters in size, the sublimation was reported to start from the surface of the single individual particles throughout the product (Trelea et al. 2009). Studies by Foerst et al. (2020) looked at the whole range of pore size on frozen bulky solids on freeze drying and confirmed the findings of these earlier studies regarding the effect of pore size as a significant impact on the drying kinetics (Liapis and Bruttini 2009). Even though the freeze drying of bulky solids with outer pores does not seem to be directly comparable with the freeze drying of foams, where pores are inside the product, the influence of the pore size can be an indication also for the behavior of foam drying. Therefore, the purpose of this study was to identify and assess how water vapor transport occurs through porous, i.e., foamed and highly viscous or solid frozen matrices, which is of equal interest for conventional and microwave-supported drying processes. The hypothesis of this study therefore was that different carbohydrate concentrations have a structural impact on the foamability and, thus, on the drying behavior of the foam. By changing the drying behavior, it can be assumed that the water vapor pathway itself will change because of the differences in lamellae thickness and inner surface area.

The drying process was observed using a freeze drying microscope, which allowed online observations of the whole freeze drying process inline, including freezing of the liquid foam and the consequent drying process. The results were compared with those of the pilot-plant experiments to validate the findings from the microstructural analysis of freeze drying.

4.3.2 Materials and methods

4.3.2.1. Materials

Polysorbate 80, which was used as foaming agent, was obtained from Sigma-Aldrich Co. LLC., (St. Louis, Missouri, USA). Maltodextrin DE6 (MDX) was purchased from Nutricia GmbH (Erlangen, Germany). All reagents were of analytical grade.

4.3.2.2. Sample preparation

Sample solutions of 200 g each were prepared by mixing and dissolving 3% (w/w) polysorbate 80 with different amounts of maltodextrin DE6 (0% to 40% in steps of 5% (w/w)) in demineralized water. The application of different maltodextrin concentrations provided the opportunity to create foam with a broad range of bubble sizes and different foam volumes, i.e., overruns. To ensure full hydration, the sample solutions were gently stirred using a magnet stirrer (Maxi Direct, Fisher Scientific GmbH, Schwerte, Germany) at 200 rpm for 12 h at 4 °C. Prior to the experiments, the sample solutions were tempered at 20 °C in a water bath (F3, Fisher Scientific GmbH, Schwerte, Germany).

4.3.2.3. Measurement of dielectric constant

The dielectric constant was measured with a dielectric kit for vials (μ WaveAnalyser, Püschner GmbH & Co. KG, Schwanewede, Germany) inside a -20 °C chamber following in principle the method of Péres-Campos et al. (2020). One milliliter of sample solution was transferred into a glass vial (1MLFBG, 40 × 8 mm, VWR International GmbH, Darmstadt, Germany) and tempered at -20 °C for at least 8 h to ensure that the temperature is in equilibrium. Thereafter, the dielectric constant was measured at 2450 MHz and calculated by the software μ WaveAnalyser (Version 3.2.0, Püschner GmbH & Co. KG, Schwanewede, Germany).

4.3.2.4. Foam preparation

A total of 150 g of the sample solution was whipped using a commercial planetary mixer (ARTISAN 5KSM150PS, KitchenAid, St. Joseph, MI, USA) for 15 min at 220 rpm and 20 °C. The mixer had a wire-whisk geometry (K45WW, KitchenAid, St. Joseph, MI, USA).

4.3.2.5. Determination of bubble size distribution and overrun

The overrun is defined as the percentage increase in volume of the foamed sample greater than the volume of the original sample, which is in our case the volume of the solution. It was determined as described by Kreuß et al. (2009) and calculated according to Equation (4.3.1), where m_S is the mass of the sample solution and m_F is the mass of the foam.

$$\text{Overrun (\%)} = \frac{m_S - m_F}{m_F} \cdot 100 \quad (4.3.1)$$

The bubble size distribution was determined using an optical microscope (Axiovert 135, Carl Zeiss AG, Oberkochen, Germany) with 10-fold magnification. The foam samples were gently

transferred to a microscope slide 15 min after the foam formation. Photographs were taken across the foam. A number of at least 300 bubbles per sample were analyzed and the d_{50} value was calculated using the software AxioVision (Version 4.8.2.0, Carl Zeiss AG, Oberkochen, Germany).

4.3.2.6. Examination of freeze drying behavior using a freeze drying microscope

Observation of the freeze drying process was made possible using a freeze drying microscope (Olympus BX51, Olympus Europa SE & Co. KG, Hamburg, Germany). Here, a single foam drop was placed on the microscope slide. A spacer between the microscope slide and cover glass prevented foam deformation. The freezing and drying processes were documented using a FireWire camera PL-A662 (PixeLINK®, Navitar Inc., New York, USA). Next to the picture, pressure, temperature and cooling rate were documented. The pressure was set using a vacuum pump (E2M1.5, Edwards Germany GmbH, Munich, Germany) that was connected to the microscope software Linksys 32 (Linkam Scientific Instruments Ltd, Surrey, UK) and controlled by the active pirani gauge APG-L-NW16i (Edwards Germany GmbH, Munich, Germany). To observe the drying process, reflected and transmitted lights were used. For tempering, the stage was equipped with a Peltier element for heating and cooling (Fig. 4.3.1). In order to achieve fast cooling rates, a liquid nitrogen vessel was connected to the stage. Due to the thin layer of sample, it was assumed that the heating of the freeze drying microscope is comparable with the volumetric heating of the microwave drier.

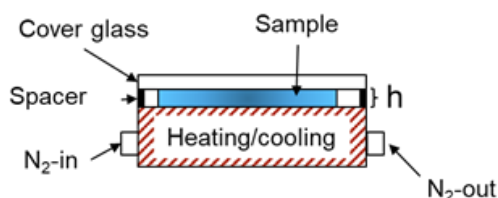


Fig. 4.3.1: Vertical cut of the heating/cooling unit inside the freeze drying microscope.

The temperature was set at a rate of $-5\text{ °C}\cdot\text{min}^{-1}$ to 0 °C . Subsequently, the temperature was set to -45 °C at a sample dependent freezing rate. In order to be able to compare microwave-assisted drying and freeze drying microscope, the freezing rates of 120 g foam samples were measured inside the -80 °C freezer. The temperature sensors were placed at the half thickness of sample and located at both relevant sides (towards the door of the freezer and in direction of the freezers cavity) and the center of the sample. The freezing rate was calculated by the mean of the temperature slopes until nucleation occurred and used for the setup in the freeze drying microscope (Table 4.3-1). During the freezing step, the pressure was set to 0.1 mbar. After the sample reached -45 °C , the sample was equilibrated for 5 min. Thereafter, the temperature was increased by $2\text{ °C}\cdot\text{min}^{-1}$ up to -25 °C and held for 90 min, while the pressure was kept constant at 0.1 mbar. Thereafter, the temperature was set at a rate of $10\text{ °C}\cdot\text{min}^{-1}$ at 20 °C . Then, the pressure was also set to ambient conditions.

Pictures were captured using reflected light and transmitted light during the cooling, freezing and drying steps. After the drying process and pressure release, a picture of the final product was taken.

Table 4.3-1: Calculated freezing rates and product thickness, L, for 120 g of foamed sample at the -80 °C freezer.

Concentration Maltodextrin, %	Freezing Rate, °C·min ⁻¹	Thickness of Samples, L, cm
10	-	4.90
20	2.5	2.16
25	2.5	1.37
30	3.5	0.85
35	6.0	0.60
40	7.0	0.34

4.3.2.7. Microwave-supported freeze drying

For the microwave-supported freeze drying process, a μ Vac0150fd microwave dryer was used. For the process control, the drying plant was connected to a computer and software μ WaveCAT (the hardware and software were both from Püschner GmbH & Co. KG, Schwanewede, Germany). We transferred 120 g foam into a 230 mm diameter sample glass and gently flattened it. The sample was frozen overnight at a -80 °C freezer (BF-U538, Buchner Labortechnik, Germany) before the drying process was started. The drying of samples was performed at 0.1 mbar and a microwave power input of 200 W. The surface temperature was measured using a pyrometer (Heitronics Infrarot Messtechnik GmbH, Wiesbaden, Germany) and set to a maximum temperature of 20 °C. The weight of the sample was recorded during the process with a scale, which was connected to the turntable. The drying process was stopped when no mass loss occurred during 10 consecutive minutes. The drying time was estimated after the drying process as the time difference between the start of the drying and 0.5% of the residual moisture. This value has been chosen because of the accuracy of the scale for low water evaporation rates. Finally, all drying runs resulted in the same residual water content of 4.5% and water activity of 0.05.

4.3.2.8. Determination of the residual water content

The initial moisture content was gravimetrically measured using Smart Turbo 6 (CEM Corp., Germany). For the determination of the water content of the dried samples, the Karl Fischer titration method (Fischer 1935) was used (Schott AG, Mainz, Germany). The analysis was conducted using automatic titrator Titro Line KF (Schott AG, Mainz, Germany). A 0.1 g dried sample was used for each measurement. All reagents used for the analysis were purchased from Sigma-Aldrich Inc. (Steinheim, Germany).

4.3.2.9. Determination of water activity

The water activity of the dried sample powder was determined at 25 °C using water-activity meter AW Sprint (Novasina AG, Lachen, Switzerland) with a sensitivity of 0.001 following practical hints described by Bell & Labuza (2000), with modifications. Standard salt solutions (Novasina AG, Lachen, Switzerland) of known water activity were used for sensor calibration at the measurement temperature.

4.3.2.10. Determination of the diffusion coefficient

In addition to the measured water activity and water content, the effective diffusion coefficient D_{eff} was calculated. The effective diffusion coefficient describes the intrinsic mass transfer property of moisture as described by Karathanos et al. (1990). It can be calculated using Fick's second law (Equation (4.3.2)), where c corresponds to the moisture content (kg water per kg dry solids) and the length of diffusion path x .

$$\frac{\partial c}{\partial t} = D_{\text{eff}} \frac{\partial^2 c}{\partial x^2} \quad (4.3.2)$$

The equation was simplified for uniform initial moisture distribution (Equation (4.3.3)) and slab geometries (Equation (4.3.4)) by Crank (1975)

$$\text{MR}(t) = \frac{MC_x - MC_e}{MC_0 - MC_e} \quad (4.3.3)$$

$$\text{MR} = \frac{8}{\pi^2} \sum_{n=1}^{\infty} \frac{1}{(2n-1)^2} \exp\left[-(2n-1)^2 \frac{\pi^2 D_{\text{eff}} t}{4L^2}\right] \quad (4.3.4)$$

where $\text{MR}(t)$ is the moisture ratio at any drying time, MC_x is the mean moisture content at the time t , MC_e is the equilibrium moisture content, MC_0 is the initial moisture content, D_{eff} is the effective diffusivity and L the thickness of the sample. The calculated thickness of the samples can be found in Table 4.3-1. For long drying processes, Equation (4.3.4) can be simplified by only using the first term in the series equation and taking the natural log, which results in Equation (4.3.5) (Tutuncu and Labuza 1996).

$$\ln \text{MR} = \ln \frac{8}{\pi^2} - \frac{\pi^2 D_{\text{eff}} t}{4L^2} \quad (4.3.5)$$

With this, a plot of $\ln \text{MR}$ with respect to the time gives a straight line with a slope, which can be used to determine D_{eff} (Equation (4.3.6)) (Salahi et al. 2015).

$$K = \frac{\pi^2 D_{\text{eff}}}{4L^2} \quad (4.3.6)$$

where K is the slope of the logarithmic moisture ratio as a function of time. It was assumed that the drying of the sample occurs from both sides simultaneously. Therefore, the thickness L was divided by two (Karathanos et al. 1990). As the microwave-supported freeze drying has

two drying sections, an average value was calculated out of the slopes of primary and secondary drying section. This was done in order to receive a value for the ability of water to leave the different product matrices with regard to the different product thicknesses and water contents. The primary drying sections refers mostly to sublimation, while in the secondary drying section, desorption and diffusion are limiting.

4.3.2.11. Statistical analysis

For solution and foam characterization, three batches of each sample formulation were prepared and each sample was analyzed in duplicate. Thus, a six-fold determination was carried out. Two samples of each formulation were investigated using the freeze drying microscope and microwave-assisted freeze drying. The mean values were plotted in the diagrams and error bars indicated the standard deviation.

4.3.3 Results and discussion

4.3.3.1. Microwave-supported freeze drying

Fig. 4.3.2 shows that the required drying time decreased from 2.5 h with 10% maltodextrin (MDX) content to 1.3 h for samples with 30% MDX content. The dashed line is guide to the eyes and shows how the speed of drying changed with different carbohydrate content. The addition of more than 30% MDX to the sample did not result in further acceleration of the drying process because a longer secondary drying stage due to the thicker lamellae of highly carbohydrate-concentrated samples was expected. Further, melting and macroscopic cracks occurred sometimes for carbohydrate concentrations above 30% MDX content (data not shown), which indicated local overpressure and overheating during the drying process. It was assumed that the dielectric properties were not the reason for the crack formation, because the dielectric constant of frozen solutions (-20 °C, 2450 MHz) were generally very similar (10% MDX 3.75 ± 0.43 ; 20% MDX 3.64 ± 0.05 ; 30% MDX 4.08 ± 0.13 and 40% MDX 4.22 ± 0.03). With regard on high penetration depth of microwaves into ice, it should be mentioned that the microwaves are able to pass the sample several times and thus, the dielectric constant provided no explanation for the differences in the heating kinetics or required drying time.

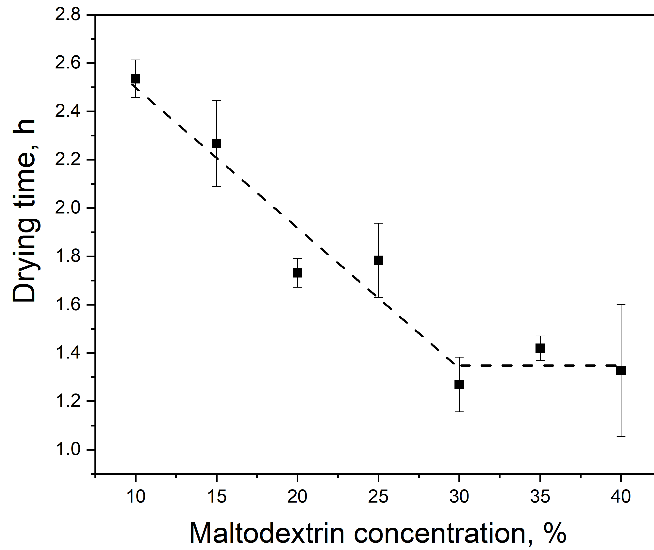


Fig. 4.3.2: Drying time of polysorbate 80 foams as a function of the maltodextrin content.

A shorter drying time resulting from the MDX addition was also reported by Ozcelik et al. (2019a) in microwave processing of raspberry foams. Similar to Ozcelik et al., a lower MDX content was expected to exhibit higher overrun due to the lower viscosity, which was expected to yield higher diffusion coefficients because of lower mass transfer resistance. This can be explained by a more efficient water pathway due to the lower effective thickness of samples with high overrun. Fig. 4.3.3 shows the apparent diffusion coefficient and the slope of the primary drying section as a function of the MDX content.

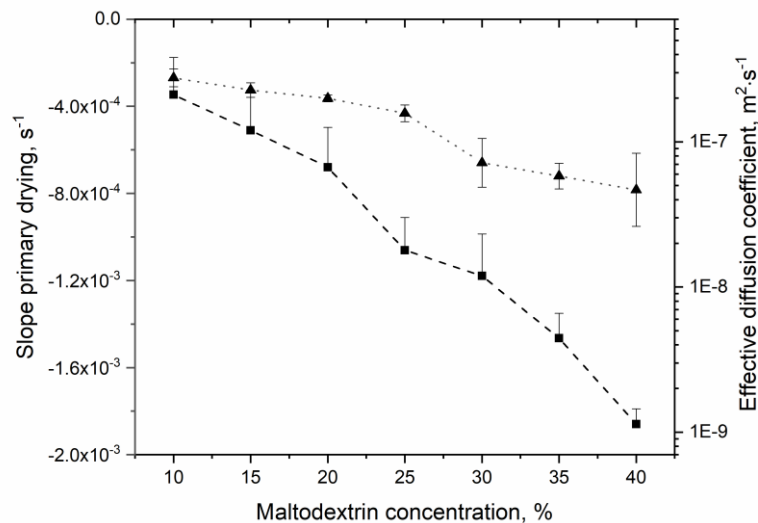


Fig. 4.3.3: Effective diffusion coefficient (■) and slope of the primary drying section (▲) as a function of the maltodextrin concentration of microwave-supported freeze drying (MWFD) dried samples.

We could observe that the effective diffusion decreased with increasing MDX content from 2.11×10^{-7} to $1.14 \times 10^{-9} \text{ m}^2 \cdot \text{s}^{-1}$, which is in accordance with results reported in the literature (Salahi et al. 2015). We assumed that the decrease in the water diffusion was a result of the

thicker lamellae. Further, the slope of the primary drying section significantly increased above MDX contents of more than 25%. This result could be due to the thinner product cake at lower overruns (Table 4.3-2), as well as the formation of cracks, which would be in accordance with the macroscopically observed cracks at the surface of the product cake. In order to be able to clarify which of these explanations apply, we will present results obtained by a freeze drying microscope in chapter 4.3.3.2. A decrease in the effective diffusion with decreasing overrun was also reported by other researchers. Kadam and Balasubramian (2011) and Thuwapanichayanan et al. (2012) investigated the influence of different foaming agents on the drying behavior and obtained a high effect of the overrun on the texture and required drying time. In contrast to our study, in both aforementioned studies the lamellae remained still liquid, and therefore, an even higher effect of overrun on the diffusivity was expected. If one compares Fig. 4.3.2 and Fig. 4.3.3, the results appear as contradictory at first sight. However, this can be explained by the fact that smaller amounts of water have to be sublimated at higher the dry matter content (maltodextrin level). This results in a decreasing drying time, which here indicates that the total water content exerted a greater effect on the drying time than the water diffusion during the secondary drying stage. This can be also observed from the plot dm/dt over the drying process (see Supplementary 4.3-1): While samples with 10% MDX showed slow but constant sublimation rate during the drying, samples with 40% MDX first had a higher rate of sublimation but remained longer in a slower sublimation stage.

The temperature and moisture ratio of the samples are shown in Fig. 4.3.4. Generally, the temperature overshoot of approximately 5 to 10 °C at the end of the drying process. While for samples with 10%–30% MDX content, the temperature increased evenly during the drying process, the temperature of the samples with 40% MDX content sample did not. Instead, the temperature largely increased in the middle of the drying process. Further, the surface temperature of the sample strongly varied, which can be observed by a higher amplitude. Both could be explained by the non-uniform heat distribution inside the sample and thus cracks appeared. These cracks made it possible to measure the hot temperature inside the sample and whereas the top of the sample surface remained comparably cold, the temperature changed with high frequency. For MDX contents below 30%, this non-uniform temperature distribution was not detected, as confirmed by optical analysis of the samples. None of the samples with MDX content below 30% exhibited non-uniform structural changes. With regards to the moisture, samples with 10%–30% MDX content exhibited more uniform drying behavior than those with 40% MDX content. Further, we could observe that in this example, the drying time was as long as for the sample with 30% MDX content.

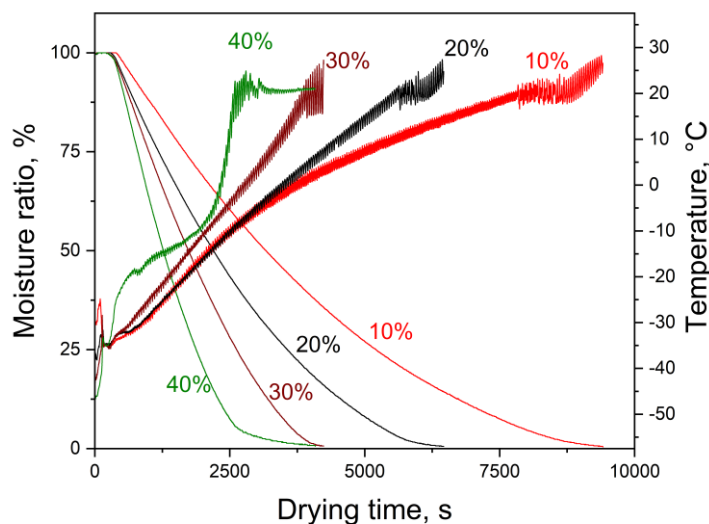


Fig. 4.3.4: Relative moisture ratio (decreasing curves) and temperature (increasing curves) during microwave-supported freeze drying of polysorbate 80 foam with different maltodextrin contents.

This result could be explained by a certain overheating of the sample. The overheating occurred randomly and within single spots, which are a so-called hotspots. While the power has to be reduced to prevent further product damage, other parts of the sample remained at low temperature. Therefore, the drying speed greatly decreased in the end of the drying as clearly shown in Fig. 4.3.3, and the final drying time was about the same as for 30% MDX concentration, which explains the larger standard deviation for MDX = 40% in Fig. 4.3.2. Samples below 40% MDX content might also form hotspots, but with non-observable intensity.

The reasons for the acceleration of the drying process between the samples with 10% and 30% MDX contents and the constant drying time for samples with MDX concentrations between 30% and 40% were investigated using a microscope that was operated under freeze drying conditions.

4.3.3.2. Freeze drying microscope results

The observation of the freeze drying process inside the freeze drying microscope was divided into five different sections: liquid foam, frozen foam, initial drying phase, mid of drying time and end of drying. Subsequent to the end of drying, the microscope was set back to ambient conditions and pictures of the final product were made. For each section, an out of single snapshots assembled picture of the transverse section was taken. In Fig. 4.3.5, liquid foams are shown using transmitted-light microscopy. As a result of the different amounts of MDX in the formulation, the viscosity varied, and thus, the bubble size varied from big bubbles at low carbohydrate concentration to small bubbles at high carbohydrate concentration. Bubble size d_{50} and the overrun value are listed in Table 4.3-2. A large reduction of bubble size and overrun could be observed with increasing MDX content.

Table 4.3-2: Bubble size d_{50} and overrun of polysorbate 80 foam at different maltodextrin concentrations.

Maltodextrin content, %	10	20	30	40
Bubble size, d_{50} , μm	553 ± 51	202 ± 29	102 ± 14	58 ± 10
Overrun, %	1671 ± 251	715 ± 71	233 ± 7	41 ± 3

We could clearly observe that the bubble size decreased less with increasing MDX concentration than the overrun did, which could be explained by the reduced number of bubbles in the highly viscous samples at high MDX concentrations. Samples with 41% overrun are commonly not defined as real foam because their gas volume fraction is below 0.5 (Wilson 1989). Therefore, these samples can be identified as bubbles in liquid, and we expect that their behavior is more similar to that of a liquid instead of that of a foam.

Further, the lamellae were shown to be thicker with increasing carbohydrate concentration, which also resulted in a darker appearance of photographs shown in Fig. 4.3.5 from left to right because the light transmission was reduced with higher MDX concentration. Less, but larger bubbles can be seen in Fig. 4.3.5A, while bubble numbers go up and bubble sizes decrease from Fig. 4.3.5A–E.

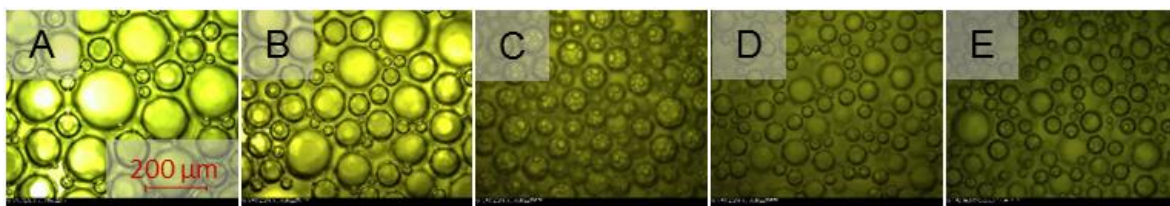


Fig. 4.3.5: Liquid polysorbate 80 foam with maltodextrin concentrations of (A) 20, (B) 25, (C) 30, (D) 35 and (E) 40% using transmitted light. The scale bar in (A) can also be applied to (B)–(E).

Fig. 4.3.6 shows the different freeze drying steps using transmitted-light microscopy. During the initial phase of drying, each bubble had its own drying front (Fig. 4.3.6C), which can be observed by the dark color around the single bubbles. However, because of its dependency on the carbohydrate concentration, these fronts appeared to very slowly progress. Therefore, the pressure inside the small bubbles increases due to the sublimation of water (Fig. 4.3.6C), until critical pressure that formed cracks was reached (Fig. 4.3.6D,E). The reason for the increase in pressure was that because of the lack of free volume, no flow pathway existed for the sublimated water. Finally, the main drying front, directed from outside to inside the sample reached the high pressure areas and, together with the cracks and formed pores inside the lamellae, allowed the sublimated gas to leave the product.

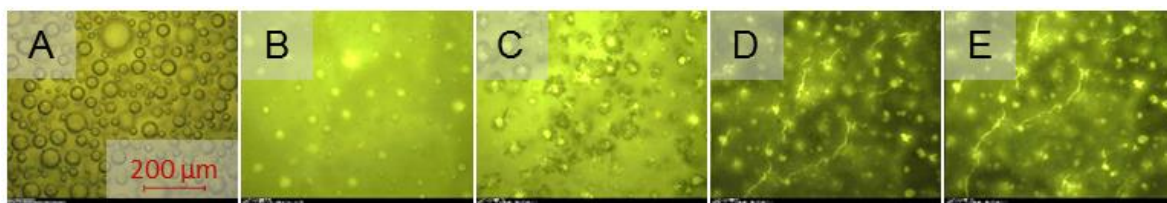


Fig. 4.3.6: Drying of a polysorbate 80 foam with 40% MDX at different stages of the drying process: (A) liquid, (B) frozen, (C) early drying, (D) mid drying, (E) final drying. The scale bar in (A) can also be applied to (B)–(E).

This showed that the drying did not take place similar to that in a loosely structured porous bulk as described by Sochanski et al. (1990), where the water was free to leave the product using the voids as channel. The issue then was how the water release happened in case of low carbohydrate concentration. Fig. 4.3.7 shows a situation during the initial drying step that compared foam containing 20% and a 40% MDX. By using reflected light, the already dried areas had a bright color, whereas the dark color indicated that the sample still contained water. We could clearly observe that for the lower MDX content the water is primarily sublimated into the bubbles (Fig. 4.3.7A), whereas for 40% MDX content an additional clearly separated drying front moved from outside to the center of the foam (Fig. 4.3.7B). This drying from outside in is more typical for the drying of solutions, as, e.g., observed by Yang et al. (2010) and supported our prediction for low overrun foam systems.

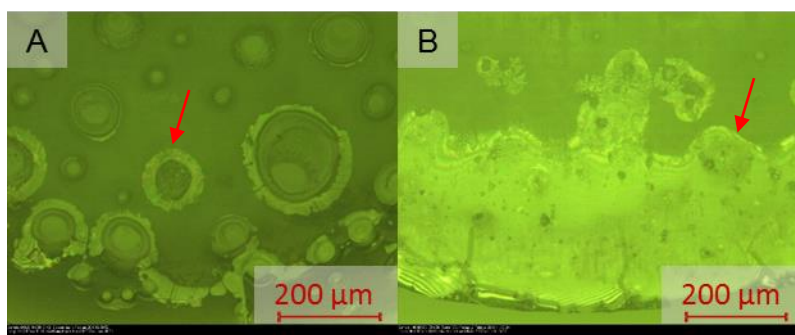


Fig. 4.3.7: Different drying mechanisms of foams with (A) 20% and (B) 40% maltodextrin (MDX) content, respectively, in the freeze drying microscope during the first drying stage.

For low carbohydrate concentrations of 10% and 20%, which resulted in more accessible volume inside the product, we expected that the drying fronts of the bubbles will combine (red arrow in Fig. 4.3.7A), providing the water vapor a channel to leave the product. This is more comparable with the expected model from Sochanski et al. (1990). Further, in the secondary drying, we required that the structure, which remained after the drying in the lamellae, must contain open pores with a low water transfer resistance. If the structure is too dense, water might slowly diffuse out of the lamellae, which could lead to a longer drying duration. The foams that were stabilized by low carbohydrate content uniformly and simultaneously became dry across the whole product because of thin lamellae and big bubbles. In contrast, the foam with the high-MDX-content behaved similar to a frozen liquid because of the thick lamellae, which

remained closed and solid during the beginning of the drying process. This condition prevented a fast transfer of water vapor through the lamellae, resulting in overpressure and crack formation. Therefore, the pathway for the water vapor transfer varied according to the carbohydrate content or the foam properties. Wang et al. (2015) investigated the foam-freeze drying of complex mannitol samples with a moderate solid content. They assumed that the drying front has to proceed throughout the product due to similar temperatures inside the sample at different positions during the first drying step. With our study, we are in agreement with this hypothesis for samples with 10–30% MDX content. Nonetheless, the microscopically detected changes of drying behavior within our samples' range show that further investigations of foam properties are necessary in order to identify the limitations of foam-freeze drying.

The final structures of the samples with 20% and 40% MDX content are shown in Fig. 4.3.8, which were assessed using transmitted-light microscopy. As a result of the dried MDX, the lamellae displayed a dark color, whereas the cracks and air voids exhibited brighter colored parts of the product. Other researchers also observed indications of liquid-like behavior in their raspberry foam with low overrun samples (Thuwapanichayanan et al. 2012), which indicated that the results were also valid for more complex systems.

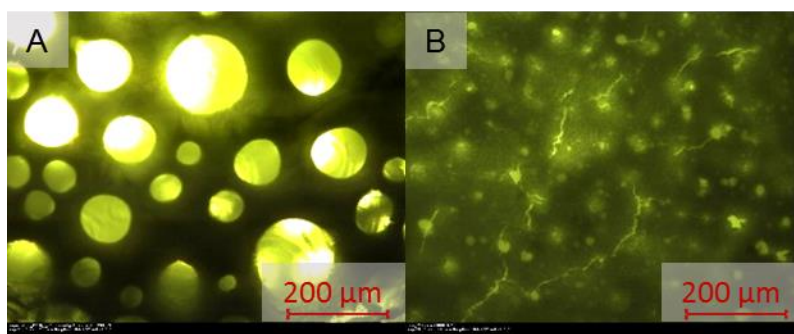


Fig. 4.3.8: Dried polysorbate 80 foam with (A) 20% and (B) 40% maltodextrin contents.

We could observe that the lamellae were intact for the samples with 20% MDX content, whereas at $c(\text{MDX}) = 40\%$ cracks occurred. This result indicated that the water vapor pathway at low concentrations occurred through the lamellae, whereas for high MDX concentration (40%), a higher pressure build-up must have occurred, because of the lower overrun and lower porosity, respectively (Fig. 4.3.9). Thus, less volume is available to take up the water vapor and cracks were created as additional pathways for the water vapor. This agrees well with the results presented in chapter 4.3.3.1. Generally, we observed that below a 25% MDX content, no cracks occurred during the first drying stage. At 30% MDX content, a few cracks were observed, and over 30% MDX content, the samples exhibited massive crack formation.

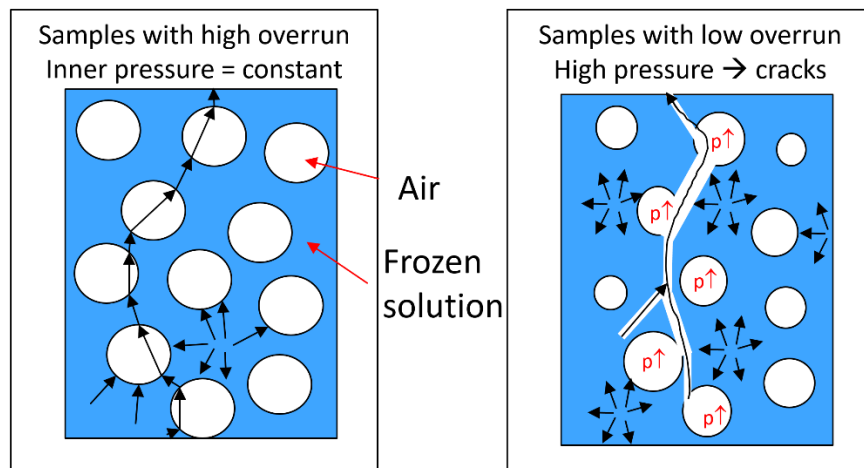


Fig. 4.3.9: Schematic pathway of water during the drying of samples with high and low overrun values.

4.3.4 Conclusion

Our study results show the cause of acceleration of the drying process due to the use of foam. For low carbohydrate concentration, a different pathway for the water vapor was found compared with that of the foam with high carbohydrate concentration was found. For low carbohydrate concentration, a simultaneous and uniform drying starting from the surfaces of the individual gas bubbles was observed across the whole product without any macroscopic channel or crack formation. The water vapor transfer occurred through the highly porous structure of dried lamellae. For high carbohydrate concentration, the thicker and denser lamellae resulted in higher water vapor transfer resistance. From this, it can be concluded that this results in a higher inner bubble pressure and bubble sublimation temperature. Crack formation therefore occurs when the inner pressure becomes too high. The cracks acted similar to channels and enabled water transfer out of the product. These new insights provide a better scientific understanding of freeze drying processes, which so far have only been phenomenologically observed. This is of relevance for a better process understanding of freeze drying and product design in food and pharmaceutical applications and can be further used for process acceleration to allow for shorter drying processes. In future studies, the effect of other sugar types on the quality of sensitive ingredients that result in a change in physiological activity or storage stability will be investigated.

Supplementary materials: The following are available online at <https://www.mdpi.com/2227-9717/8/11/1463/s1>, Supplementary 4.3-1: Sublimation rate of foams with MDX content between 10–40%.

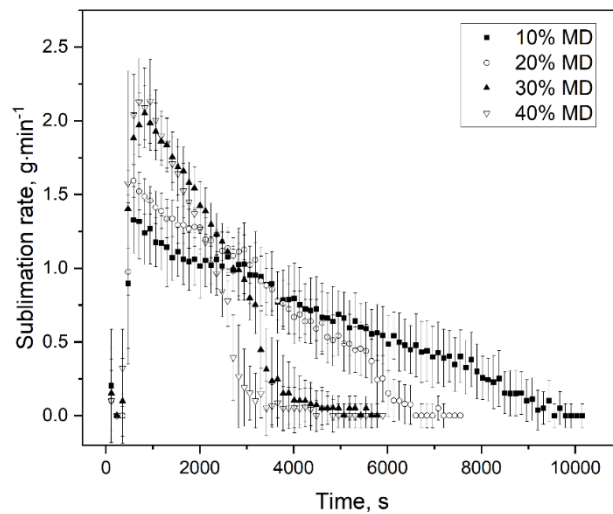
Author contributions: Experimental investigation, P.K. and A.T.; data curation, P.K. and A.T.; writing—original draft preparation, P.K.; writing—review and editing, U.K. All authors have read and agreed to the published version of the manuscript.

Funding: This IGF Project of the FEI was supported via AiF 18819N within the program for promoting the Industrial Collective Research (IGF) of the German Ministry of Economic Affairs and Energy (BMWi), based on a resolution of the German Parliament.

Acknowledgments: We would like to thank Christian Hansen A/S (Copenhagen, Denmark) for providing the freeze drying microscope. We also want to thank Prof. Petra Först at Technical University of Munich for her help with the freeze drying microscope.

Conflicts of interest: The authors declare no conflict of interest.

4.3.5 Supplementary



Supplementary 4.3-1: Sublimation rate of foams with MDX content between 10–40%.

4.4 Foam structure preservation during microwave-assisted vacuum drying: Significance of interfacial and dielectric properties of the bulk phase of foams from polysorbate 80-maltodextrin dispersions

Summary and contribution of the doctoral candidate

For foam mat drying, the stability of the foam throughout the process is a mandatory parameter since the drying speed and the product quality decrease in case of foam collapse. Therefore, the foam must be able to withstand the mechanical and thermal stress during the drying process. From the previous study, shown in chapter 4.1, it was known that sugars could influence the foam properties by the promotion of H-bonds between surfactants at the interface or the formation of H-bonds between surfactant and saccharide. Therefore, this study hypothesized that by influencing intermolecular interactions, the addition of maltodextrin in different amounts would also influence the surface rheological properties and the surface elasticity. As a result, the overall foam stability would be influenced by the addition of maltodextrin. Besides, the dielectric properties of the investigated formulations were investigated to gain information about their heating properties. Finally, the investigated formulations were dried with conventional and microwave-assisted vacuum drying to find differences and to relate the findings from interfacial properties to the foam decay behavior of the samples.

It was shown that the surface elasticity was strongly dependent on the used concentration of maltodextrin. Further, it was found that surface elasticity was an important property for the stabilization of foams during the drying process. Samples with a $\tan(\varphi) < 0.2$ seemed suitable for both, conventional and microwave-assisted vacuum drying. However, for MWVD, an indication was found that the dielectric properties of the foaming agents were important for the foam stability during the drying process. In contrast, the dielectric properties of the formulation were of minor importance. Overall, an influence of maltodextrin content on foam stability during vacuum drying processes was found.

The substantial contribution of the doctoral candidate was the conception and design of the experiments. Further, he was substantially involved in the performance of experiments and acquired parts of the data for the manuscript, and interpreted the data set. Furthermore, the critical literature review and chiefly writing of the manuscript were done by the candidate. Co-authors contributed to the experimental part and/or in the discussion of the results and provided input to the drafted manuscript prior to and during submission.

Foam Structure Preservation during Microwave-Assisted Vacuum Drying: Significance of Interfacial and Dielectric Properties of the Bulk Phase of Foams from Polysorbate 80–Maltodextrin Dispersions³

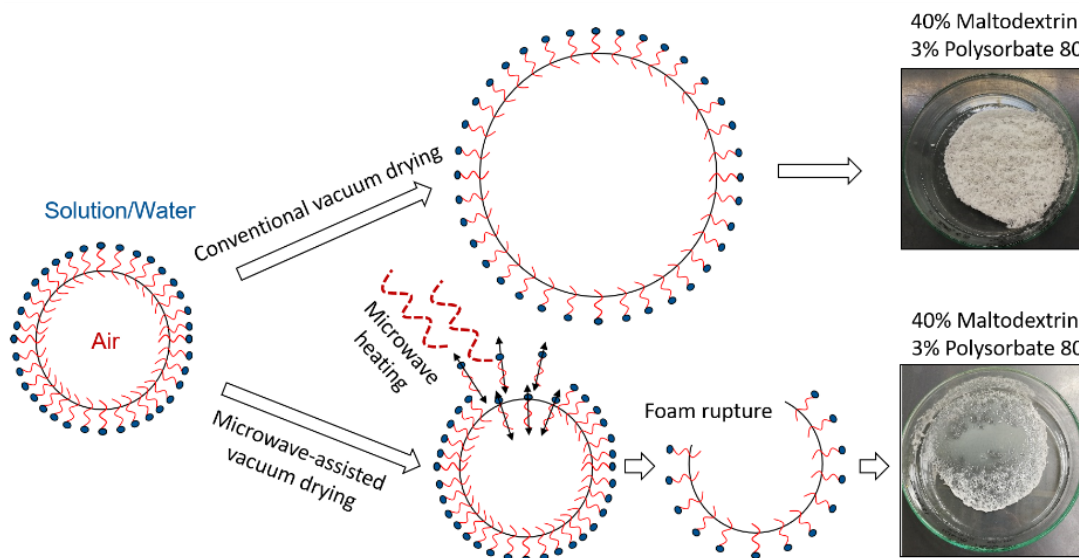
by Peter Kubbutat^{1,*}, Ulrich Kulozik¹ and Jannika Dombrowski^{1,2}

¹Chair of Food and Bioprocess Engineering, TUM School of Life Sciences, Technical University of Munich, Weihenstephaner Berg 1, 85354 Freising, Germany

²Nestlé Research, Société des Produits Nestlé SA, Route du Jorat 57, 1000 Lausanne, Switzerland

* Correspondence: peter.kubbutat@tum.de

Received: 24 March 2021; Revised: 3 May 2021; Accepted: 20 May 2021; Published: 22 May 2021



Abstract:

This study aimed at examining the cause of differences in the structure preservation of polysorbate 80–maltodextrin foams during microwave-assisted vacuum drying (MWVD) versus conventional vacuum drying (CVD). Aqueous dispersions of 3% polysorbate 80 and 0–40% maltodextrin were characterized for their dielectric and interfacial properties, and results were related to their drying performance in a foamed state. Surface tension and surface dilatational properties as well as dielectric properties clearly responded to the variation in the maltodextrin content. Likewise, the foam structure preservation during CVD was linked to the maltodextrin concentration. Regarding MWVD, however, foams collapsed at all conditions tested. Nevertheless, if the structure during MWVD remained stable, the drying time was significantly reduced. Eventually, this finding could be linked to the dielectric properties of polysorbate 80 rather than its adsorption kinetics and surface film viscoelasticity as its resonant frequency fell within the working frequency of the microwave drying plant.

Keywords: vacuum drying; surfactant; polysaccharide; foam decay; resonant frequency

³ Original publication: Kubbutat, P.; Kulozik, U.; Dombrowski, J. (2021) Foam Structure Preservation during Microwave-Assisted Vacuum Drying: Significance of Interfacial and Dielectric Properties of the Bulk Phase of Foams from Polysorbate 80–Maltodextrin Dispersions. *Foods*, 10, 6, 1163, <https://doi.org/10.3390/foods10061163> Adaptions of the manuscript refer to enumeration, citation style, spelling, notation of units and format. Permission for reuse of article is granted by MDPI and authors. References of all chapters are merged at the end of the dissertation.

4.4.1 Introduction

For the preservation of heat-sensitive biological material (e.g., bacterial cultures (Ambros et al. 2018; Bauer et al. 2012) enzymes (Jesus and Filho 2011) or pharmaceutical ingredients (McLoughlin et al. 2003)), vacuum drying has evolved into a promising alternative to time- and energy-intensive freeze drying. Besides advantages in the specific energy demand (Gehrmann et al. 2009) and drying time (Santivarangkna et al. 2007a), vacuum drying was shown to yield products of increased storage stability as compared to freeze drying. The increased storage stability was linked to product shrinkage during dehydration (Foerst et al. 2012), which, however, entails a prolongation of the third drying stage. In addition, due to the compactness of the dried product structure, its grindability is impaired. In this context, Ambros et al. (2019b) reported that microwave assistance can reduce the vacuum drying time by about 95%. This significant effect was related to the volumetric energy input of the microwaves allowing for a high mass transfer over all drying stages. Furthermore, controlled product aeration (i.e., foaming) prior to microwave-assisted vacuum drying (MWVD) was proposed to tackle the drawback of conventional vacuum drying (CVD) in terms of poor product grindability (Ambros et al. 2019a). Additionally, the drying process can be accelerated by means of foaming. This can be attributed to the higher specific surface of an aerated versus a non-aerated product as well as the presence of lamellae, which act as capillaries during the drying process, transporting the water to the product's surface (Rajkumar et al. 2007).

Overall, MWVD of foamed materials was shown to display a promising concept. However, it is important to note that product formulation (e.g., foaming agent, protectant, carrier) and characteristics (e.g., foam characteristics) as well as process conditions (e.g., pressure level, microwave power level, drying protocol) need to be well adapted and controlled (Ratti and Kudra 2006a). Therewith, foam structure stability and thus product quality, besides process efficiency, are ensured. In order to avoid detrimental foam collapse during drying and further optimize MWVD in terms of the drying time and resulting product quality, a more in-depth understanding of the interdependency of the above-mentioned influencing factors is required (Sankat and Castaigne 2004). It was assumed that interfacial and/or dielectric properties of the material to be dried would play a key role. Thereby, the former allow for conclusions regarding adsorption kinetics and the stability of the interfacial film against mechanical stress (e.g., stretching) and are associated with foamability and foam stability (Georgieva et al. 2009; Rodríguez Patino et al. 2008). The latter provide insights into the interaction of the material to be dried with the electromagnetic field of the microwave and are key for process understanding (Guo and Zhu 2014). To the authors' best knowledge, neither interfacial characteristics nor dielectric properties of surfactant–polysaccharide or protein–polysaccharide dispersions have been investigated in the context of microwave-assisted vacuum drying, thus far. Therefore, the

objective of the present study was to evaluate these characteristics (i.e., surface tension and surface dilatational rheology, dielectric constant and loss factor, resonant frequency and quality factor) for polysorbate 80–maltodextrin dispersions and to correlate them with the samples' drying performance in terms of foam structure preservation during MWVD versus CVD. In this model system, the non-ionic surfactant polysorbate 80 served as a foaming agent, whereas the polysaccharide maltodextrin was used to enhance foam stability by means of increasing the bulk viscosity. In addition, maltodextrin is widely applied as a protectant or carrier for sensitive biological material during drying (Ambros et al. 2019b; Jaya et al. 2006; Jaya and Das 2004). The behavior of whey protein–maltodextrin-based matrices was examined in a further study (Kubbutat et al. 2021b).

4.4.2 Materials and methods

4.4.2.1. Materials and preparation of sample dispersions

Sample dispersions of 200 g each were prepared by blending 3.0% w/w polysorbate 80 (Tween 80; Gerbu Biotechnik GmbH, Heidelberg, Germany) with different amounts (i.e., 0.0–40.0% w/w) of maltodextrin DE6 (MDX; Nutricia GmbH, Erlangen, Germany) and dissolving the dry mix in deionized water (Milli-Q Integral 3, Merck KGaG, Darmstadt, Germany). To ensure full hydration, the sample dispersions were gently stirred using a magnet stirrer (Maxi Direct, Fisher Scientific GmbH, Schwerte, Germany) at 200 rpm for 12 h at 4 °C. Prior to the experiments, the sample dispersions were tempered at 20 °C with a water bath (F3, Fisher Scientific GmbH, Schwerte, Germany).

Unless mentioned otherwise, measurements were performed at 20 °C and at least in triplicate using independent batches of sample dispersions. Error bars represent the calculated standard deviation.

4.4.2.2. Surface tension and surface dilatational properties of the bulk phase

Time-dependent evolution of surface tension σ was determined by the pendant drop method using the DSA100R (Krüss GmbH, Hamburg, Germany). A drop of 12 μl was formed at the tip of a capillary ($d_i = 1.81$ mm, Krüss GmbH, Hamburg, Germany) and its contour was monitored for 120 min. Extraction of surface tension was conducted by drop shape analysis using the software Advance (Krüss GmbH, Hamburg, Germany).

Upon reaching quasi-equilibrium surface tension, surface dilatational properties were determined by the oscillating drop method. For this, the pendant drop at a drop age of 60 min was exposed to a sinusoidal oscillation with a frequency of 0.1 Hz for a duration of 100 s. The amplitude was set to 200–800‰ in order to achieve a change in surface area by 2.5–3.5%. Data fitting according to Lucasson and van den Tempel (1972) allowed for the estimation of surface dilatational elasticity E' and surface dilatational viscosity E'' (Equation 4.4.1 – 4.4.3):

$$E = \frac{\Delta\sigma}{\Delta A/A_0} \quad (4.4.1)$$

$$E' = |E|\cos(\varphi) \quad (4.4.2)$$

$$E'' = |E|\sin(\varphi) \quad (4.4.3)$$

where E is the complex viscoelastic modulus, $\Delta A/A_0$ is the amplitude of the surface area oscillation and φ is the phase angle between surface tension oscillation and surface area oscillation. The tangent φ was calculated by dividing E''/E' according to Conde et al. (2005).

4.4.2.3. Dielectric properties of the bulk phase

Dielectric properties of the sample dispersions were measured with the μ WaveAnalyser (Püschner GmbH & Co. KG, Schwanewede, Germany) over a broad temperature range from -40 to $+40$ °C. For this, 300 μ l of sample dispersion was filled into a 1 ml glass vial, which was then sealed with a lock (1MLFBG, VWR International GmbH, Darmstadt, Germany). For each measurement point, the filled vial and the μ WaveAnalyser were tempered at the respective target temperature within a climate chamber. After an equilibration time of 6 h, measurements were performed at a frequency between 2400 and 2500 MHz against an empty vial. Based on the response of the sample dispersion towards the emitted frequency, the software μ WaveAnalyser Version 3.2.0 (Püschner GmbH & Co. KG, Schwanewede, Germany) calculates the dielectric constant ϵ' , the dielectric loss ϵ'' , the resonant frequency f_{res} and the quality factor Q (Pueschner GmbH & Co. KG 2008). The dielectric constant is a measure of the polarizability of a material, whereas the dielectric loss is a parameter for the physical conversion of electromagnetic radiation into heat. In addition, the loss factor $\tan(\delta)$ describes the ability of the sample dispersion to take up energy from the electromagnetic field and is defined by the ratio of loss factor and dielectric constant (Equation, 4.4.4) (Bart 2005):

$$\tan(\delta) = \frac{\epsilon''}{\epsilon'} \quad (4.4.4)$$

Further, the penetration depth PD can be calculated according to Equation (4.4.5) (Radoń and Włodarczyk 2019):

$$PD = \frac{\lambda_{2450\text{MHz}}}{2\pi} \frac{\sqrt{\epsilon'}}{\epsilon''} \quad (4.4.5)$$

The penetration depth describes the depth until the power density has decreased to $1/e$ of its initial value and depends on the wavelength λ . In this study, the wavelength was assumed with 2450 MHz.

4.4.2.4. Foam preparation

Foams were prepared by means of whipping with a commercial planetary mixer (KitchenAid ARTISAN 5KSM105PS, Whirlpool Corp., Greenville, United States of America) equipped with a wire whisk geometry (K45WW, Whirlpool Corp., Greenville, United States of America). Per foam, 150 g of sample dispersion was whipped for 15 min at 220 rpm. Immediately after foam formation, 15 g of foamed sample was gently transferred to a cylindrical crystallization glass with a diameter of 200 nm (VWR International GmbH, Darmstadt, Germany) and dried as described in chapter 4.4.2.5. The resulting foam properties and viscosity values of the investigated sample dispersions are published in a previous study (Kubbutat and Kulozik 2021b).

4.4.2.5. Foam drying and product characterization

Foams were dried by means of two different techniques: conventional vacuum drying (CVD) and microwave-assisted vacuum drying (MWVD). For CVD, a pilot freeze dryer (Delta 1-24LSC; Martin Christ Gefriertrocknungsanlagen GmbH, Osterode am Harz, Germany) was operated at a chamber pressure of 15 mbar and a shelf temperature of 20 °C. The foams were dried for 16 h. In case of foam collapse, drying was stopped 10 min after the collapse occurred. For MWVD, the microwave drying plant μ Vac0150fd (Püschner GmbH & Co. KG, Schwane-wede, Germany) was used. Process control was conducted with the software μ WaveCAT (Püschner GmbH & Co. KG, Schwane-wede, Germany). A typical MWVD process is shown in Fig. 4.4.1. Similar to CVD, MWVD was performed at 15 mbar. The maximum temperature was limited to 20 °C, and a microwave power input of 80 W was set. The drying process was stopped 10 min after foam collapse or when no mass loss was detected during 10 consecutive minutes. For successfully dried samples, the drying time was between 45 and 90 min. The appearance of the resulting product structures was optically described.

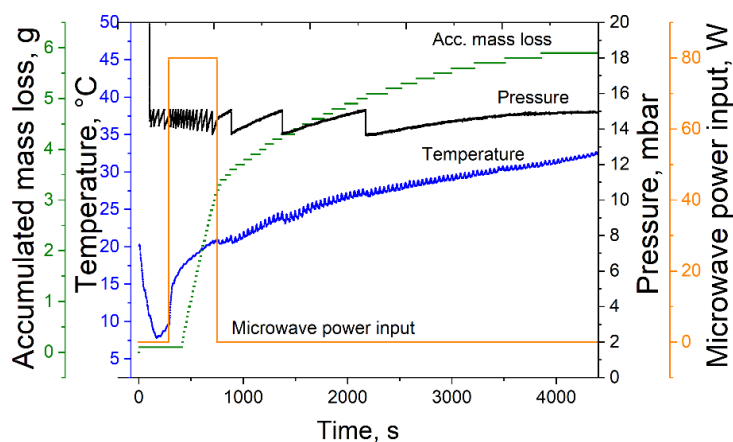


Fig. 4.4.1: Exemplary microwave-assisted foam vacuum drying process at 15 mbar, 80 W microwave power input and a sample temperature of 20 °C.

4.4.3 Results and discussion

4.4.3.1. Foam drying

For the investigation of the interrelation between foam structure and drying behavior as a function of the heating technique, foams were prepared from polysorbate 80 at 3.0% w/w in combination with 10–40% w/w maltodextrin (MDX). Thereby, an increase in the MDX concentration led to an increase in the sample dispersion viscosity, which in turn resulted in a decrease in the overrun as well as the bubble size of the formed foams (results not shown). In terms of heating method, the foams were either subjected to conventional vacuum drying (CVD) or microwave-assisted vacuum drying (MWVD). For both drying processes, a maximum product temperature of 20 °C was set. Overall, this approach gave the opportunity to distinguish heating method-specific effects and to identify relevant product properties for a successful drying process.

Fig. 4.4.2 shows the different product structures obtained after either CVD or MWVD as a function of the MDX concentration. Overall, both drying techniques, as well as MDX content, had a clear impact on the appearance of the resulting product structures. For both drying techniques, foam structure preservation increased with increasing MDX concentration, though CVD was clearly superior to MWVD. In the latter case, all samples collapsed during the drying process, yielding highly viscous liquids at the bottom of the sample containers. By contrast, by CVD, a foam-like structure was observed for samples containing 30 or 40% MDX, whereas for 10 and 20% MDX, foam collapse occurred during the first 30 min of drying. A better foam preservation during vacuum drying as a result of saccharide addition was also observed by Jangle and Pisal (2012) investigating the impact of sucrose and mannitol on the vacuum foam drying of bovine serum albumin. The necessary amount of saccharide to obtain a foamy structure after the drying was comparable (>20% w/v). This is interesting because the viscosity of a 20% sucrose dispersion is expected to be lower than a 20% maltodextrin dispersion, and the viscosity should preserve the foam structure (Ambros et al. 2019a). A reason for this difference might be that in the recent study, foam formation was conducted before the drying process was started. Thereby, the foam was destabilized while the pressure was decreased, whereas, in the study of Jangle and Pisal, the vacuum step was necessary to form the foam. Hence, in our study, the foam expanded even before it got heated, which resulted in higher mechanical stress.

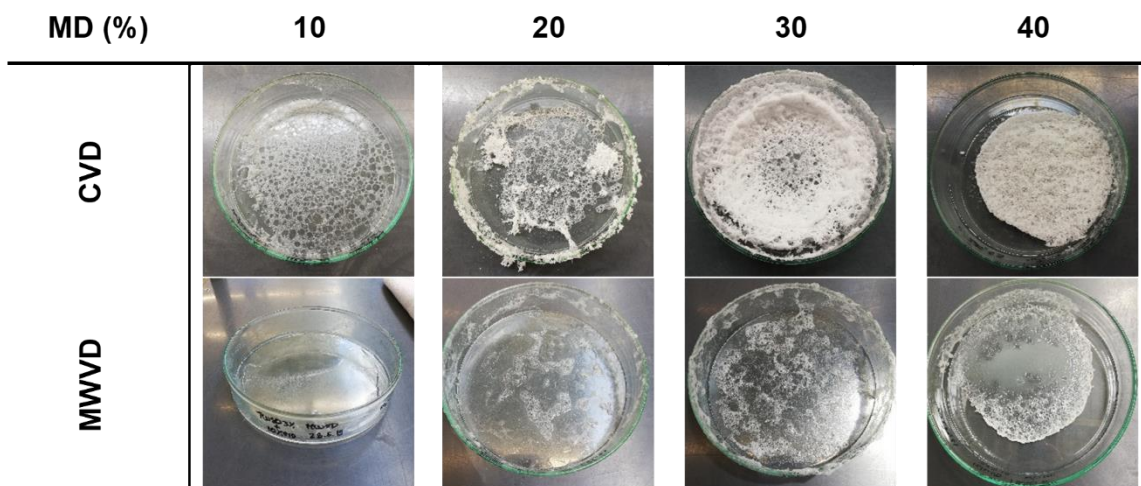


Fig. 4.4.2: Impact of maltodextrin (MDX) concentration and drying method on the appearance of the resulting product structures.

Overall, the results show that CVD was better suited to preserve foam structures from polysorbate 80 in combination with MDX than MWVD. This raised the question of the specific relationship between the type of energy input and the surface properties of polysorbate 80 with MDX. In this context, this study aimed at distinguishing properties being relevant for structure preservation and successful drying. In order to close this knowledge gap, surface tension and surface dilatational properties, as well as dielectric properties of the sample dispersions, were determined.

4.4.3.2. Surface tension and surface dilatational properties of the bulk phase

Firstly, the evolution of surface tension of the different sample dispersions (i.e., polysorbate 80 with 0–40% MDX) was measured for a period of 7200 s. The obtained results are displayed in Fig. 4.4.3. The surface activity refers to the rate of initial surface tension decrease (Marinova et al. 2009), which was calculated from the slope of the surface tension within the first 5 s. In general, all sample dispersions exhibited a relatively high surface activity, which is characterized by the fact that quasi-equilibrium surface tension was almost reached within the first few seconds. The slight further decrease in surface tension over time was considered rather insignificant as compared to the very initial decrease.

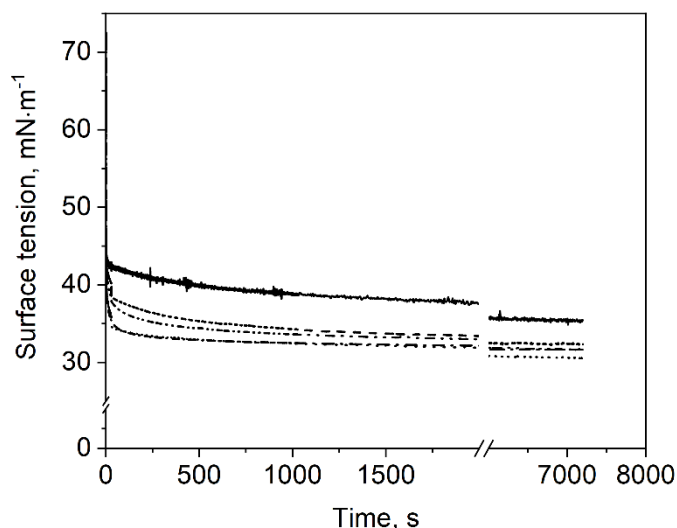


Fig. 4.4.3: Impact of maltodextrin concentration on the time-dependent surface tension of polysorbate 80: (-) 0% MDX, (- -) 10% MDX, (····) 20% MDX, (-·-·) 30% MDX, (- - -) 40% MDX.

It was observed that samples with MDX showed higher surface activity and lower surface tension than the reference sample dispersion without MDX. The surface activity increased from -6.0 at 0% MDX to $-7.4 \text{ mN}\cdot\text{m}^{-1}\cdot\text{s}^{-1}$ with 30% MDX. The 40% MDX samples showed a slightly lower value of $-6.8 \text{ mN}\cdot\text{m}^{-1}\cdot\text{s}^{-1}$. Quasi-equilibrium surface tension of samples containing MDX was around $33 \text{ mN}\cdot\text{m}^{-1}$, whereas for 0% MDX, a value of $37 \text{ mN}\cdot\text{m}^{-1}$ was obtained. A possible explanation for this behavior could stem from the presence of surface-active molecules such as native starch lipids and proteins, originating from the maltodextrin manufacturing process (Pycia et al. 2017; Shogren and Biresaw 2007). However, the surface tension of MDX dispersions with an MDX content between 10 and 40% and without polysorbate 80 was reported to be in equilibrium between 71.2 and $72.5 \text{ mN}\cdot\text{m}^{-1}$ (Kubbutat and Kulozik 2021b). Hence, the contamination of MDX with surface-active components seems not to be the reason for the observed differences in surface tension. Therefore, we assume that the high viscosity of 40% MDX samples inhibited the polysorbate to move to the new surface and was therefore the reason for the slightly lower surface activity. Further, strong hydrogen bonds and hydrophobic interactions between polysorbate 80 and MDX may change the surface activity of polysorbate 80 as also suggested by Semenova et al. (2003). Thereby, the surfactant might be modified via non-covalent interaction by extending the ethylene oxide group of polysorbate. Consequently, polysorbate 80–MDX mixtures could lower the surface tension more than samples which contain only polysorbate 80. On the other hand, this might also be the reason for the slower adsorption of samples with 40% MDX, as the interactions might result in a steric repulsion at the surface in the presence of high carbohydrate concentrations.

The lowest surface tension was obtained for sample dispersions containing 10 or 20% MDX, whereas the surface tension was slightly higher for sample dispersions with 30 and 40% MDX. This could be due to the increasing viscosity of the investigated sample dispersions with increasing MDX concentration. Thereby, diffusion and adsorption of the surface-active molecules at the air/water interface might be hindered, resulting in a higher surface tension within the time frame investigated. Nevertheless, MDX had an enhancing effect on surface activity and surface tension as compared to the reference sample dispersion without MDX.

Overall, the results show that surface activity and surface tension are not indicative for structure preservation during drying (Fig. 4.4.2).

Besides surface tension, the different sample dispersions were also characterized in terms of their surface dilatational properties. Surface dilatational properties are deemed indicative of surface film stability, which was assumed to be of importance in view of gas expansion under vacuum as well as bubble deformation during drying. The results on surface dilatational elasticity E' and surface dilatational viscosity E'' are shown in Fig. 4.4.4 as a function of the MDX concentration. In terms of E'' , no clear dependence on the MDX concentration could be observed, though values slightly increased with increasing MDX concentration from about 3.5 to 5.8 $\text{mN}\cdot\text{m}^{-1}$. Nonetheless, the very slight increase in E'' could be due to the increased total solids content of the sample dispersions with increasing MDX concentration, which in turn showed a positive effect during drying. Unlike surface tension, surface dilatational properties and especially E' strongly depended on the MDX content. By comparison, results on E' followed a “u” shape with a minimum at 25% MDX. Thereby, the relative change in surface dilatational elasticity as a function of the MDX concentration was quite high, with absolute values starting at 20.1 $\text{mN}\cdot\text{m}^{-1}$ at 0% MDX, decreasing to 7.5 $\text{mN}\cdot\text{m}^{-1}$ at 25% MDX and increasing again towards 21.7 $\text{mN}\cdot\text{m}^{-1}$ at 40% MDX. This can also be described by $\tan(\varphi)$, where 0 represents a perfect elastic behavior of the film (Table 4.4-1) (Baeza et al. 2006; Conde and Rodríguez Patino 2005). The surface showed most elastic behavior at low ($\tan(\varphi) = 0.2\text{--}0.24$ at 0–5% MDX) and high MDX ($\tan(\varphi) = 0.28$ at 40% MDX), while for 20% MDX, the surface exhibited the lowest elasticity ($\tan(\varphi) = 0.53$). However, in comparison with protein-stabilized systems, the obtained $\tan(\varphi)$ for our system is quite high. For example, Beaza et al. (2006) investigated the influence of different additives to β -lactoglobulin and obtained $\tan(\varphi)$ values of < 0.2 . An explanation for this difference might be protein network formation by means of intermolecular interactions between protein molecules such as electrostatic interactions or hydrogen bonds. By contrast, small non-ionic surfactants such as polysorbate 80 are mainly interacting via hydrogen bonds.

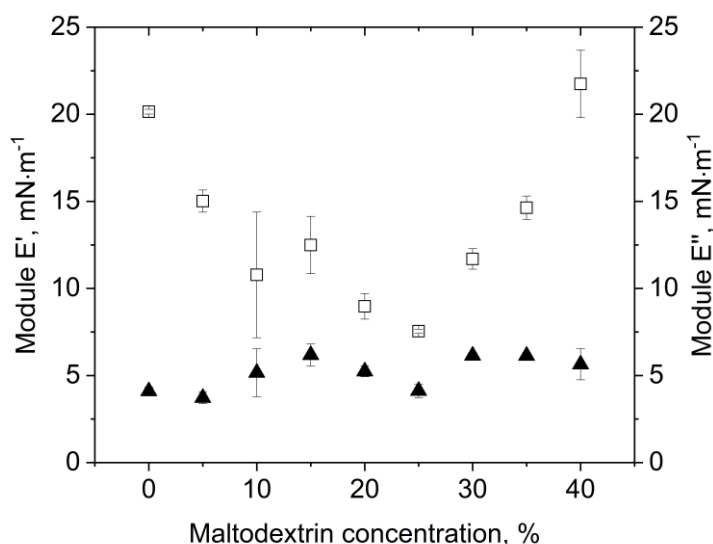


Fig. 4.4.4: Impact of MDX concentration on surface dilatational properties of polysorbate 80: (□) surface dilatational elasticity E' ; (▲) surface dilatational viscosity E'' at an amplitude of 500‰.

Table 4.4-1: Calculated $\tan(\varphi)$ of samples with 3% polysorbate 80 and an MDX content between 0 and 40% at 20 °C and an amplitude of 500‰.

c(MDX), %	0	5	10	15	20	25	30	35	40
$\tan(\varphi), -$	0.20	0.24	0.45	0.46	0.53	0.50	0.48	0.40	0.28

Overall, the surface of polysorbate-stabilized foams showed low elastic behavior, which could be problematic regarding the high mechanical stress during the drying process.

However, no clear correlation could be resolved between drying performance in terms of structure preservation and surface dilatational elasticity.

The effect of better stability at higher total solid content could be explained as such that the high viscosity of the bulk phase prevents the bubbles to expand too quickly. During drying, the lamellae become very thin, and the surface area increases. This in turn might result in the occurrence of holes in the surface films whereby foam collapse is triggered, eventually. The higher MDX content could slow this down and enable the foaming agent to cover the surface quickly enough to prevent foam collapse. In terms of conventional vacuum drying, an MDX concentration of $\geq 30\%$ seemed favorable in terms of formation of elastic surface films, resulting in structure preservation during drying.

However, the results do not explain the observed differences between CVD and MWVD processes. Therefore, it was considered necessary to investigate in more depth the microwave-specific properties of the different sample dispersions. Therewith, it was aimed to

better understand the underlying mechanisms allowing for specific conclusions regarding future product design.

4.4.3.3. Dielectric properties of the bulk phase

The dielectric properties of polysorbate 80 dispersions with various contents of MDX are shown in Fig. 4.4.5. The dielectric constant decreased with increasing sugar concentration, while the dielectric loss factor slightly increased. A comparable trend for increasing carbohydrate concentration was also observed by Roebuck et al. (1972) during their investigation of dielectric properties of carbohydrates using a microwave frequency of 3 GHz. They stated that the reason for the decrease in the dielectric constant was due to fewer polarizable dipole moments due to less free water in the samples. The increase in the dielectric loss factor with increasing carbohydrate content can be explained by a better stabilization of hydrogen bonds in the presence of carbohydrates. Haggis et al. (1952) stated that due to better stabilized hydrogen bonds in the presence of organic molecules, the relaxation frequency of water is lowered, whereby the dielectric loss increases. Therefore, our findings are in accordance with our expectations and findings from the literature.

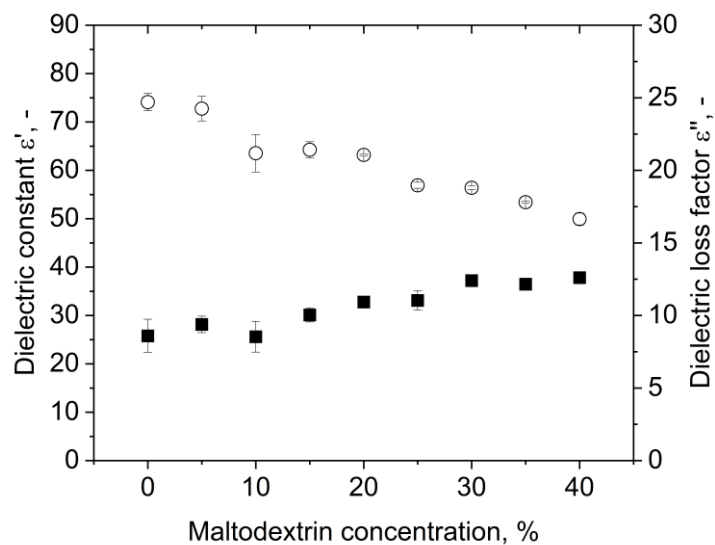


Fig. 4.4.5: Impact of MDX concentration on the dielectric properties of dispersions with 3% polysorbate 80. Symbols: (○) dielectric constant ϵ' , (■) dielectric loss ϵ'' .

As a result of the increasing dielectric loss and decreasing dielectric constant, the value for $\tan(\delta)$, which is a parameter for the ability of the material to converse radiation power into heat, increased (Table 4.4-2). Therefore, the samples were heated more efficiently with the higher sugar content. However, this might be problematic for the uniformity of the heating process: the more efficient the heating, the lower the penetration depth according to Equation (4.4.5). For the investigated samples, the penetration depth of the bulk decreased from 7.67 at 0%

MDX to 3.84 cm at 40% MDX. Therefore, the characteristics of the heating are less volumetric with increasing MDX because more energy is converted into heat within a shorter distance. As a result, the probability of hot and cold spot formation is increased. The bubbles are assumed to not be heated extensively because the bulk phase converts the energy much more efficiently than the air inside the bubbles. Consequently, the penetration depth into the foam will increase with higher overrun values, which means that the differences in the heating pattern are expected to be even higher. However, no differences in hot spot formation were detected, which was contributed to the foam expansion during the drying process.

Table 4.4-2: Calculated $\tan(\delta)$ for dispersions with 3% polysorbate 80 and an MDX content between 0 and 40% at 20 °C.

c(MDX), %	0	5	10	15	20	25	30	35	40
$\tan(\delta)$, -	0.12	0.13	0.14	0.16	0.17	0.20	0.22	0.23	0.26

In Fig. 4.4.6, the resonant frequency of polysorbate 80 dispersions with an MDX content between 0 and 40% is shown. It was observed that with increasing sugar content, the resonant frequency shifted from 1951.3 ± 5.7 to 2039.2 ± 5.6 MHz. This seems to be plausible, as the addition of organic molecules increases the resonant frequency of water (Zhang et al. 2019).

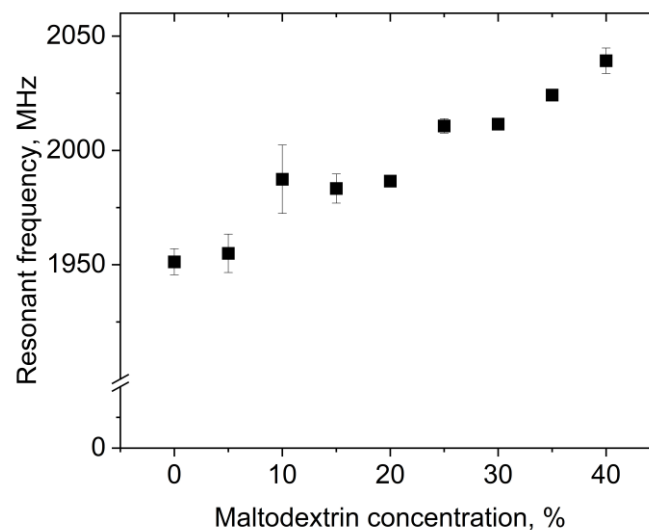


Fig. 4.4.6: Impact of MDX concentration on the resonant frequency of dispersions with 3% polysorbate 80.

Summing up the results on the dielectric properties of the dispersion, the samples were able to convert radiation more efficiently into heat at higher sugar contents. The faster and concentrated heating resulted in harsher heating conditions. Nevertheless, we observed better preservation of shape and structure at higher MDX contents. Hence, the dielectric properties of the complex dispersion do not explain the collapse of the foam during the MWVD process.

In order to more deeply address this question, different concentrations of MDX without a foaming agent (i.e., polysorbate 80) were tested (data not shown), but they did not give a hint for the drying behavior of the samples. Hence, a dispersion of 100% foaming agent was examined in view of its dielectric properties. In Fig. 4.4.7, the complex reflection coefficient S_{11} depending on the frequency is shown. This value represents the interactions of a material with the electromagnetic wave if it is impinged with a certain frequency. The frequency where the interactions are the strongest is called resonant frequency, which is at 2445 MHz for the pure surfactant. This matches the frequency band which the microwave drying plant emits to apply power to the sample (i.e., 2450 ± 50 MHz). Therefore, it appears that a so-called frequency catastrophe happened at the air/water interface, as schematically shown in Fig. 4.4.8. Due to the overlapping microwave and resonant frequencies, the ethylene group of the surfactant is polarized very efficiently and at a high frequency. Further, interactions between water and the ethylene groups of polysorbate might be affected by the radiation (Epstein et al. 1983), which might result in lower interface stability. Due to the high applied power, the movement of the surfactant caused hole formation within the surfactant layer. This in turn resulted in a collapse of the foam structure during microwave application.

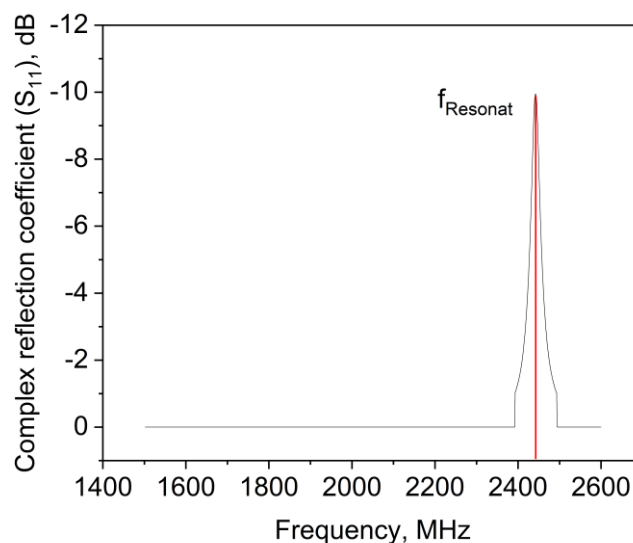


Fig. 4.4.7: Complex reflection coefficient S_{11} of pure polysorbate 80.

For high sugar concentrations and, consequently, thick lamellae, this effect can be suppressed by the high viscosity of the bulk phase. However, due to the quick expansion of the air bubbles during the vacuum and heating process, it could be that the counteracting forces become too weak. In a first step, the air bubbles would show coalescence with other bubbles until the necessary amount of surfactant to stabilize the interface is too low. Then, the bubble and the foam would collapse.

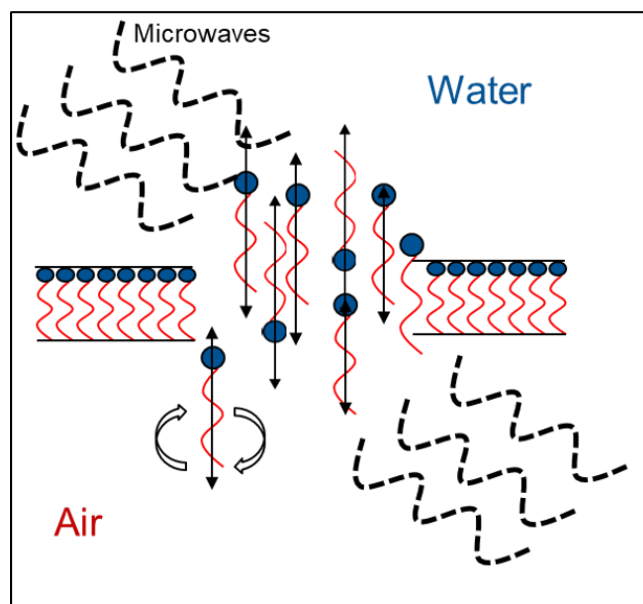


Fig. 4.4.8: Schematic representation of the behavior of polysorbate 80 at the air/water interface during foam drying.

Observations during the drying process showed that the foam started to collapse when the microwave power was on and stopped decaying right after turning the microwave power off (Fig. 4.4.1). This indicates strongly that the resonant frequency of the foaming agent had a strong impact on the foam decay and not the overall dielectric properties of the bulk phase. Finally, the dielectric properties of polysorbate 80 seem to be one of the main reasons for the foam decay during MWVD.

4.4.4 Conclusions

In this study, the behavior of polysorbate 80–maltodextrin foams during vacuum drying processes with different heating methods was investigated. It was shown that there is not one single parameter that is overall important to achieve a successful drying process. Nevertheless, surface dilatational rheology seems an important parameter because a certain elasticity ($\tan(\varphi) < 0.4$) of the surface is mandatory to withstand the mechanic stress during the evacuation of the drying plant. For the case of MWVD, it was not clear if just the dielectric properties of the surfactant had this massive impact on foam stability during the drying process. However, the results indicate that the dielectric properties of the foaming agent and the surface dilatational rheology of the complex system are responsible for its behavior during microwave-assisted processes, which is a new insight related to microwave-assisted drying. Further, a certain ratio of E''/E' expressed as $\tan(\varphi) < 0.2$ was shown to be necessary for successful drying with MWVD, and the resonant frequency of the foaming agent should not match the working frequency of the microwave drying plant (2450 ± 50 MHz). As the dielectric properties change with the temperature, it would be interesting to investigate these parameters at different, commonly used temperatures for vacuum drying. Further, it would be of interest to

determine the importance of effects at the molecular level to better understand the behavior of foam during the drying process. Besides surfactants, proteins are commonly used as foaming agents, which is why we investigated the behavior of protein samples during MWVD in a second study. Further, it would be of interest to use other microwave sources to determine the specific effect of the microwave frequency.

Author contributions: P.K.: conceptualization, methodology, investigation, writing—original draft, writing—review and editing, visualization; U.K.: writing—review and editing, resources, supervision, funding acquisition; J.D.: conceptualization, writing—original draft, writing—review and editing. All authors have read and agreed to the published version of the manuscript.

Funding: This research project was supported by the German Ministry of Economics and Energy (via AiF) and the FEI (Forschungskreis der Ernährungsindustrie e.V., Bonn), Project AiF 18819 N. This work was supported by the Technical University of Munich (TUM) in the framework of Open Access Publishing Program.

Data availability statement: Data will be available upon request from the corresponding author.

Acknowledgments: The authors would like to thank Krüss GmbH for providing the DSA100R. The authors would like to thank Luísa Leitão for helping with the experimental data collection.

Conflicts of interest: The authors declare no conflict of interest. The funders had no role in the design of the study; in the collection, analyses, or interpretation of data; in the writing of the manuscript, or in the decision to publish the results.

4.5 Influence of interfacial characteristics and dielectric properties on foam structure preservation during microwave-assisted vacuum drying of whey protein isolate-maltodextrin dispersions

Summary and contribution of the doctoral candidate

The study aimed at investigating surface tension, surface dilatational characteristics, and dielectric properties for whey protein isolate-maltodextrin dispersions and correlating them with the samples' performance during MWVD and CVD.

It was hypothesized that surface activity and surface dilatational properties of the main product constituents would indicate foam structural stability during drying. This assumption was based on the fact that foams are exposed to thermal stress and mechanical stress (e.g., bubble expansion, oscillation, rupture, and regeneration). Besides, the dielectric properties of the product dispersion were supposed to allow for a better understanding of its interaction with the electromagnetic field during MWVD.

It was shown that the surface tension decreased with increasing MDX content while the surface activity index increased. One explanation for this was the interactions between MDX and whey proteins based on hydrogen bonds and steric hindrance. However, no linkage between foam decay during drying and surface tension or surface activity index was possible. The surface dilatational properties were considered as key properties for successful foam drying. A further key finding was that $\tan(\delta)$ increased with increasing MDX content, reflecting a faster heating of the product. However, concerning foam stability, the dielectric properties were of minor importance.

The substantial contribution of the doctoral candidate was the conception and design of the experiments. Further, he was substantially involved in the performance of experiments and acquired parts of the data for the manuscript, and interpreted the data set. Furthermore, the critical literature review and chiefly writing of the manuscript were done by the candidate. Co-authors contributed to the experimental part and/or in the discussion of the results and provided input to the drafted manuscript prior to and during submission.

Influence of interfacial characteristics and dielectric properties on foam structure preservation during microwave-assisted vacuum drying of whey protein isolate-maltodextrin dispersions⁴

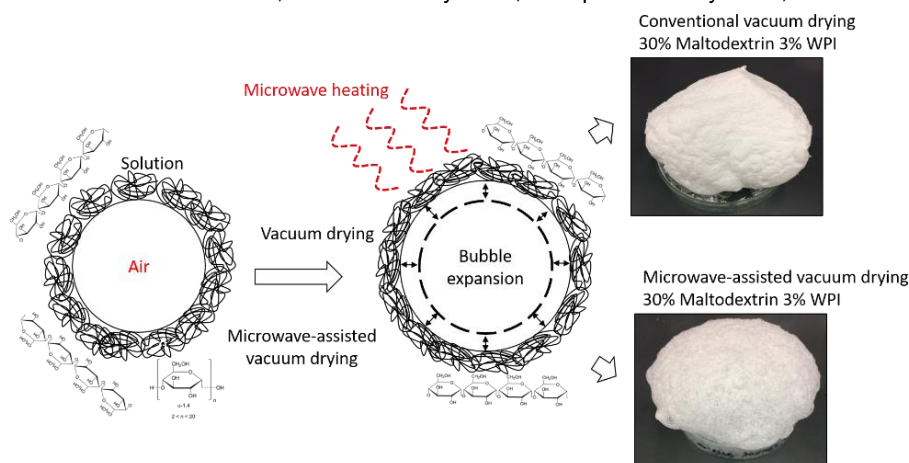
Peter Kubbutat^{1,*}, Ulrich Kulozik¹ and Jannika Dombrowski^{1,2}

¹Chair of Food and Bioprocess Engineering, School of Life Science, Technical University of Munich, 85354 Freising, Germany

²New affiliation: Nestlé Research, Société des Produits Nestlé SA, Route du Jorat 57, 1000 Lausanne 26, Switzerland.

* Correspondence: peter.kubbutat@tum.de

Received: 4 March 2021; Revised: 4 May 2021; Accepted: 16 May 2021; Published: 18 May 2021



Abstract:

This study aimed at assessing the correlation between interfacial and dielectric properties of whey protein isolate (WPI)-maltodextrin (MDX) dispersions and their foam structure stability during conventional vacuum drying (CVD) and microwave-assisted vacuum drying (MWVD). Interestingly, the presence of MDX clearly increased the surface activity of WPI, whereas the surface dilatational properties were rather unaffected. Besides, loss factor and resonant frequency linearly increased with MDX concentration, while the dielectric constant decreased. Regarding drying, foam structure preservation during CVD was mainly correlated with the dilatational elasticity. Thereby, all samples remained stable throughout the drying process. Compared to CVD, MWVD required $\geq 20\%$ MDX to avoid foam collapse. In addition, MWVD-dried samples exhibited larger bubble sizes, which was linked to the volumetric heating and higher mechanical stress as compared to CVD. Overall, high surface dilatational elasticity and bulk viscosity were identified as key parameters to ensure foam structure preservation during vacuum drying.

Keywords: Polysaccharide, Protein, Dielectric properties, Surface dilatational rheology, Vacuum drying, Microwave-assisted vacuum drying

⁴ Original publication: Kubbutat, P.; Kulozik, U. (2021) Influence of interfacial characteristics and dielectric properties on foam structure preservation during microwave-assisted vacuum drying of whey protein isolate-maltodextrin dispersions. *Journal of Food Engineering*, 308: 110691, <https://doi.org/10.1016/j.jfoodeng.2021.110691>. Adapted original manuscript. Adaptions of the manuscript refer to enumeration, citation style, spelling, notation of units and format. Permission for reuse of article is granted by Elsevier Ltd.

References of all chapters are merged at the end of the dissertation.

4.5.1 Introduction

During the last few decades, vacuum drying has turned into an interesting alternative to freeze drying. This is not only attributable to advantages in specific energy demand (Gehrmann et al. 2009) and drying time (Santivarangkna et al. 2007a), but also to a relatively low thermal stress allowing for the preservation of heat- and freeze-sensitive biological materials (Ambros et al. 2016; Bauer et al. 2012; Jesus and Filho 2011; Hajare et al. 2006; McLoughlin et al. 2003). Furthermore, vacuum dried products were reported to exhibit an enhanced storage stability as compared to freeze-dried materials, which was mainly related to product shrinkage during dehydration (Foerst et al. 2012). Unfortunately, compaction of the product structure during drying entails a prolonged third drying stage. In addition, grindability of the final product is mostly impaired. Recent approaches to tackle these drawbacks include the combination of vacuum and microwave drying (i.e., microwave-assisted vacuum drying (MWVD)) as well as a controlled product aeration (i.e., foaming) prior to drying (Ambros et al. 2019a). According to Ambros et al. (2019b), MWVD allowed for a reduction of drying time by about 95% as compared to conventional vacuum drying (CVD). Foaming prior to MWVD entailed an even further acceleration of the process besides its positive effect on product grindability. On the one hand, this can be explained by the volumetric energy input of microwaves enabling a high mass transfer over all drying stages. On the other hand, foaming increases the product's specific surface area, while lamellae between bubbles act as capillaries through which water can be transported to the product's surface during drying (Rajkumar et al. 2007).

In this regard it is important to note that the beneficial effect of microwaves and foaming on process efficiency and product quality only applies if the foam structure does not collapse during drying. Here, it may not be neglected that foams are thermodynamically instable and therefore continuously undergo structural changes in terms of foam volume, liquid content and bubble size distribution (Damodaran 2005). Hence, in order to ensure a successful and efficient drying, not only the process conditions (e.g., pressure level, microwave power level, drying protocol), but also foam characteristics via the product formulation (e.g., foaming agent, protectant, carrier) and aeration method (e.g., whipping, decompression) need to be well controlled (Ambros et al. 2019a; Ratti and Kudra 2006a).

In view of product formulation, it was hypothesized that surface activity and surface dilatational properties of the main product constituents would be indicative of foam structural stability during drying. This assumption was based on the fact that foams are not only exposed to thermal stress, but also to significant mechanical stress (e.g., bubble expansion, oscillation, rupture and regeneration). Besides, dielectric properties of the product dispersion were supposed to allow for a better understanding of its interaction with the electromagnetic field of the microwave during MWVD (Guo and Zhu 2014).

In general, foam formation and stabilization requires the presence of surface-active molecules such as surfactants or proteins. In terms of foam formation, surfactants often outclass proteins due to their higher surface activity resulting from their lower molecular weight and higher structural flexibility. However, in terms of foam stability, proteins are usually superior to surfactants (Saint-Jalmes et al. 2005) as they are able to strongly interact intermolecularly at the air/water interface allowing for the formation of viscoelastic films (Georgieva et al. 2009; Rodríguez Patino et al. 2008).

Based on this, the question arose of whether surfactants or proteins are better suited to ensure foam structural stability during vacuum drying processes (i.e., CVD or MWVD). To the authors' best knowledge, neither interfacial characteristics nor dielectric properties of surfactant-polysaccharide or protein-polysaccharide dispersions have been investigated in the context of MWVD, so far.

Therefore, this study aimed at investigating surface tension, surface dilatational characteristics, dielectric constant and loss factor, resonant frequency and quality factor for whey protein isolate-maltodextrin dispersions and correlating them with the samples' performance during MWVD versus CVD. In this model system, whey protein isolate served as foaming agent, whereas the polysaccharide maltodextrin was used to enhance foam stability by means of increasing bulk viscosity. The behavior of polysorbate 80-maltodextrin-based matrices was examined in a separate study (Kubbutat and Kulozik 2021a).

4.5.2 Methods

4.5.2.1. Materials and preparation of sample solutions

Whey protein isolate (WPI), which was used as foaming agent, was obtained from Davisco Foods International Inc. (Bipro®, Eden Prairie, MN, USA). Maltodextrin DE6 (MDX) served as thickening agent and was purchased from Nutricia GmbH (Erlangen, Germany).

Sample dispersions of 200 g each were prepared by mixing and dissolving 3% (w/w) WPI and different amounts of MDX (0–40% (w/w) in demineralized water. To ensure full hydration, the dispersions were gently mixed for 12 h at 4 °C using a magnetic stirrer. Prior to the experiments, the sample dispersions were tempered at 20 °C in a water bath.

4.5.2.2. Determination of surface tension

The time-dependent evolution of surface tension σ was determined by the pendant drop method using the DSA100 (Krüss GmbH, Hamburg, Germany). A drop of 12 μ l was formed at the tip of a needle (NE 95, $\varnothing = 1.81$ mm, Krüss GmbH, Hamburg, Germany) and the drop shape was recorded with a high-speed camera (UI-3060CP R2, IDS Imaging Development Systems GmbH, Obersulm, Germany) for a period of 120 min (frame rate: 10 fps for $t \leq 30$ s and 1 fps for $t > 30$ s). For data analysis, the software ADVANCE was used (Krüss GmbH,

Hamburg, Germany). Reported values on quasi-equilibrium surface tension refer to the average of data points acquired within the last 30 s of each measurement. All measurements were performed at 20 °C.

The surface activity index was calculated according to Marinova et al. (2009), based on the initial decrease of surface tension (i.e., $t = 5$ s). As initial state, the surface tension of water at 20 °C ($72.8 \text{ mN}\cdot\text{m}^{-1}$ (Pallas and Harrison 1990)) was used.

4.5.2.3. Determination of surface dilatational properties

The surface dilatational properties were determined subsequent to surface tension using the same equipment and software (chapter 4.5.2.2). The pendant drop in quasi-equilibrium conditions, i.e., after 120 min, was subjected to sinusoidal oscillation at 0.1 Hz for 100 s. The amplitude was set to 200–800‰ to induce a change of surface area by 2.5–3.5%.

Based on the obtained data on the changes of surface tension $\Delta\sigma$ and drop surface area $\Delta A/A$, the complex viscoelastic modulus $|E|$ was calculated ((Equation 4.5.1), Lucassen and van den Tempel (1972)) with φ , the phase angle between surface tension oscillation and surface area oscillation, the surface dilatational elasticity E' and the surface dilatational viscosity E'' were determined (Equation 4.5.2 and 4.5.3)

$$E = \frac{\Delta\sigma}{\frac{\Delta A}{A}} = |E|e^{i\varphi} = E' + iE'' \quad (4.5.1)$$

$$E' = |E|\cos(\varphi) \quad (4.5.2)$$

$$E'' = |E|\sin(\varphi) \quad (4.5.3)$$

4.5.2.4. Dielectric properties of the bulk phase

Dielectric properties of the bulk phase were determined with the μ WaveAnalyser (Püschner GmbH & Co. KG, Schwanewede, Germany) within a frequency band of 2400 and 2500 MHz in 1 MHz steps. For this, 300 μl of sample dispersion were filled into 1 ml glass vials (1MLFBG, VWR International GmbH, Darmstadt, Germany) and sealed. Vials and device were tempered in a climate chamber to the measurement temperature, i.e., 4, 10, 20, 30, or 40 °C. As reference, an empty vial was used. For each temperature step, a new sample was used to prevent temperature-dependent changes of the sample dispersions due to prior heating or cooling. The dielectric constant ϵ' , dielectric loss ϵ'' , resonant frequency f_{res} as well as the quality factor Q were calculated using the software μ WaveAnalyser Version 3.2.0 (Püschner GmbH & Co. KG, Schwanewede, Germany). Further, $\tan(\delta)$ was calculated, which describes the samples' ability to absorb energy from the electromagnetic field (Equation 4.5.4) (Bart 2005).

$$\tan(\delta) = \frac{\varepsilon''}{\varepsilon'} \quad (4.5.4)$$

In addition, the penetration depth (PD) was determined according to Equation 4.5.5.:

$$\text{Overrun (\%)} = \frac{m_S - m_F}{m_F} \cdot 100 \quad (4.5.5)$$

The penetration depth describes the depth up to which the power density has decreased to 1/e of its initial value and depends on the wavelength λ , the dielectric constant, and the dielectric loss. In this study, the wavelength was assumed with 2450 MHz.

4.5.2.5. Foam preparation

150 g of sample dispersion were whipped for 15 min at 220 rpm and 20 °C with a commercial planetary mixer (KitchenAid ARTISAN 5KSM150PS, Whirlpool Corp., Greenville, United States of America), equipped with a wire whisk geometry (K45WW, Whirlpool Corp., Greenville, United States of America). After foam formation, 15 g of sample were gently transferred into a cylindrical crystallization glass with a diameter of 200 mm (VWR International GmbH, Darmstadt, Germany).

4.5.2.6. Drying process

The foamed samples were dried by means of conventional vacuum drying (CVD) and microwave-assisted vacuum drying (MWVD).

For CVD, a pilot freeze dryer model Delta 1-24LSC (Martin Christ Gefriertrocknungsanlagen GmbH, Osterode am Harz, Germany) was used. The pressure during the main drying step was set to 15 mbar, the shelf temperature to 20 °C. The foams were dried for 16 h, except for those that collapsed. In case of irreversible foam collapse, the drying process was stopped 10 min after it occurred.

For MWVD, the pilot plant unit μ Vac0150fd (Fig. 4.5.1, Püschner GmbH & Co. KG, Schwanewede, Germany) was used. For process control, the drying plant was connected to a computer using the software μ WaveCAT (Püschner GmbH & Co. KG, Schwanewede, Germany). Like CVD, the pressure was set to 15 mbar and the maximum temperature to 20 °C. The microwave power input was set to 80 W, which was the lowest adjustable power input. The mass loss was measured by a scale connected to the turntable. The drying process was stopped 10 min after foam collapse, or if no mass loss occurred during 10 consecutive minutes.

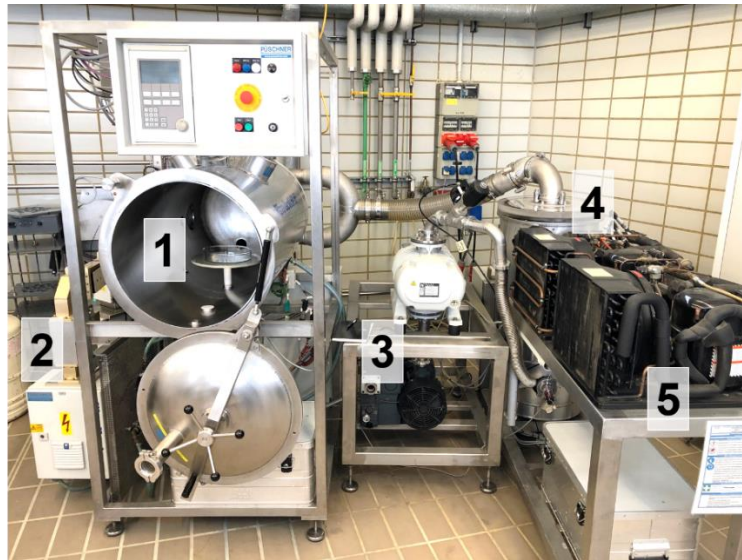


Fig. 4.5.1: Microwave drying plant μ Vac0150fd with turntable and sample glass (1: Drying chamber; 2: Microwave generator with hollow guide; 3: Vacuum pump; 4: Condenser; 5: Cooling device).

A scheme of a typical MWVD process is shown in Fig. 4.5.2. The microwave power is applied only for a short period at the beginning of the drying process and was turned off as soon as the set temperature is reached. Therewith, overheating shall be prevented. Nonetheless, a consecutive increase in temperature occurs, which is a result of partial overheating (i.e., hotspot formation) due to the heat conduction-related delay of hot area detection inside the product. It is to note that on the process side there is no possibility to actively cool the product. In consequence, an overheating by up to 10 °C can be observed in case of an advanced process duration. Overall, this partial overheating did not show a negative impact on foam stability during the drying process as the samples were already largely dehydrated at this stage.

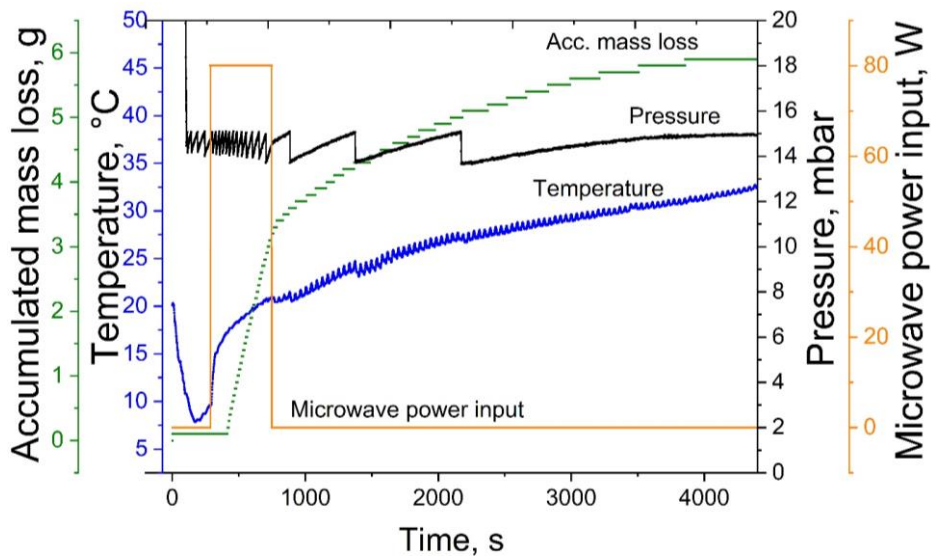


Fig. 4.5.2: Scheme of MWVD process with time-dependent mass loss (green), temperature (blue), and microwave power input (orange).

After the drying process, the foams were optically analyzed and evaluated. Because collapsed foams imply various disadvantages like reduced product quality or impaired further processing properties (Sankat and Castaigne 2004), a successfully dried product was defined by an aerated structure without collapse during drying.

4.5.2.7. Statistics

All experiments were performed at least in triplicate using independent batches of sample dispersions. Error bars represent the standard deviation of samples.

4.5.3 Results and discussion

4.5.3.1. Conventional versus microwave-assisted vacuum foam drying

The combination of vacuum and microwaves for the drying of foams is a promising hybrid for fast and high-quality processing of foods and pharmaceuticals (Walters et al. 2014; Ratti and Kudra 2006a). However, both processes differ in terms of heating and drying speed, which implies different requirements for the samples' foam properties. In order to specify these differences, dispersions of 3% WPI with 10–40% MDX were foamed and then subjected to conventional (CVD) or microwave-assisted vacuum drying (MWVD). While WPI served as a foaming agent, MDX at different concentration levels was used to modify bulk viscosity. Thereby, the gradual increase in MDX led to a decrease of overrun and bubble size.

Due to the volumetric heating, it was expected that MWVD would be faster than CVD. Furthermore, a shorter drying time in combination with an increased evaporation area (Sangamithra et al. 2015) was assumed to reduce foam decay as compared to CVD.

Product structures resulting from CVD and MWVD are shown in Fig. 4.5.3. During CVD, it was observed that all samples retained their foam structure. Although certain foam collapse occurred for 10 and 20% MDX, the foam structures were preserved for the most part. By comparison, for samples with 30 and 40% MDX, the foams remained stable until the end of the drying process. For MWVD, samples with 20, 30, and 40% MDX were stable throughout the process and resulted in aerated products. Only for samples with 10% MDX complete foam collapse occurred as shown in Fig. 4.5.3. Overall, foam decay during drying was more pronounced for MWVD than for CVD. This observation could be related to differences in the capacity of the respective vacuum pumps installed in the two drying plants. For MWVD, pressure decrease happened faster than for CVD, which in turn was assumed to imply higher mechanical stress, potentially triggering foam collapse. However, monitoring of the initial phase of the MWVD process revealed that vacuum creation as such did not induce foam collapse, it actually happened after a few minutes of microwave power input. In this regard, (Ratti and Kudra 2006a) stated that foams need to be stable for at least 1 h in order to withstand vacuum drying

conditions. Findings from a preliminary study on the foaming properties of WPI-MDX dispersions (2.5% w/w WPI with 1–10% w/w MDX; results not shown) suggested that 10% MDX might not have been enough to appropriately prevent foam structure destabilization, as drainage rate at ambient pressure was still relatively high. Presumably, foam structures from sample dispersions with 10% MDX were too fragile to withstand MWVD conditions.

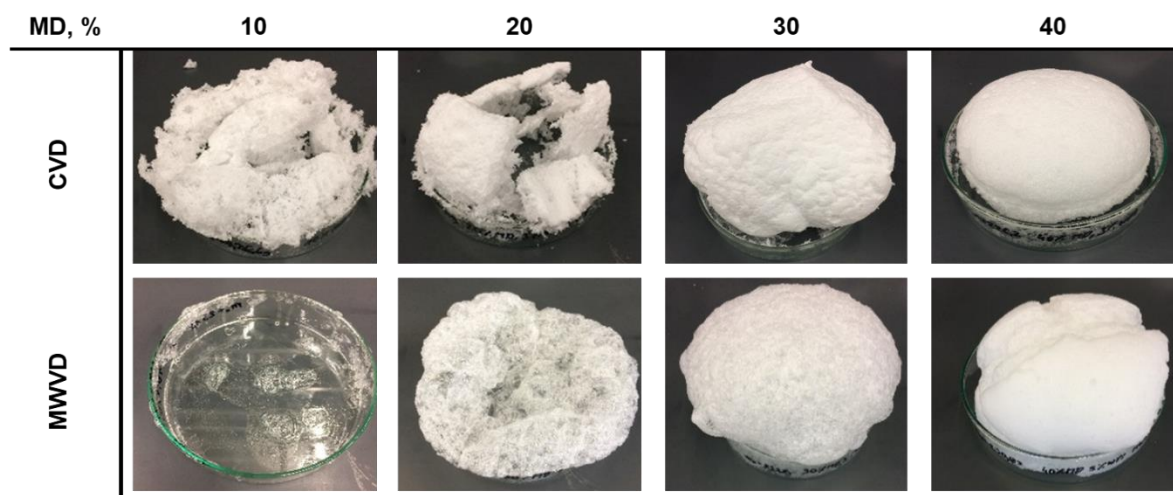


Fig. 4.5.3: Product structure of foams from 3% WPI with 10, 20, 30, or 40% MDX after drying.

Besides the differences in foam collapse during CVD and MWVD as a function of MDX content, the resulting structures also exhibited different bubble sizes. As appears from Fig. 4.5.3, the bubble size of MWVD-dried foams was higher as for CVD. This could be explained by the highly efficient and volumetric heating of microwaves, resulting in very fast bubble expansion, which in turn triggers film rupture and bubble coalescence. In contrast, it was supposed that higher evaporation rates would keep bubbles separated (Sangamithra et al. 2015) and would promote the formation of finer pores and new bubbles (Sankat and Castaigne 2004), which in turn would result in a better preservation of aerated structures during drying. It seems logical that a formation of new bubbles could also occur during MWVD and CVD as a result of boiling. However, this finding by Sankat and Castaigne (2004) refers to hot air drying of foamed banana puree with relatively low overrun. In addition, no vacuum was applied. Therefore, the process can be considered gentler in terms of mechanical stress as compared to CVD and MWVD, and thus result in better bubble preservation.

Referring to the results displayed in Fig. 4.5.3, for MWVD, the rate of new bubble formation might have been lower than the rate of bubble collapse, which would explain the observed foam collapse. However, foam collapse always happened within a few seconds, whereas a foam collapse due to too slow reformation of bubbles was expected to occur over the whole drying process. Further, when the foam collapsed completely, no reformation of bubbles was

observed. This might be due to a too high viscosity of the remaining liquid, which hindered the formation of new bubbles.

Further, the evaporation of water resulted in a concentration of MDX and protein, which influenced, on the one hand, the viscosity but also might have influenced the interfacial elasticity and thereby overall foam stability (Maldonado-Valderrama and Patino 2010). However, higher foaming agent concentrations do not necessarily need to have a significant impact on the interfacial elasticity as shown by Wang and Narsimhan (2005) for β -lactoglobulin concentrations between 0.01 and 0.5%. Therefore, due to concentration, the interfacial elasticity might have increased. However, the different formulations with an MDX content between 10 and 40% had probably a higher impact on the foam stability than the concentration of foaming agent throughout the drying process.

Overall, the comparison of both drying techniques clearly showed that foam structure preservation and therewith, drying performance is a fragile interplay between process conditions and foam properties. In order to better understand the differences between the samples as a function of MDX content as well as the specificity of the microwave drying process, interfacial characteristics and dielectric properties of the sample dispersions were investigated.

4.5.3.2. Surface tension

Fig. 4.5.4 displays the time-dependent evolution of surface tension of WPI as a function of MDX content in the range of 0–40%. It appears that increasing the MDX content from 0% to 30% resulted in a clear enhancement of surface activity when referring to the respective surface tensions at 120 min. This might be explainable by the presence of surface-active residuals from the manufacturing process of MDX (Pycia et al. 2017; Shogren and Biresaw 2007). However, as discussed in chapter 4.5.3.3., this might also be due to interactions between WPI and MDX based on hydrogen bonds and steric hindrance.

It is to note that for samples with 40% MDX, the surface tension appeared to increase during the first seconds of the measurement (Fig. 4.5.4). This displays an artefact and is attributed to both the method and the high viscosity of the dispersion. Furthermore, it is to mention that a quasi-equilibrium state was not reached within the 2 h of measurement. This can also be reduced to the viscosity and applied to all sample dispersions investigated. In consequence of the relatively high viscosity, protein molecule mobility and ability to rearrange at the interface might have been impaired, thus leading to a deceleration of adsorption (Baeza et al. 2006; Baeza et al. 2005).

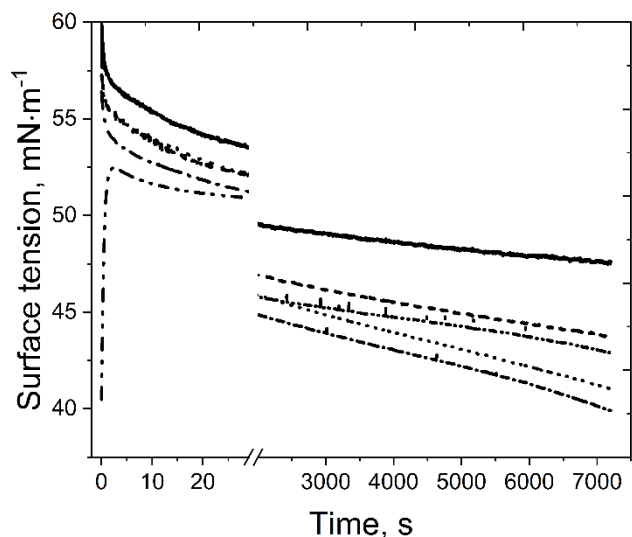


Fig. 4.5.4: Surface tension of 3% WPI dispersions with 0 [—], 10 [---], 20 [· · ·], 30 [— ·] or 40% [— · ·] MDX at 20 °C.

Nonetheless, the obtained data was considered suitable to reflect the changes occurring during foam drying. This assumption is based on the fact that surface age of the prepared foams was only about 30–60 min at the time of drying and thus would not reach an equilibrium state.

Overall, the effect was most pronounced at 40% MDX as viscosity at this condition was highest. As appears from Fig. 4.5.4, the surface tension of this sample at 2 h was even higher as for the sample dispersions with 20 and 30% MDX. However, it was assumed that the surface tension would further decrease and finally reach an even lower level.

As proposed by Marinova et al. (2009), surface tension data was used to estimate a surface activity index based on the initial decrease of surface tension (i.e., $t = 5$ s). It was observed that the surface activity index increased from $-3.43 \text{ mN m}^{-1} \cdot \text{s}^{-1}$ at 0% MDX to $-4.05 \text{ mN m}^{-1} \cdot \text{s}^{-1}$ at 40% MDX. Furthermore, the obtained data shows that the MDX-related viscosity increase (data not shown) did not impair the initial surface adsorption of WPI.

Apart from its effect on bulk viscosity, the increase in surface activity index with increasing MDX content could serve as an explanation for the higher structural stability of the respective foams during drying. Both pressure decrease and heating induce bubble expansion and thus, increase the surface area. In order to prevent bubble rupture, the newly formed air/water interface needs to be quickly stabilized by surface-active components. Hence, high surface activity is key to counteract foam destabilization in a highly dynamic situation such as during vacuum drying.

4.5.3.3. Surface dilatational properties

Surface dilatational characteristics are often used as an indicator of foam stability as they are supposed to reflect intermolecular interactions (e.g., protein-protein interactions) within the surface film. In this regard, Fig. 4.5.4 shows the impact of MDX concentration on the surface dilatational elasticity (E') and surface dilatational viscosity (E'') of WPI. Overall, results for E' and E'' are in a typical range for protein-stabilized air/water interfaces (Dombrowski et al. 2017) and indicate viscoelastic behavior.

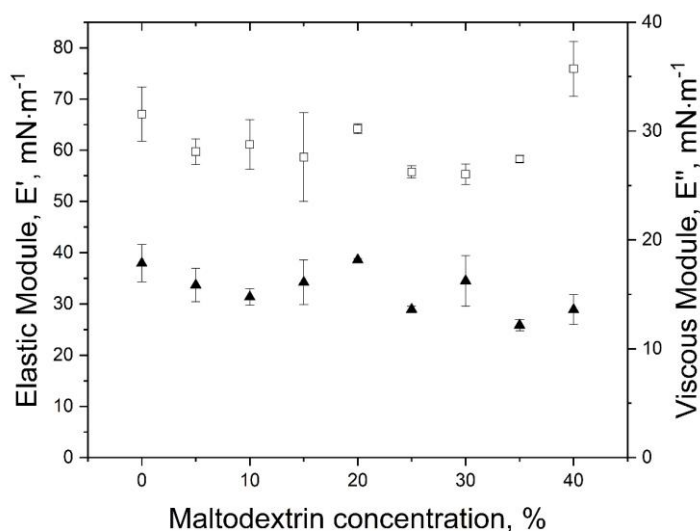


Fig. 4.5.5: Impact of MDX concentration on surface dilatational properties of WPI: (\square) surface dilatational elasticity E' , (\blacktriangle) surface dilatational viscosity E'' at an amplitude of 500%.

Regarding the effect of MDX content, no clear trend could be observed. Nonetheless, E' seemed to slightly decrease with increasing MDX content until 35% ($58 \text{ mN}\cdot\text{m}^{-1}$), whereas at 40% MDX ($76 \text{ mN}\cdot\text{m}^{-1}$), E' was significantly increased as compared to 0% MDX ($67 \text{ mN}\cdot\text{m}^{-1}$). One explanation for this increase at high concentrations might be macromolecular crowding, resulting in a change of protein-protein interactions (Yadav 2013; Laurent 1995). In consequence, interactions between WPI and MDX could be reinforced, resulting in higher E' . By comparison, E'' remained at a relatively constant level of about $15 \text{ mN}\cdot\text{m}^{-1}$.

Besides, $\tan(\varphi)$ was used to more clearly emphasize the elastic contribution to surface film viscoelasticity. The respective data are summarized in Table 4.5-1, where a value of zero would indicate a perfectly elastic system (Baeza et al. 2006; Conde and Rodríguez Patino 2005). The most elastic samples were found for MDX concentrations above 30%. Therefore, it was expected that the mechanical stress occurring during drying and affecting foam structural stability would be lowest for those samples. This is based on the assumption that surface elasticity imparts bubble stability.

Table 4.5-1: Tan(ϕ) of WPI dispersions as a function of MDX content.

c(MDX), %	0	5	10	15	20	25	30	35	40
tan(ϕ), -	0.27± 0.01	0.27± 0.04	0.24± 0.02	0.27± 0.01	0.28± 0.00	0.24± 0.01	0.29± 0.03	0.21± 0.01	0.18± 0.01

The decrease of tan(ϕ) for MDX > 30% could be explained by interactions between whey proteins and MDX. As MDX is an uncharged molecule, these interactions should be of hydrophilic and/or hydrophobic nature (Semenova et al. 2003), rather than electrostatic. In this regard, it could be possible that WPI components and MDX form surface-active complexes, which are interfering with the interface – a mechanism that is often described in literature (Wangsakan et al. 2004; Dickinson 2003). Besides, a certain thermodynamic incompatibility of the polysaccharide/protein system could have promoted protein-protein interactions at the air/water interface (Baeza et al. 2006). In contrast to our findings, Baeza et al. (2006) observed a decrease of surface elasticity for β -lg-polysaccharide mixtures (λ -carrageenan, propylene glycol alginate) due to reduced protein-protein interactions. One reason for this different observation could be the lower applied foaming agent concentration (0.1% w/w) in comparison to our study (3% w/w), whereby few interactions between polysaccharide and foaming agent have higher impact on the elastic behavior of the film. Further to that, the polysaccharides investigated by Baeza et al. (2006) were ionic and therefore, different interactions like electrostatic interactions between polysaccharide and protein are expected compared to the non-ionic maltodextrin in our study. Furthermore, for MDX concentrations above 30%, the protein molecules might have been concentrated at the air/water interface as a result of excluded volume (Baeza et al. 2006; Carp et al. 1999). Thereby, as indicated above, a strengthening of protein-protein interactions might have been the reason for the increased surface elasticity. Similar observations were reported by Tsapkina et al. (1992), who investigated the behavior of aqueous 11S-globulin-dextran mixtures at an n-decane interface. According to their findings, the interfacial protein concentration was increased due to excluded volume.

Furthermore, as whey proteins carry a strongly negative surface charge at neutral pH, certain gaps in between adsorbed protein molecules might allow for a co-adsorption of MDX as proposed for other polysaccharides in protein systems (Bouyer et al. 2012; Baeza et al. 2005). This co-adsorption might influence surface dilatational properties as suggested by Sangamithra et al. (2015). However, in our study, higher protein concentrations were used and therefore it was assumed that the surface was completely covered and hence, this effect was considered less likely.

Besides the changes in surface elasticity, interactions between maltodextrin molecules might have influenced the foam decay during the drying, as they influenced the firmness of the foam

as a result of interactions between non-polar glucose units among two maltodextrin molecules as also stated by Duan et al. (2001). Thereby, the foam structure was preserved and stabilized during the second half of the drying process.

Despite the observation of an MDX concentration-dependent change of surface elasticity, the overall surface elasticity of all investigated dispersions was high ($\tan(\varphi) < 0.3$). Therefore, the overall stability was high enough to withstand the drying conditions independently of the drying process technology, whereas the size of the bubbles increased more at microwave-assisted processed compared to CVD (Fig. 4.5.3).

However, neither surface tension nor surface rheology was dependent on the used drying technique and could therefore not explain the differences between conventionally and microwave processed samples. In order to explain the observed differences, the heating properties of the solutions inside a microwave were investigated. In addition to the impact of MDX content, the influence of the temperature was examined.

4.5.3.4. Dielectric properties of the bulk phase

The dielectric properties of WPI dispersions with varying MDX content are shown in Fig. 4.5.6A. The dielectric constant linearly decreased with increasing MDX content from 76 at 0% MDX to 41 at 40% MDX. A reason for this could be that the molecule rotation in the alternating microwave field was limited by the molecule size due to the binding of free water to the polysaccharide. For comparison, the dielectric constant of pure water is about 80 (Archer and Wang 1990; Haggis et al. 1952).

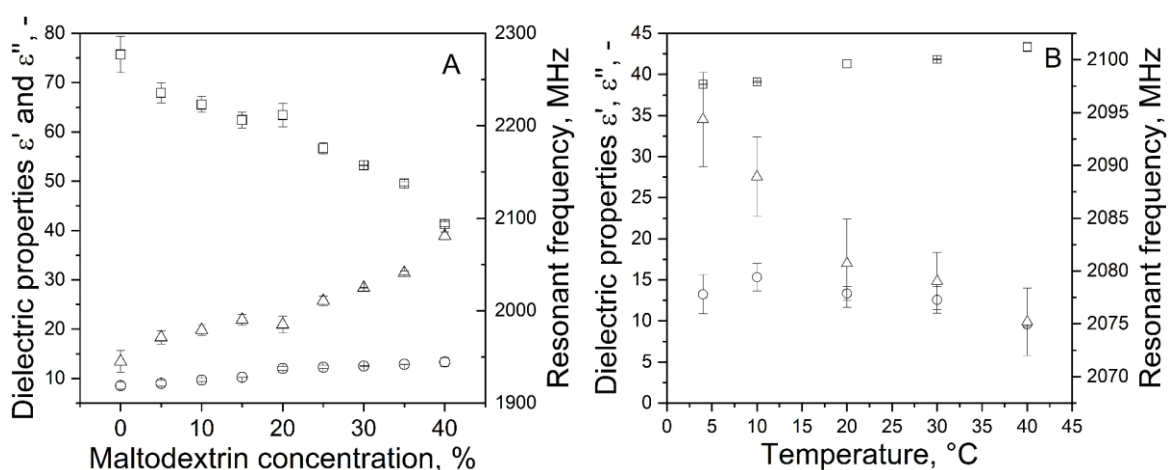


Fig. 4.5.6: (A) Dielectric constant ϵ' (□), dielectric loss ϵ'' (○) and resonant frequency (Δ) of 3% WPI dispersions in dependence of MDX content at 20 °C and (B) dielectric constant ϵ' (□), dielectric loss ϵ'' (○) and resonant frequency (Δ) of 3% WPI-40% MDX dispersions as a function of temperature.

In a study about the dielectric properties of potato starch and other carbohydrates, Roebuck et al. (1972) stated that adsorbed water is not or only slightly polarizable by microwaves. As a

result, the dielectric constant decreased with increasing carbohydrate content. This would be following our results on MDX. However, it is worth to note that the influence of adsorbed water on the dielectric properties strongly depends on the applied microwave frequency and that for lower frequencies the adsorbed water has a significant impact on the dielectric properties (Radoń and Włodarczyk 2019). In contrast to the dielectric constant, the dielectric loss factor slightly increased with increasing MDX content (i.e., from about 9 at 0% MDX content to 13 at 40%). This might be a result of the stabilizing interactions between OH-groups and the alternating microwave field (Tulasidas et al. 1995; Roebuck et al. 1972). Further, the resonant frequency increased from 1945 MHz without MDX to 2080 MHz for samples with 40% MDX content. Similar findings have been reported for the evolution of the dielectric properties of carbohydrate solutions (e.g., potato starch, glucose, or sucrose) in dependence on their total solids content (Liao et al. 2001; Roebuck et al. 1972).

In Fig. 4.5.6B, the dielectric constant, dielectric loss factor, and the resonant frequency of 40% MDX samples are shown for temperatures between 4 and 40 °C. This temperature range was expected to occur during the vacuum drying process, low temperatures due to high evaporation rates, and the high temperatures due to hotspot formation. It was observed that the dielectric constant increased with temperature, while resonant frequency and loss factor decreased.

A second-order polynomial fit of the resonant frequency in dependency of MDX content (data not shown) revealed that the resonant frequency reached above around 80% MDX the ISM bandwidth (2400 MHz), which would result in very efficient heating of the product. Reaching this MDX content during the drying process seems likely, as the residual water content of the samples was around 5%. Hence, one could expect that the foam would collapse due to high thermal stress at the end of the drying due to better absorption of microwave energy. However, against this expectation, the foam remained stable. One explanation for this could be the temperature dependency of the resonant frequency as shown in Fig. 4.5.6B. Therefore, it can be stated that the MDX content would have to be much higher than 80% MDX, as the resonant frequency decreased with the increasing temperature of the product. Even for the unlikely event that the resonant frequency was within the working frequency of the microwave, the thick lamellae and the high viscosity of the bulk phase might have suppressed the expansion of the bubbles and the collapse of the foam (Ambros et al. 2019a). Furthermore, parts of the sample might have already been dry and solid, which could have resulted in a good stabilization of the wet residual sections inside the foam cake. Hence, it seems meaningful that the resonant frequency of a formulation matches the working frequency of the microwave as long as the interface is elastic and the viscosity of the bulk phase is high enough.

Table 4.5-2 Tan(δ) and penetration depth (PD) for WPI dispersions as a function of MDX content at 20 °C.

c(MDX), %	0	5	10	15	20	25	30	35	40
tan(δ), -	0.12	0.13	0.14	0.16	0.17	0.20	0.22	0.23	0.26
PD, cm	8.60	7.33	6.58	5.93	5.12	4.48	4.13	3.74	3.01

In addition to the different overall foam decay behavior of CVD and MWVD treated samples, larger bubbles were obtained for microwave-assisted dried samples, as shown in chapter 4.5.3.1. Those can be explained by the specific heating of polar substances like water due to the application of microwaves (Radoń and Włodarczyk 2019). The liquid lamellae are heating the gas inside the bubbles, which expands and increases the size of the bubbles. Due to higher tan(δ) the energy will be converted more efficiently into heat. Furthermore, the heating will be less volumetric due to a lower penetration depth (Table 4.5-2). However, the harsher heating was more concise for higher moisture samples as compared to samples with higher solid content. This can be explained by longer heating periods of the product, which in combination with a delayed temperature measurement due to higher overrun, resulted in a higher thermal stress. This might be an additional explanation, why foams with lower MDX content were not stable throughout the drying process. Therefore, we assumed that the combination of specific heating and high mechanical stress, as already discussed in chapter 4.5.3.1, was the reason for the different bubble sizes of MWVD and CVD samples.

4.5.4 Conclusion

In this study, the behavior of pre-foamed WPI-MDX samples was investigated during CVD and MWVD. It was shown that for CVD, all examined samples remained stable throughout the process, while during the mechanically and thermally more challenging MWVD foams with less than 20% MDX collapsed. To find a correlation between foam collapse occurring during the drying process and the dispersions' properties, their surface activity, surface dilatational properties, and dielectric properties were investigated.

The surface tension decreased with increasing MDX content, while the surface activity index increased. This was attributed to the interaction between MDX and whey proteins based on hydrogen bonds and steric hindrance. However, foam decay during drying could not be linked to surface tension or surface activity index. The surface elasticity was already relatively high at MDX concentrations between 0 and 30% and even further increased for MDX > 30%. This was attributed to the excluded volume due to the hydration of the polysaccharide as well as steric hindrance. Overall, surface dilatational properties were considered key for successful foam drying. A key finding was that tan(δ) increased with increasing MDX content, which reflects a faster heating of the product. However, concerning foam stability, the dielectric properties were of minor importance, especially for samples with high MDX content. Nonetheless,

the change of dielectric properties with increasing MDX content as well as temperature shows the complexity of defining or adapting product formulation and process conditions for MWVD. Therefore, it is recommended to measure those properties for samples, which are intended to be dried with MWVD.

Nevertheless, surface activity, surface dilatational properties, and dielectric properties are known to change with biopolymer type and concentration, viscosity, and temperature. Therefore, and to be able to draw more generalized conclusions, further surface-active molecules (e.g. ionic surfactants or plant proteins) also in combination with other commonly used polysaccharides (e.g., pectin or xanthan) would need to be investigated in terms of their foam structural stability during vacuum drying.

Author contributions: Peter Kubbutat, Conceptualization, Methodology, Investigation, Writing – original draft, Writing – review & editing, Visualization. Ulrich Kulozik, Writing – review & editing, Resources, Supervision, Funding acquisition, Jannika Dombrowski, Conceptualization, Writing – original draft, Writing – review & editing

Declaration of competing interest: The authors declare that they have no known competing financial interests or personal relationships that could have appeared to influence the work reported in this paper.

Acknowledgments: This research project was supported by the German Ministry of Economics and Energy (via AiF) and the FEI (Forschungskreis der Ernährungsindustrie e.V., Bonn), Project AiF 18819 N. The authors would like to thank Krüss GmbH for providing the DSA100R.

4.6 Stability of foams in vacuum drying processes. Effects of interactions between sugars, proteins, and surfactants on foam stability and dried foam properties

The aim of the study was to investigate the influence of different sugar types and concentrations on the foam decay behavior in vacuum and microwave-assisted vacuum drying of polysorbate 80 and β -lactoglobulin stabilized foams on a molecular, surface, and macroscopic level. Regarding the molecular interaction level, the second virial coefficient, A_2 , was determined to measure the impact of saccharide addition on intermolecular attraction or repulsion of surfactants or proteins as foaming agents. Further, the surface tension, surface activity, and the surface dilatational properties of the samples were determined. In addition, samples were dried in vacuum and microwave-assisted vacuum drying, and the foam decay behavior during the drying process related to the properties of the solutions.

It was found that the repulsion between surfactant micelles was not significantly influenced by the added saccharides. In contrast, the repulsion of proteins was significantly lowered in the presence of saccharides and strongly dependent on the used type of saccharide. The surface tension and surface activity were influenced for all investigated systems and independent on the used foaming agent. However, no correlation between surface tension or surface activity and the foam decay during the drying process was obtained. The surface dilatational properties were massively influenced by the type and concentration of saccharides. Surfactant stabilized foams became more brittle with higher saccharide concentration. This was attributed to the easy detachment and attachment of surfactants at the air-water interface. While surfactants usually cover the surface fastly, the reattachment might be hindered due to interactions with saccharides. In contrast, protein stabilized foams became more elastic, which was attributed to the preferential exclusion effect. Most foams utilizing polysorbate 80 collapsed during VD or MWVD, while nearly all investigated foams using β -Ig remained stable. It was found that a good prediction of the foam decay during the drying process can be made using a combination of E' and $\tan(\varphi)$. Samples with high E' and low $\tan(\varphi)$ were most suited for the drying with VD or MWVD.

The substantial contribution of the doctoral candidate was the conception and design of the experiments. Further, he was substantially involved in the performance of experiments and acquired parts of the data for the manuscript, and interpreted the data set. Furthermore, the critical literature review and chiefly writing of the manuscript were done by the candidate. Co-authors contributed to the experimental part and/or in the discussion of the results and provided input to the drafted manuscript prior to and during submission.

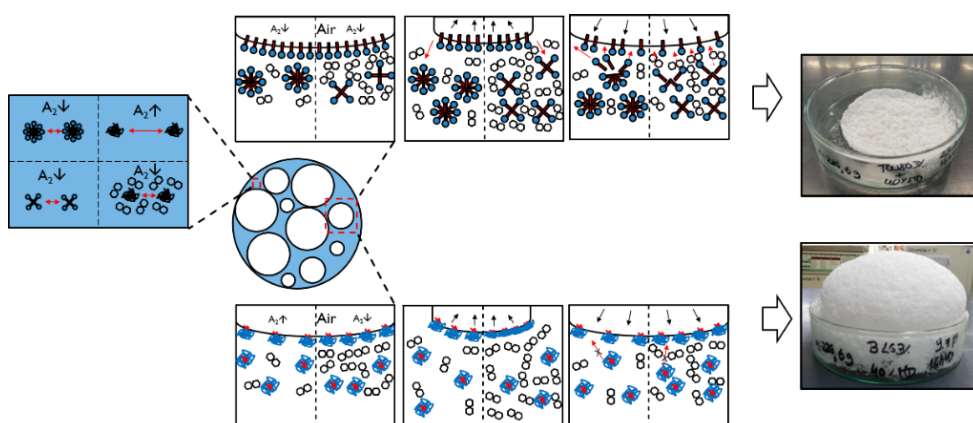
Stability of foams in vacuum drying processes. Effects of interactions between sugars, proteins, and surfactants on foam stability and dried foam properties⁵

Peter Kubbutat^{1,*}, Luísa Leitão¹, Ulrich Kulozik¹

¹Chair of Food and Bioprocess Engineering, School of Life Science, Technical University of Munich, 85354 Freising, Germany

*Correspondence: peter.kubbutat@tum.de

Received: 7 July 2021; Revised: 5 August 2021; Accepted: 11 August 2021; Published: 13 August 2021



Abstract:

The hypothesis was that saccharides mediate interactions between surface-active components and that this will have an impact on foam decay during the drying process. Static light scattering was performed to determine changes in interactions between the foam stabilizer on a molecular level. Further, pendant drop and oscillating drop measurements were performed to examine the surface tension and surface rheology. Foams were dried in conventional as well as microwave-supported vacuum dryers. Final foam properties were determined. It was shown that the addition of sugars, often added as protective substances for sensitive organic molecules, resulted in lower repulsion between different types of surface-active components, namely poly-sorbate 80 and β -lactoglobulin (β -lg). Differences in impact of the types of sugars and between different types of surfactant, protein, and small molecules were observed influencing the foam decay behavior. The interfacial properties of polysorbate 80 and β -lg were influenced by the type of the used sugars. The surface elasticity of protein stabilized surfaces was higher compared to that of polysorbate stabilized systems. Protein stabilized systems remained more stable compared to polysorbate systems, which was also affected by the used saccharide. Overall, a correlation between molecular interactions and foam decay behavior was found.

Keywords: Foam; Saccharides; Static light scattering; Molecular interactions; Surface tension; Surface rheology; Vacuum drying; Microwave drying

⁵ Original publication: Kubbutat, P.; Leitão, L.; Kulozik, U. (2021) | Stability of foams in vacuum drying processes – Effects of interactions between sugars, proteins, and surfactants on foam stability and dried foam properties, *Foods*, 10, 8, 1876, <https://doi.org/10.3390/foods10081876>. Adapted original manuscript. Adaptions of the manuscript refer to enumeration, citation style, spelling, notation of units and format. Permission for reuse of article is granted by the authors and MDPI. References of all chapters are merged at the end of the dissertation.

4.6.1 Introduction

In order to preserve sensitive, high-value food or pharmaceuticals components, products are stored refrigerated or even frozen. Another option is to dry products to prolong shelf life. (Heldman et al. 2019)

One way to remove water from products containing components sensitive to heat or oxidation is vacuum drying, which avoids excessive thermal stress by lower boiling point temperatures (Walters et al. 2014; Santivarangkna et al. 2007b) as applied to oxygen-sensitive materials like fruits or proteins (Bhandari et al. 2013). Sugars are often added as protective substances to prevent or mitigate structural changes and related losses in activity of organic material like enzymes or microorganisms. However, vacuum drying is limited in production capacity due to batch operation in most cases and the small size of vacuum chambers and long required drying times. Furthermore, the shrinkage of vacuum-dried products is higher compared to – e.g., freeze drying – but lower than hot-air dried products (Balzarini et al. 2018; Jaya and Das 2003). Moreover, vacuum dried products are elastic and, therefore difficult to mill to obtain powders and they are slow in rehydration due to their compact structure.

One way to overcome most of these problems is to aerate the product before or at the beginning of the drying process (Huang et al. 2015; Ratti and Kudra 2006a). Thereby, the surface area increases and the lamellae act as capillaries, transferring the water to the product's surface, which results in faster drying (Rajkumar et al. 2007) and a porous structure of the dried product (Huang et al. 2015; Sangamithra et al. 2015; Kadam et al. 2012). However, the heat transfer into the product is lower, as the height of the product increases and the air voids inside the foam are acting as an insulator.

As the water transport occurs through the lamellae, the foam must be structurally stable, even drying processes imposing harsh conditions (Ambros et al. 2019b; Ratti and Kudra 2006a). The main factors affecting liquid foam stability are disjoining pressure, viscoelasticity of the surfactant film, and interfacial tension. These factors are directly correlated with the leading causes of foam instability, namely liquid drainage, gas disproportionation, and bubble coalescence, all of which result in liquid film thinning and rupture (Georgieva et al. 2009; Damodaran 2005). Therefore, knowledge about the interactions between foaming agents, foam stabilizing additives, and foam stability under processing stress is of great importance, as these factors influence the foaming capacity of the starting solution and the resulting foam stability (Davis and Foegeding 2007).

In order to improve the heat transfer into foams, microwave technology can be applied instead of heat conduction by heated shelves (Foerst et al. 2012; Kardum et al. 2001). Microwaves are principally able to volumetrically heat the product across the entire product to the point of the

moving drying front. As a result, the drying speed increases immensely (Kardum et al. 2001). Therefore, different researchers reported that the combination of foaming and vacuum drying is beneficial to increase the drying speed and to improve the structure of the dried product (Ambros et al. 2019b; Ambros et al. 2016). However, most of these studies are investigating protein stabilized and complex systems like fruits foams or bacteria suspensions (Kadam et al. 2012; Foerst et al. 2012; Bauer et al. 2012). In conjunction with added sugars, complex situations occur, which have not been intensely studied so far. Sugars might have an additional role in this regard, next to their protective effect against thermal and dehydration stress on sensitive organic molecules.

Few studies used small surfactants or stabilizing foaming agent-sugar combinations when studying foam stability during vacuum drying (Jangle and Pisal 2012; Ohtake et al. 2011; Abdul-Fattah et al. 2007a). To the best of our knowledge, studies investigating the impact of surfactant-stabilized foams in accelerated microwave-assisted vacuum drying are lacking. Interactions of polysorbate 80 and various sugars, also added as protective agents of sensitive organic material like therapeutic proteins, enzymes, or microorganisms, and their impact on the foam properties was investigated in a previous study (Kubbutat and Kulozik 2021b). Therein, it was shown that sugars influence the interaction of surfactants at the air-water interface and change foam properties, mainly bubble size, firmness, or stability, depending on the used type of saccharide. However, surface rheology was not investigated, which is essential for the characterization of mechanical foam stability (Davis and Foegeding 2007). Hence, the impact of saccharides on different foam stabilizer systems regarding foam stability during vacuum and microwave-assisted vacuum drying is still largely unknown.

Therefore, the aim of the study was to investigate the influence of different sugar types and concentrations on the foam decay behaviour during vacuum, and microwave-assisted vacuum drying of polysorbate and β -lactoglobulin (β -lg) stabilized foams. Sorbitol, maltose, sucrose, and maltodextrin were added to polysorbate 80 and β -lg solutions, and those complex solutions were investigated on a molecular, surface, and macroscopic level. Regarding the molecular interaction level, the second virial coefficient, A_2 , was determined to measure the impact of saccharide addition on intermolecular attraction or repulsion of surfactants or proteins as foaming agents. In order to be able to determine molecular interactions, β -lg was used instead of whey protein isolate. The results were used to explain differences in surface tension and surface rheology. Finally, it was aimed at finding a correlation between molecular interactions, interface properties, and dried foam properties. The hypothesis was that the sugars are interacting differently with proteins and surfactants due to H-bonds or conformational differences of the saccharide structure, which directly influence the interfacial properties and, therefore, the foam preservation in vacuum drying of foams. Further, it was expected to gain relevant

insights from comparing vacuum drying (VD) and microwave-assisted vacuum drying (MWVD) since different formulations will influence the heating properties during MWVD.

4.6.2 Materials and methods

4.6.2.1 Materials

As foaming agent, polysorbate 80 (average molecular weight (M_w) 1310 g·mol⁻¹ (Merck KGaA 2020), PS80, Sigma-Aldrich Chemie GmbH, Taufkirchen, Germany) and isolated β -lactoglobulin ($M_w = 18.4$ kg·mol⁻¹, β -lg, in house production, purity >98%; method of production described by Toro-Sierra et al. (2013) were used. The total protein content was measured with a VarioMaxCube (Elementar Analysensysteme GmbH, Langenselbold, Germany), which measures the nitrogen content in a sample with thermal combustion according to the method of Dumas (Dumas 1831). The saccharides D-sorbitol ($M_w = 182.2$ g·mol⁻¹, SOB, Gerbu Biotechnik GmbH, Heidelberg, Germany), D-maltose ($M_w = 342.3$ g·mol⁻¹, MTO, Gerbu Biotechnik GmbH, Heidelberg, Germany), sucrose ($M_w = 342.3$ g·mol⁻¹, SUC, Carl Roth GmbH, Karlsruhe, Germany) and maltodextrin DE6 ($M_w = 2880$ g·mol⁻¹ (Castro et al. 2016), MDX, Nutricia GmbH, Erlangen, Germany) were used as thickening agents. MilliQ-Water was used to prepare the solutions. Toluene was sourced from Merck (KGaA, Darmstadt, Germany).

Sample dispersions of 200 g each were prepared by mixing and dissolving 3% (w/w) β -lg or polysorbate 80 and different amounts of saccharide (i.e., 10%, 20%, 30%, 35% or 40% (w/w)) in demineralized water. Sample solutions were dissolved at 20 °C and stirred at 200 rpm for 12 h in a 4 °C chamber to ensure complete dissolution of the added sugars. Before use, the samples were tempered at 20 °C in a water bath (F3, Fisher Scientific GmbH, Schwerte, Germany) and stirred using a magnetic stirrer (Maxi Direct, Fisher Scientific GmbH, Schwerte, Germany) at 200 rpm.

The critical micelle concentration (CMC) of PS80 in water was provided by the manufacturer with 13–15 mg·l⁻¹ or 0.012 mM at 20–25 °C (Merck KGaA 2020).

4.6.2.2 Static light scattering measurements

In order to determine the second virial coefficient A_2 , angular and concentration-dependent static light scattering measurements were performed using an ALV/CGS-3 goniometer system (ALV-Laser Vertriebsgesellschaft mbH, Langen, Germany). The goniometer was equipped with a 22 mW HeNe laser, providing coherent and monochromatic light with a wavelength of 632.8 nm at 20 °C. The experimental design was based on that of Antipova and Semenova (1997), which were using static light scattering at for the investigation of surface activity of 11S globulin. For the measurement, angles between $30^\circ < \theta < 150^\circ$ were utilized with 10° increments. Three consecutive individual runs with a data collection time of 10 s were averaged for each angle observation. Data was rejected, and runs were repeated if the intensity fluctuation

was higher than 10%. The refractive indices n of all solvents and toluene were measured using the refractometer 74268 (Carl Zeiss AG, Oberkochen, Germany).

Samples with 1% (w/w) β -lg or 3% (w/w) polysorbate 80 in combination with different maltodextrin (0–2.5% (w/w)), maltose, sucrose, sorbitol (1–7.5% (w/w)) concentrations, regarded as solvents, were investigated against toluene. For data analysis (i.e., static Berry plot analysis (Berry 1966)), the ALV Correlator Software Version 3.0 (ALV-Laser Vertriebsgesellschaft mbH, Langen, Germany) was used to determine the second osmotic virial coefficient A_2 . Thereby, extrapolation of the scattering vector q as well as the protein concentration c towards zero was done by applying a linear regression model, respectively, according to the method also described by Dombrowski et al. (2017).

4.6.2.3 Pendent drop and oscillating drop measurement

Surface tension and surface rheology of polysorbate 80 (3% w/w), as well as β -lactoglobulin (3% w/w) at different concentrations of sorbitol, maltose, sucrose and maltodextrin (0–40% w/w), were measured using a DSA100 (Krüss GmbH, Hamburg, Germany) at 20 °C. For the analysis, the samples were transferred into a syringe, and a drop of 12 μ l was pressed out of a stainless steel needle with a diameter of 1.81 mm. The ADVANCE software (Krüss GmbH, Hamburg, Germany) was used for data analysis and processing, which allowed the determination in the water-air phase of drop surface tension and rheology.

For pendent drop measurement, the picture analysis was done for the first 30 s with 10 frames per second (fps), thereafter for 1000 s with 2.5 fps and finally for 6170 s with 0.25 fps. Therefore, the evaluation of surface tension was monitored for a duration of 7200 s in total for each drop. The surface tension was computed by the software using Young-Laplace formula. The initial slope of surface tension over time (e.g., $d\sigma/dt=10$ s) was used to determine the surface activity according to the description of Marinova et al. (2009).

For the determination of the surface rheology, the surface of the formed drop was firstly brought into quasi-equilibrium, which for polysorbate samples was after 30 min and for β -lg samples was 60 min. Thereafter, the drop was subjected to a sinusoidal oscillation for 100 s with a frequency of 0.1 Hz at an amplitude of 400‰. The oscillatory deformation of the drop surface was ~3.2–5%, which was proved to be in the linear viscoelastic region (data not shown). Three consecutive individual runs were performed for each drop. The complex viscoelastic (E), elastic (storage modulus, E'), and viscous (loss modulus, E'') moduli were calculated by the software using data fitting according to Lucassen and Van den Tempel (1972). The $\tan(\varphi)$ was calculated according to Conde and Rodriguez Patino (2005) (Equation 4.6.1):

$$\tan(\varphi) = \frac{E''}{E'} \quad (4.6.1)$$

4.6.2.4 Foam formation and vacuum drying

In order to produce foams under comparable conditions, 200 g solutions were prepared for each sample. After sample preparation, as described in chapter 4.6.2.1, 150 g of solution was stirred with a planetary rotor-stator mixer (KitchenAid ARTISAN 5KSM150PS, Whirlpool Corp., Greenville, Ohio, USA) with a wire wisp geometry at 220 rpm and 20 °C for 15 min. Directly after that, 15 g of foam was gently transferred into a cylindrical crystallization glass with $d=200$ mm (VWR International GmbH, Darmstadt, Germany). Afterwards, the sample was immediately transferred into the drying plant.

For conventional vacuum drying, a freeze-dryer model Delta 1-24LSC (Martin Christ Gefriertrocknungsanlagen GmbH, Osterode am Harz, Germany) was used. The shelf temperature was set to 20 °C and the pressure was reduced to 15 mbar. The foams were dried for 16 h, except for the foams that completely collapsed. For the latter, the drying process was stopped 30 min after the collapse occurred because no further re-formation of foamy structures was expected 30 min after foam collapse.

The microwave-supported vacuum drying processes were performed using a microwave dryer model μ Vac0150fd (Püschner Microwave Power Systems GmbH & Co. KG, Schwanewede, Germany). The microwave drying plant was controlled by the software μ WaveCAT (Püschner Microwave Power Systems GmbH & Co. KG, Schwanewede, Germany) and allowed process monitoring by the measured weight, temperature, or pressure. The sample weight was measured by an inline scale, which was connected to the turntable, and the product temperature was assessed by a pyrometer. A detailed description of the drying plant can be found in Ambros et al. (2016). The drying process was performed at 15 mbar, 80 W microwave power input, and 20 °C max. product temperature. The process was stopped after no mass loss occurred during 10 consecutive minutes or when the foam collapsed during the drying process.

At least two dryings for each formulation were performed.

4.6.2.5 Analysis of dried samples

Samples, which did not collapse during the drying process were characterized by the residual water content and water activity. In addition, the shape of the solidified pores and the overall foam structure were investigated. For the evaluation of water content and water activity, the dried samples were ground inside an electric coffee mill (PC-KSW 1021, Mühle Clatronic International GmbH, Kempen, Germany) for 15 s in order to obtain a homogeneous powder.

The residual water content was measured using Karl-Fischer titration. The analysis was conducted using a volumetric compact titrator V20S (Mettler-Toledo GmbH, Gießen, Germany). After a pre-titration period of 300 seconds, about 0.05 g sample was added and dissolved for 300 s in a 1:1 (v/v) mixture of Hydranal®-Formamid (Fisher Scientific GmbH,

Schwerte, Germany) dry and Hydranal®-Methanol Rapid (Fisher Scientific GmbH, Schwerte, Germany). After dissolution, the titration with iodine started immediately. A two-fold determination of the moisture content was done, which considering duplicate dried foams, resulted in a four-fold determination of moisture content.

The water activity was conducted in a HygroLab (Rotronic AG, Bassersdorf, Germany) at 25 °C. The measurement was stopped automatically after the value was in equilibrium. A two-fold determination of the water activity was done, which, considering duplicate dried foams, resulted in a four-fold determination of the water activity.

4.6.2.6 Statistical analysis

Error bars represent the standard deviation of samples. Lines are guide to the eye. Statistical significance of mean values was evaluated using OriginPro software (Originlab Corp., Northampton, Massachusetts, USA).

4.6.3 Results and discussion

4.6.3.1 Influence of the type of sugar on the interactions between surface-active components

In order to assess the molecular interactions and behavior of the different foaming agent-sugar systems, A_2 was obtained through the employment of the Berry's method (Berry 1966) to measured SLS data. Briefly, the A_2 value indicates the direction and magnitude of overall intermolecular forces between two particles in solution by its charge and value, respectively. Positive A_2 values correspond to net repulsive forces (where protein-solvent interactions are favored over protein-protein interactions), whereas negative values represent net attractive forces (George et al. 1997).

The second virial coefficient, A_2 , of polysorbate and β -lactoglobulin in the presence of sorbitol, sucrose, maltose, and maltodextrin is shown in Table 4.6-1. The values indicate a trend of repulsive or attractive interactions due to the addition of the investigated saccharides at high sugar concentrations.

Table 4.6-1: Second virial coefficient A_2 of polysorbate 80 and β -lactoglobulin solutions in the appearance of different saccharides at 20 °C.

Foaming agent	Saccharide	A_2 (10^{-7} , mol·dm ³ ·g ⁻²)
Polysorbate 80	Sorbitol	1.38 ± 0.36 ^a
	Sucrose	1.08 ± 0.33 ^a
	Maltose	1.18 ± 0.22 ^a
	Maltodextrin	1.20 ± 0.20 ^a
β -lactoglobulin	Sorbitol	11.30 ± 2.61 ^b
	Sucrose	14.17 ± 7.86 ^b
	Maltose	6.80 ± 1.73 ^b
	Maltodextrin	9.58 ± 3.39 ^b

^{a, b} Means in the same column with different letters indicate significant differences (P<0.05)

For polysorbate samples, the interactions are between $1.38 \cdot 10^{-7}$ for sorbitol and $1.08 \cdot 10^{-7}$ mol·dm³·g⁻² for sucrose, respectively. For β -lg, the value for sucrose ($14.2 \cdot 10^{-7}$ mol·dm³·g⁻²) was the highest, while maltose showed the lowest value ($6.8 \cdot 10^{-7}$ mol·dm³·g⁻²). In other words, the values were much lower for polysorbate samples compared to β -lg samples. However, all samples showed positive A_2 values, thus indicating that the molecules of the foaming agent repulsed each other in the presence of saccharides and that the tendency for aggregation was lowered as well.

Since for polysorbate samples, the used concentration was much higher than the CMC (Merck KGaA 2020), it can be assumed that the molecules were associated with forming spherical micelles (Karjiban et al. 2012; Kerwin 2008). As PS80 is a non-ionic surfactant and the sugars are neutrally charged, electrostatic interactions between polysorbate and saccharides were not likely to play a role. This would also be an explanation for the differences in A_2 between PS80 and β -lg samples. Due to the lack of electrostatic interactions, H-bonds must have been the major interaction type, as already discussed in a previous study about the foaming properties of PS80 foams in the presence of saccharides (Kubbutat and Kulozik 2021b). However, effects like molecular crowding or the incorporation of PS80 into maltodextrin were not observed in the obtained data. This might be due to concentration differences between the previous (up to 60% saccharide concentration) and the actual study (up to 7.5%).

For all investigated saccharides, the A_2 values were $1.3 \pm 0.1 \cdot 10^{-7}$ mol·dm³·g⁻². This is remarkably similar to the A_2 values, found by Richtering et al. (1988) for octa(ethylene glycol) n-tetradecylether (C14E8) in water at 20 °C ($1.1 \cdot 10^{-7}$ mol·dm³·g⁻²). No significant differences between sugar types were detected. This was unexpected, as the investigated sugar types were assumed to have a different ability to form H-bonds due to a different number of potential H-bonding groups and structural differences. Comparable effects were also described by Ali et al. (2019) during their investigation of different types of sugars in aqueous glycine solutions. Further, the modification of hydrophobic interactions between non-ionic surfactants resulting from added saccharides, as described by Claesson et al. (2006) was not detectable. Therefore, it appears likely that the concentration of polysorbate was too high or the concentration of saccharides was too low to detect differences.

In comparison, differences between sugar types in protein samples were more pronounced. All β -lg samples showed a high positive A_2 indicating a higher repulsive character than in the samples containing PS80. One explanation for the high virial coefficient would be that β -lg has a highly negative zeta-potential at neutral pH (Engelhardt et al. 2013), resulting in strong repulsive forces between single molecules. However, the obtained A_2 values were lower than the reported A_2 value for β -lg in pure water by Dombrowski et al. (2018), which was about $15 \cdot 10^{-7}$ mol·dm³·g⁻². Hence, it seems that the saccharides shielded the surface charge and

lowered the repulsive forces down to nearly a third of the value of that of no added saccharide. This could be explained by the preferential exclusion mechanism as reported by Timasheff and Lee (Timasheff 1993; Lee and Timasheff 1981). Due to the higher affinity of the used saccharides for water compared to the affinity of β -lg, water migrated from the protein surface to the bulk solution, leaving the protein preferentially hydrated. Further, the saccharide, now occupying layers adjacent to the hydration layer that surrounds the protein, can act as shielding matter. Thereby, it reduced the charge interactions between β -lg molecules and excluded volume between the proteins in the solution. In total, the repulsive character decreased with the increasing ability of preferential exclusion. Comparable observations were also made by Antipova and Semenova (1997) during their investigation of the influence of dextran and maltodextrin on the surface activity of 11S globulin at the air-water interface. Furthermore, maltodextrin could also sterically hinder interactions between protein molecules due to its molecular size and potentially form clusters, resulting in an effective decrease of A_2 towards zero. Nonetheless, it should be mentioned that maltodextrin consists of saccharides with different chain lengths (Pycia et al. 2017; Shogren and Biresaw 2007; Chronakis 1998b). Therefore, the data correspond to a saccharide mixture, which might influence the value obtained.

Therefore, differences between the sugar types can be attributed to the different structural and chemical properties of the saccharides. Various sugars have different abilities to form H-bonds (Lerbret et al. 2005; Engelsen and Monteiro 2001) and/or to sterically disturb interactions between proteins due to structural differences (Ali et al. 2019).

4.6.3.2. Impact of sugar type and concentration on the surface tension and surface activity of polysorbate and β -lactoglobulin stabilized foams

Besides the second virial coefficient, the surface tension and the surface activity were determined. It was expected that the observed differences in higher A_2 influence the surface activity of foaming agents, as also observed for 11S globulin in the presence of different saccharides (Antipova and Semenova 1997). Surface tension values of sugar dispersions without surfactant are published in Kubbutat and Kulozik (2021b) and showed only a slight decrease in surface tension with increasing saccharide concentration.

The impact of sugar concentration on the surface tension is shown in Fig. 4.6.1. It is clearly observable that the final surface tension of β -lg samples was almost independent of the used sugar and higher compared to polysorbate samples. Further, with the addition of saccharides, β -lg showed slightly higher surface tensions than the control. In contrast, for polysorbate samples, it was found that the higher the saccharide content, the lower the surface tension.

With regard to chapter 4.6.3.1, polysorbate 80 has a lower A_2 value compared to β -lg. Thereby, the polysorbate molecules do not repel as strongly as proteins, and the resulting concentration

at the surface is higher. In addition, all sugars seem to moderate the interaction between polysorbate 80 and air, as the surface tension lowers with saccharide concentration. This is in accordance with a previous study on the influence of sugars on the foam properties of polysorbate 80 foams (Kubbutat and Kulozik 2021b) and can be explained by strong hydrogen bonds between sugar and polysorbate as well as between sugar and water. Further, Staples et al. (1996) stated that sorbitol is able to interact with the ethylene-oxide groups of polysorbate and adsorb at its hydrophilic head group, resulting in lower surface tension. The formation of H-bonds can also be observed by the decrease of CMC of non-ionic surfactants in the presence of saccharides, as found by Acharya et al. (1999).

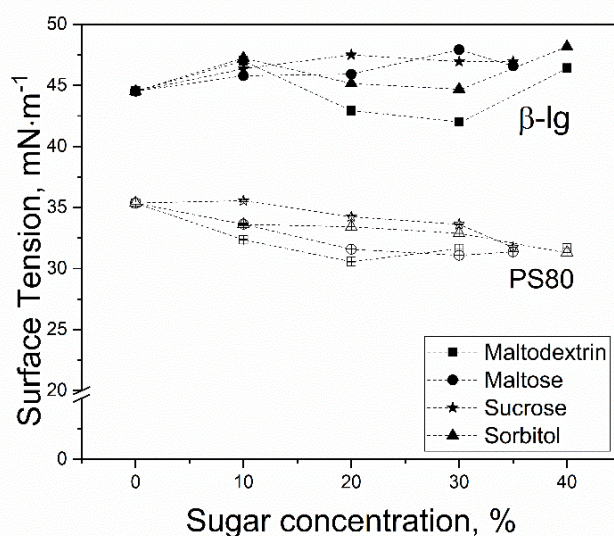


Fig. 4.6.1: Surface tension of polysorbate 80 (empty symbols) and β -lactoglobulin (filled symbols) with different concentrations of added sugar after an equilibrium time of 7200 s at 20 °C, where (■) corresponds to maltodextrin, (●) to maltose, (○) to sucrose and (▲) to sorbitol, respectively.

The authors stated that the reduction in CMC was a result of water-carbohydrate interactions, which were lowering the monomer-stabilizing so-called 'iceberg formation' around non-polar tails of surfactants (Shinoda et al. 1987). The 'iceberg formation' became less pronounced through the strong H-bonds between water and sugar, resulting in the destabilization of the surfactants monomer state followed by a faster formation of micelles and, therefore, a lower CMC (Acharya et al. 1999). As this effect seemed to appear for all investigated saccharides, the surface tension lowered with increasing sugar content.

The high repulsion can explain the higher surface tension of protein samples between the protein molecules described and discussed in chapter 4.6.3.1. As shown in Fig. 4.6.1, there was no constant trend for surface tension in dependency of the sugar concentration observable. However, as A_2 decreased due to the addition of sugar, the surface tension should do so, too, like molecules at the air-water interface repelled each other less. However, this was not

observed. A possible explanation might be that the A_2 value was obtained from different sugar concentrations, and therefore, an overall trend was described. This might also be the reason for the high standard deviation of A_2 .

However, the increasing surface tension might also be a result of two contradictive mechanisms. On one side, the sugars are shielding the charges of the proteins resulting in higher surface concentration, but on the other side, they are stabilizing the natural conformation of the protein, which made the protein interaction with the surface unfavorable. Antipova and Semenova (1997) found during their study of 11S globulin in the presence of sucrose and glucose that proteins have an increased affinity to the aqueous phase with added saccharides and contributed this to strong hydrogen bonds resulting in excluding volume. Even though the concentrations used in our study were much higher, we also detected concentration-dependent changes. One explanation for this could be solvophobic effects, which might have occurred due to strong hydrogen bonds between sugar and water. Thus, the water is less accessible for the protein, whereby the protein gains an increased affinity to move to the hydrophobic air bubble surface. Nevertheless, even though the saccharide concentration was higher than in the study of Antipova and Semenova (1997), the mechanisms leading to the shift of surface tension seem to be comparable. An increasing surface tension was also found for the addition of erythritol or sucrose to WPI dispersions in studies of Nastaj et al. (2021; 2020). The increasing surface tension was explained by less adsorption of proteins at the air-water interface due to the high viscosity of the bulk phase (Nastaj et al. 2021) or differences in protein concentrations (Nastaj et al. 2020).

Table 4.6-2: Calculated surface activity of samples with polysorbate 80 and β -lactoglobulin in the presence of added saccharides with content between 0 and 30% at 20 °C.

c(Saccharide, %)	β -lactoglobulin, $\text{mN}\cdot\text{m}^{-1}\cdot\text{s}^{-1}$				Polysorbate 80, $\text{mN}\cdot\text{m}^{-1}\cdot\text{s}^{-1}$			
	Sorbitol	Sucrose	Maltose	Maltodextrin	Sorbitol	Sucrose	Maltose	Maltodextrin
0	-1.62 $\pm 0.35^a$	-1.62 $\pm 0.35^a$	-1.62 $\pm 0.35^a$	-1.62 $\pm 0.35^a$	-12.53 $\pm 6.44^a$	-12.53 $\pm 6.44^a$	-12.53 $\pm 6.44^a$	-12.53 $\pm 6.44^a$
10	-1.60 $\pm 0.26^a$	-1.79 $\pm 0.31^a$	-1.51 $\pm 0.34^a$	-1.40 $\pm 0.30^a$	-12.72 $\pm 6.55^a$	-13.02 $\pm 7.01^a$	-14.63 $\pm 7.75^a$	-4.40 $\pm 1.80^{a,c}$
20	-1.56 $\pm 0.29^a$	-2.26 $\pm 0.46^a$	-1.32 $\pm 0.19^a$	-2.38 $\pm 0.68^a$	-13.18 $\pm 6.81^a$	-14.29 $\pm 7.33^a$	-14.95 $\pm 8.06^a$	-1.07 $\pm 0.12^b$
30	-1.18 $\pm 0.16^a$	-2.33 $\pm 0.40^a$	-1.37 $\pm 0.11^a$	-2.46 $\pm 0.56^a$	-2.35 $\pm 0.82^a$	-4.82 $\pm 2.05^a$	-5.00 $\pm 2.21^a$	-1.67 $\pm 0.38^{b,c}$

^{a, b, c} Means in the same column with different letters indicate significant differences ($P < 0.05$)

The surface activity, calculated by the method of Marinova et al. (2009), is shown in Table 4.6-2. For β -lg samples, it can be observed that the surface activity for sucrose and maltodextrin was increasing with increasing saccharide concentration, while for sorbitol and maltose, the value was slightly decreasing. Polysorbate samples were showing stable or slightly increasing surface activities up to a saccharide concentration of 30%. Only for MDX-PS80 samples, the surface activity was steadily decreasing. If the surface activity had an influence on

the foam decay during the drying process, it would be expected that for samples with higher surface activity, the foams remain most stable. The reason is that the foam expands during the drying due to evaporation, heating, and low pressure, whereby the surface area increases, which has to be newly covered by foaming agents.

The A_2 values for all PS80-carbohydrate mixtures were similar, which was unexpected. However, the explanation might be that the carbohydrates moderated the interactions of PS80 via their H-bonds and the formation of clusters, as discussed above. Thereby, the surface activity increased. At high sugar concentrations, the viscosity of the samples increased so much that the mobility of the PS80 molecules was decreased, resulting in slower surface adsorption. In addition, the formation of sugar clusters, which could integrate PS80, would lower the surface activity (Dickinson 1998). Consequently, at a particular saccharide concentration (here, 30% w/w), the surface activity would significantly decrease.

For maltodextrin, a different behavior was observed as the surface activity decreased steadily. An explanation for this might be that maltodextrin can interact and form complexes with surfactants, as reported by several researchers (Wangsakan et al. 2004; Semenova et al. 2003). Semenova et al. (2003) reported that maltodextrin was able to integrate PS80 into the structure of MDX due to H-bonds between the polyethylene-head of PS80 and the OH-groups of MDX. In addition, Wangsakan et al. (2004) explained that complexes between MDX and surfactants might have a different impact on the surface tension depending on the surface-active component resulting from the promotion of the formation of 3D maltodextrin structures. Further, maltodextrin might be able to sterically hinder the surfactant from moving to the surface (Dickinson 1998), which should also be dependent on the size and structure of the foaming agent. This might also be an explanation for the detection of a different trend for β -Ig compared to PS80.

The increasing surface activity of β -Ig samples can be explained by the excluded volume, as described above (Antipova and Semenova 1997). However, sorbitol and maltose showed decreasing trends. As carbohydrates can form H-bonds in different numbers and strengths (Ali et al. 2019), it seems logical that the carbohydrates differ in their behavior. The high ability to moderate hydrophobic interactions of sorbitol might explain the observed decreasing surface activity. As sorbitol stabilized the native structure of the proteins (Fujita et al. 1982), this effect might be strengthened by higher concentration, and the affinity of β -Ig to the aqueous phase might be higher, thus decreasing the surface activity (Antipova and Semenova 1997).

In summary, a correlation between the second virial coefficient and the surface tension was identified. However, differences in carbohydrates do not seem to be directly in accordance with this, which can be attributed to a too-generous statement and experimental design of the A_2 . In order to gain more detailed information about the influence of molecular interactions between the foaming agents and sugars, it would be helpful to study concentration-dependent

values for A_2 additionally. Regarding the previously discussed data, it was expected that the surface rheology would be significantly influenced by the sugars, as their presence affects the surface activity of the foaming agents (Małysa et al. 1991).

4.6.3.3 Impact of the sugar type and concentration on the surface rheology of polysorbate and β -lactoglobulin stabilized foams

The influence of sugar type on the surface rheology is shown in Fig. 4.6.2. It can be clearly observed that the elastic moduli of polysorbate 80 samples were much lower than of protein systems. Furthermore, apparent differences between the investigated sugar types were detectable. The elastic modulus E' of 3% β -lg without saccharide was around $60 \text{ mN}\cdot\text{m}^{-1}$, which seems comparable to the obtained E' values reported by Lexis and Willenbacher (2014) for 1% β -lg solutions. The high elastic moduli of protein samples can be explained by a structural rearrangement of proteins at the air-water interface. Thereby, proteins were interacting with each other via hydrophobic interactions or aggregation and ionic interactions at the hydrophilic parts of the proteins, which prevent detachment from the surface.

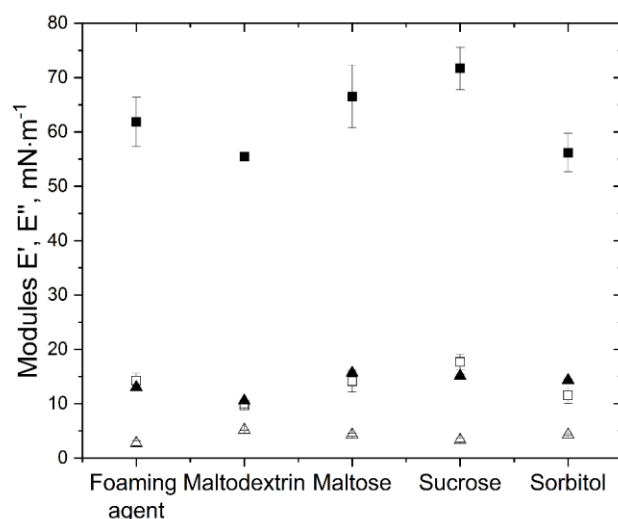


Fig. 4.6.2: Influence of sugar type on the elastic (E' , squares) and viscoelastic (E'' , triangles) moduli of polysorbate (empty symbols) and β -lactoglobulin (filled symbols) samples pure or with a saccharide concentration of 20%.

The added saccharides promoted those interactions by H-bond formation in the presence of saccharides. Thereby, the proteins at the surface connect with each other, and a high viscoelastic behavior can be observed, as shown by other research groups (Dombrowski et al. 2018; Braunschweig et al. 2016; Engelhardt et al. 2013). In addition, the increase of E' due to the addition of saccharides can be attributed to preferential exclusion, as discussed in the previous sections. Further, due to lowering repulsive forces (see chapter 4.6.3.1), the interactions between proteins are stronger, resulting in a more elastic behavior, as also was observed and

described for the addition of ions by Dombrowski et al. (2018). As already discussed, the major interactions between saccharides and polysorbate are H-bonds. As the interactions between polysorbate molecules at the interface were expected to be much lower when compared to those of proteins, it was assumed that they would easily detach and attach at the surface, as well as move along the surface layer to compensate gaps of lack of surfactant in the interface (Damodaran 2005; Wilde et al. 2004). In the presence of saccharides, this would be even easier, as the CMC is decreasing with increasing sugar content (Sharma and Rakshit 2004; Staples et al. 1996). However, for disaccharides, only a small increase in E' was observable.

Table 4.6-3: Calculated $\tan(\varphi)$, - for samples with polysorbate 80 or β -lactoglobulin at a saccharide concentration of 20% at 20 °C.

	Foaming agent	Maltodextrin	Maltose	Sucrose	Sorbitol
Polysorbate 80	0.21±0.03 ^a	0.54±0.02 ^b	0.28±0.02 ^c	0.22±0.02 ^a	0.31±0.01 ^{c,d}
β -lactoglobulin	0.23±0.01 ^a	0.18±0.01 ^b	0.22±0.01 ^{a,c}	0.25±0.02 ^{a,c}	0.21±0.01 ^{a,c}

^{a, b, c, d} Means in the same column with different letters indicate significant differences ($P < 0.05$)

In Table 4.6-3, the calculated $\tan(\varphi)$ for samples with 20% saccharide content is shown. A $\tan(\varphi)$ of zero would represent a perfect elastic behavior of the film (Baeza et al. 2006; Conde and Rodríguez Patino 2005). The highest difference between the protein and surfactant samples was detected for maltodextrin (β -lg = 0.18 ± 0.01, PS80 = 0.54 ± 0.01). For maltose and sorbitol, surfactant samples had about a 40–50% higher $\tan(\varphi)$ value, which is following the already discussed behavior of PS80 at the surface. For 20% sucrose, no clear difference was obtained in comparison to the foaming agent. This was attributed to the low concentration since $\tan(\varphi)$ was influenced at higher sucrose concentrations.

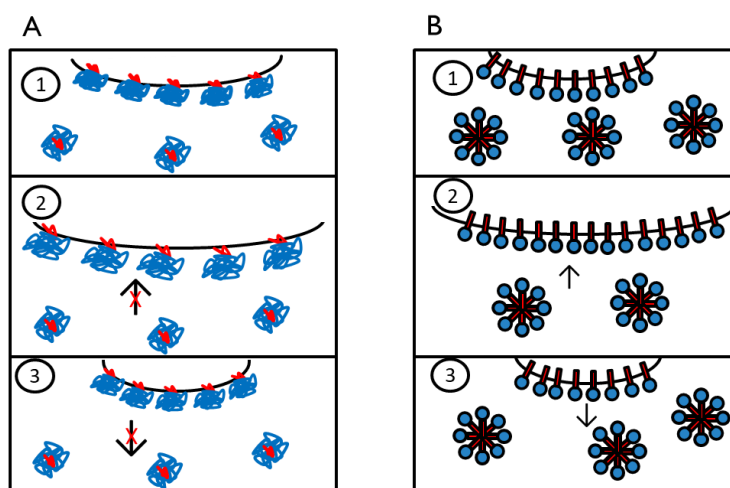


Fig. 4.6.3: Schematic differences at the air-water interface between β -lactoglobulin (A) and polysorbate 80 (B) samples during oscillation.

A much lower $\tan(\varphi)$ was also observed by Davis and Foegeding (2007) during their investigation of the impact of sucrose on the rheological properties of different proteins. However, Davis and Foegeding (2007) did not find a specific explanation but highlighted the importance of knowledge about the properties of the solutions to understand the interfaces' rheological properties. Nonetheless, with increasing concentration, sucrose followed a clear trend as visibly observable in Fig. 4.6.3. Therefore, it was postulated that the change in $\tan(\varphi)$ required a higher concentration than 20%.

The influence of sugar concentration on the $\tan(\varphi)$ will be discussed, considering the different foaming agents. Samples with polysorbate are shown in Fig. 4.6.4A. It was clearly observable that with increasing saccharide concentration, the $\tan(\varphi)$ also increased. Therefore, it was assumed that this was linked to the higher viscosity of the bulk phase near the interface.

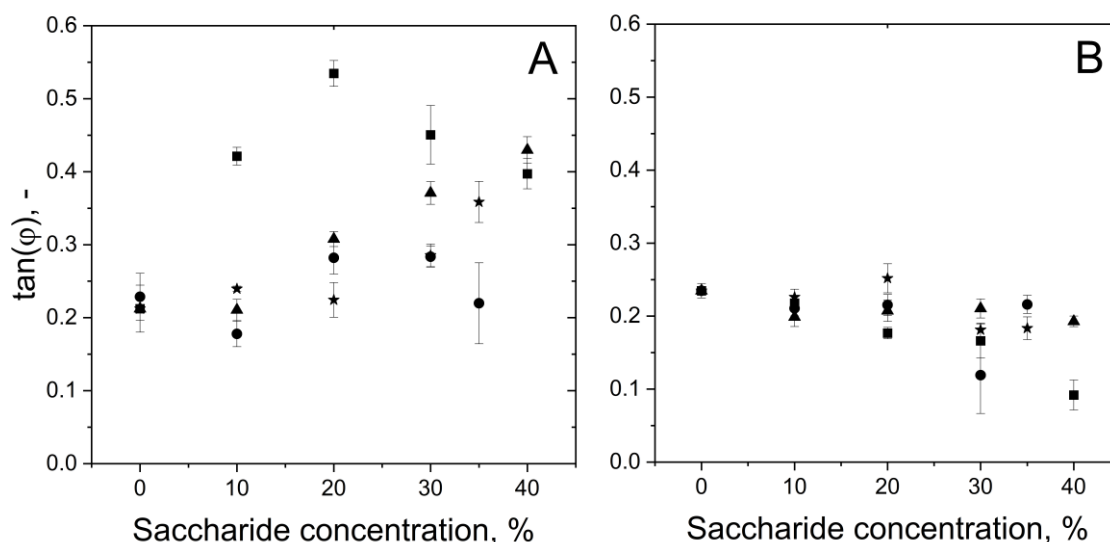


Fig. 4.6.4: Influence of different saccharide concentrations on the calculated $\tan(\varphi)$ of polysorbate 80 (A) and β -lactoglobulin (B) samples at the air-water interface, with sorbitol (▲), sucrose (★), maltose (●) and maltodextrin (■).

As we think that polysorbate had a high ability to attach and detach from the surface (Fig. 4.6.3), the reattachment during oscillation might have been hindered due to the high viscosity of the solution or by steric hindrance of saccharide molecules and H-bonds between polysorbate and saccharides. Thereby, the surface became more brittle, as the newly formed surface during expansion was not immediately covered by polysorbate and the $\tan(\varphi)$ consequently increased. This would also agree with the obtained data of surface activity, which decreased sharply as discussed in chapter 4.6.3.2. One exception was again maltodextrin, which had the most significant changes within the investigated range of saccharide concentration and decreased clearly between a concentration of 20 and 40%. While the increase of $\tan(\varphi)$ can also be explained by the increase of viscosity and the hindrance of reattachment of the surfactant,

the decrease of $\tan(\varphi)$ must have a different origin. As this behavior only occurred with maltodextrin and polysorbate, it was assumed that the interactions between polysorbate and maltodextrin must be responsible for that behavior. Since maltodextrin can incorporate polysorbate molecules (Semenova et al. 2003), those complexes might be located around the interface. Thereby, the MDX integrated polysorbate molecules could stabilize the surface during oscillation as MDX decreases their mobility, and thus, the detachment process would be less likely. However, this effect can only appear if other MDX molecules hinder the MDX-PS80 complexes from moving, as it is assumed to occur at high polysaccharide concentrations (Dickinson 1998). In contrast, samples with β -lg showed decreasing $\tan(\varphi)$ with increasing sugar concentration. This can be attributed to the stabilization of the surface by the formation of H-bonds that moderate the interactions between proteins. Due to the addition of sugars, A_2 decreased, promoting the intermolecular interactions between proteins. Furthermore, the sugars can be preferentially excluded and hence can form a shell around the protein layer at the surface. Thereby, the surface stability and consequently elasticity increased with increasing sugar concentration. Therefore, the observed behavior was in accordance with the obtained results from SLS and PDM. A scheme of how the authors imagine that sugar concentration influenced the surface rheology is shown in Fig. 4.6.5.

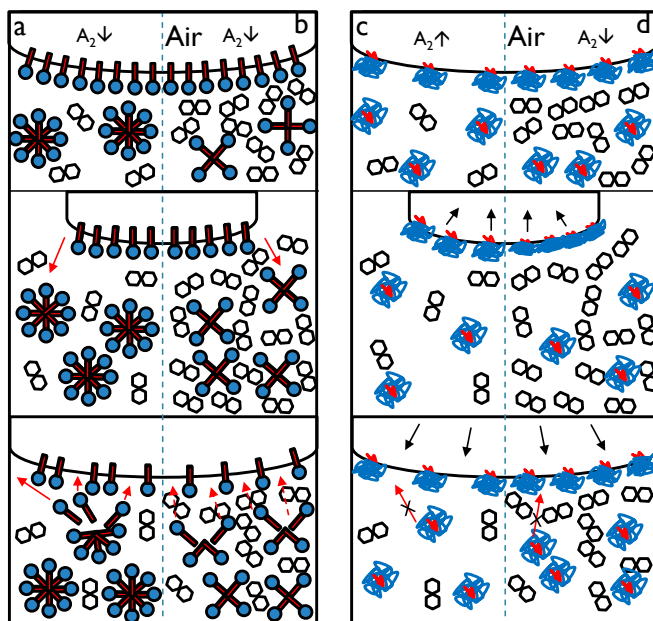


Fig. 4.6.5: Schematic comparison of the impact of low (a, c) and high (b, d) sugar concentrations on the behavior of surfactants (a, b) and proteins (c, d) at the air-water interface.

Taking chapters 4.6.3.1–4.6.3.3 into consideration, it was expected that foams stabilized with β -lg would show less decay over time than those stabilized with polysorbate. The reason for this statement is the increasing elastic behavior of the surface with added sugar and the increased stability of the interface due to H-bonding between sugars and proteins. Since the

surface activity of surfactant-saccharide formulations decreased sharply with high sugar content, it was expected that the advantage of small surfactants (e.g. the fast adsorption at the interface) would be neglected, resulting in a higher chance of foam collapse.

4.6.3.4 Drying behavior of with sugar thickened foam matrices

On the basis of the observed differences in molecular interactions and surface properties of different saccharide-foaming agent mixtures as discussed above, their influence on the structural stabilization of foams during vacuum drying, different vacuum drying experiments were assessed to correlate sample properties and drying results. As the molecular interactions and surface rheology discussed in the previous chapters are still present within the different formulations, but sample and not process-related, the discussion about the aforementioned will be brief. Nonetheless, the relevant sample properties show great influence, as shown below.

The residual water content ($10 \pm 2\%$) and the water activity (0.35 ± 0.1) for all investigated samples were independent of the used formulation. At the same time, the drying time for CVD was constantly set to 16 h, and the MWVD needed between 1.3 and 2 h until the drying was finished (data not shown).

In Fig. 4.6.6, the structure of the vacuum-dried β -lactoglobulin and polysorbate 80 stabilized foams are shown. It can be clearly observed that most PS80 stabilized foams collapsed during the first 15 min of the drying process. Only samples with maltodextrin remained stable until the end of the process. In contrast, protein samples remained stable independently of the used sugar. Here, maltose and maltodextrin showed the best results as their foam structure was preserved the best. The foams with added sucrose or sorbitol showed better foam structure but were more compact than maltose and maltodextrin. However, it was shown that the combination of surfactant and additives results in different foam stabilities, best observable for polysorbate stabilized foams.

No apparent influence of A_2 on the drying behavior was observed for polysorbate, as the A_2 value was similar between all investigated sugars. While all investigated sugars improved the surface properties of polysorbate due to H-bonds, the surface was getting less elastic with increasing saccharide concentration. However, interactions between polysorbate and maltodextrin, as suggested in the literature (Semenova et al. 2003; Antipova and Semenova 1997), might be the reason for the high viscosity of the solution and moreover, for the prevention of foam decay during the drying process. Those interactions were only found for MDX and not for the other investigated saccharides. Further, polysaccharides were able to block the lamellae at high concentrations by their high water binding capacity and steric stabilization (Dickinson 1998), preventing drainage and consequently foam decay, while disaccharides and sorbitol seemed not to be able to do so. However, all samples stabilized with proteins remained stable, indicating that the sugar type was not the only reason for the decay. Therefore, complex

interactions between the foaming agent and the saccharide were assumed, keeping the water inside the lamellae before drainage occurs, so that the interface remains stable until solidification.

In contrast, β -lg samples showed for all in this study investigated property an improvement with the addition of sugar. On a molecular level, the charges got shielded, reducing the A_2 , and promoting the interactions between attached protein molecules. This resulted in the high elastic behavior of the interface, consequently leading to stabilization of the foam during the drying process. In contrast, higher surface tension in equilibrium did not result in worse preservation of foam. This result was also obtained for the surface activity, which was low compared to that of surfactant mixtures. One explanation for this might be that the interface was already formed, and therefore, high concentrations of foaming agents were already present at the air-water interface. Thereby, the differences between protein and surfactant samples would be lower, as the velocity of surface attachment would be negligible. In summary, all investigated combinations of β -lg and saccharide were dried successfully.

	Sorbitol, 40%	Sucrose, 35%	Maltose, 35%	Maltodextrin, 40%
Polysorbate 80 stabilized foams				
	$t_{collapse} = 13.1 \pm 0.9$ min	$t_{collapse} = 14.7 \pm 3.1$ min	$t_{collapse} = 11.6 \pm 0.8$ min	No collapse
β -lactoglobulin stabilized foams				
	No collapse	No collapse	No collapse	No collapse

Fig. 4.6.6: Impact of sugar types on the foam decay in conventional vacuum drying with regard to the used foaming agents and saccharides.

As samples containing maltodextrin remained the most stable for both foaming agent systems, those were selected for assessing the influence of sugar concentration on foam decay during drying. As observable in Fig. 4.6.7, the addition of MDX with 30 and 40% content resulted in a stable product for PS80 foams, whereas foams with 10 and 20% MDX content collapsed. One reason for this might be the higher viscosity of high carbohydrate samples. The higher viscosity of the liquid phase improves the stability of foams, as proven in several studies about foam properties (Ambros et al. 2019b; Lazidis et al. 2016; Pisal et al. 2006; Damodaran 2005). Therefore, it is evident that a foam structure with a high viscosity is more easily stabilized

against decay when compared to foams with a low viscosity. However, as β -lg samples remained stable and assuming that the viscosity between PS80 samples and β -lg samples did not differ greatly, this is less likely to be the explanation for the observed differences. Here, it was interestingly found that the $\tan(\phi)$ of maltodextrin samples correlated with the result of a successful drying process as observable for PS80-MDX mixtures between 20 and 40%. This was attributed to the interactions between maltodextrin and polysorbate, promoting a stabilization of the interface while it was mechanically treated (chapter 4.6.3.2). Therefore, the obtained results from samples with different polysaccharide content support this explanation. Further, this would also explain why the other investigated saccharides were not able to prevent foam decay during the drying process, since for the other saccharides, the $\tan(\phi)$ increased with increasing sugar content. However, regarding the $\tan(\phi)$ and the saccharide concentration, two contrasting effects were observed for PS80: on the one hand, the higher the saccharide concentration, the higher $\tan(\phi)$, which indicates a less elastic surface. On the other hand, the higher the saccharide concentration, the higher the viscosity of the solution, lowering the drainage speed and stabilizing the foam. Therefore, it is assumed that each mixture of saccharide and foaming agent has an optimum, resulting in overall best foam preservation properties during the drying process.

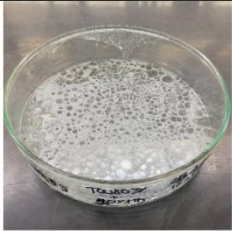
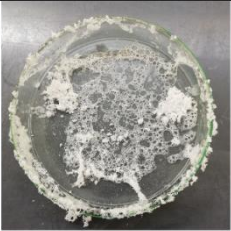

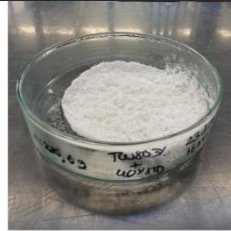

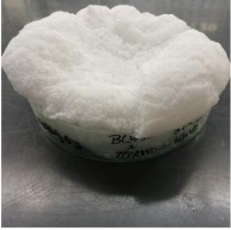
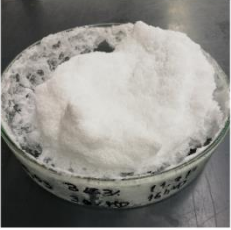

		Maltodextrin concentration, %			
		10	20	30	40
Conventional Vacuum Drying	Polysorbate 80 stabilized foams	 $t_{\text{collapse}} = 11.6 \pm 1.5 \text{ min}$	 $t_{\text{collapse}} = 7.1 \pm 0.9 \text{ min}$	 ($t_{\text{collapse}} = \sim 30 \text{ min}$)	 No collapse
	β -lactoglobulin stabilized foams	 No collapse	 No collapse	 No collapse	 No collapse

Fig. 4.6.7: Foam structure after conventional vacuum drying for polysorbate 80 and β -lactoglobulin foam with a maltodextrin concentration between 10 and 40%.

Furthermore, the specific interactions between foaming agent and thickener would result in a for each formulation unique foam structure in the end of the drying process.

Besides the investigation of samples in CVD, microwave-assisted vacuum drying was performed. Differences between CVD and MWVD were assumed because components added to stabilize organic material or to increase foam stability by increased viscosity could affect

MWVD due to their dielectric properties, whereas VD would only be affected by the molecular interfacial behavior of foam stabilizing substances. The obtained water activity and residual moisture content of microwave-processed samples were slightly higher compared to that of CVD samples (10–12% instead of 8–10%). But it should be mentioned that no drying-kinetic was assessed for the CVD samples, and therefore, the results cannot be directly compared. However, the potential in decreasing drying time due to the use of microwaves for heating could be clearly demonstrated. Further, it was assumed that due to higher evaporation rates during MWVD, the bubbles are better separated from each other (Sangamithra et al. 2015) and that the formation of new bubbles and finer pores are promoted (Sankat and Castaigne 2004), whereby the aerated structure would be stabilized against foam decay. However, the influence of these mechanisms on the overall foam preservation is dependent on the process conditions, drying stage and product formulation. Therefore it can not be stated which one dominates on the foam preservation during the drying process.

In Fig. 4.6.8, the obtained structures for MDX concentration between 10 and 40% for both foaming systems are shown. The obtained results were clearly different compared to those of CVD: For PS80 stabilized systems, no foam remained stable during drying. The reason for this might be the too low surface elasticity of PS80 samples, as well as the dielectric properties of the solution as suggested in a previous study (Kubbutat et al. 2021a). Herein, it was stated that the used microwave frequency matched with the resonance frequency of the foaming agent, which resulted in a decay of the foam. As it was found in this work that the elasticity of the surface was increasing with high saccharide concentration, the evidence here supports this theory. Besides, the re-formation of foam due to high evaporation rates during MWVD did not result in better preservation of the foamy structure in comparison to samples dried with VD (Fig. 4.6.7). In contrast to Sankat and Castaigne (2004), the samples were dried using a vacuum, which resulted in less thermal stress but higher mechanical stress. Thereby, the bubbles collapsed faster than new foam was generated due to the evaporation resulting in an overall foam collapse.

β -lg preserved the foam structure much better. However, the size of the obtained solidified bubbles was bigger, and the structure was coarser compared to the results of CVD. This might be due to the volumetric heating and faster drying. Thereby, the bubbles might have expanded more compared to CVD dryings before they solidified. Nonetheless, even for these harsh conditions, β -lg samples remained stable throughout the drying process. This was also proven for the other sugar- β -lg matrices (data not shown).

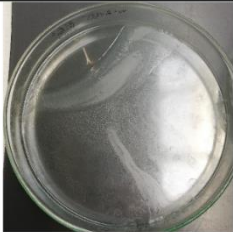







Maltodextrin concentration, %		10	20	30	40
Microwave-assisted Vacuum Drying	Polysorbate 80 stabilized foams	 $t_{collapse} = 9.2 \pm 3.4 \text{ min}$	 $t_{collapse} = 27.1 \pm 3.5 \text{ min}$	 $t_{collapse} = 13.2 \pm 3.7 \text{ min}$	 $t_{collapse} = 6.7 \pm 0.1 \text{ min}$
	β -lactoglobulin stabilized foams	 No collapse	 No collapse	 No collapse	 No collapse

Fig. 4.6.8: Obtained foam structure after microwave-assisted vacuum drying of polysorbate 80 and β -lactoglobulin foams with a maltodextrin content between 10 and 40%.

4.6.4 Conclusions

The obtained data demonstrate the importance of gaining knowledge about the solutions' properties to understand the foam decay behavior during vacuum and microwave vacuum drying. Significant differences between surfactant and proteins systems were found as well as between the impact of different types of saccharides on foam stability. Further, the obtained data indicated that all investigated saccharides promoted H-bonds and, therefore, indirectly or directly influenced the interactions between surface-active components. A decrease of repulsion between proteins was observed, which was correlated to the shielding effect by the added saccharides. However, the interactions within the different saccharide-foaming agent systems differed strongly, and therefore, general assumptions regarding the success of foam drying are difficult to make.

On a molecular level, the addition of saccharides had nearly no influence on the interactions between surfactants. However, if the surfactant forms complexes with the used saccharide, this statement loses its ground, as observed for maltodextrin. If it is assumed that those complexes are predominantly formed by polymers and not by small sugar alcohols or disaccharides, this effect would not be expected for most of the added excipients in the pharmaceutical industry. However, the addition of polysaccharides as thickening agents is quite common in the food industry and should be considered for other areas, too.

The addition of saccharides to β -lactoglobulin solutions improved the surface properties of the system. Repulsion between β -lg molecules was lowered, and the intermolecular interactions at the interface were promoted. Thereby, the surface tension was slightly lowered. However, no correlation between surface tension, surface activity, and foam decay during drying was

found. In contrast, the obtained results of surface rheology were well correlating with the obtained drying results. All β -lg samples showed high elastic behavior at the interface and preserved the foam structure during the drying. Nevertheless, polysorbate samples were also showing high elastic surfaces (low $\tan(\varphi)$) for some saccharide concentrations, and therefore the $\tan(\varphi)$ can not be used as an overall explanation. However, a good prediction of foam decay during the drying process can be made using a combination of E' and $\tan(\varphi)$. Therefore, it is recommended to test formulations, which should be vacuum foam dried, for their surface rheological properties.

The obtained microwave processed samples always showed more indications for foam decay compared to CVD samples. This was attributed to the harsher drying conditions as a result of faster evaporation and more efficient heating. However, β -lactoglobulin stabilized samples were robust enough to withstand those conditions. Investigations about the dielectric properties of the solutions might also be relevant to go deeper into the drying technology and the optimization of drying parameters, such as microwave power input, vacuum pressure, and drying temperature. With regard to the foam preservation, a formulation of 3% β -lg and 40% MD was best suited.

Overall, a correlation between molecular and interfacial properties and the drying results in terms of maintaining stable foams was established. This could be used for an upfront characterization of solutions to predict the drying behavior. Further, it can be estimated that samples using whey protein isolate instead of β -lg result in comparable product characteristics as shown in a previous study (Kubbutat et al. 2021b).

Author contributions: Conceptualization, P.K.; methodology, P.K.; validation, P.K. and L.L.; formal analysis, P.K. and L.L.; investigation, P.K. and L.L.; resources, U.K.; data curation, P.K. and L.L.; writing—original draft preparation, P.K.; writing—review and editing, P.K., L.L. and U.K.; visualization, P.K.; supervision, U.K.; project administration, P.K and U.K.; funding acquisition, U.K. All authors have read and agreed to the published version of the manuscript

Funding: This IGF Project of the FEI (AiF 18819 N) was supported via AiF within the program for promoting the Industrial Collective Research (IGF) of the German Ministry of Economic Affairs and Energy (BMWi), based on a resolution of the German Parliament.

Data availability statement: Data is contained within the article.

Acknowledgments: We would like to thank Krüss GmbH for providing the DSA100.

Conflicts of interest: The authors declare no conflict of interest.

4.7 Influence foam properties and excipients on the residual stability of β -galactosidase after microwave-assisted freeze drying

4.7.1 Introduction

Using foamed matrices offers several advantages in drying processes compared to the use of non-foamed products (Ratti and Kudra 2006b). However, foams differ in their properties and bulk phase, whereby the drying process can be influenced. Of particular interest is to preserve the foamy matrix throughout the drying process (Ratti and Kudra 2006a), which is obviously more challenging if the bulk phase is liquid and vacuum is applied compared to a solid foam during, e.g., freeze drying. However, there is a lack of information about the influence of foam properties on the product quality of freeze-dried samples. It seems clear that changes in water-vapor transport (chapter 4.3) impacts drying performance and product quality. Therefore, this study aimed to investigate the influence of foam properties on the residual enzyme activity of β -galactosidase for microwave-assisted freeze drying. The hypothesis was that by changing the foam structure, the product quality or residual enzyme activity of β -galactosidase is influenced as a result of differences in the water vapor pathway. A drying, which occurs throughout the product, was expected to be most gentle while drying with single drying fronts as observed for solutions, or high-density foams, was expected to damage the enzyme activity due to local overheating and higher internal pressure.

Further, it was examined if other foam thickeners than maltodextrin show comparable influence on the drying process. In case of similar behavior, it should be possible to point out for the product quality relevant foam properties, which can be used independently on the used type of saccharides. Besides applying other saccharides, the influence of the commonly used excipient glycerin on the product quality was investigated and related to different foam properties.

4.7.2 Results and discussion

In order to investigate the influence of excipients and foam properties on the residual enzyme activity after MWFD, different foam formulations with 3% polysorbate 80, maltodextrin (0–40% w/w) or maltose (0–50%), and the equivalent amount of 5% β -Gal raw solution were used. The dispersions were whipped according to the method described in chapter 4.1. 120 g of foamed sample were dried with microwave-assisted freeze drying at 200 W, 20 °C product temperature, and 0.1 mbar and compared with the drying results from conventionally freeze-dried samples (24 h, 20 °C shelf temperature, 0.1 mbar). Details for foam formation and microwave-assisted freeze drying can be found in chapter 4.3. No significant differences in foam properties were found between samples without β -Gal, raw β -Gal, and dialyzed β -Gal at equivalent maltodextrin content (data not shown).

In a first step, the influence of maltodextrin content in the formulations was investigated. Therefore, samples with 10–40% MDX were prepared according to the method described in chapter 4.1 and 4.2. The whipped and frozen samples were dried with microwave-assisted freeze drying at 0.1 mbar, and a power input of 200 W. Besides, experiments with non-dialyzed β -Gal were investigated to prove the estimated problems, which may occur due to the higher evaporation temperature of glycerin.

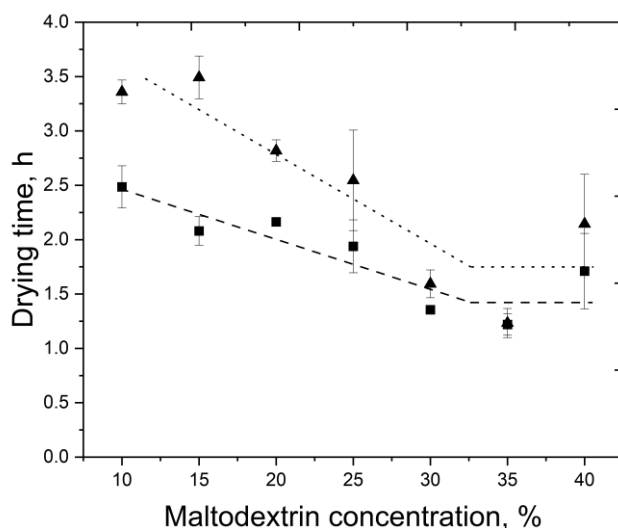


Fig. 4.7.1: Required drying time for samples with MDX content between 10 and 40% with the addition of dialyzed (\blacktriangle) and non-dialyzed (\blacksquare) β -galactosidase at 200 W and 0.1 mbar.

The drying time of samples with variable MDX content and added non-dialyzed or dialyzed β -Gal is shown in Fig. 4.7.1. For all samples, the necessary drying time decreased with increasing MDX concentration up to 30% MDX. Above 30% MDX content, the drying time remained equal to samples with 30% MDX or even increased. The decreasing drying times are contradictory to the results from the literature, where a higher overrun resulted in faster drying of the samples due to higher effective diffusion (Thuwapanichayanan et al. 2012; Kadam and Balasubramanian 2011). However, the experiments in literature were performed with samples that had the same volume. In contrast to this, the samples in this study had the same initial mass. Thereby, the sample height varied for different formulations (higher overrun at low MDX content, see Table 4.7-1). Therefore, the product height had a higher impact on the drying behavior than the change in effective diffusion, which has also been found for samples without added β -Gal (Kubbutat et al. 2020) and for the MWFD of raspberry foams (Ozcelik et al. 2019a). Further, the drying rate did not increase about an MDX content above 30%, which can be attributed to overheating of the high-density samples (Kubbutat et al. 2020). Thereby, longer and more frequent cooling periods were necessary to process the samples at a maximum surface temperature of 20 °C, which extended the drying time.

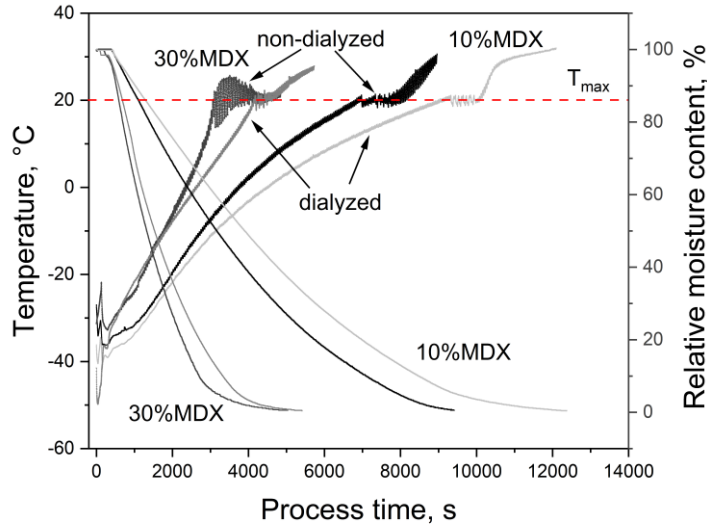


Fig. 4.7.2: Temperature and relative moisture content during the microwave-assisted freeze drying process of samples with 10 or 30% MDX and added β -Gal at 0.1 mbar and 200 W.

Samples with glycerin generally dried faster than samples without glycerin, especially at MDX concentrations between 10 and 25%. At higher MDX concentrations, the necessary drying time was more or less the same. The rise of temperature during MWFD for samples of 10 and 30% MDX with added non-dialyzed and dialyzed β -Gal is shown in Fig. 4.7.2. The maximally reached temperature seems comparable and independent of the used formulation. However, glycerin-containing samples heated more efficiently, as clearly observable for both shown formulations. This observation explains why samples with non-dialyzed β -Gal dried faster compared to their dialyzed equivalents. This can be explained by the slightly higher $\tan(\delta)$ for dialyzed (0.12) and non-dialyzed β -Gal (0.15), which results in more efficient heating of the sample. However, those values were measured at room temperature, and the freeze drying process was running at much lower pressure and temperature. Nonetheless, glycerin has a much higher boiling point than water, and therefore, heating occurred in even water-free regions (Glycerine Producers' Association 1963). Thereby, the product was heated more efficiently compared to samples with dialyzed β -Gal. Hence, the question raised now was if the non-specific heating of water damaged the enzyme during the drying process.

The residual enzyme activity in dependency of the maltodextrin content is shown in Fig. 4.7.3. Samples prepared with non-dialyzed β -Gal showed an increasing residual enzyme activity with increasing MDX content between 10 and 20% MDX, followed by a plateau phase at about 80–90% enzyme activity. For MDX concentrations above 30% MDX, decreasing residual enzyme activity was observed. For samples containing dialyzed β -Gal, a slightly decreasing trend between 10 and 30% MDX is observable. A more pronounced decreasing trend was observed

for increasing MDX concentrations above 30%. Hence, samples with or without glycerin differed more clearly for low MDX concentrations, whereas no difference was further detectable at MDX content above 30%.

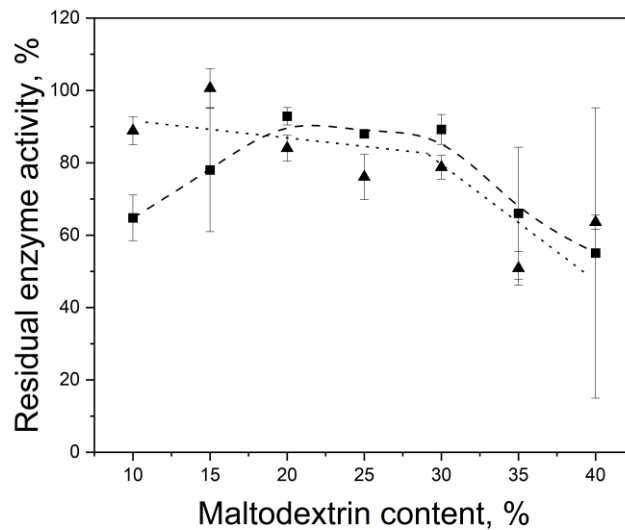


Fig. 4.7.3: Enzyme activity of β -galactosidase after microwave-assisted freeze drying for samples with MDX content between 10 and 40% with (\blacktriangle) dialyzed β -galactosidase and (\blacksquare) non-dialyzed β -galactosidase.

The decreasing trend at high MDX concentrations can be explained by the strong overheating of the samples, which was also detectable by the necessary drying time. Thereby, the enzyme got thermally damaged and lost its enzymatic activity. However, it is worth noting that the highest measured temperature was about 30 °C for nearly finished samples. As no damaging effect of sample preparation was found, it was assumed that the temperature inside the sample was higher than 40–50 °C (see chapter 4.2). However, the overheating due to a too dense product structure would not explain the differences for samples with an MDX content between 10 and 20%. One explanation could be differences in dielectric properties and the presence of non-evaporating glycerin. When the glycerin is not evaporated, it concentrates within the drying process. Thereby, the heating of the product gets more intensive within the progressing drying process, which can result in local overheating of the product and consequently damage of the enzyme. This would be less problematic if the temperature can be measured with low latency, as it is assumed for thin layered products. In the case of voluminous samples, due to heat transduction delayed temperature measurement is problematic. Even though this was a problem for both sample types, the glycerin itself intensified the problem. Therefore, the residual enzyme activity was lower for samples with glycerin compared to those without glycerin.

Besides, the influence of foam characteristics on product quality was investigated. Only results for dialyzed samples are shown to determine just the effect of foam properties and not mixing

it up with the effects of up-concentrating glycerin. Some foam properties of MWFD dried samples are shown in Table 4.7-1. The discussion of how differently sugars interact with polysorbate 80 and how they influence foam properties can be found in chapter 4.1.

Table 4.7-1: Properties of foams with 3% polysorbate 80 and added maltose (MTO) and maltodextrin (MDX).

Formulation		Overrun	Drainage	Firmness	Bubble size, d_{50}	IQR
% w/w	Type	%	%	mNm	μm	μm
10	MDX	1671 \pm 251	66.1 \pm 6.1	15.5 \pm 3.9	553 \pm 51	616 \pm 60
15	MDX	1108 \pm 62	70.0 \pm 0.9	22.0 \pm 2.0	300 \pm 10	471 \pm 29
20	MDX	715 \pm 70	69.5 \pm 1.5	28.2 \pm 2.8	202 \pm 28	235 \pm 84
25	MDX	459 \pm 34	31.8 \pm 5.8	26.9 \pm 1.5	118 \pm 14	110 \pm 18
30	MDX	234 \pm 7	17.7 \pm 9.7	32.7 \pm 2.1	102 \pm 14	63 \pm 0
35	MDX	144 \pm 16	0.0 \pm 0.0	34.7 \pm 1.8	64 \pm 3	41 \pm 7
40	MDX	41 \pm 3	0.0 \pm 0.0	41.3 \pm 6.5	59 \pm 10	26 \pm 9
20	MTO	1578 \pm 128	59.7 \pm 3.8	22.3 \pm 0.7	422 \pm 22	406 \pm 122
30	MTO	1429 \pm 57	66.1 \pm 3.8	24.7 \pm 1.0	300 \pm 38	455 \pm 44
40	MTO	1058 \pm 13	54.9 \pm 10.5	23.1 \pm 1.9	201 \pm 47	291 \pm 39
50	MTO	701 \pm 13	1.2 \pm 2.1	24.5 \pm 1.8	102 \pm 12	174 \pm 15

The drainage of foams seemed not to be relevant for the product quality of MWFD treated samples because the foams were frozen within a short period, and no drainage during the freezing process was detected. This was also assumed for the measured firmness of the foams because the frozen foams were solid and not deformable. In addition, the bubble size and the interquartile range were measured.

The plot of drying time as function of overrun is shown in Fig. 4.7.4A. One can observe that the drying time decreases with decreasing overrun. This is also valid for the investigated maltose samples, which shows that the linear correlation between drying time and overrun is independent of the used saccharide. However, for overrun values above 1600% and below 140%, this statement does not necessarily become true as a result of overheating due to delayed heat measurement or too dense product structures. Further, if one compares the mean bubble size of MTO and MDX containing foams (Table 4.7-1), one would assume that due to higher specific surface, foams with added maltose would dry faster than formulations with added maltodextrin. However, this was not the case (Fig. 4.7.4A), which indicates that the size of the bubbles needs to be related to the number of bubbles and that differences in bubble size or bubble size distribution do not necessarily result in different drying behavior. Therefore, the overrun value seems to be the foam properties, which is best suited to predict the drying time.

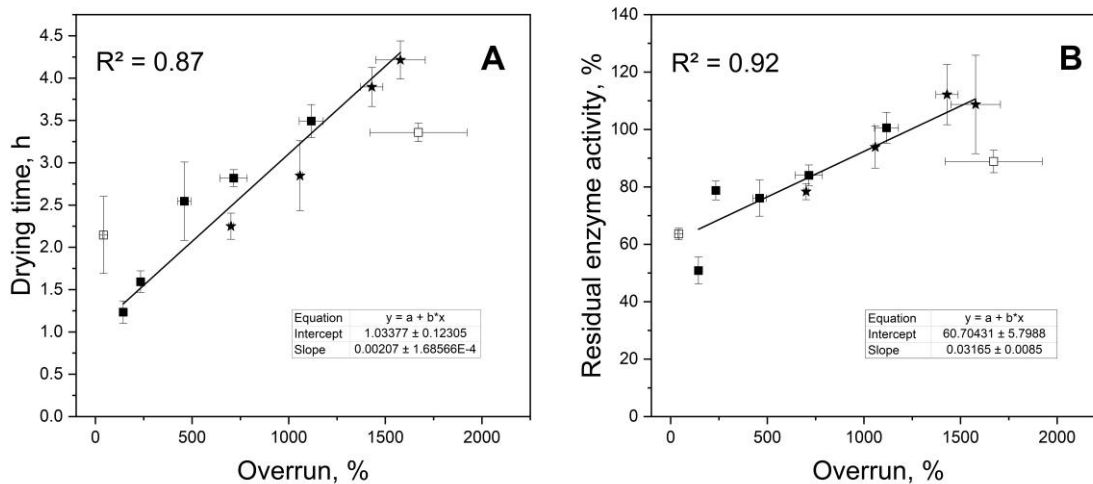


Fig. 4.7.4: (A) Required drying time and (B) residual enzyme activity of β -galactosidase for microwave-assisted freeze-dried samples with 3% polysorbate 80 and maltodextrin (■) or maltose (★).

In Fig. 4.7.4B, the residual enzyme activity after MWFD in relation to the foams overrun is shown. It was observed that with increasing overrun, the residual enzyme activity increased. As for the drying time, this was independent of the used saccharide. However, formulations with maltose showed generally higher overrun values and, therefore, higher residual enzymatic activity. The relation between residual enzyme activity and overrun could indicate a too high volumetric power density during the drying process, which would result in high temperature inside the lamellae. This is more present for samples with low overrun because their lamellae are thicker and their structure is denser compared to that of foams with high overrun (Fig. 4.7.5). The detection by temperature measurement might have failed due to a too fast progressing drying and due to low heat conduction, as already discussed. However, the observed decreasing enzyme activity strongly indicates the local overheating.

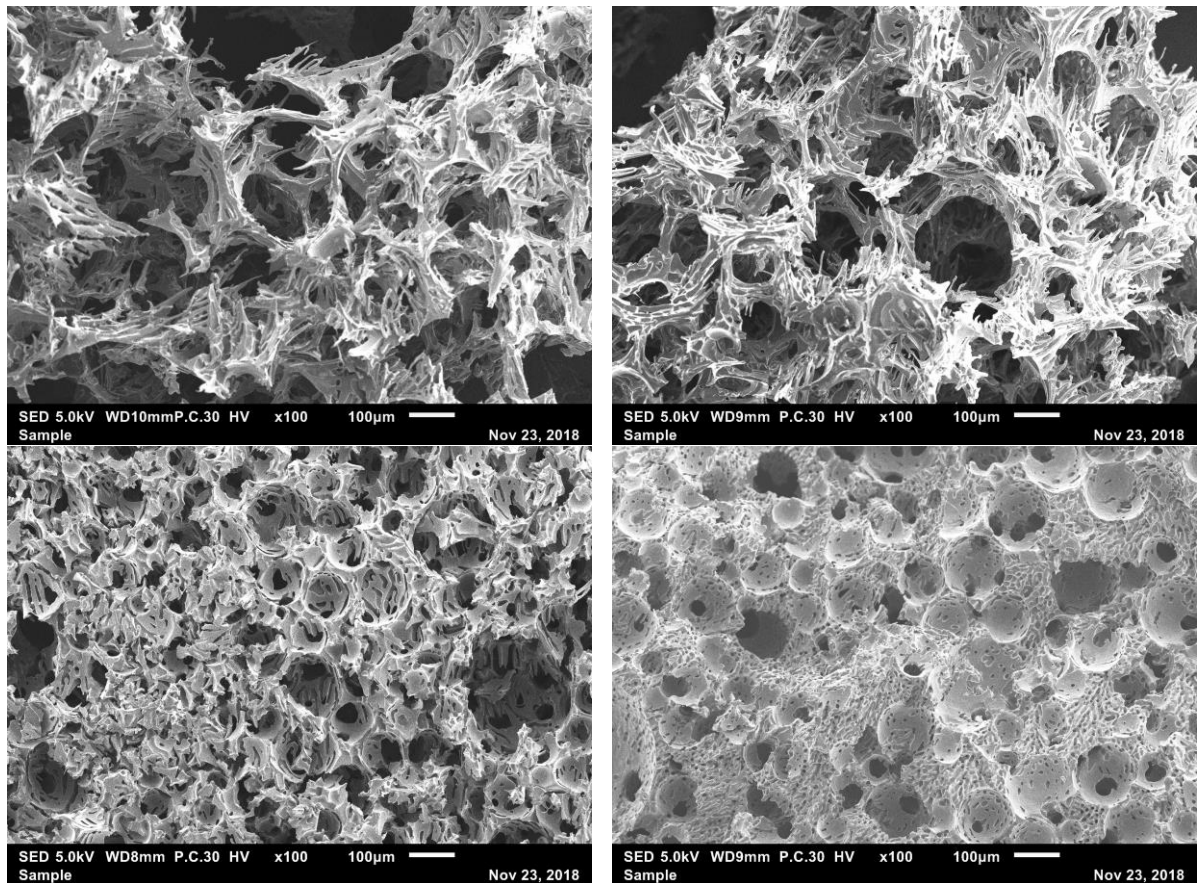


Fig. 4.7.5: Scanning electron microscope pictures of microwave-assisted freeze-dried polysorbate 80 foams with β -galactosidase and (A) 10% MDX, (B), 20% MDX, (C) 30% MDX, and (D) 40% MDX.

4.7.3 Conclusion

The impact of saccharide concentration on the drying behavior of foams during microwave-assisted freeze drying was investigated. Further, the influence of excipients like glycerin on the drying speed and the residual enzyme activity was determined. The drying speed was increased due to the heating of concentrated glycerin. However, the high evaporation rates were challenging due to high water vapor transfer resistance and which could cause overheating. Therefore, good product quality was only obtained within the optimum product properties and process conditions. Therefore, the addition of a microwave-absorber or microwave-reflecting plates, which are suggested to be added in order to increase the drying speed during microwave-assisted freeze drying (Wang et al. 2020; İçöz et al. 2004), seem to be unnecessary or even counter-productive for the drying of heat-sensitive substances. Foam properties like drainage, firmness, bubble size, and bubble size distribution showed no clear influence on the drying speed or the product quality. Further, it was shown that the drying speed can be directly affected by the overrun. Furthermore, it was shown that very high or low overrun values cause problems due to overheating, which can lower the quality of the product. Best product quality was achieved for foams with high overrun, independent of the used saccharide, which can be used to design other formulations. This additionally indicates that the volumetric power input

plays a major role in the preservation of biological substances during microwave-assisted freeze drying.

4.8 Influence of microwave power input and product temperature on the residual activity of β -galactosidase in microwave-assisted vacuum and freeze drying

4.8.1 Introduction

In literature, microwave power input and maximum product temperature are mentioned as important process parameters for the product quality of microwave-processed samples (Ambros et al. 2016; Duan et al. 2007; Hu et al. 2006). In general, it was shown that with higher product temperature, the product quality decreased, which was attributed to the denaturation of enzymes or the thermal degradation of the product. Further, with higher microwave power input, the product quality decreased, which was due to too high temperature or the formation of hot- and coldspots. However, the absolute power input should have theoretically no influence on the microwave-field distribution, which needs to be further investigated. Further, no investigation of heat-sensitive materials during microwave-assisted foam freeze drying was found. Therefore, the hypothesis was that the MWFD of foamy structures will result in high drying speed and product quality even at high microwave power input levels. The formation of hotspots should be reduced since the foam matrix decreases the heating stress and offers simultaneous drying throughout the product, as theoretically shown by Sochanski et al. (1990) and the previous study about water vapor pathways during MWFD (chapter 4.3). Microwave-assisted foam vacuum drying of sensitive biologicals was only found for microorganisms but not for proteins or enzymes (Ambros et al. 2019b). It was expected that the used enzyme was even more sensitive to heat and dehydration stress than microorganisms. Hence, it was mandatory to use combinations of lower pressure and product temperature. Further, the influence of process parameters for microwave-assisted drying of foamed matrices on the product quality of β -galactosidase was investigated.

4.8.2 Results and discussion

Besides the influence of foam properties, the influence of microwave power input and the height of the sample on the product quality were investigated. For this, samples with 30% MDX, 3% polysorbate 80, and 5% β -galactosidase were dried with a microwave power input between 120 and 240 W. Besides, the influence of the set maximum temperature (20, 25, and 30 °C and sample height (0.85 and 1.71 cm) were investigated. The hypothesis was that with increasing microwave power input, the drying time decreases and that with increasing product height, the drying rate decreases.

The required drying time and the residual enzyme activity of β -galactosidase of samples prepared with polysorbate 80 and 30% MDX are shown in Fig. 4.8.1. One can see that the drying time decreases with increasing microwave power input until a power input of about $1.8 \text{ W}\cdot\text{g}^{-1}$.

Dehydration occurred faster as the difference between inside and outside the product increased with increasing microwave power input, as Abbasi and Azari (2009) stated for the microwave-freeze drying of onion slices or by Feng et al. (2001) for sliced apples. Above, the required drying time reached a plateau. This can be explained by plasma formation, which mainly occurred in the second half of the drying process. The formation of plasma during the drying process is generally unacceptable because the product and the drying plant can be damaged (Duan et al. 2010b). However, for the case of plasma formation within this experimental setup, the drying plant stopped the process, and the user restarted the process manually. Interestingly, and for most of the time, no second appearance of plasma was detected, and the process could continue without further interruptions. Plasma discharge was also observed by Ambros et al. (2018) during the MWFD of lactobacilli above a microwave power input of $2 \text{ W}\cdot\text{g}^{-1}$, which is slightly higher than the first occurrence in this study. This difference can be explained by a different load (100 g) and pressure (0.6 mbar). Because the probability of corona discharge is strongly related to the chamber pressure (Metaxas and Meredith 1988), the pressure was always set to the minimal possible value, which the plant could provide (0.1 mbar). Furthermore, it is known that increasing the pressure destabilizes the product as a result of higher sublimation temperature (Ambros et al. 2018), and thereby the collapse temperature can be reached easier. However, the influence on the drying rate differs for conventional and microwave-assisted freeze drying: In conventional freeze drying, an increased pressure or a collapsed structure results in lower drying rates (Pikal and Shah 1990), while in MWFD, the collapse of a structure leads to an increase of dielectric properties, which result in even higher drying rates (Ambros et al. 2018).

Besides, Fig. 4.8.1 shows that the drying process resulted in more damage of β -Gal with a microwave input power above $1.8 \text{ W}\cdot\text{g}^{-1}$. On the one hand, the corona discharge might have damaged the enzyme. On the other hand, it was not clear if the plasma occurrence resulted in the additional damage of β -Gal or the thermal stress, which could be attributed to the higher microwave power. In Fig. 4.8.2, the obtained product structure after the MWFD at different microwave power inputs is shown. The cakes remained stable for power input values between 1.0 and $1.7 \text{ W}\cdot\text{g}^{-1}$. However, occasionally cracks occurred (Fig. 4.8.2B or C), which were assumed to be unproblematic, because no other optical or enzymatic damage was observed. In contrast to this, the cake was destroyed for power input values with high probability above $1.7 \text{ W}\cdot\text{g}^{-1}$ (Fig. 4.8.2D). This can be explained by a too high energy absorption, which resulted in higher sublimation rates at the same internal product resistance, as has been already discussed in chapter 4.3.

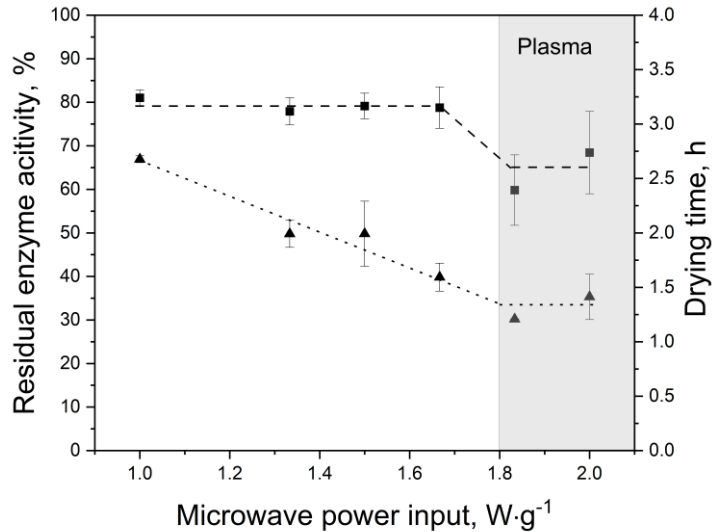


Fig. 4.8.1: Residual enzyme activity and necessary drying time of polysorbate 80 foams with a maltodextrin content of 30% and added β -galactosidase, dried with microwave-assisted freeze drying at a microwave input power of 1.0–2.0 $W \cdot g^{-1}$ at 0.1 mbar.

Thereby, the internal pressure increased until the product was melting. With the change from solid to liquid state, the firmness of the product was lost, and the pressure was released within an explosion of the product cake. Further, the change from frozen to the liquid state increased the dielectric properties (Regier et al. 2016), which resulted in the formation of hotspots. Product collapse was also found in studies investigating the influence on process conditions on the drying of raspberry foams (Ozcelik et al. 2019b) or the drying of bacteria (Ambros et al. 2018).

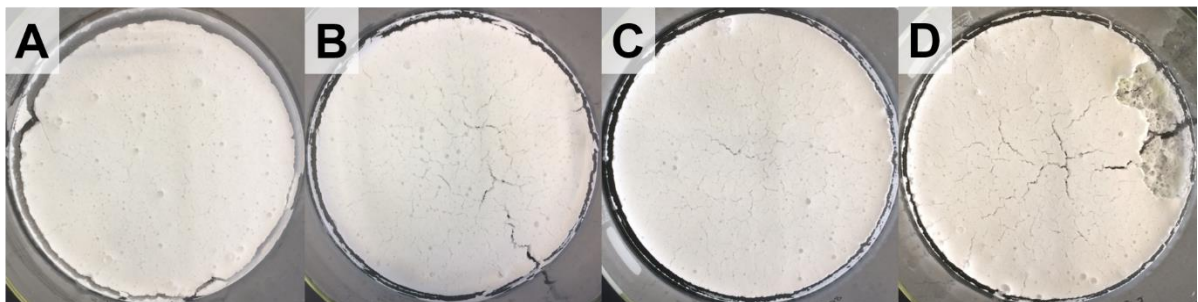


Fig. 4.8.2: Samples with 30% maltodextrin, 3% polysorbate 80 and 5% β -gal after microwave-assisted freeze drying using a power input of (A) 1.0 $W \cdot g^{-1}$, (B) 1.5 $W \cdot g^{-1}$, (C) 1.7 $W \cdot g^{-1}$, and (D) 2.0 $W \cdot g^{-1}$.

Different maximal temperatures and product heights were used to investigate the formation of hotspots and the influence of delayed temperature measurement on the residual enzyme activity. In Fig. 4.8.3, the maximum residual enzyme activity for products with a height of 0.85 and 1.71 cm in dependency on the set maximum temperature is shown. One can see that for a set maximal temperature of 20 °C, no differences were obtained for the different product's

height. However, the standard deviation was slightly higher for samples with 1 cm. Nonetheless, this indicates that at a surface temperature of 20 °C, the process was stable and controllable. In contrast to this finding, samples processed with a maximum temperature of 25 or 30 °C showed a massive loss of enzyme activity compared to samples processed at 20 °C. Further, the loss of enzyme activity was higher for thicker samples compared to thin ones.

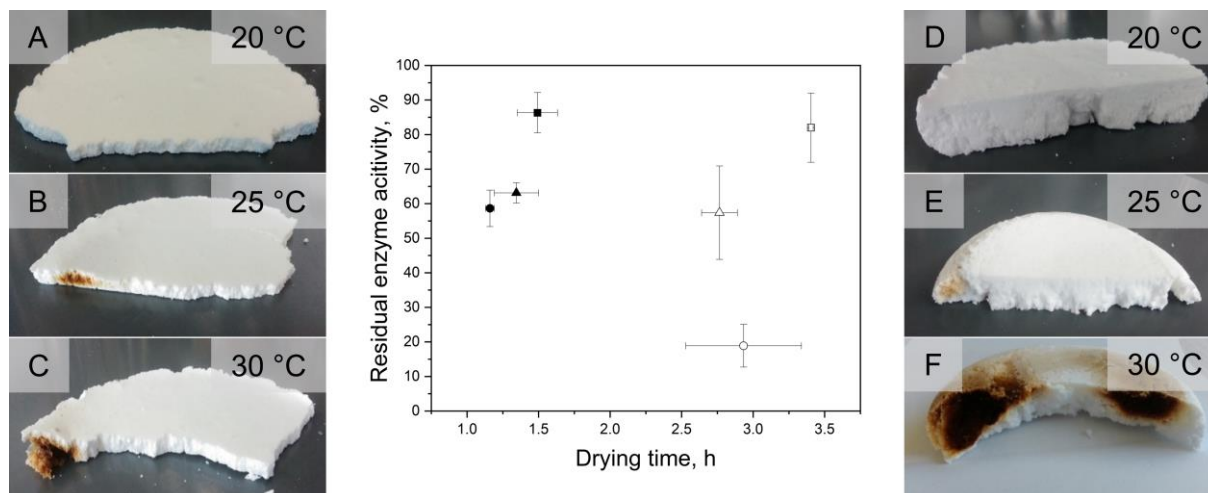


Fig. 4.8.3: Influence of product height (A–C and full symbols: 0.86 cm, D–F and empty symbols: 1.71 cm) and maximal set surface temperature on the required drying time and residual enzyme activity of β -galactosidase for microwave-assisted freeze drying of polysorbate 80 foams with 30% MDX content at $1.7 \text{ W}\cdot\text{g}^{-1}$ and a maximum temperature of 20 °C (■), 25 °C (▲) and 30 °C (●).

In Fig. 4.8.4, the surface temperature and the relative moisture content during the drying process are shown. If one compares the temperature for the different samples, one can see that the maximum temperature was reached at about 10–20% residual moisture content for samples with 1.71 cm height and below 10% moisture content for samples with a height of 0.86 cm. One explanation for the high loss of enzyme activity was that the residual moisture was distributed non-uniformly within the product cake. Thereby massive overheating occurred, as a high amount of microwave energy coupled into the product within a small volume. Thereby, a loss of enzyme activity was observed, which appear to take place even for products with low moisture content.

This explanation was also supported by photographs of the dried products (Fig. 4.8.3A–F). Samples, dried at 20 °C, remained stable during the drying process, and no color change occurred. For samples dried at 25–30 °C, intense browning occurred at the corner of the sample, which can be an indication of edging effects (Fig. 4.8.3). The heating of corners was also theoretically predicted by Brodie (2008) for the microwave-heating of cylindrical agar gels and is strongly dependent on the used diameter of the cylinder (Romano et al. 2005). However, the effect of excessive corner heating was unexpected because a flattening of this temperature distribution was expected as a result of the low dielectric properties during freeze drying.

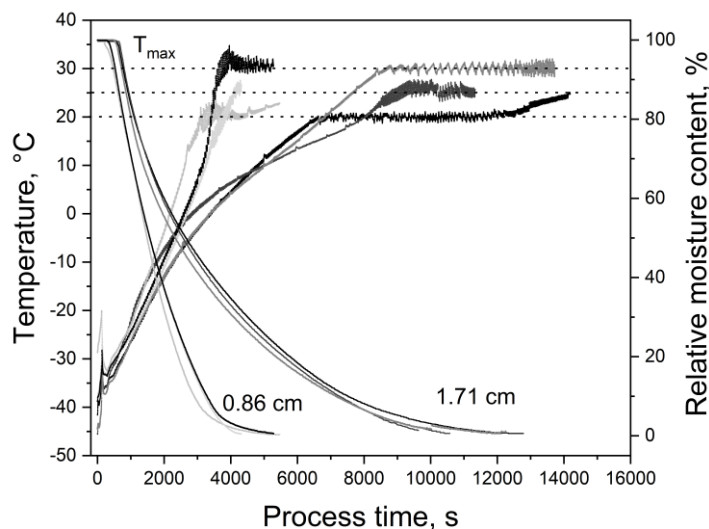


Fig. 4.8.4: Product temperature and relative moisture content within the drying process for microwave-assisted freeze drying of polysorbate 80 foams with 30% MDX content at $1.7 \text{ W}\cdot\text{g}^{-1}$ and a maximum set temperature of $20 \text{ }^\circ\text{C}$, $25 \text{ }^\circ\text{C}$, and $30 \text{ }^\circ\text{C}$.

One explanation would be the low thermal conductivity of foams due to the incorporated air. Thereby, temperature differences would be pronounced, which was also stated for liquid samples by Van Remmen et al. (1996). Besides, the most intense browning occurred for thick samples at $30 \text{ }^\circ\text{C}$ temperature, which indicates the overheating, as mentioned above. The dark-brown or black color clearly shows that the temperature inside must have been much higher than the measured surface temperature of $30 \text{ }^\circ\text{C}$ and supports the findings from chapter 4.7 as well as the decreased residual enzyme activity.

Besides microwave-assisted freeze drying, microwave-assisted vacuum drying was performed. As already discussed in chapters 4.4–4.6, only a few formulations retain their foam structure throughout the drying process. Best results were obtained using a whey protein isolate-maltodextrin formulation, and therefore, the following results are about the influence of process conditions on the residual enzyme activity of β -Gal of foams with 40% maltodextrin and 2.5% whey protein isolate.

In Fig. 4.8.5A, the required drying time and the residual enzyme activity of β -Gal after MWVD of WPI foams with an MDX content of 40% are shown. Because of the volume expansion during the evacuation of the process chamber and the heating during the drying process, a maximal sample size of 70 g could be processed. In contrast to freeze drying, the required drying time was not correlating with the microwave power input, and the end of the drying process was reached within about 1 h. The residual enzyme activity was slightly lower compared to that of MWFD (Fig. 4.8.1) except for samples processed at $5.7 \text{ W}\cdot\text{g}^{-1}$. This can be

explained as follows: During vacuum drying, the formulation concentrates due to the evaporation of water. On the one hand, this generates a harmful environment for the enzyme, which was also found for conventional vacuum drying (Fig. 4.4.5B). On the other hand, electromagnetic energy is more efficiently converted into heat, as discussed in chapter 4.4.

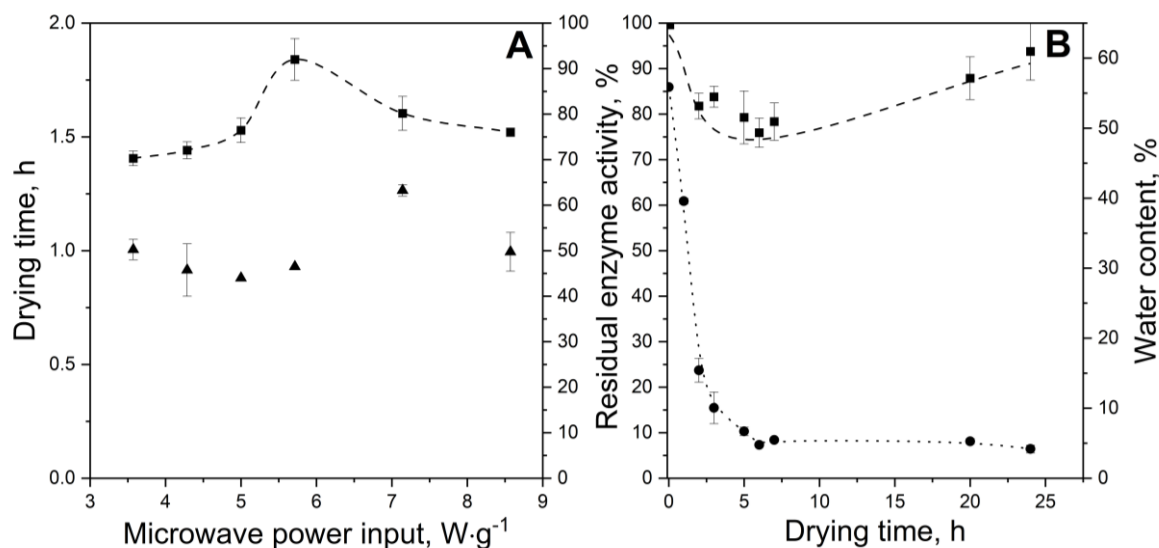


Fig. 4.8.5: (A) Required drying time (▲) and residual enzyme activity of β -galactosidase (■) after microwave-assisted vacuum drying at microwave power input between 3.6 and 8.6 $\text{W}\cdot\text{g}^{-1}$, and (B) residual enzyme activity of β -galactosidase (■) and water content (●) of foam samples containing polysorbate 80 and 40% maltodextrin during conventional vacuum drying.

Therefore, the drying has to proceed as fast as possible to solidify the product, which will also reduce the dielectric heat conversion. The slight increase in residual enzyme activity for microwave power input between 3.6 and 5.0 $\text{W}\cdot\text{g}^{-1}$ indicates that those harmful conditions were overcome faster, resulting in an optimum process condition at 5.7 $\text{W}\cdot\text{g}^{-1}$. However, for higher microwave input power, the sample overheated, whereby cooling steps were necessary before the solidification occurred. Thereby, the enzyme remained longer at unfavorable conditions, and the residual enzyme activity was low. Comparable behavior was also found for the vacuum drying of lactobacilli for relative water loss of 60–80% and a water activity of 0.4–0.6 (Ambros et al. 2019b; Ambros et al. 2018; Foerst and Kulozik 2012). All studies refer to the observed higher inactivation rate of the bacillus to the unfavorable environmental conditions and conclude that those conditions should be as short as possible to retain the product's quality. Further, a moisture content-dependent change of residual activity of β -Gal during freeze drying was reported by Jiang and Nail (1998). However, no explanation for the observed relationship between moisture content and residual enzyme activity was given. Further, these authors observed over-drying for β -Gal for a residual moisture content below 10%, but their formulations did not contain any lyoprotectant, whereby over-drying can be reached easier (Jiang and Nail 1998). In contrast, no over-drying was observed during conventional and microwave-assisted

vacuum drying. Even though the drying of microorganisms or the freeze drying of enzymes cannot be directly compared to the vacuum drying of proteins and enzymes, this explanation for the decrease in enzyme activity seems to be also applicable here.

4.8.3 Conclusion

Microwave power input and sample height were investigated to detect limitations in heat conduction or sublimation. It was shown that due to overly high power input, the quality of the sample can get lowered and that the probability of plasma occurring increased. Further, browning and loss of quality can be attributed to too retarded temperature detection. Further, it is worth noting that the temperature was only measured in a single spot and that, therefore, a thermographic temperature detection would be a better tool compared to the used pyrometer to prevent hotspots and thermal runaway. Furthermore, even for thin samples, a loss of enzyme activity was obtained if the maximal temperature was set to a higher temperature than 20 °C. Because the temperature measurement is much more reliable for thin products, the degradation of enzymes can also be an indication of a too high water vapor resistance, which would cause thermal runaway, as already discussed in chapter 4.7 and 4.3. Overall, thin layer products seem to be better suited for drying in microwave-assisted drying plants than thick samples, which can mainly be attributed to problems in temperature measurement and inner product resistance.

4.9 Up-Scaling of microwave-assisted freeze drying by generating small spherical foamy samples

4.9.1 Introduction

The upscaling of a microwave-assisted process is often challenging due to the requirement of a uniform microwave field distribution or economic reasons (Regier et al. 2016; Benaskar et al. 2011; Heindl and Müller 2007; Datta 2001). Since the microwave field distribution is never entirely even, the upscaling of plants just by increasing their size and periphery seems not to be practical. Instead, only a specific area inside the product cavity, where the field distribution is relatively uniform, is suited for the microwave processing (Regier et al. 2016). In addition to the limitation of the drying plant, the products need to be suited for higher absolute microwave power input as they can start to deteriorate due to overheating in case of mass-dependent microwave power input. Hence, the success of an upscaling depends on both product and plant properties.

This study aimed to determine the best ways to upscale microwave-assisted freeze drying of sensitive biomolecules. In previous chapters, the advantages of the use of foam matrices were described. Further, in chapter 4.8, the influence of process parameters was investigated, and it was found that above a power input of $1.8 \text{ W}\cdot\text{g}^{-1}$, the probability of plasma formation increases.

Two different strategies were examined: The first strategy was to determine the maximal possible water transfer rate, where the product and the drying process remained stable. For this, a linear and a quadratic relation between sample weight and power input to larger amounts of product was applied.

For the second strategy, the foam was frozen as small spheres in liquid nitrogen. Thereby, the product's surface was increased compared to the use of foam cakes, as used in the previous chapters. The hypothesis was that due to the higher surface area and smaller thickness of spheres, the required drying time would decrease due to higher water transfer rates. Furthermore, it was assumed that a larger amount of product can be dried without structural collapse because the internal resistance within the bulk of spheres was lower than that of a compact foam cake. Hence, by using spherical foam drops, the drying speed and the processable amount of product would be improved.

4.9.2 Results and discussion

Upscaling using most suitable combinations of process conditions and sample size

In Fig. 4.9.1, the water loss coefficient for different power input levels for foams with 30% MDX content is shown. With increasing microwave power input, the effective diffusion coefficient increases until a power input of $1.83 \text{ W}\cdot\text{g}^{-1}$. One explanation for this would be that the plant

was limited to this sublimation rate due to too small diameters of pipes between the product chamber and the condenser, which would also explain the found plateau between $1.83 \text{ W}\cdot\text{g}^{-1}$ and $2.0 \text{ W}\cdot\text{g}^{-1}$. Further, the higher difference in effective diffusion coefficient between 1.7 and $1.83 \text{ W}\cdot\text{g}^{-1}$ can be explained by cracks, which occurred during the drying at high drying rates (chapter 4.8). Besides, higher pressure inside the product chamber or directly above the product can cause problems like melting or plasma formation. With increasing power input, the electrical field strength increases, and with increasing pressure ($<0.1 \text{ mbar}$), the probability of plasma formation increases, as described by Metaxas and Meredith (1988). Thereby, the product, as well as the process stability, decrease, as already discussed in the previous chapter. As a result, the most promising compromise between drying speed and process stability ($1.7 \text{ W}\cdot\text{g}^{-1}$) provided an effective diffusion coefficient of about $2.0 \cdot 10^{-7} \text{ m}^2\cdot\text{s}^{-1}$.

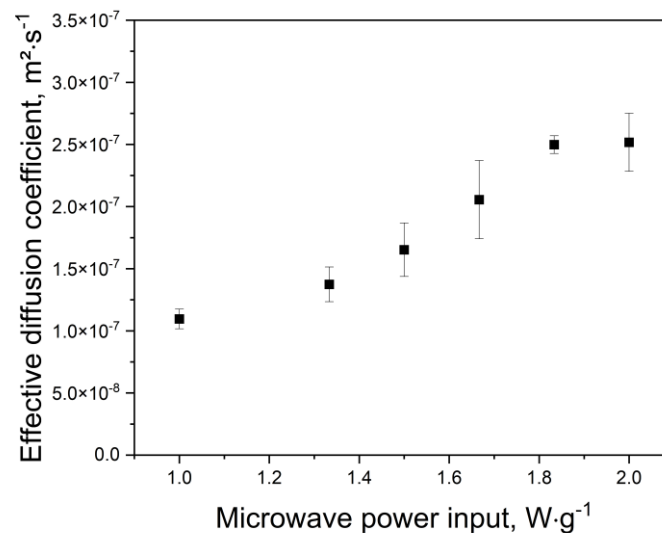


Fig. 4.9.1: Calculated effective diffusion coefficients for 120 samples of polysorbate 80 foams with 30% MDX and a microwave power input between 1.0 and $2.0 \text{ W}\cdot\text{g}^{-1}$.

In a second step, the combination of power input and product mass was adjusted to other combinations of power and mass. With increasing product mass, the samples were getting thicker, and the power had to be reduced to remain a stable product. Therefore, a negative linear and exponential relation between power and product weight was assumed. The aim of this experiment was to obtain the same product quality for different combinations of product weight and microwave power input. The investigated combinations of microwave-power input and product mass are shown in Table 4.9-1. Plasma occurred and reignited throughout the process for 80 g samples, processed at 440 W , and was therefore not further mentioned for the discussion because the process was not stable and the product collapsed.

Table 4.9-1: Investigated combinations of microwave power input and sample weight using negative linear or exponential relationship between sample weight and microwave power input.

Sample weight, g	60	80	100	120	140	160	180
Linear, W	-	240	220	200	180	160	-
Exponential, W	800	450	288	200	147	113	89

Interestingly, plasma did not occur for samples processed at 800 W, if during the secondary drying, the power input was reduced to 200 W. In Fig. 4.9.2A, the effective diffusion coefficient D_{eff} for different power input levels and product weights is shown. One can see that using a linear relationship between power input level and product weight resulted in values closer to the target value of $2.05 \times 10^{-7} \text{ m}^2 \cdot \text{s}^{-1}$. Besides, the required drying time for the drying of different sample weights is shown in Fig. 4.9.2.

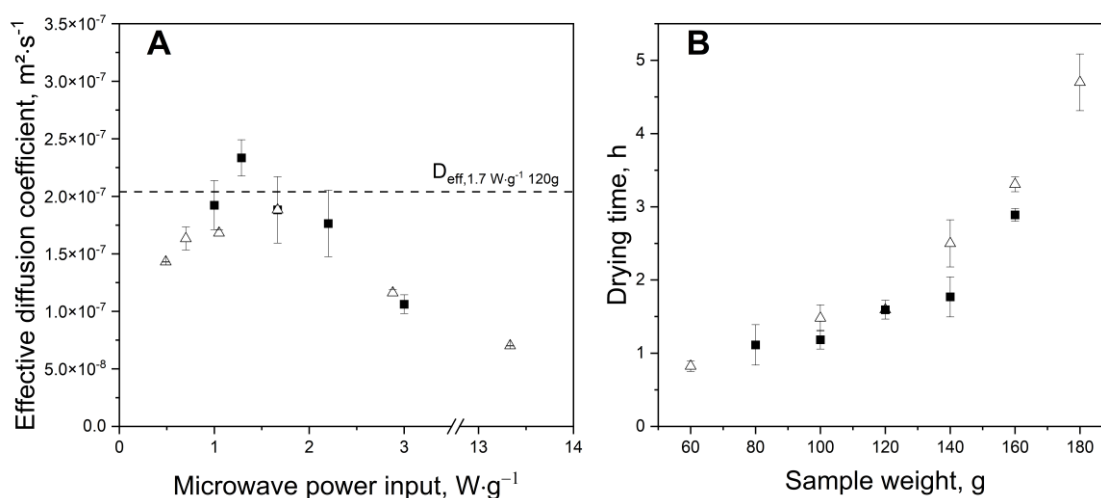


Fig. 4.9.2: Effective diffusion coefficients for different microwave-power input–sample weight combinations (A) and the required drying time over the sample weigh (B) using a linear (■) or exponential (Δ) power to weight adjustment.

Using a negative exponential relation between microwave power input and product weight resulted in slightly higher drying times for thick samples compared to the use of a linear relation. In contrast, for thin samples, an exponential relation was equal to the use of a linear relationship. For linear relationship, the drying time increased slightly and linearly between 80 and 140 g. For samples with higher mass, the required drying time increased more. This indicates that with a certain thickness of the foam, the inner resistance decreases the efficiency of the drying process or that the power input was too slow for an efficient drying process. This clearly shows that for more mass, the strategy has to be changed. One way would be to increase the shelf area by, e.g., using a sample glass with a larger diameter while remaining the same

product thickness. However, microwaves facilities are designed to heat a product within a specific area, and outside this area, the microwave field is usually distributed very randomly. Therefore, processing a product outside the specific area would increase the probability of obtaining hot- and cold spots inside the product. Besides, by increasing the shelf size, the turntable would not work anymore. Therefore, it was not possible to increase the shelf size inside the microwave cavity.

Besides the differences in diffusion coefficients, the product stability was investigated. Both, linear and exponential correlation resulted in only slight cracking, but nearly no melting or burning, except samples with 100 g. Even with linear correlation, burning occurred, which clearly shows the impact of slight differences in power-mass ratio. The residual enzyme activity after the drying process is shown in Fig. 4.9.3. Interestingly, the residual enzyme activity was higher for exponential power input and high product weight. One explanation is that the volumetric power input was the lowest for high mass and low power input. Thereby, the product was heated more uniformly. Further, local overheating was minimized, and thereby, the residual enzyme activity was higher compared to a moderate combination of power input and product weight. This shows that much lower microwave power input has to be used to prevent damage from the target substance, especially for higher product thickness.

Summing up, using a negative linear relationship between power input and sample weight was suitable to dry different sample sizes within a comparable time and quality. The obtained drying time scaled linearly with dried sample weight, and the residual enzyme activity remained at the same level. However, the experiments showed that the volumetric power input, which was chosen for 120 g and 200 W, was slightly too high and that by a decrease of the volumetric power input, the product quality was improved.

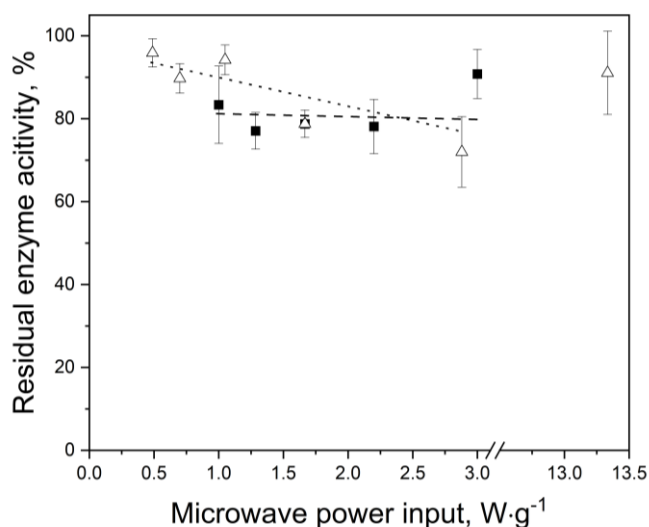


Fig. 4.9.3: Comparison of residual enzyme activity of β -galactosidase for samples with negative linear (■) and exponential (△) adjustment of microwave power input and sample weight.

Upscaling using foam droplets

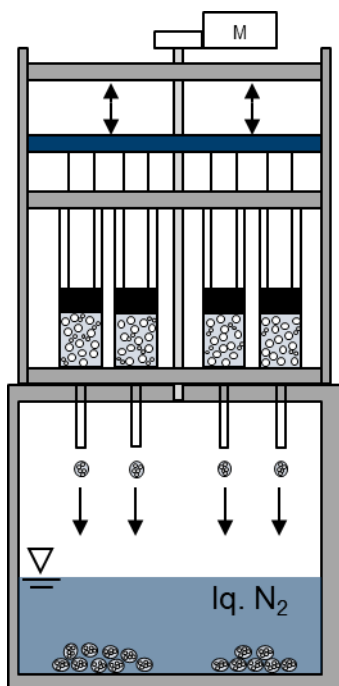


Fig. 4.9.4: Simplified scheme of the plant for the production of spherical foam drops using liquid nitrogen.

Because the inner resistance of the product was the main challenging property for the up-scale, samples were frozen as drops in liquid nitrogen to obtain a higher specific surface and to minimize the specific thickness. A scheme of the developed device for the reproducible production of spherical foam droplets is shown in Fig. 4.9.4. After the foam formation, the foam is gently transferred into ten syringes and mounted into the device. After that, a speed-controlled engine pushes a plate on the stamp of the syringes. The shape of the droplets and the rate of droplet aggregation during the freezing process can be controlled by the engine speed. A mounted stirrer prevented by separation the freezing of liquid droplets on still frozen ones (not shown in the scheme). The hypothesis was that the higher specific surface due to faster freezing and the smaller specific thickness (i.e., the diameter of drops) results in faster drying and easier upscaling compared to the processing of product cakes. Experiments were

performed with solution droplets and foam droplets.

In Fig. 4.9.5, the required drying time and the residual enzyme activity after MWFD is shown. One can see that the residual enzyme activity of solution droplets is slightly higher than for foamed droplets for 160 g samples. However, for other sample sizes, no significant difference in residual enzyme activity could be observed, and therefore, it was assumed that this has been an outlier. Besides, the residual enzyme activity of dried droplets was equal or even a bit higher compared to the residual enzyme activity of dried cakes. This was attributed to the smaller effective thickness of the samples, whereby the water vapor could easily leave the product. However, cakes dried equal or even faster than droplets. This is at first sight contradictory, because of the higher specific surface of the foam droplets. However, the higher specific surface led to faster drying, mainly during the primary drying section, whereas the secondary drying was slower for foam droplets. The reason for this is the open structure of foam cakes (Fig. 4.7.5), while foam droplets are much more compact, as a result of smaller ice-crystals and better preservation of bubble size due to the faster freezing process.

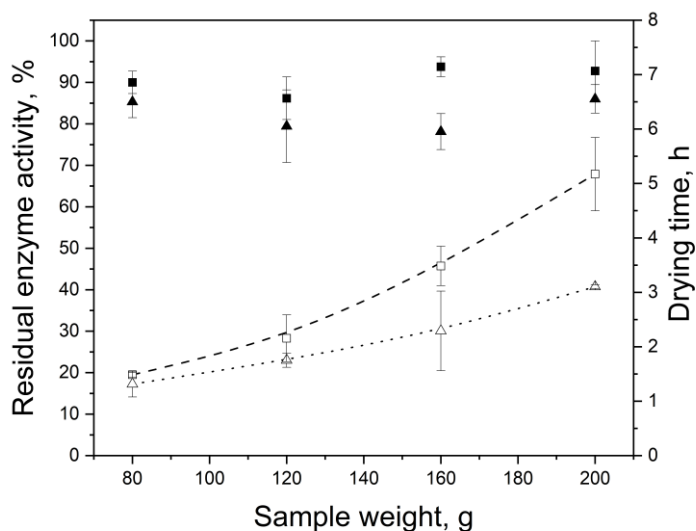


Fig. 4.9.5: Residual enzyme activity of β -gal after microwave-assisted freeze drying at 200 W and required drying time for solution droplets (and foam droplets with a sample weight between 80 and 180 g).

This argumentation is also supported by the drying rates (data not shown) and the SEM pictures of solution droplets, foam droplets, and foam cake after microwave-assisted freeze drying (Fig. 4.9.6). Residuals of lamellae are much more porous for foam cakes than foam droplets, resulting in lower residual water content and faster secondary drying. Besides, the residual water content of solution droplets was about 30% higher ($5.73 \pm 0.99\%$) compared to that of dried foam droplets ($4.05 \pm 0.32\%$). Therefore, it can be concluded that besides the internal surface area, their accessibility is of significant importance for the drying speed. In another experiment, the influence of different freezing rates on the drying time of foams using poloxamer F-108 combined with 30% maltodextrin and 5% β -galactosidase was investigated. The drying time of foam droplets was 2.73 ± 0.53 h, while in liquid nitrogen frozen foam cakes needed 3.02 ± 0.51 h, and foam cakes, frozen in a -80 °C freezer required 2.15 ± 0.45 h, respectively. Therefore, it was assumed that the unexpected shorter drying of polysorbate and maltodextrin-containing foam cakes and droplets can be mainly attributed to the different freezing rates. Therefore, the order of drying speed of the investigated product structures can be simplified as followed: foam droplets>foam cake>solution droplets>solution cake.

Further, the influence of different microwave power inputs on the residual enzyme activity of β -galactosidase for the MWFD of 120 g foam droplets was investigated (Fig. 4.9.7). One can see that the residual enzyme activity decreased between 160 and 180 W and then reached a plateau at about 80% residual enzyme activity. This is different from the drying of product cakes because, at a microwave power input above $1.6 \text{ W}\cdot\text{g}^{-1}$, the enzyme was damaged by overheating and plasma occurrence. This was obviously not the case for the drying of foam

droplets, which indicates that due to the use of droplets, a higher gravimetric power input can be applied to the product.

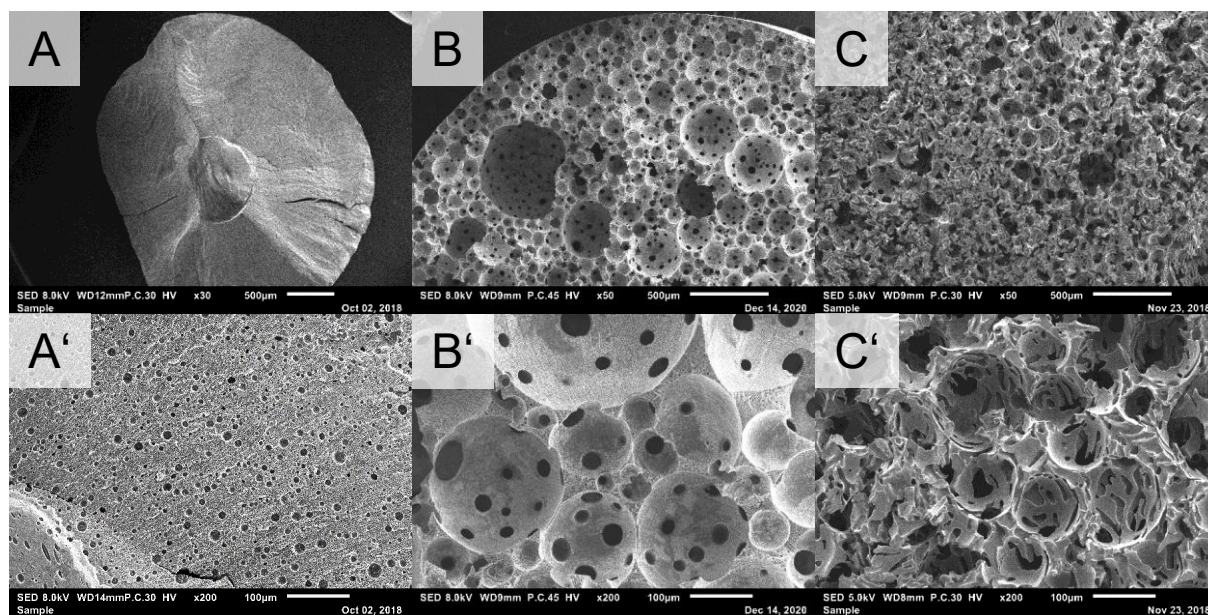


Fig. 4.9.6: Scanning electron microscope pictures of solution droplets (A, 30-fold); A', 200-fold), foam droplets (B, 50-fold; B', 200-fold), and product cake (C, 50-fold; C', 200-fold) after microwave-assisted freeze drying.

However, for samples with a power input of 240 W, slight and local browning at the surface of the center bulk was observed, which was assumed to occur due to a focus of the microwave field and inefficient rotation of the turntable. However, the area where browning occurred was small and did not influence the average residual enzyme activity of the sample (Fig. 4.9.7). Further, the drying time was significantly higher compared to samples processed with 220 W microwave energy input. This can be explained by a non-stable process due to an increase in operating pressure. Due to the comparable high microwave-power input and a too-small diameter of the connecting pipes between the product chamber and condenser, the pressure inside the drying chamber increased up to 0.32 mbar. This is over three times higher than the set pressure of 0.1 mbar and resulted in lower efficiency of the drying process because cooling cycles were more frequently needed. In literature, higher pressure during freeze drying processes is also known to increase the drying rate up to a pressure of 1.3 mbar due to easier convection and heating in between samples on a drying shelf (Pikal 1990a). However, in microwave-assisted drying, the products are heated volumetrically, and therefore, heat convection or conduction has a much lower influence on the drying speed. Furthermore, high pressure can destabilize the product due to too high sublimation temperature and the collapse of the product (Pikal 1990b; Pikal and Shah 1990).

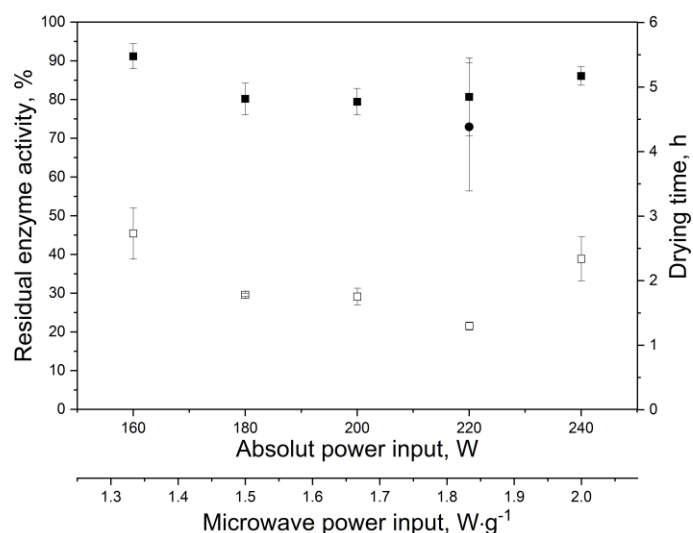


Fig. 4.9.7: Residual enzyme activity of β -gal (■) and required drying time (□) for 120 g of foam droplets dried at a microwave power input of 160–240 W and residual enzyme activity of 600 g foam droplets (●) dried at 220 W.

Suppose one assumes more efficient heating of larger samples during upscale as a result of better absorption and less microwave reflection. In that case, this problem might be even more pronounced with larger samples. Therefore, the microwave power input was not further scaled to the sample size, and samples for a 600 g upscale were processed with 220 W to prevent the melting or collapse of the product. Further, the upscale samples were dried inside a polypropylene drum instead of a sample glass (Fig. 4.9.8).

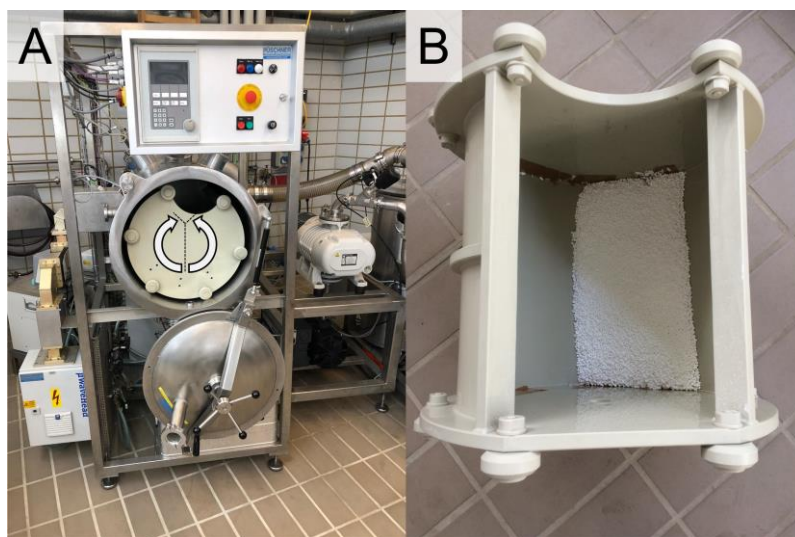


Fig. 4.9.8: Microwave drying plant equipped with drum(A) and dried foam drops after MWFD inside the polypropylene drum (B).

Thereby, the product layer did not get too thick, and due to a rotation of the drum with changing direction ($\pm 80^\circ$), the samples were mixed during the drying process. However, the drum was not connected to the scale, and therefore, the end of the drying could not be determined online.

Because it was expected that the drying time does not linearly scale with the sample weight, a drying time of 10 h was predetermined. The residual enzyme activity for the upscale experiment was $73.0 \pm 16.7\%$ and was therefore slightly lower compared to the 120 g samples at 220 W ($80.7 \pm 10.1\%$). This was unexpected, because the volumetric power input was much lower for the 600 g samples compared to samples with 120 g. One possible explanation could be the over-drying of the upscaled samples (Severo et al. 2017; Breen et al. 2001; Pikal and Shah 1997). Due to the missing connection to the scale, the necessary drying time was only presumed. However, the analysis of the temperature data (data not shown) hinted that the drying process was nearly finished within 6–7 h because the temperature was stable and only slightly increasing due to passive heating by the chamber wall. Thereby, the average residual water content inside the samples was $2.75 \pm 0.34\%$, much lower compared to the samples with 220 W and 120 g sample weight, where the end of the drying was controlled by a scale ($3.56 \pm 0.08\%$).

4.9.3 Conclusion

Different investigations on the up- or downscale of microwave-assisted freeze drying were performed, and limitations of product and drying plant were shown. By using a negative linear relationship between product weight and microwave power input up- and downscale of product mass can be done. However, upscaling is strongly limited by the internal water vapor resistance and the uniformity of the products' heating. Further, the water vapor has to be transferred towards the condenser to keep the drying process stable. This might be challenging, because the volume of vapor is immense due to the low pressure during freeze drying. Therefore, the upscale within an existing microwave-drying plant is difficult. Nonetheless, a successful upscale concept was shown within a feasibility study, using a drying drum and spherical foam drops. A five times higher sample weight was successfully dried and showed comparable residual enzyme activity to smaller batches. The end of the drying process was assumed to scale with the sample weight linearly. However, the process control was limited, and therefore, further experiments are required to find optimal conditions. Further, one limitation might be the use of super-cool liquids to retain the spherical shape of the drops during freezing. The use of freezing protection agents seems to be mandatory for freeze-sensitive substances, and due to the high freezing rate, annealing is recommended in order to increase the drying speed. Besides, an easy way to upscale and dry solutions instead of foams was found, which is new for microwave-assisted freeze drying of biological substances.

By using a bulk of droplets, high amounts of samples can be dried within one batch without having problems with too high water vapor transport resistance inside the product. Therefore, foamed sensitive substances in droplet form might be best suited for the gentle preservation using MWFD.

5 Overall discussion and main findings

5.1 Influence of saccharides on the properties of surfactant or protein stabilized foams

Saccharides are frequently used in the pharmaceutical industry as freezing or lyoprotectants. Besides, by the addition of saccharides, the viscosity of a product can be adjusted, which affects the foam properties (Wilson 1989). This increase in viscosity was always declared as the property influencing aspect for the formation of foams. However, in biotechnology, saccharides are known to interact and to stabilize proteins due to their hydrogen bonds, preferential exclusion, or preferential hydration. Moreover, the modulation of interactions between surfactants and proteins in the presence of saccharides showed that even non-ionic surfactants can be influenced by saccharides. Therefore, it was hypothesized that in addition to the increase in viscosity, foam properties would also be affected by the saccharide type and concentration-dependent interactions between foam forming and foam stabilizing components. For this purpose, the properties of foams using four different saccharides (sorbitol, sucrose, maltose, and maltodextrin) at different concentrations in combination with polysorbate 80 were investigated. It was found that the foam properties were influenced by the viscosity of the solution. In addition, a significant influence of concentration and type of saccharides was obtained. This was attributed to hydrogen bonds between surfactant and saccharide, which influenced the foaming properties of polysorbate 80. Comparable observations were made by Staples et al. (1996) in their study on the influence of sorbitol on the adsorption behavior of surfactants at the air-water interface. Further to that, the incorporation of surfactants in polysaccharides, as also assumed by Semenova et al. (2003) for small nonionic surfactants in the presence of maltodextrin, may have an influence on the surface properties of the surfactant. Therefore, differences in surface properties were expected as a result of changes in the number and strength of H-bonds in the presence of saccharides. The type of saccharides had a strong influence on the foam properties. However, the differences between maltose and sucrose were small. Nevertheless, the results clearly showed that not only the viscosity influences the foam properties. However, only surfactant-stabilized foams were investigated so far, where major interactions are of hydrophilic or hydrophobic character. It is expected that for protein stabilized foams the influence of saccharides is much more complex and stronger, since ionic interactions are present and changes in tertiary structures have been reported in the literature (Arakawa and Timasheff 1982; Lee and Timasheff 1981). Therefore, the knowledge of interactions between saccharides and foaming agents is critical to the design of foamed products, and it is expected that those interactions have an influence on foam stability during vacuum drying processes.

5.2 Foam stability during microwave-assisted vacuum drying

The stability of foams throughout the drying process is a mandatory criterion for a successful drying process and high product quality (Ratti and Kudra 2006a; Sankat and Castaigne 2004). Therefore, investigations on foam decay behavior during vacuum and microwave-assisted vacuum drying were carried out using different foaming agents and thickeners.

The hypothesis was that due to interactions between saccharides and surfactant or other surface-active substances, foam stability is affected during conventional or microwave-assisted vacuum drying. To this end, three different studies were conducted to investigate on a multiscale level the behavior of polysorbate 80 (chapter 4.4), whey protein isolate (chapter 4.5), and β -lactoglobulin stabilized foams (chapter 4.6) during vacuum drying. It was assumed that the use of different foaming agents in combination with various types and concentrations of disaccharides or polysaccharides would exhibit differences in molecular interactions, leading to different surface dilatational properties and thus varying foam stability during the drying process. The dielectric properties of formulations with different saccharides and saccharide concentrations were investigated. Furthermore, the influence of the change in dielectric properties during the drying process was investigated.

In the first part, the influence of different maltodextrin contents in polysorbate 80 foams on foam decay during vacuum and microwave-assisted vacuum drying was investigated. The hypothesis was that with increasing maltodextrin content, the interactions between surfactant and polysaccharide become more pronounced, resulting in differences in foam decay. Foam stability increased with increasing maltodextrin content, and foams were produced at MDX concentrations above 30% that were stable throughout the vacuum drying process.

In contrast, all formulations collapsed for microwave-assisted vacuum drying during the drying process. No correlation was found between the surface activity or surface tension and the foam decay during the drying process.

It was assumed that due to the high surfactant concentration and the overall high surface tension decrease rates, the influence of different maltodextrin contents was negligible. However, at an 40% MDX content, a slight decrease in surface activity was observed, attributed to the bulk's increased viscosity. Further, it was found that with increasing maltodextrin content, the surface dilatational rheology was affected. The highest surface dilatational elasticity was found for MDX concentrations between 10 and 35% MDX. This was hypothesized to be due to hydrophobic interactions between MDX molecules and the formation of hydrogen bonds between surfactant and polysaccharides, as also suggested by Semenova et al. (2003) for the interaction between small non-ionic surfactants and maltodextrin. Further, the dielectric properties of the bulk were investigated. It was found that with increasing maltodextrin content, dielectric

heat conversion became more efficient. In addition, the resonant frequency of polysorbate 80 was within the operating frequency of the microwave system. Therefore, one assumption was that a high power conversion at the air-liquid interface resulted in a structural collapse during microwave-assisted drying, whereas in conventional vacuum drying, this effect was absent, and the foam structure remained stable. However, this study could not fully clarify whether the dielectric properties were of major importance. Nevertheless, the study has initiated a discussion on the suitability of excipients for the purpose of microwave-assisted vacuum drying and highlighted the fragile relationship between foam properties, process conditions and drying success of products processed with microwave-assisted vacuum drying.

In a second part, studies were conducted on whey protein isolate-stabilized foams during microwave-assisted vacuum drying with different maltodextrin concentrations. The hypothesis was that due to interactions between proteins and maltodextrin, such as hydrogen bonding, the foam decay could be affected during the drying process. These should be different compared to nonionic surfactant-stabilized systems because proteins are charged and thus, ionic and electrostatic interactions affect the overall interactions. Furthermore, it was assumed that maltodextrin influences the interaction between protein molecules, and therefore, influences the surface dilatational rheology. It was shown that with a higher concentration of maltodextrin, the surface tension decreased, while the surface elasticity of the air-water interfaces increased. The surface elasticity was significantly higher compared to surfactant-stabilized surfaces, which was explained by the stronger intermolecular interactions between proteins compared to non-ionic small surfactants. The dielectric properties showed that with increasing MDX concentration, the dielectric heat conversion efficiency increases. In comparison to the drying of surfactant foams, all foams were structurally stable throughout the conventional vacuum drying. For MWVD, samples with a maltodextrin content above 10% remained stable throughout the drying process. Therefore, this study provided an indication that the surface dilatational rheology was of major importance to stabilize the structure of aerated products during CVD and MDVD. It was further shown that with increasing saccharide concentration, the products are heated more efficiently in MWVD.

Since in the two previously discussed studies the thickening agent was maltodextrin, the influence of different saccharides in combination with surfactants or proteins was investigated in a third study (chapter 4.6). Polysorbate 80 was used as a surfactant in combination with sucrose, sorbitol, maltose, and maltodextrin as thickening agents. Furthermore, β -lactoglobulin was utilized as a protein-based foaming agent instead of WPI to be able to investigate the intermolecular interactions between proteins in the presence of saccharides on a molecular level utilizing static light scattering. Repulsive and attractive interactions were expressed by the second virial coefficient A_2 , as was done for other protein-saccharide mixtures by Antipova and

Semenova (1997). The hypothesis was that different saccharides influence the molecular interactions individually and that thereby the surface dilatational rheology of the air-water interface is changed. Surface dilatation rheology was hypothesized in Sections 4.4 and 4.5 to be one of the most important properties for stabilizing foams during vacuum drying. Therefore, it was assumed that the investigated saccharides differ in their ability to stabilize foams during (microwave-assisted) vacuum drying.

Polysorbate samples were found to have significantly lower A_2 compared to β -lg samples, which was attributed to their non-ionic nature. As a result, repulsion was lower than that of protein samples, and it was assumed that the surface concentration at the air-water interface of the surfactant was higher than that of β -lg. This was also related to the lower surface tension of surfactant-stabilized samples. For polysorbate 80 samples, no significant difference was found for different sugars, while samples with β -lg showed higher A_2 for sucrose and sorbitol compared to maltose or maltodextrin. This was attributed to preferential exclusion mechanisms, whereby the proteins were stabilized by saccharides, resulting in higher repulsion and lower aggregation rate, supporting the native structure of the proteins (Timasheff 1992). Besides, the surface activity of surfactant-containing systems was much higher compared to protein-containing systems. However, with increasing saccharide concentration, the surface activity decreased, which could be attributed to the higher viscosity of the system. Anyway, as already discussed in the previous studies, the surface activity was not expected to have an effect on the foam stability during vacuum drying since the foam was already formed and the concentration of surface-active components was high. In addition, surface dilatation rheology was investigated, and various saccharides were found to affect the surface elasticity of polysorbate 80-stabilized systems. This was attributed to the formation of H-bonds between polysorbate and saccharides, which affected the speed of reattachment on the interface. Since proteins are known to not detach from the air-water interface once they have been attached (Dörfler 2002), the surface elasticity of β -lg stabilized systems was not significantly influenced. However, it was assumed that due to preferential exclusion, proteins were stabilized by saccharides in the solvated and attached state, as both states are the thermodynamically most stable conformation in the liquid or interface region. This would also explain why the surface elasticity was more elastic with increasing saccharide concentration, which was a big contrast to the polysorbate 80 stabilized foams. The CVD experiments showed that the above differences had a significant effect on the foam stability during vacuum drying. While all formulations with polysorbate 80, except those with maltodextrin, collapsed during the drying process, all formulations using β -lg were stable enough to withstand the process conditions. One explanation for this was the high viscosity of the bulk phase. However, samples with the same viscosity but other thickening agent collapsed. This indicated that besides the bulk's viscosity, the surface elasticity had an influence on the foam stability. However, no successful drying was achieved

for microwave-assisted vacuum drying of polysorbate 80-maltodextrin formulations, as already discussed in the previous studies. It was found that the collapse time does not correlate with the viscosity. This shows that the foam decay cannot only be attributed to a viscosity increase and that interfacial and foam properties play a major role in the stabilization of foams during the drying process. In contrast, all β -lg stabilized samples showed foamy structures after the MWVD process and remained therefore structurally stable. Overall, a correlation between molecular and surface dilatatory properties was established and their influence on the drying success of foamy structures in conventional and microwave-assisted vacuum drying processes was demonstrated.

Therefore, two properties seem most important for the vacuum or microwave-assisted vacuum drying of foams: The surface elasticity and the dielectric properties of the foaming agent. In terms of the foam properties, smaller bubbles sizes are preferred, because their expansion during the drying process is less than that of initially large bubbles. Further, the viscosity of the bulk phase should be high enough to prevent the foam from collapsing due to the additional thinning of the lamellae.

5.3 Influence of foam structures on the microwave-assisted freeze drying process

The influence of aerated structures on the drying behavior during conventional and microwave-assisted freeze drying was investigated. The hypothesis was that aerated structures dry simultaneously throughout the product and not like a liquid with a clear drying front. It was shown that the drying time was significantly decreased by using aerated matrices, and that microwave-assisted freeze drying resulted in high-quality samples. However, significant differences were observed for the water vapor release and the drying behavior dependent on the used overrun of the sample. Foams with moderate and high overrun dried evenly throughout the product. Similar findings were reported by Sochanski et al. (1990) for the drying of foamed milk. However, for foams with an overrun below 100%, a clear sublimation front was observed. Therefore, one finding was that frozen foams behave differently during freeze drying processes. If one compares the results from chapters 4.3 and 4.7., one can see that this change in water vapor transport has a strong impact on the drying behavior and product quality. The reason for this is that due to the higher water vapor resistance inside the products, the temperature and the pressure increased. As temperature control in microwave-drying can be only done by single spots (glass fiber optic) or surface temperature measurement (pyrometer, thermographic camera), the time delay between overheating and detection of too high temperatures can result in product instabilities. If the water transport resistance is low due to thin lamellae and a high specific surface, the probability of local overheating decreases significantly.

In addition, the volumetric power input is much lower for samples with high overrun, as the microwaves are mainly absorbed within the lamellae. Even if overheating and overpressure occur, thin lamellae are forming cracks easier, and thereby overheating by a too high sublimation rate becomes less likely. However, with increasing overrun, the required drying time increased, as also shown for foamed raspberry pulp during MWFD (Ozcelik et al. 2019a), which can be attributed to a higher water content in the samples and recondensation effects (Wang and Shi 1998).

Overall, it was found that foams positively influence the drying behavior during microwave-assisted freeze drying in different ways: Aerated structures lower the volumetric power input, increase the internal and external surface area, decrease the water vapor transfer resistance, and thereby counteract overheating effects during microwave-assisted heating.

5.4 Influence of process parameters on the product quality of microwave-assisted vacuum and freeze drying of aerated product matrices

Different combinations of microwave-power input and sample size were examined to find stable process conditions and produce high-quality products. The hypothesis was that by using an aerated matrix, high microwave power input can be used and that the drying time linearly decreases with increasing applied power. It was shown that the drying time could be reduced linearly with increasing power input. However, for power input above $1.8 \text{ W}\cdot\text{g}^{-1}$, overheating and plasma occurred. Thereby, the drying process became unstable, and the product quality decreased. Further, the problem of overheating was highlighted by the use of different product heights and demonstrated how important the inner water vapor resistance is for the product quality during microwave-assisted freeze drying. By increasing the product height, the inner water vapor resistance increases, and thereby, the inner pressure and temperature. As a result, the product is damaged even at moderate microwave power input. This effect was also found for the microwave-assisted vacuum drying of porous media by Péré and Rodier (2002). Since their study was about vacuum drying, where samples are still liquid, this effect was assumed to be even more pronounced for frozen products in MWFD. A way to solve this problem could be the use of a formulation yielding higher overruns, because then the lamellae are getting thinner, and consequently, the water vapor transfer resistance decreases due to the shorter distance the water vapor has to travel through the solid material. However, if the area where the microwave field seems suitable for the drying process is too small or space is limited, this is not always possible. Therefore, it is recommended to use only moderate microwave power input with about $0.8\text{--}2.5 \text{ W}\cdot\text{g}^{-1}$ even at higher loads to prevent plasma formation and product collapse. Besides, it was shown that with higher surface temperature, hot-spots were more pronounced and the probability of product instabilities increased. This was attributed to

the difficult temperature measurement of the foamed systems, since only the surface temperature can be measured. Thereby, heat conduction, which is bad for foams, comes into play for the detection of hot spots. Therefore, the maximum temperature should be chosen with care and low enough to be able to find hot spots before damage occurred to the product.

5.5 Up-scaling of microwave-assisted drying processes

The results from chapter 4.9 show clearly that the upscaling of microwave-assisted drying processes is challenging. No upscale experiments could be performed for microwave-assisted vacuum drying because the space within the product cavity was limited. Hence, the upscale of microwave-assisted vacuum drying requires other drying plant dimensions or a mechanical solution to keep the volume under a certain level. However, no suitable solution was found for the existing plant.

For microwave-assisted freeze drying, the area does not necessarily increase that much with the product load, since the product does not expand during the process. Nonetheless, issues due to changes in microwave field distribution and occurring hot- and coldspots are expected if the diameter of the sample is increased. Two different strategies were examined. One was to find a relation between product size and microwave power input to decrease the drying speed in order to increase the throughput of different products or batches. A second strategy was to utilize spherical foam drops in order to increase the surface area and decrease internal water vapor transport resistance.

It was found that a comparable product quality for different product mass can be achieved by using a negative linear relationship between microwave power input and sample weight. The reason for this was that by increasing the sample weight, the product height necessarily increases. Thereby, the water vapor resistance increased, and less power can be used to dry the product. As a result, the required drying time increased. Further, plasma formation became a problem when high microwave power input was used for small product weights (above $1.8 \text{ W}\cdot\text{g}^{-1}$). Thereby, the product can be damaged, and the process gets unstable. Therefore, the first strategy was highly limited to the product's dimensions and the gravimetric power input.

The use of foam drops instead of a single cake was promising for large amounts of product. The foam drops could be dried faster than product cakes, which were frozen with the same freezing rate, and no differences in product quality were observed. Furthermore, no product collapse or melting was observed, even at high power input values, which showed that the formation of drops was a suitable way to increase the mass transfer out of the sample. Samples of 80 up to 600 g were successfully dried, resulting in comparable product quality in comparison to conventional freeze drying processes. In addition, by using foam drops, a positive linear

relationship between microwave power input and sample weight might be possible because the water vapor transport resistance should be equal for every single drop. However, the probability of plasma formation was still a problem, especially at high drying rates and a high product load. Therefore, one assumption was that due to high sublimation rates, a comparable high pressure close to the sample's surface might cause plasma formation. One possible way to prevent plasma formation due to too high sublimation rates would be to decrease the overall pressure and the temperature of the condenser. Thereby, the suction of water vapor due to pressure differences between condenser and product chamber would be more efficient. However, lower pressure also requires a larger diameter of the pipes connecting the condenser and product chamber. Therefore, this connection could be the limitation in the upscale-process, as found for the drying of foam drops combined with high microwave power input. Because the connection between those two chambers cannot be modified easily, it is recommended to oversize this critical part of the drying plant when microwave-drying plants are developed to gain flexibility in process control and sample size.

5.6 Overall conclusion and perspectives

Microwave-assisted vacuum drying and microwave-assisted freeze drying are suited for the drying of sensitive biomolecules. A further acceleration and better product quality can be achieved by using a foamed product matrix. Thereby, the inner water vapor resistance of products decreases, and the heating of the product is more volumetric and uniform compared to the drying of solutions.

Generally, it was shown that for the use of non-frozen formulations in VD or MWVD, different sugars show a strong influence on the drying success and product quality. This was attributed to interactions between surface-active components and saccharides, which influenced the foam properties, heating, and consequently the evaporation during the drying process. The initial foam properties had a significant influence on the foam decay during vacuum drying. Despite of high microwave power input, there was no browning observed for all investigated formulation in VD or MWVD. It was assumed that due to boiling, which results in a mixing of the sample, the overheating was less pronounced than in MWFD. In MWFD, single components or sugars showed no significant influence on the drying process. However, the structure of the frozen foam had a massive influence on water vapor transport resistance. For unfavorable formulations and processing conditions, massive overheating was observed. Besides, excipients with lower freezing temperature or higher sublimation temperature than water like, e.g., glycerin can cause overheating due to more efficient energy conversion. Further, in the case of higher sublimation temperatures than that of water, even water-free samples can be heated in the presence of other microwave absorbers. This can cause damage to the amorphous structure or the target substance. Hence, formulations need to be designed regarding

the initial foam properties and physical properties for MWFD, while for MWVD, the initial foam properties and the molecular interactions in bulk phase and interface are of higher relevance.

The foam structure had a significant impact on the quality of the product and the required drying time. As an overview, the different bulk and foam properties and their importance for MWFD and MWVD are listed in Table 5.6-1.

Table 5.6-1: Importance of different foam properties for successfully drying with microwave-assisted vacuum or freeze drying.

	Bubble size	Bubble size distribution	Drainage	Overrun	Firmness	Surface activity	Surface elasticity	Dielectric properties
MWFD	+	0	0	++	--	--	--	0
MWVD	+	++	+	+	0	0	++	++

For MWVD, the initial bubble size should be small and the bubble size distribution as narrow as possible to obtain uniform expansion during the pressure release and the heating of the product. Thereby, the probability of a foam collapse decreases. Best results in terms of foam stability and process stability were obtained for protein-stabilized foams, whereas surfactant-stabilized foams collapsed during the drying process. However, with a collapsed product structure, the sample required much longer drying times, and due to shrinkage, the grindability was poor. Therefore, the stability of a foam throughout the drying is essential for the product quality (Ratti and Kudra 2006a; Sankat and Castaigne 2004). However, foams stability during MWVD is highly challenging. High surface elasticity is necessary to maintain the integrity of bubbles, which can easily collapse due to mechanical stress. This stress was mainly attributed to the expansion in a vacuum and the high evaporation rate. A further challenge is that the dielectric properties are changing throughout the drying process, whereby also the evaporation and heating properties of the samples are permanently changing. The most efficient heat conversion of microwaves is expected within the second half of the drying when the concentration of the bulk phase is prior to solidification. However, for MWVD, the dielectric properties of the foaming agent might have a significant impact on the foam stability during the drying process and should have its resonant frequency outside the operating range of the microwave drying plant. Further, the expansion of the product during the pressure release and the heating presents a limitation for the development of formulations and the upscaling of the process. The drying time can be drastically decreased in comparison to conventional vacuum drying due to the volumetric heating of the samples. The product quality in terms of residual enzyme activity is strongly dependent on the microwave power input, and therefore, is evaporation rate dependent. However, at suitable conditions, the residual enzyme activity of microwave-assisted vacuum drying can be higher compared to conventional vacuum drying. This is due to the faster passing of harmful conditions (e.g., unfavorable pH-value), which occur because of concentration during the drying process. Further, samples processed with microwave-assisted

vacuum drying have comparable product quality to freeze-dried samples. A comparison of conventional and microwave-assisted vacuum- and freeze drying of foamed samples is shown in Fig. 5.6.1, and MWVD seems suitable for the drying of sensitive biomolecules like enzymes, immunoglobulins, and proteins.

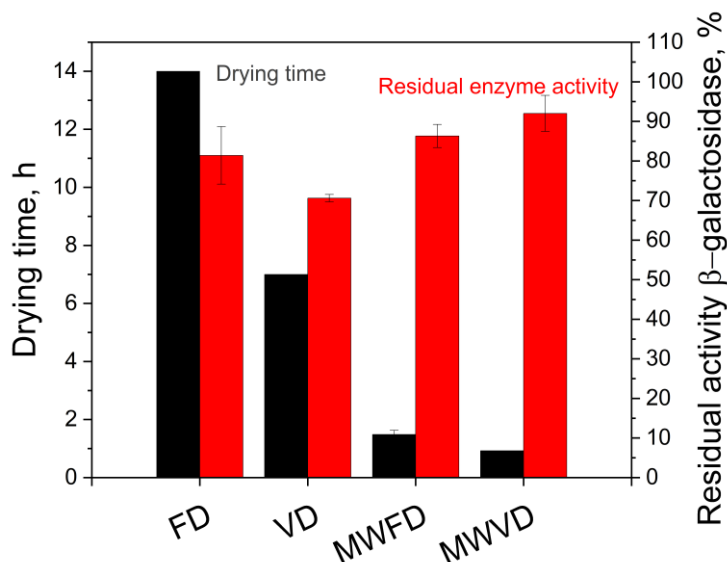


Fig. 5.6.1: Comparison of required drying time and residual enzyme activity of foam matrices using freeze drying (FD), vacuum drying (VD), microwave-assisted freeze drying (MWFD), and microwave-assisted vacuum drying (MVVD).

In MWFD, the initial foam properties strongly influenced the drying behavior. During the freezing step, drainage may occur and should be prevented as much as possible to obtain a uniform, frozen sample. Further, the fastest dryings were obtained for samples with an overrun value of about 150%, whereas high enzyme activity was obtained at much higher overrun values. This indicates that the water vapor transfer resistance within the foam results in damage to the enzyme due to partial overheating. Another explanation for the lower product quality might be the recondensing of water vapor within the foam structure due to pressure and, consequently, temperature differences. These are more pronounced for porous media in combination with microwave-drying than for conventional freeze drying, as also mentioned by Wang and Shi (1998). The reason is the circulation of vapor inside and between voids as well as the volumetric heating character of microwaves. However, due to recondensation, thermal and mechanical stress could also occur at already dried areas, which could result in lower residual enzyme activity. Since this phenomenon is strongly dependent on the voids' properties and the volumetric heating, the combination of overrun, bubble size, and bubble size distribution seem to be most relevant for a successful microwave-assisted freeze drying process. The dielectric properties of the samples were, in general, low because of the frozen state, and

therefore, differences in between formulations seem negligible. However, it should be mentioned that all ingredients should be in a solid-state, because the ability of heat conversion from microwave significantly increases if the ingredient is liquid and not frozen.

The formation of plasma is a problem, which is still a challenge in microwave-assisted freeze drying. High sublimation rates in combination with unsuitable plant design can cause corona discharge, which results in damage to the product or drying plant. One solution would be to decrease the pressure to a minimum. However, it has to be considered the dimensions of the plant regarding water vapor transport from product to condenser chamber. Further, for products with a big volume, the dielectric field distribution must be considered and optimized to prevent hot spots and cold spots, because practical applications like a turntable are not suitable for pilot-scale. One way to solve this problem would be the use of semiconductors, where the frequency can be varied within a certain bandwidth, resulting in different microwave modes. This would distribute the power input into the product and could prevent local hot- or cold spots. However, the development of a control logarithm might be challenging and highly specific for single products. Further, the temperature measurement during microwave-assisted drying is generally problematic, as it is only a surface measurement or a very small local spot. Therefore, it would be of interest to develop a method where the temperature of the product can be determined better to be able to react immediately to local overheating.

Overall, a compromise needs to be found between an acceleration of the drying process and the resulting product quality for each single target biomolecule. The easiest way to do so is the adjustment of the foams' overrun. Therefore, microwave-assisted freeze drying is a promising approach to reduce the required drying time while the product quality is the same as for conventional freeze drying. Due to the efficient heating of microwaves, the product's inner water vapor transfer resistance is an important property. Low microwave-power input is important to prevent the product from damage. By using an aerated matrix with an overrun above 50%, the water vapor transfer resistance can be decreased significantly. Further, samples begin to dry simultaneously throughout the product, and thereby, volumetric heating becomes much more suitable for the drying process. Hence, the use of aerated matrices is highly recommended for the microwave-assisted freeze drying of sensitive biomolecules.

6 References

- Abdul-Fattah, Ahmad M.; Truong-Le, Vu; Yee, Luisa; Nguyen, Lauren; Kalonia, Devendra S.; Cicerone, Marcus T.; Pikal, Michael J. (2007a): Drying-induced variations in physico-chemical properties of amorphous pharmaceuticals and their impact on stability (I): stability of a monoclonal antibody. In *J. Pharm. Sci.* 96 (8), pp. 1983–2008. DOI: 10.1002/jps.20859.
- Abdul-Fattah, Ahmad M.; Truong-Le, Vu; Yee, Luisa; Pan, Emilie; Ao, Yi; Kalonia, Devendra S.; Pikal, Michael J. (2007b): Drying-induced variations in physico-chemical properties of amorphous pharmaceuticals and their impact on Stability II. Stability of a vaccine. In *Pharm. Res.*, pp. 715–727. DOI: 10.1007/s11095-006-9191-2.
- Abiad, M. G.; Carvajal, M. T.; Campanella, O. H. (2009): A Review on Methods and Theories to Describe the Glass Transition Phenomenon. Applications in Food and Pharmaceutical Products. In *Food Eng. Rev.* 1 (2), pp. 105–132. DOI: 10.1007/s12393-009-9009-1.
- Acharya, Kamala Rani; Bhattacharyya, Subhash C.; Moulik, Satya P. (1999): Effects of carbohydrates on the solution properties of surfactants and dye–micelle complexation. In *J. Photochem. Photobiol.* 122 (1), pp. 47–52. DOI: 10.1016/S1010-6030(99)00003-9.
- Adams, G. D.; Irons, L. I. (1993): Some implications of structural collapse during freeze-drying using *Erwinia caratovora* L-asparaginase as a model. In *J. Chem. Technol. Biotechnol.* 58 (1), pp. 71–76. DOI: 10.1002/jctb.280580110.
- Aizawa, H. (2009): Morphology of polysorbate 80 (Tween 80) micelles in aqueous 1,4-dioxane solutions. In *J. Appl. Crystallogr.* 42 (4), pp. 592–596. DOI: 10.1107/S002188980902295X.
- Alhalaweh, A.; Alzghoul, A.; Mahlin, D.; Bergström, C. A. S. (2015): Physical stability of drugs after storage above and below the glass transition temperature. Relationship to glass-forming ability. In *Int. J. Pharm.* 495 (1), pp. 312–317. DOI: 10.1016/j.ijpharm.2015.08.101.
- Ali, A.; Bidhuri, P.; Malik, N. A.; Uzair, S. (2019): Density, viscosity, and refractive index of mono-, di-, and tri-saccharides in aqueous glycine solutions at different temperatures. In *Arab. J. Chem.* 12 (7), pp. 1684–1694. DOI: 10.1016/j.arabjc.2014.08.027.
- Allison, S. D.; Chang, B.; Randolph, T. W.; Carpenter, J. F. (1999): Hydrogen bonding between sugar and protein is responsible for inhibition of dehydration-induced protein unfolding. In *Arch. Biochem. Biophys.* 365 (2), pp. 289–298. DOI: 10.1006/abbi.1999.1175.

- Alvino Granados, A. E.; Fongin, S.; Hagura, Y.; Kawai, K. (2019): Continuously Distributed Glass Transition of Maca (*Lepidium meyenii* Walpers) Powder and Impact on Caking Properties. In *Food Biophysics* 14 (4), pp. 437–445. DOI: 10.1007/s11483-019-09593-z.
- Ambros, S.; Bauer, S. A. W.; Shylkina, L.; Foerst, P.; Kulozik, U. (2016): Microwave-Vacuum Drying of Lactic Acid Bacteria. Influence of Process Parameters on Survival and Acidification Activity. In *Food Bioprocess Technol.* 9 (11), pp. 1901–1911. DOI: 10.1007/s11947-016-1768-0.
- Ambros, S.; Dombrowski, J.; Boettger, D.; Kulozik, U. (2019a): Structure-Function-Process Relationship for Microwave Vacuum Drying of Lactic Acid Bacteria in Aerated Matrices. In *Food Bioprocess Technol.* 12 (3), pp. 395–408.
- Ambros, S.; Dombrowski, J.; Boettger, D.; Kulozik, U. (2019b): The Concept of Microwave Foam Drying Under Vacuum. A Gentle Preservation Method for Sensitive Biological Material. In *J. Food Sci.* 84 (7), pp. 1682–1691. DOI: 10.1111/1750-3841.14698.
- Ambros, S.; Mayer, R.; Schumann, B.; Kulozik, U. (2018): Microwave-freeze drying of lactic acid bacteria: Influence of process parameters on drying behavior and viability. In *Innovative Food Sci. Emerging Technol.* 48, pp. 90–98. DOI: 10.1016/j.ifset.2018.05.020.
- Antipova, A. S.; Semenova, M. G. (1997): Effect of neutral carbohydrate structure in the set glucose/sucrose/maltodextrin/dextran on protein surface activity at the air/water interface. In *Food Hydrocolloids* 11 (1), pp. 71–77. DOI: 10.1016/S0268-005X(97)80013-6.
- Arakawa, T.; Kita, Y.; Carpenter, J. F. (1991): Protein-solvent interactions in pharmaceutical formulations. In *Pharm. Res.* 8 (3), pp. 285–291. DOI: 10.1023/a:1015825027737.
- Arakawa, T.; Timasheff, S. N. (1982): Stabilization of protein structure by sugars. In *Biochemistry* 21 (25), pp. 6536–6544. DOI: 10.1021/bi00268a033.
- Archer, Donald G.; Wang, Peiming (1990): The Dielectric Constant of Water and Debye-Hückel Limiting Law Slopes. In *J. Phys. Chem. Ref. Data* 19 (2), pp. 371–411. DOI: 10.1063/1.555853.
- Aumann, E.; Hildemann, L. M.; Tabazadeh, A. (2010): Measuring and modeling the composition and temperature-dependence of surface tension for organic solutions. In *Atmos. Environ.* 44 (3), pp. 329–337. DOI: 10.1016/j.atmosenv.2009.10.033.
- Baeza, R.; Pilosof, A. M. R.; Sanchez, C. C.; Rodríguez Patino, J. M. (2006): Adsorption and rheological properties of biopolymers at the air-water interface. In *AIChE J.* 52 (7), pp. 2627–2638. DOI: 10.1002/aic.10855.

- Baeza, Rosa; Carrera Sanchez, Cecilio; Pilosof, Ana M.R.; Rodríguez Patino, Juan M. (2005): Interactions of polysaccharides with β -lactoglobulin adsorbed films at the air–water interface. In *Food Hydrocolloids* 19 (2), pp. 239–248. DOI: 10.1016/j.foodhyd.2004.06.002.
- Bakaltcheva, I.; O'Sullivan, A. M.; Hmel, P.; Ogbu, H. (2007): Freeze-dried whole plasma. Evaluating sucrose, trehalose, sorbitol, mannitol and glycine as stabilizers. In *Thromb. Res.* 120 (1), pp. 105–116. DOI: 10.1016/j.thromres.2006.07.005.
- Bals, A.; Kulozik, U. (2003): The influence of the pore size, the foaming temperature and the viscosity of the continuous phase on the properties of foams produced by membrane foaming. In *J. Membr. Sci.* 220 (1-2), pp. 5–11. DOI: 10.1016/S0376-7388(03)00168-6.
- Balzarini, M. F.; Reinheimer, M. A.; Ciappini, M. C.; Scenna, N. J. (2018): Comparative study of hot air and vacuum drying on the drying kinetics and physicochemical properties of chicory roots. In *J. Food Sci. Technol.*, pp. 4067–4078. DOI: 10.1007/s13197-018-3333-5.
- Bart, J. C. J. (2005): Additives in polymers. Industrial analysis and applications. Reprinted with corrections. Chichester: Wiley.
- Basedow, A. M.; Möschl, G. A.; Schmidt, P. C. (2008): Sorbitol Instant an Excipient with Unique Tableting Properties. In *Drug Dev. Ind. Pharm.* 12 (11-13), pp. 2061–2089. DOI: 10.3109/03639048609042624.
- Bauer, S. A. W.; Schneider, S.; Behr, J.; Kulozik, U.; Foerst, P. (2012): Combined influence of fermentation and drying conditions on survival and metabolic activity of starter and probiotic cultures after low-temperature vacuum drying. In *J. Biotechnol.* 159 (4), pp. 351–357. DOI: 10.1016/j.jbiotec.2011.06.010.
- Bell, L. N.; Labuza, T. P. (2000): Moisture Sorption: Practical Aspects of Isotherm Measurement and Use. 2nd ed. St. Paul MN: American Association of Cereal Chemists.
- Bellows, R. J.; King, C. J. (1972): Freeze-drying of aqueous solutions. Maximum allowable operating temperature. In *Cryobiology* 9 (6), pp. 559–561. DOI: 10.1016/0011-2240(72)90179-4.
- BeMiller, J. N. (2019): Carbohydrate chemistry for food scientists. Third edition. London: WP. Available online at <https://www.sciencedirect.com/science/book/9780128120699>.
- Benaskar, F.; Ben-Abdelmoumen, A.; Patil, N. G.; Rebrov, E. V.; Meuldijk, J.; Hulshof, L. A. et al. (2011): Cost Analysis for a Continuously Operated Fine Chemicals Production Plant at 10 Kg/Day Using a Combination of Microprocessing and Microwave Heating. In *J. Flow Chem.* 1 (2), pp. 74–89. DOI: 10.1556/jfchem.2011.00015.

- Bergeron, V. (1999): Forces and structure in thin liquid soap films. In *J. Phys.: Condens. Matter* 11 (19), R215-R238. DOI: 10.1088/0953-8984/11/19/201.
- Berry, G. C. (1966): Thermodynamic and Conformational Properties of Polystyrene. I. Light-Scattering Studies on Dilute Solutions of Linear Polystyrenes. In *J. Chem. Phys.* 44 (12), pp. 4550–4564. DOI: 10.1063/1.1726673.
- Bey, H.; Wintzenrieth, Frédéric; Ronsin, Olivier; Höhler, Reinhard; Cohen-Addad, Sylvie (2017): Stabilization of foams by the combined effects of an insoluble gas species and gelation. In *Soft Matter* 13 (38), pp. 6816–6830. DOI: 10.1039/c6sm02191c.
- Bezulgues, J.-B.; Serieye, S.; Crosset-Perrotin, L.; Leser, M. E. (2008): Interfacial and foaming properties of some food grade low molecular weight surfactants. In *Colloids Surf., A* 331 (1-2), pp. 56–62. DOI: 10.1016/j.colsurfa.2008.07.022.
- Bhandari, Bhesh; Bansal, Nidhi; Zhang, Min (2013): Handbook of food powders. Processes and properties. Oxford, Cambridge, Philadelphia: Woodhead Publishing (Woodhead Publishing series in food, technology and nutrition, 255).
- Blanchard, J.; Fink, W.; Duffy, J. (1977): Effect of sorbitol on interaction of phenolic preservatives with polysorbate 80. In *J. Pharm. Sci.* 66 (10), pp. 1470–1473.
- Blanchard, P. H.; Katz, F. R. (2006): Starch Hydrolysates. In Alistair M. Stephen, Glyn O. Phillips, Peter A. Williams (Eds.): Food polysaccharides and their applications. 2nd ed. Boca Raton, FL: CRC/Taylor & Francis (Food science and technology), pp. 119–145.
- Bock, K.; Lemieux, R. U. (1982): The conformational properties of sucrose in aqueous solution. Intramolecular hydrogen-bonding. In *Carbohydr Res* 100 (1), pp. 63–74. DOI: 10.1016/S0008-6215(00)81026-5.
- Boisen, Sigurd; Bech-Andersen, Steen; Eggum, Bjørn O. (1987): A Critical View on the Conversion Factor 6.25 from Total Nitrogen to Protein. In *Acta. Agric. Scand.* 37 (3), pp. 299–304. DOI: 10.1080/00015128709436560.
- Boon, M.A; Janssen, A.E.M; van 't Riet, K. (2000): Effect of temperature and enzyme origin on the enzymatic synthesis of oligosaccharides. In *Enzyme Microb. Technol.* 26 (2-4), pp. 271–281. DOI: 10.1016/S0141-0229(99)00167-2.
- Boos, Julia; Drenckhan, Wiebke; Stubenrauch, Cosima (2013): Protocol for Studying Aqueous Foams Stabilized by Surfactant Mixtures. In *J. Surfact. Deterg.* 16 (1), pp. 1–12. DOI: 10.1007/s11743-012-1416-2.
- Borglum, G. B.; Sternberg, M. Z. (1972): Properties of a fungal lactase. In *J. Food Sci.* 37 (4), pp. 619–623. DOI: 10.1111/j.1365-2621.1972.tb02707.x.

- Bos, A. M.; van Vliet, T. (2001): Interfacial rheological properties of adsorbed protein layers and surfactants. A review. In *Adv. Colloid. Interface Sci.* 91 (3), pp. 437–471. DOI: 10.1016/S0001-8686(00)00077-4.
- Bouyer, Eléonore; Mekhloufi, Ghazlene; Rosilio, Véronique; Grossiord, Jean-Louis; Agnely, Florence (2012): Proteins, polysaccharides, and their complexes used as stabilizers for emulsions: alternatives to synthetic surfactants in the pharmaceutical field? In *Int. J. Pharm.* 436 (1-2), pp. 359–378. DOI: 10.1016/j.ijpharm.2012.06.052.
- Braunschweig, Björn; Schulze-Zachau, Felix; Nagel, Eva; Engelhardt, Kathrin; Stoyanov, Stefan; Gochev, Georgi et al. (2016): Specific effects of Ca(2+) ions and molecular structure of β -lactoglobulin interfacial layers that drive macroscopic foam stability. In *Soft Matter* 12 (27), pp. 5995–6004. DOI: 10.1039/C6SM00636A.
- Breen, E. D.; Curley, J. G.; Overcashier, D. E.; Hsu, C. C.; Shire, S. J. (2001): Effect of moisture on the stability of a lyophilized humanized monoclonal antibody formulation. In *Pharm. Res.* 18 (9), pp. 1345–1353. DOI: 10.1023/A:1013054431517.
- Briceño-Ahumada, Z.; Langevin, D. (2017): On the influence of surfactant on the coarsening of aqueous foams. In *Adv. Colloid. Interface Sci.* 244, pp. 124–131. DOI: 10.1016/j.cis.2015.11.005.
- Brodie, G. (2008): The Influence of Load Geometry on Temperature Distribution During Microwave Heating. In *Trans. ASABE* 51 (4), pp. 1401–1413. DOI: 10.13031/2013.25224.
- Browne, C. A. (1912): Handbook of Sugar Analysis. New York: John Wiley and Sons.
- Brygidyr, A. M.; Rzepecka, M. A.; McConnell, M. B. (1977): Characterization and Drying of Tomato Paste Foam by Hot Air and Microwave Energy. In *Can. Inst. Food Technol. J.* 10 (4), pp. 313–319. DOI: 10.1016/S0315-5463(77)73553-9.
- Cantat, Isabelle; Cohen-Addad, Sylvie; Elias, Florence; Graner, François; Höhler, Reinhard; Pitois, Olivier et al. (2013): Foams: Structure and Dynamics. Oxford, UK: Oxford University Press.
- Carp, D.J; Bartholomai, G.B; Pilosof, A.M.R (1999): Electrophoretic studies for determining soy proteins–xanthan gum interactions in foams. In *Colloids Surf., B* 12 (3-6), pp. 309–316. DOI: 10.1016/S0927-7765(98)00085-X.
- Carpenter, J. F.; Arakawa, T.; Crowe, J. H. (1992): Interactions of stabilizing additives with proteins during freeze-thawing and freeze-drying. In *Dev. Biol. Stand.* 74, 225-38; discussion 238-9.

- Carpenter, J. F.; Crowe, J. H. (1989): An infrared spectroscopic study of the interactions of carbohydrates with dried proteins. In *Biochemistry* 28 (9), pp. 3916–3922. DOI: 10.1021/bi00435a044.
- Carpenter, J. F.; Pikal, M. J.; Chang, B. S.; Randolph, T. W. (1997): Rational design of stable lyophilized protein formulations. Some practical advice. In *Pharm. Res.* 14 (8), pp. 969–975. DOI: 10.1023/a:1012180707283.
- Castro, Natalia; Durrieu, Vanessa; Raynaud, Christine; Rouilly, Antoine (2016): Influence of DE-value on the physicochemical properties of maltodextrin for melt extrusion processes. In *Carbohydr. Polym.* 144, pp. 464–473. DOI: 10.1016/j.carbpol.2016.03.004.
- Chandrasekaran, S.; Ramanathan, S.; Basak, Tanmay (2013): Microwave food processing—A review. In *Food Res. Int.* 52 (1), pp. 243–261. DOI: 10.1016/j.foodres.2013.02.033.
- Chang, Liuquan Lucy; Pikal, Michael J. (2009): Mechanisms of protein stabilization in the solid state. In *J. Pharm. Sci.* 98 (9), pp. 2886–2908. DOI: 10.1002/jps.21825.
- Chang, Liuquan Lucy; Shepherd, Deanna; Sun, Joanna; Ouellette, David; Grant, Kathleen L.; Tang, Xiaolin Charlie; Pikal, Michael J. (2005): Mechanism of protein stabilization by sugars during freeze-drying and storage. Native structure preservation, specific interaction, and/or immobilization in a glassy matrix? In *J. Pharm. Sci.* 94 (7), pp. 1427–1444. DOI: 10.1002/jps.20364.
- Charman, S. A.; Mason, K. L.; Charman, W. N. (1993): Techniques for assessing the effects of pharmaceutical excipients on the aggregation of porcine growth hormone. In *Pharm. Res.* 10 (7), pp. 954–962. DOI: 10.1023/a:1018994102218.
- Chatterjee, Koustuv; Shalaev, Evgenyi Y.; Suryanarayanan, Raj (2005): Partially crystalline systems in lyophilization. II. Withstanding collapse at high primary drying temperatures and impact on protein activity recovery. In *J. Pharm. Sci.* 94 (4), pp. 809–820. DOI: 10.1002/jps.20304.
- Chaudhari, Smruti P.; Dugar, Rohit P. (2017): Application of surfactants in solid dispersion technology for improving solubility of poorly water soluble drugs. In *J. Drug Deliv. Sci. Technol.* 41, pp. 68–77. DOI: 10.1016/j.jddst.2017.06.010.
- Chauhan, S.; Sharma, Vivek; Sharma, Kundan (2013): Maltodextrin–SDS interactions. Volumetric, viscometric and surface tension study. In *Fluid Phase Equilib.* 354 (7), pp. 236–244. DOI: 10.1016/j.fluid.2013.06.051.

- Chitu, T.; Vessot, S.; Peczalski, R.; Andrieu, J.; Woinet, B.; Françon, A. (2015): Influence of Operating Conditions on the Freeze-Drying of Frozen Particles in a Fixed Bed and Modeling Data. In *Drying Technol.* 33 (15-16), pp. 1892–1898. DOI: 10.1080/07373937.2015.1066386.
- Chou, Danny K.; Krishnamurthy, Rajesh; Randolph, Theodore W.; Carpenter, John F.; Manning, Mark Cornell (2005): Effects of Tween 20 and Tween 80 on the stability of Albutropin during agitation. In *J. Pharm. Sci.* 94 (6), pp. 1368–1381. DOI: 10.1002/jps.20365.
- Chronakis, I. S. (1998a): On the molecular characteristics, compositional properties, and structural-functional mechanisms of maltodextrins. A review. In *Crit. Rev. Food Sci. Nutr.* 38 (7), pp. 599–637. DOI: 10.1080/10408699891274327.
- Chronakis, I. S. (1998b): On the molecular characteristics, compositional properties, and structural-functional mechanisms of maltodextrins. A review. In *Crit. Rev. Food Sci. Nutr.* 38 (7), pp. 599–637. DOI: 10.1080/10408699891274327.
- Chung, Hyun-Jung; Lim, Seung-Taik (2006): Physical Aging of Amorphous Starches (A Review). In *Starch - Stärke* 58 (12), pp. 599–610. DOI: 10.1002/star.200600547.
- Claesson, Per M.; Kjellin, Mikael; Rojas, Orlando J.; Stubenrauch, Cosima (2006): Short-range interactions between non-ionic surfactant layers. In *Phys. Chem. Chem. Phys.* 8 (47), pp. 5501–5514. DOI: 10.1039/b610295f.
- Clark, D. C.; Coke, M.; Smith, L.J., Wilson, D.R. (1989): The Formation and Stabilisation of Protein Foams. In A. J. Wilson (Ed.): *Foams. Physics, Chemistry and Structure*. Berlin Heidelberg New York: Springer-Verlag, pp. 55–68.
- Conde, José Miñones; Rodríguez Patino, Juan M. (2005): Rheological Properties of Hydrolysates of Proteins from Extracted Sunflower Flour Adsorbed at the Air–Water Interface. In *Ind. Eng. Chem. Res.* 44 (20), pp. 7761–7769. DOI: 10.1021/ie0506163.
- Coors, Esther A.; Seybold, Heidi; Merk, Hans F.; Mahler, Vera (2005): Polysorbate 80 in medical products and nonimmunologic anaphylactoid reactions. In *Ann. Allergy Asthma Immunol.* 95 (6), pp. 593–599. DOI: 10.1016/s1081-1206(10)61024-1.
- Crank, J. (1975): *The mathematics of diffusion*. 2. ed., reprint. Oxford, UK: Clarendon Press.
- Dachmann, E.; Hengst, C.; Ozcelik, M.; Kulozik, U.; Dombrowski, J. (2018): Impact of Hydrocolloids and Homogenization Treatment on the Foaming Properties of Raspberry Fruit Puree. In *Food Bioprocess Technol.* 11 (12), pp. 2253–2264. DOI: 10.1007/s11947-018-2179-1.
- Damodaran, Srinivasan (2005): Protein Stabilization of Emulsions and Foams. In *J. Food Sci.* 70 (3), R54-R66. DOI: 10.1111/j.1365-2621.2005.tb07150.x.

- Dash, Ranjeet Prasad; Srinivas, Nuggehally R.; Babu, R. Jayachandra (2019): Use of sorbitol as pharmaceutical excipient in the present day formulations - issues and challenges for drug absorption and bioavailability. In *Drug Dev. Ind. Pharm.* 45 (9), pp. 1421–1429. DOI: 10.1080/03639045.2019.1640722.
- Datta, Ashim K. (Ed.) (2001): Handbook of Microwave Technology for Food Application: CRC Press.
- Davies, J. D.: "Freeze-dried foam dosage form." U.S. Patent No. 4,642,903. 17 Feb. 1987.
- Davis, J. P.; Foegeding, E. A. (2007): Comparisons of the foaming and interfacial properties of whey protein isolate and egg white proteins. In *Colloids Surf., B* 54 (2), pp. 200–210. DOI: 10.1016/j.colsurfb.2006.10.017.
- Dereymaker, Aswin; van den Mooter, Guy (2015): The peculiar behavior of the glass transition temperature of amorphous drug-polymer films coated on inert sugar spheres. In *J. Pharm. Sci.* 104 (5), pp. 1759–1766. DOI: 10.1002/jps.24395.
- Dibben, D. (2001): Electromagnetics: Fundamental Aspects and Numerical Modeling. In Ashim K. Datta (Ed.): Handbook of Microwave Technology for Food Application: CRC Press, pp. 1–32.
- Dickinson, E. (1989): Protein Adsorption at Liquid Interfaces and the Relationship to Foam Stability. In A. J. Wilson (Ed.): *Foams. Physics, Chemistry and Structure*. Berlin Heidelberg New York: Springer-Verlag, pp. 39–53.
- Dickinson, Eric (1998): Stability and rheological implications of electrostatic milk protein–polysaccharide interactions. In *Trends Food Sci. Technol.* 9 (10), pp. 347–354. DOI: 10.1016/S0924-2244(98)00057-0.
- Dickinson, Eric (2003): Hydrocolloids at interfaces and the influence on the properties of dispersed systems. In *Food Hydrocolloids* 17 (1), pp. 25–39. DOI: 10.1016/S0268-005X(01)00120-5.
- Dokic-Baucal, Ljubica; Dokic, Petar; Jakovljevic, Jovan (2004): Influence of different maltodextrins on properties of O/W emulsions. In *Food Hydrocolloids* 18 (2), pp. 233–239. DOI: 10.1016/S0268-005X(03)00068-7.
- Dombrowski, J.; Gschwendtner, M.; Kulozik, U. (2017): Evaluation of structural characteristics determining surface and foaming properties of β -lactoglobulin aggregates. In *Colloids Surf., A* 516 (4), pp. 286–295. DOI: 10.1016/j.colsurfa.2016.12.045.
- Dombrowski, Jannika; Gschwendtner, Matthias; Saalfeld, Daniel; Kulozik, Ulrich (2018): Salt-dependent interaction behavior of β -Lactoglobulin molecules in relation to their surface

- and foaming properties. In *Colloids Surf., A* 558, pp. 455–462. DOI: 10.1016/j.colsurfa.2018.09.015.
- Domingues, Lucília; Lima, Nelson; Teixeira, José A. (2005): *Aspergillus niger* β -galactosidase production by yeast in a continuous high cell density reactor. In *Process Biochem.* 40 (3-4), pp. 1151–1154. DOI: 10.1016/j.procbio.2004.04.016.
- Dörfler, H. D. (2002): Grenzflächen und kolloid-disperse Systeme. Physik und Chemie ; mit 579, zum Teil farbigen Abb. und 88 Tabellen. Berlin: Springer.
- Drenckhan, Wiebke; Hutzler, Stefan (2015): Structure and energy of liquid foams. In *Adv. Colloid. Interface Sci.* 224, pp. 1–16. DOI: 10.1016/j.cis.2015.05.004.
- Drouzas, A. E.; Schubert, H. (1996): Microwave application in vacuum drying of fruits. In *J. Food Eng.* 28 (2), pp. 203–209. DOI: 10.1016/0260-8774(95)00040-2.
- Drouzas, A.E; Tsami, E.; Saravacos, G.D (1999): Microwave/vacuum drying of model fruit gels. In *J. Food Eng.* 39 (2), pp. 117–122. DOI: 10.1016/S0260-8774(98)00133-2.
- Duan, X.; Hall, J. A.; Nikaido, H.; Quioco, F. A. (2001): Crystal structures of the maltodextrin/maltose-binding protein complexed with reduced oligosaccharides. Flexibility of tertiary structure and ligand binding. In *J. Mol. Biol.* 306 (5), pp. 1115–1126. DOI: 10.1006/jmbi.2001.4456.
- Duan, X.; Zhang, M.; Mujumdar, A. S.; Wang, R. (2010a): Trends in Microwave-Assisted Freeze Drying of Foods. In *Drying Technol.* 28 (4), pp. 444–453. DOI: 10.1080/07373931003609666.
- Duan, Xu; Ren, Guang Yue; Zhu, Wen Xue (2012): Microwave Freeze Drying of Apple Slices Based on the Dielectric Properties. In *Drying Technol.* 30 (5), pp. 535–541. DOI: 10.1080/07373937.2011.648783.
- Duan, Xu; Zhang, Min; Mujumdar, Arun S. (2007): Studies on the Microwave Freeze Drying Technique and Sterilization Characteristics of Cabbage. In *Drying Technol.* 25 (10), pp. 1725–1731. DOI: 10.1080/07373930701591044.
- Duan, Xu; Zhang, Min; Mujumdar, Arun S.; Wang, Shaojin (2010b): Microwave freeze drying of sea cucumber (*Stichopus japonicus*). In *J. Food Eng.* 96 (4), pp. 491–497. DOI: 10.1016/j.jfoodeng.2009.08.031.
- Dumas, J. B. A. (1831): Procédes de l'analyse organique. In *Ann. Chim. Phys* 47, pp. 198–213.

- Durance, T. D.; Yaghmaee, P. (2011): 4.51 - Microwave Dehydration of Food and Food Ingredients. In Murray Moo-Young (Ed.): *Comprehensive biotechnology*. [principles and practices in industry, agriculture, medicine and the environment] ; vol. 1 - 6. 2. ed., [elektronische Ressource]. Amsterdam: Elsevier, pp. 617–628.
- Edwards, R. A.; Jacobson, A. L.; Huber, R. E. (1990): Thermal denaturation of beta-galactosidase and of two site-specific mutants. In *Biochemistry* 29 (49), pp. 11001–11008. DOI: 10.1021/bi00501a019.
- Ellis, A. L.; Norton, A. B.; Mills, T. B.; Norton, I. T. (2017): Stabilisation of foams by agar gel particles. In *Food Hydrocolloids* 73, pp. 222–228. DOI: 10.1016/j.foodhyd.2017.06.038.
- Engelhardt, Kathrin; Lexis, Meike; Gochev, Georgi; Konnerth, Christoph; Miller, Reinhard; Wilenbacher, Norbert et al. (2013): pH effects on the molecular structure of β -lactoglobulin modified air-water interfaces and its impact on foam rheology. In *Langmuir*, pp. 11646–11655. DOI: 10.1021/la402729g.
- Engelsen, S. B.; Monteiro, C. (2001): The diluted aqueous solvation of carbohydrates as inferred from molecular dynamics simulations and NMR spectroscopy. In *Biophys. Chem.* 93 (2-3), pp. 103–127. DOI: 10.1016/S0301-4622(01)00215-0.
- Epstein, Benjamin R.; Foster, Kenneth R.; Mackay, Raymond A. (1983): Microwave dielectric properties of ionic and nonionic microemulsions. In *J. Colloid Interface Sci.* 95 (1), pp. 218–227. DOI: 10.1016/0021-9797(83)90090-5.
- Fainerman, V. B.; Miller, R. (2005): Equilibrium and Dynamic Characteristics of Protein Adsorption Layers at Gas-Liquid Interfaces. Theoretical and Experimental Data. In *Colloid J* 67 (4), pp. 393–404. DOI: 10.1007/s10595-005-0110-8.
- Falade, K. O.; Solademi, O. J. (2010): Modelling of air drying of fresh and blanched sweet potato slices. In *Int. J. Food Sci. Technol.* 45 (2), pp. 278–288. DOI: 10.1111/j.1365-2621.2009.02133.x.
- Fameau, Anne-Laure; Salonen, Anniina (2014): Effect of particles and aggregated structures on the foam stability and aging. In *C.R. Physique* 15 (8-9), pp. 748–760. DOI: 10.1016/j.crhy.2014.09.009.
- Fan, Kai; Zhang, Min; Mujumdar, Arun S. (2019): Recent developments in high efficient freeze-drying of fruits and vegetables assisted by microwave. A review. In *Crit. Rev. Food Sci. Nutr.* 59 (8), pp. 1357–1366. DOI: 10.1080/10408398.2017.1420624.
- Feng, H.; Tang, J.; Cavalieri, R. P.; Plumb, O. A. (2001): Heat and mass transport in microwave drying of porous materials in a spouted bed. In *AIChE J.* 47 (7), pp. 1499–1512. DOI: 10.1002/aic.690470704.

- Fischer, K. (1935): Neues Verfahren zur maßanalytischen Bestimmung des Wassergehalts von Flüssigkeiten und festen Körpern. In *Angew. Chem.* 48 (26), pp. 394–396.
- Flickinger, M. C. (Ed.) (2013): *Downstream industrial biotechnology. Recovery and purification.* Hoboken New Jersey: John Wiley & Sons Inc. Publication.
- Foerst, P.; Gruber, S.; Schulz, M.; Vorhauer, N.; Tsotsas, E. (2020): Characterization of Lyophilization of Frozen Bulky Solids. In *Chem. Eng. Technol.* 43 (5), pp. 789–796. DOI: 10.1002/ceat.201900500.
- Foerst, P.; Kulozik, U.; Schmitt, M.; Bauer, S.; Santivarangkna, C. (2012): Storage stability of vacuum-dried probiotic bacterium *Lactobacillus paracasei* F19. In *Food Bioprod. Process.* 90 (2), pp. 295–300. DOI: 10.1016/j.fbp.2011.06.004.
- Foerst, Petra; Kulozik, Ulrich (2012): Modelling the Dynamic Inactivation of the Probiotic Bacterium *L. Paracasei* ssp. *Paracasei* During a Low-Temperature Drying Process Based on Stationary Data in Concentrated Systems. In *Food Bioprocess Technol.* 5 (6), pp. 2419–2427. DOI: 10.1007/s11947-011-0560-4.
- Fonseca, Fernanda; Passot, Stéphanie; Cunin, Olivier; Marin, Michèle (2004): Collapse temperature of freeze-dried *Lactobacillus bulgaricus* suspensions and protective media. In *Biotechnol. Prog.* 20 (1), pp. 229–238. DOI: 10.1021/bp034136n.
- Fonte, Pedro; Lino, Paulo Roque; Seabra, Vítor; Almeida, António J.; Reis, Salette; Sarmiento, Bruno (2016): Annealing as a tool for the optimization of lyophilization and ensuring of the stability of protein-loaded PLGA nanoparticles. In *Int. J. Pharm.* 503 (1-2), pp. 163–173. DOI: 10.1016/j.ijpharm.2016.03.011.
- Fowler, A. V.; Zabin, I. (1977): The amino acid sequence of beta-galactosidase of *Escherichia coli*. In *Proc. Natl. Acad. Sci. USA* 74 (4), pp. 1507–1510. DOI: 10.1073/pnas.74.4.1507.
- Francesconi, Carlos Fernando de Magalhães; Machado, Marta Brenner; Steinwurz, Flavio; Nones, Rodrigo Bremer; Quilici, Flávio Antonio; Catapani, Wilson Roberto et al. (2016): Oral administration of exogenous lactase in tablets for patients diagnosed with lactose intolerance due to primary hypolactasia. In *Arq. Gastroenterol.* 53 (4), pp. 228–234. DOI: 10.1590/s0004-28032016000400004.
- Fujita, Yukihiisa; Iwasa, Yasuchika; Noda, Yukinao (1982): The Effect of Polyhydric Alcohols on the Thermal Denaturation of Lysozyme as Measured by Differential Scanning Calorimetry. In *BCSJ* 55 (6), pp. 1896–1900. DOI: 10.1246/bcsj.55.1896.
- Fumagalli, F.; Silveira, A. M. (2005): Quality Evaluation of Microwave-Dried Packham's Triumph Pear. In *Drying Technol.* 23 (9-11), pp. 2215–2226. DOI: 10.1080/07373930500212701.

- Galema, S. A.; Hoeliland, H. (1991): Stereochemical aspects of hydration of carbohydrates in aqueous solutions. 3. Density and ultrasound measurements. In *J. Phys. Chem.* 95 (13), pp. 5321–5326, checked on sa.
- Gehrmann, D.; Esper, G.; Schuhmann, H. (2009): *Trocknungstechnik in der Lebensmittelindustrie*. 1. Aufl. Hamburg: B. Behr's Verlag.
- Gekko, K.; Timasheff, S. N. (1981): Mechanism of protein stabilization by glycerol: preferential hydration in glycerol-water mixtures. In *Biochemistry* 20 (16), pp. 4667–4676. DOI: 10.1021/bi00519a023.
- George, A.; Chiang, Y.; Guo, B.; Arabshahi, A.; Cai, Z.; Wilson, W. William (1997): [6] Second virial coefficient as predictor in protein crystal growth. In : *Macromolecular Crystallography Part A*, vol. 276: Elsevier (Methods in Enzymology), pp. 100–110.
- Georgieva, Daniela; Cagna, Alain; Langevin, Dominique (2009): Link between surface elasticity and foam stability. In *Soft Matter* 5 (10), p. 2063. DOI: 10.1039/B822568K.
- Glycerine Producers' Association (1963): *Physical properties of glycerine and its solutions*. New York, NY: Glycerine Producers' Association.
- Gómez, G.; Pikal, M. J.; Rodríguez-Hornedo, N. (2001): Effect of initial buffer composition on pH changes during far-from-equilibrium freezing of sodium phosphate buffer solutions. In *Pharm. Res.* 18 (1), pp. 90–97. DOI: 10.1023/A:1011082911917.
- Grasmeijer, N.; Stankovic, M.; Waard, H. de; Frijlink, H. W.; Hinrichs, W. L. J. (2013): Unraveling protein stabilization mechanisms: vitrification and water replacement in a glass transition temperature controlled system. In *Biochim. Biophys. Acta* 1834 (4), pp. 763–769. DOI: 10.1016/j.bbapap.2013.01.020.
- Grembecka, M. (2018): Sugar Alcohols as Sugar Substitutes in Food Industry. In Jean-Michel Mérillon, Kishan Gopal Ramawat (Eds.): *Sweeteners. Pharmacology, Biotechnology, and Applications*. Cham: Springer International Publishing (Reference Series in Phytochemistry), pp. 1–27.
- Grumbach, Eric S.; Fountain, Kenneth J. (2010): *Comprehensive guide to HILIC. Hydrophilic interaction chromatography*. Milford MA: Waters.
- Guignot, S.; Faure, S.; Vignes-Adler, M.; Pitois, O. (2010): Liquid and particles retention in foamed suspensions. In *Chem. Eng. Sci.* 65 (8), pp. 2579–2585. DOI: 10.1016/j.ces.2009.12.039.
- Guo, Wenchuan; Zhu, Xinhua (2014): Dielectric Properties of Red Pepper Powder Related to Radiofrequency and Microwave Drying. In *Food Bioprocess Technol.* 7 (12), pp. 3591–3601. DOI: 10.1007/s11947-014-1375-x.

- Haggis, G. H.; Hasted, J. B.; Buchanan, T. J. (1952): The Dielectric Properties of Water in Solutions. In *J. Chem. Phys.* 20 (9), pp. 1452–1465. DOI: 10.1063/1.1700780.
- Hajare, Ashok; More, Harinath; Pisal, Sambhaji (2006): Vacuum foam drying: New technology for preservation of sensitive biomolecules. In *Pharma Times* 38 (6), pp. 28–30, checked on 1/2/2020.
- Hancock, B. C.; Shamblin, S. L.; Zografi, G. (1995): Molecular mobility of amorphous pharmaceutical solids below their glass transition temperatures. In *Pharm. Res.* 12 (6), pp. 799–806. DOI: 10.1023/a:1016292416526.
- Heindl, A.; Müller, J. (2007): Microwave drying of medicinal and aromatic plants. In *Stewart Postharvest Rev.* 3 (4), pp. 1–6. DOI: 10.2212/spr.2007.4.3.
- Heldman, Dennis R.; Lund, Daryl B.; Sabliov, Cristina M. (2019): Handbook of food engineering. Third edition. Boca Raton, Florida: CRC Press/Taylor & Francis Group.
- Hertendorf, Martin S.; Moshy, Raymond J.; Seltzer, Edward (1970): Foam drying in the food industry. In *CRC crit. rev. food technol.* 1 (1), pp. 25–70. DOI: 10.1080/10408397009527099.
- Hillgren, Anna; Lindgren, Jan; Aldén, Maggie (2002): Protection mechanism of Tween 80 during freeze–thawing of a model protein, LDH. In *Int. J. Pharm.* 237 (1-2), pp. 57–69. DOI: 10.1016/S0378-5173(02)00021-2.
- Hirai, Mitsuhiro; Ajito, Satoshi; Sugiyama, Masaaki; Iwase, Hiroki; Takata, Shin-Ichi; Shimizu, Nobutaka et al. (2018): Direct Evidence for the Effect of Glycerol on Protein Hydration and Thermal Structural Transition. In *Biophys. J.* 115 (2), pp. 313–327. DOI: 10.1016/j.bpj.2018.06.005.
- Hu, Qing-guo; Zhang, Min; Mujumdar, Arun S.; Xiao, Gong-nian; Jin-cai, Sun (2006): Drying of edamames by hot air and vacuum microwave combination. In *J. Food Eng.* 77 (4), pp. 977–982. DOI: 10.1016/j.jfoodeng.2005.08.025.
- Huang, J.; Yang, Z.-H.; Zeng, G.-M.; Wang, H.-L.; Yan, J.-W.; Xu, H.-Y.; Gou, C.-L. (2015): A novel approach for improving the drying behavior of sludge by the appropriate foaming pretreatment. In *Water Res.* 68, pp. 667–669. DOI: 10.1016/j.watres.2014.10.036.
- Hupperts, T. (2010): Foaming properties of milk. A review of the influence of composition and processing. In *Int. J. Dairy Technol.* 63 (4), pp. 477–488. DOI: 10.1111/j.1471-0307.2010.00629.x.
- İçöz, D.; Sumnu, G.; Sahin, S. (2004): Color and Texture Development During Microwave and Conventional Baking of Breads. In *Int. J. Food Prop.* 7 (2), pp. 201–213. DOI: 10.1081/JFP-120025396.

- Jangle, R. D.; Pisal, S. S. (2012): Vacuum foam drying: an alternative to lyophilization for biomolecule preservation. In *Indian J. Pharm. Sci.* 74 (2), pp. 91–100. DOI: 10.4103/0250-474x.103837.
- Jaya, S.; Das, H. (2003): A Vacuum Drying Model for Mango Pulp. In *Drying Technol.* 21 (7), pp. 1215–1234. DOI: 10.1081/DRT-120023177.
- Jaya, S.; Das, H. (2004): Effect of maltodextrin, glycerol monostearate and tricalcium phosphate on vacuum dried mango powder properties. In *J. Food Eng.* 63 (2), pp. 125–134. DOI: 10.1016/S0260-8774(03)00135-3.
- Jaya, S.; Das, H.; Mani, S. (2006): Optimization of Maltodextrin and Tricalcium Phosphate for Producing Vacuum Dried Mango Powder. In *Int. J. Food Prop.* 9 (1), pp. 13–24. DOI: 10.1080/10942910500217666.
- Jesus, Sérgio S. de; Filho, Rubens Maciel (2011): Optimizing Drying Conditions for the Microwave Vacuum Drying of Enzymes. In *Drying Technol.* 29 (15), pp. 1828–1835. DOI: 10.1080/07373937.2011.605977.
- Jiang, Hao; Zhang, Min; Mujumdar, Arun S. (2010): Microwave Freeze-Drying Characteristics of Banana Crisps. In *Drying Technol.* 28 (12), pp. 1377–1384. DOI: 10.1080/07373937.2010.482702.
- Jiang, Shan; Nail, Steven L. (1998): Effect of process conditions on recovery of protein activity after freezing and freeze-drying. In *Eur. J. Pharm. Biopharm.* 45 (3), pp. 249–257. DOI: 10.1016/S0939-6411(98)00007-1.
- Juers, D. H.; Heightman, T. D.; Vasella, A.; McCarter, J. D.; Mackenzie, L.; Withers, S. G.; Matthews, B. W. (2001): A structural view of the action of *Escherichia coli* (lacZ) beta-galactosidase. In *Biochemistry* 40 (49), pp. 14781–14794. DOI: 10.1021/bi011727i.
- Juers, Douglas H.; Matthews, Brian W.; Huber, Reuben E. (2012): LacZ β -galactosidase: structure and function of an enzyme of historical and molecular biological importance. In *Protein Sci.* 21 (12), pp. 1792–1807. DOI: 10.1002/pro.2165.
- Kaatze, U. (1997): The dielectric properties of water in its different states of interaction. In *J. Solution Chem.* 26, pp. 1049–1112.
- Kadam, D. M.; Balasubramanian, S. (2011): Foam mat drying of tomato juice. In *J. Food Process. Preserv.* 35 (4), pp. 488–495. DOI: 10.1111/j.1745-4549.2010.00492.x.
- Kadam, Dattatreya M.; Wilson, Robin A.; Kaur, Sumandeep; Manisha (2012): Influence of Foam Mat Drying on Quality of Tomato Powder. In *Int. J. Food Prop.* 15 (1), pp. 211–220. DOI: 10.1080/10942911003763701.

- Karamoko, Gaoussou; Danthine, Sabine; Olive, Gilles; Blecker, Christophe (2013): Interfacial and Foaming Properties of Two Types of Total Proteose-Peptide Fractions. In *Food Bioprocess Technol.* 6 (8), pp. 1944–1952. DOI: 10.1007/s11947-012-0916-4.
- Karathanos, V. T.; Villalbobos, G.; Saravacos, G. D. (1990): Comparison of Two Methods of Estimation of the Effective Moisture Diffusivity from Drying Data. In *J. Food Sci.* 55 (1), pp. 218–231.
- Kardum, J. P.; Sander, A.; Skansi, D. (2001): Comparison of convective, vacuum, and microwave drying chlorpropamide. In *Drying Technol.* 19 (1), pp. 167–183. DOI: 10.1081/DRT-100001359.
- Karim, A. A.; Wai, C. C. (1999): Foam-mat drying of starfruit (*Averrhoa carambola* L.) purée. Stability and air drying characteristics. In *Food Chem.* 64 (3), pp. 337–343. DOI: 10.1016/S0308-8146(98)00119-8.
- Karjiban, Roghayeh Abedi; Basri, Mahiran; Rahman, Mohd Basyaruddin Abdul; Salleh, Abu Bakar (2012): Structural Properties of Nonionic Tween80 Micelle in Water Elucidated by Molecular Dynamics Simulation. In *APCBEE Procedia* 3, pp. 287–297. DOI: 10.1016/j.apcbee.2012.06.084.
- Kerwin, Bruce A. (2008): Polysorbates 20 and 80 used in the formulation of protein biotherapeutics. Structure and degradation pathways. In *J. Pharm. Sci.* 97 (8), pp. 2924–2935. DOI: 10.1002/jps.21190.
- Kessler, H.-G. (2006): Lebensmittel- und Bioverfahrenstechnik. Molkereitechnologie. 4th ed. München: Verlag A. Kessler.
- Khamjae, T.; Rojanakorn, T. (2018): Foam-mat drying of passion fruit aril. In *Int. Food Res. J.* 25 (1), pp. 204–212.
- King, V.A.-E.; Su, J. T. (1993): Dehydration of *Lactobacillus acidophilus*. In *Process Biochem.* 28 (1), pp. 47–52. DOI: 10.1016/0032-9592(94)80035-9.
- King, V.A.-E.; Zall, R. R.; Ludington, D. C. (1989): Controlled Low-Temperature Vacuum Dehydration. A New Approach for Low-Temperature and Low-Pressure Food Drying. In *J. Food Sci.* 54 (6), pp. 1573–1579. DOI: 10.1111/j.1365-2621.1989.tb05163.x.
- Kinsella, E. (1981): Functional properties of proteins: Possible relationship between structure and function in foams. In *Food Chem.* (7), pp. 273–288.
- Kishore, Devesh; Kundu, Suman; Kayastha, Arvind M. (2012): Thermal, chemical and pH induced denaturation of a multimeric β -galactosidase reveals multiple unfolding pathways. In *PloS one* 7 (11), e50380. DOI: 10.1371/journal.pone.0050380.

- Klein, David R. (2012): Organic chemistry. Hoboken, NJ: Wiley.
- Klein, Manuela Poletto; Sant'Ana, Voltaire; Hertz, Plinho Francisco; Rodrigues, Rafael Costa; Ninow, Jorge Luiz (2018): Kinetics and Thermodynamics of Thermal Inactivation of β -Galactosidase from *Aspergillus oryzae*. In *Braz. arch. biol. technol.* 61 (0). DOI: 10.1590/1678-4324-2018160489.
- Kolhe, Parag; Amend, Elizabeth; Singh, Satish K. (2010): Impact of freezing on pH of buffered solutions and consequences for monoclonal antibody aggregation. In *Biotechnol. Prog.* 26 (3), pp. 727–733. DOI: 10.1002/btpr.377.
- Köpf, E.; Frieß, W. (2016): Proteinformulierung: Vom Molekül zum Medikament. Protein pharmaceuticals: challenges and approaches. In *Pharmakon* 4 (2), pp. 125–133. DOI: 10.1691/pn.20160015.
- Kreuz, M.; Krause, I.; Kulozik, U. (2009): Influence of glycosylation on foaming properties of bovine caseinomacropptide. In *Int. Dairy J.* 19 (12), pp. 715–720. DOI: 10.1016/j.idairyj.2009.06.012.
- Kubbutat, P.; Kulozik, U. (2021a): Interactions of Sugar Alcohol, Di-Saccharides and Polysaccharides with Polysorbate 80 as Surfactant in the Stabilization of Foams. In *Colloids Surf., A*, pp. accepted. DOI: 10.1016/j.colsurfa.2021.126349.
- Kubbutat, P.; Kulozik, U.; Dombrowski, J. (2021a): Foam Structure Preservation during Microwave-Assisted Vacuum Drying: Significance of Interfacial and Dielectric Properties of the Bulk Phase of Foams from Polysorbate 80–Maltodextrin Dispersions. In *Foods* 10, p. 1163. DOI: 10.3390/foods10061163.
- Kubbutat, P.; Tauchnitz, A.; Kulozik, U. (2020): Water Vapor Pathways during Freeze-Drying of Foamed Product Matrices Stabilized by Maltodextrin at Different Concentrations. In *Processes* 8 (11), p. 1463. DOI: 10.3390/pr8111463.
- Kubbutat, Peter; Kulozik, Ulrich (2021b): Interactions of sugar alcohol, di-saccharides and polysaccharides with polysorbate 80 as surfactant in the stabilization of foams. In *Colloids Surf., A* 616, p. 126349. DOI: 10.1016/j.colsurfa.2021.126349.
- Kubbutat, Peter; Kulozik, Ulrich; Dombrowski, Jannika (2021b): Influence of interfacial characteristics and dielectric properties on foam structure preservation during microwave-assisted vacuum drying of whey protein isolate-maltodextrin dispersions. In *J. Food Eng.*, p. 110691. DOI: 10.1016/j.jfoodeng.2021.110691.
- Kudra, T.; Ratti, C. (2006): Foam-mat drying: Energy and cost analyses. In *Can. Biosyst. Eng.* 48, pp. 27–32, checked on 1/3/2020.

- Lau, C. K.; Dickinson, E. (2005): Instability and structural change in an aerated system containing egg albumen and invert sugar. In *Food Hydrocolloids* 19 (1), pp. 111–121. DOI: 10.1016/j.foodhyd.2004.04.020.
- Lau, Cathy Ka; Dickinson, Eric (2007): Stabilization of aerated sugar particle systems at high sugar particle concentrations. In *Colloids Surf., A* 301 (1-3), pp. 289–300. DOI: 10.1016/j.colsurfa.2006.12.074.
- Laurent, T. C. (1995): An early look at macromolecular crowding. In *Biophys. Chem.* 57, pp. 7–14.
- Lazidis, A.; Hancocks, R. D.; Spyropoulos, F.; Kreuz, M.; Berrocal, R.; Norton, I. T. (2016): Whey protein fluid gels for the stabilisation of foams. In *Food Hydrocolloids* 53 (1–3), pp. 209–217. DOI: 10.1016/j.foodhyd.2015.02.022.
- Lee, J. C.; Timasheff, S. N. (1981): The stabilization of proteins by sucrose. In *J. Biol. Chem.* 14 (14), pp. 7193–7201, checked on 11/19/2018.
- Legucha-Ballesteros, D.; Miller, D. P.; Zhang, J. (2002): Residual Water in Amorphous Solids: Measurement and Effects on Stability. In Harry Levine (Ed.): *Amorphous Food and Pharmaceutical Systems*. Cambridge: Royal Society of Chemistry, pp. 275–316.
- Lerbret, A.; Bordat, P.; Affouard, F.; Descamps, M.; Migliardo, F. (2005): How homogeneous are the trehalose, maltose, and sucrose water solutions? An insight from molecular dynamics simulations. In *J. Phys. Chem. B* 109 (21), pp. 11046–11057. DOI: 10.1021/jp0468657.
- Lexis, M.; Willenbacher, N. (2014): Yield stress and elasticity of aqueous foams from protein and surfactant solutions – The role of continuous phase viscosity and interfacial properties. In *Colloids Surf., A* 459, pp. 177–185. DOI: 10.1016/j.colsurfa.2014.06.030.
- Liao, X.; Raghavan, V. G.; Meda, V.; Yaylayan, V. A. (2001): Dielectric properties of supersaturated alpha-D-glucose aqueous solutions at 2450 MHz. In *J. Microw. Power Electromagn. Energy* 36 (3), pp. 131–138. DOI: 10.1080/08327823.2001.11688455.
- Liapis, A. I.; Bruttini, R. (2009): A mathematical model for the spray freeze drying process. The drying of frozen particles in trays and in vials on trays. In *Int. J. Heat Mass Transfer* 52 (1-2), pp. 100–111. DOI: 10.1016/j.ijheatmasstransfer.2008.06.026.
- Lide, David; Bruno, Thomas J.; Rumble, John R. (2019): *CRC handbook of chemistry and physics*. A ready-reference book of chemical and physical data. 100th edition.
- Lin, Tein M.; D. Durance, Timothy; Scaman, Christine H. (1998): Characterization of vacuum microwave, air and freeze dried carrot slices. In *Food Res. Int.* 31 (2), pp. 111–117. DOI: 10.1016/S0963-9969(98)00070-2.

- Liu, Yanhong; Tang, Juming; Mao, Zhihui (2009): Analysis of bread dielectric properties using mixture equations. In *J. Food Eng.* 93 (1), pp. 72–79. DOI: 10.1016/j.jfoodeng.2008.12.032.
- Lobo, F. A.; Nascimento, M. A.; Domingues, J. R.; Falcão, D. Q.; Hernanz, D.; Heredia, F. J.; Lima A., Kátia G. de (2017): Foam mat drying of Tommy Atkins mango. Effects of air temperature and concentrations of soy lecithin and carboxymethylcellulose on phenolic composition, mangiferin, and antioxidant capacity. In *Food Chem.* 221, pp. 258–266. DOI: 10.1016/j.foodchem.2016.10.080.
- Loveday, Simon M. (2016): β -Lactoglobulin heat denaturation. A critical assessment of kinetic modelling. In *Int. Dairy J.* 52, pp. 92–100. DOI: 10.1016/j.idairyj.2015.08.001.
- Lu, Xiaofeng; Pikal, Michael J. (2004): Freeze-drying of mannitol-trehalose-sodium chloride-based formulations: the impact of annealing on dry layer resistance to mass transfer and cake structure. In *Pharm. Dev. Technol.* 9 (1), pp. 85–95. DOI: 10.1081/pdt-120027421.
- Lucassen, J.; van den Tempel, M. (1972): Dynamic measurements of dilational properties of a liquid interface. In *Chem. Eng. Sci.* 27 (6), pp. 1283–1291. DOI: 10.1016/0009-2509(72)80104-0.
- Lucasson, J. (1981): Dynamic properties of free liquid films and foams. In E. H. Lucassen-Reynders (Ed.): Anionic surfactants. Physical chemistry of surfactant action. New York: Dekker (Surfactant science series, 11), pp. 217–265.
- Lueckel, B.; Helk, B.; Bodmer, D.; Leuenberger, H. (1998): Effects of formulation and process variables on the aggregation of freeze-dried interleukin-6 (IL-6) after lyophilization and on storage. In *Pharm. Dev. Technol.* 3 (3), pp. 337–346. DOI: 10.3109/10837459809009861.
- Maldonado-Valderrama, Julia; Patino, Juan M. Rodríguez (2010): Interfacial rheology of protein–surfactant mixtures. In *Curr. Opin. Colloid Interface Sci.* 15 (4), pp. 271–282. DOI: 10.1016/j.cocis.2009.12.004.
- Małysa, K.; Miller, R.; Lunkenheimer, K. (1991): Relationship between foam stability and surface elasticity forces. Fatty acid solutions. In *Colloids Surf.* 53 (1), pp. 47–62. DOI: 10.1016/0166-6622(91)80035-M.
- Manassero, Carlos A.; David-Briand, Elisabeth; Vaudagna, Sergio R.; Anton, Marc; Speroni, Francisco (2018): Calcium Addition, pH, and High Hydrostatic Pressure Effects on Soybean Protein Isolates—Part 1. Colloidal Stability Improvement. In *Food Bioprocess Technol.* 11 (6), pp. 1125–1138. DOI: 10.1007/s11947-018-2084-7.

- Manning, Mark Cornell; Chou, Danny K.; Murphy, Brian M.; Payne, Robert W.; Katayama, Derrick S. (2010): Stability of protein pharmaceuticals: an update. In *Pharm. Res.* 27 (4), pp. 544–575. DOI: 10.1007/s11095-009-0045-6.
- Marinova, Krastanka G.; Basheva, Elka S.; Nenova, Boriana; Temelska, Mila; Mirarefi, Amir Y.; Campbell, Bruce; Ivanov, Ivan B. (2009): Physico-chemical factors controlling the foamability and foam stability of milk proteins: Sodium caseinate and whey protein concentrates. In *Food Hydrocolloids* 23 (7), pp. 1864–1876. DOI: 10.1016/j.foodhyd.2009.03.003.
- Marze, S.; Guillermic, R. M.; Saint-Jalmes, A. (2009): Oscillatory rheology of aqueous foams. Surfactant, liquid fraction, experimental protocol and aging effects. In *Soft Matter* 5 (9), p. 1937. DOI: 10.1039/b817543h.
- Mayer-Miebach, E.; Behsnilian, D.; Regier, M.; Schuchmann, H. P. (2005): Thermal processing of carrots. Lycopene stability and isomerisation with regard to antioxidant potential. In *Food Res. Int.* 38 (8-9), pp. 1103–1108. DOI: 10.1016/j.foodres.2005.03.018.
- McKenzie, Hugh A. (Ed.) (1970): Milk proteins. Chemistry and molecular biology. Volume I. ebrary, Inc. New York: Academic Press. Available online at <http://www.sciencedirect.com/science/book/9780124852013>.
- McKenzie, Hugh A. (Ed.) (1971): Milk proteins. Chemistry and Molecular Biology. Volume II. ebrary, Inc. New York: Academic Press. Available online at <http://www.sciencedirect.com/science/book/9780124852020>.
- McLoughlin, C. M.; McMinn, W. A. M.; Magee, T. R. A. (2003): Microwave-Vacuum Drying of Pharmaceutical Powders. In *Drying Technol.* 21 (9), pp. 1719–1733. DOI: 10.1081/DRT-120025505.
- Mensink, Maarten A.; Frijlink, Henderik W.; van der Voort Maarschalk, Kees; Hinrichs, Wouter L. J. (2017): How sugars protect proteins in the solid state and during drying (review). Mechanisms of stabilization in relation to stress conditions. In *Eur. J. Pharm. Biopharm.* 114, pp. 288–295. DOI: 10.1016/j.ejpb.2017.01.024.
- Merck & Co., Inc (1989): The Merck Index: An Encyclopaedia of Chemicals, Drugs and Biologicals: An Encyclopedia of Chemicals, Drugs, and Biologicals. 11th Ed. Rahway - USA: Merck & Co.
- Merck KGaA (2020): TWEEN® 80 P1754, 9005-65-6. Available online at <https://www.sigmaaldrich.com/catalog/product/sial/p1754?lang=de®ion=DE>, updated on 10/19/2020, checked on 10/19/2020.

- Metaxas, A. C.; Meredith, Roger J. (1988): Industrial microwave heating. Reprinted. London: The Institution of Engineering and Technology (IEE power engineering series, 4).
- Mortensen, Alicja (2016): Sweeteners permitted in the European Union. Safety aspects. In *Scand. J. Food Nutr.* 50 (3), pp. 104–116. DOI: 10.1080/17482970600982719.
- Mullin, J. (1995): Microwave Processing. In G. W. Gould (Ed.): *New Methods of Food Preservation*. Boston, MA, s.l.: Springer US, pp. 112–134.
- Muthukumaran, A.; Ratti, C.; Raghavan, V. G. S. (2008): Foam-Mat Freeze Drying of Egg White—Mathematical Modeling Part II. Freeze Drying and Modeling. In *Drying Technol.* 26 (4), pp. 513–518. DOI: 10.1080/07373930801929615.
- Nabors, Lyn O'Brien (Ed.) (2001): *Alternative sweeteners*. 3. ed., rev. and expanded. New York, NY: Marcel Dekker (Food science and technology, 112). Available online at <http://www.loc.gov/catdir/enhancements/fy0647/2001028939-d.html>.
- Nail, Steve L.; Akers, Michael J. (2002): *Development and Manufacture of Protein Pharmaceuticals*. Boston, MA: Springer US (Pharmaceutical Biotechnology, 14).
- Nastaj, M.; Sołowiej, B. G.; Terpiłowski, K.; Mleko, S. (2020): Effect of erythritol on physicochemical properties of reformulated high protein meringues obtained from whey protein isolate. In *Int. Dairy J.* 105, p. 104672. DOI: 10.1016/j.idairyj.2020.104672.
- Nastaj, Maciej; Mleko, Stanisław; Terpiłowski, Konrad; Tomczyńska-Mleko, Marta (2021): Effect of Sucrose on Physicochemical Properties of High-Protein Meringues Obtained from Whey Protein Isolate. In *Appl. Sci.* 11 (11), p. 4764. DOI: 10.3390/app11114764.
- Noel, Timothy R.; Parker, Roger; Brownsey, Geoffrey J.; Farhat, Imad A.; MacNaughtan, William; Ring, Stephen G. (2005): Physical aging of starch, maltodextrin, and maltose. In *J. Agric. Food Chem.* 53 (22), pp. 8580–8585. DOI: 10.1021/jf0580770.
- Ohtake, Satoshi; Martin, Russell; Saxena, Atul; Pham, Binh; Chiueh, Gary; Osorio, Manuel et al. (2011): Room temperature stabilization of oral, live attenuated *Salmonella enterica* serovar Typhi-vectored vaccines. In *Vaccine* 29 (15), pp. 2761–2771. DOI: 10.1016/j.vaccine.2011.01.093.
- Ohtake, Satoshi; Schebor, Carolina; Palecek, Sean P.; Pablo, Juan J. de (2004): Effect of pH, counter ion, and phosphate concentration on the glass transition temperature of freeze-dried sugar-phosphate mixtures. In *Pharm. Res.* 21 (9), pp. 1615–1621. DOI: 10.1023/B:PHAM.0000041456.19377.87.
- Ortiz, Maria Eugenia; Bleckwedel, Juliana; Raya, Raúl R.; Mozzi, Fernanda (2013): Biotechnological and in situ food production of polyols by lactic acid bacteria. In *Appl. Microbiol. Biotechnol.* 97 (11), pp. 4713–4726. DOI: 10.1007/s00253-013-4884-z.

- Owusu-Apenten, R.K (2002): Food protein analysis. Quantitative effects on processing. New York: Marcel Dekker (Food science and technology, 118).
- Ozcelik, M.; Ambros, S.; Heigl, A.; Dachmann, E.; Kulozik, U. (2019a): Impact of hydrocolloid addition and microwave processing condition on drying behavior of foamed raspberry puree. In *J. Food Eng.* 240, pp. 83–91. DOI: 10.1016/j.jfoodeng.2018.07.001.
- Ozcelik, M.; Heigl, A.; Kulozik, U.; Ambros, S. (2019b): Effect of hydrocolloid addition and microwave-assisted freeze drying on the characteristics of foamed raspberry puree. In *Innovative Food Sci. Emerging Technol.* 56, p. 102183. DOI: 10.1016/j.ifset.2019.102183.
- Pallas, N. R.; Harrison, Y. (1990): An automated drop shape apparatus and the surface tension of pure water. In *Colloids Surf.* 43 (2), pp. 169–194. DOI: 10.1016/0166-6622(90)80287-E.
- Panesar, Reeba; Panesar, Parmjit S.; Singh, Ram S.; Kennedy, John F.; Bera, Manav B. (2007): Production of lactose-hydrolyzed milk using ethanol permeabilized yeast cells. In *Food Chem.* 101 (2), pp. 786–790. DOI: 10.1016/j.foodchem.2006.02.064.
- Parashar, Archana; Jin, Yiqiong; Mason, Beth; Chae, Michael; Bressler, David C. (2016): Incorporation of whey permeate, a dairy effluent, in ethanol fermentation to provide a zero waste solution for the dairy industry. In *Int. J. Dairy Sci.* 99 (3), pp. 1859–1867. DOI: 10.3168/jds.2015-10059.
- Passot, Stéphanie; Fonseca, Fernanda; Barbouche, Naziha; Marin, Michèle; Alarcon-Lorca, Muriel; Rolland, Dominique; Rapaud, Michel (2007): Effect of product temperature during primary drying on the long-term stability of lyophilized proteins. In *Pharm. Dev. Technol.* 12 (6), pp. 543–553. DOI: 10.1080/10837450701563459.
- Patapoff, T. W.; Overcashier, D. E. (2002): The Importance of Freezing on Lyophilization Cycle Development. In *BioPharm* 15 (3), pp. 16–21.
- Péré, C.; Rodier, E. (2002): Microwave vacuum drying of porous media: experimental study and qualitative considerations of internal transfers. In *Chem. Eng. Process.* 41 (5), pp. 427–436. DOI: 10.1016/S0255-2701(01)00161-1.
- Pérez-Campos, Rafael; Fayos-Fernández, José; Lozano-Guerrero, Antonio José; Martínez-González, Antonio; Monzó-Cabrera, Juan; Mediavilla, Irene et al. (2020): Permittivity Measurements for Cypress and Rockrose Biomass Versus Temperature, Density, and Moisture Content. In *Sensors (Basel)* 20 (17). DOI: 10.3390/s20174684.
- Permyakov, Eugene A.; Morozova, Ludmila A.; Burstein, Edward A. (1985): Cation binding effects on the pH, thermal and urea denaturation transitions in α -lactalbumin. In *Biophys. Chem.* 21 (1), pp. 21–31. DOI: 10.1016/0301-4622(85)85003-1.

- Phillips, L. G.; Haque, Z.; Kinsella, E. (1987): A Method for the Measurement of Foam Formation and Stability. In *J. Food Sci.* 52 (4), pp. 1074–1077.
- Pickering, S. U. (1907): CXCVI.—Emulsions. In *J. Chem. Soc., Trans.* 91 (0), pp. 2001–2021. DOI: 10.1039/CT9079102001.
- Pikal, M. J. (1990a): Freeze-drying of proteins. Part I: Process design. In *BioPharm* 3 (8), pp. 18–27.
- Pikal, M. J. (1990b): Freeze-drying of proteins. Part II: Formulation selection. In *BioPharm* 3 (9), pp. 26–30.
- Pikal, M. J.; Shah, S. (1997): Intravial distribution of moisture during the secondary drying stage of freeze drying. In *PDA J. Pharm. Sci. Technol.* 51 (1), pp. 17–24.
- Pikal, Michael J.; Shah, Saroj (1990): The collapse temperature in freeze drying: Dependence on measurement methodology and rate of water removal from the glassy phase. In *Int. J. Pharm.* 62 (2-3), pp. 165–186. DOI: 10.1016/0378-5173(90)90231-R.
- Pisal, Sambhaji; Wawde, Gopal; Salvankar, Shailendra; Lade, Sanjay; Kadam, Shivajirao (2006): Vacuum foam drying for preservation of LaSota virus. Effect of additives. In *AAPS PharmSciTech* 7 (3), p. 60. DOI: 10.1208/pt070360.
- Posocco, P.; Perazzo, A.; Preziosi, V.; Laurini, E.; Pricl, S.; Guido, S. (2016): Interfacial tension of oil/water emulsions with mixed non-ionic surfactants. Comparison between experiments and molecular simulations. In *RSC Adv.* 6 (6), pp. 4723–4729. DOI: 10.1039/C5RA24262B.
- Pueschner GmbH & Co. KG (2008): Dielectric Measurement Kit WaveAnalyser: Short Technical Notes. Available online at https://www.pueschner.com/downloads/product-news/werb_mwmess_techDaten_en.pdf, checked on 5/26/2021.
- Purdon, C. H.; Haigh, J. M.; Surber, C.; Smith, E. W. (2003): Foam Drug Delivery in Dermatology. In *Am. J. Drug Delivery* 1 (1), pp. 71–75. DOI: 10.2165/00137696-200301010-00006.
- Pycia, Karolina; Juszczak, Lesław; Gałkowska, Dorota (2016): Effect of native potato starch maltodextrins on stability and rheological properties of albumin foams. In *Starch - Stärke* 68 (7-8), pp. 611–620. DOI: 10.1002/star.201500156.
- Pycia, Karolina; Juszczak, Lesław; Gałkowska, Dorota; Socha, Robert; Jaworska, Grażyna (2017): Maltodextrins from chemically modified starches. Production and characteristics. In *Starch - Stärke* 69 (5-6), p. 1600199. DOI: 10.1002/star.201600199.

- Qadri, O. S.; Srivastava, A. K. (2017): Microwave-Assisted Foam Mat Drying of Guava Pulp. Drying Kinetics and Effect on Quality Attributes. In *J. Food Process Eng.* 40 (1), e12295. DOI: 10.1111/jfpe.12295.
- Radoń, Adrian; Włodarczyk, Patryk (2019): Influence of water on the dielectric properties, electrical conductivity and microwave absorption properties of amorphous yellow dextrin. In *Cellulose* 26 (5), pp. 2987–2998. DOI: 10.1007/s10570-019-02324-0.
- Raharitisfa, N.; Ratti, C. (2010): Foam-mat freeze-drying of apple juice Part 2. Stability of dry products during storage. In *J. Food Process Eng.* 33 (23), pp. 341–364. DOI: 10.1111/j.1745-4530.2009.00517.x.
- Rajkumar, P.; Kailappan, R.; Viswanathan, R.; Raghavan, G.S.V. (2007): Drying characteristics of foamed alphonso mango pulp in a continuous type foam mat dryer. In *J. Food Eng.* 79 (4), pp. 1452–1459. DOI: 10.1016/j.jfoodeng.2006.04.027.
- Rao, M. V.; Dutta, S. M. (1978): Lactase activity of microorganisms. In *Folia Microbiol. (Praha)* 23 (3), pp. 210–215. DOI: 10.1007/BF02876581.
- Ratti, C.; Kudra, T. (2006a): Drying of Foamed Biological Materials. Opportunities and Challenges. In *Drying Technol.* 24 (9), pp. 1101–1108. DOI: 10.1080/07373930600778213.
- Ratti, C.; Kudra, T. (2006b): Foam-mat drying: Energy and cost analyses. In *Can. Biosyst. Eng.* 48, pp. 27–32, checked on 1/3/2020.
- Ratti, Cristina (Ed.) (2008): Advances in food dehydration. ebrary, Inc. Boca Raton, FL: CRC Press/Taylor & Francis (Contemporary food engineering, 5). Available online at <http://site.ebrary.com/lib/alltitles/docDetail.action?docID=10257460>.
- Regier, Marc; Knoerzer, Kai; Schubert, Helmar (Eds.) (2016): Microwave Processing of Foods. 2nd ed. Cambridge: Elsevier Science & Technology (Woodhead Publishing Series in Food Science, Technology and Nutrition). Available online at <https://ebookcentral.proquest.com/lib/gbv/detail.action?docID=4732259>.
- Reif, G. (1934): Über den Nachweis von Sorbit in Obsterzeugnissen. In *Zeitschr. f. Untersuchung der Lebensmittel* 68 (2), pp. 179–186. DOI: 10.1007/BF01663308.
- Richtering, Walter H.; Burchard, Walther; Jahns, E.; Finkelmann, H. (1988): Light scattering from aqueous solutions of a nonionic surfactant (C14E8) in a wide concentration range. In *J. Phys. Chem.* 92 (21), pp. 6032–6040. DOI: 10.1021/j100332a039.
- Rico-Díaz, Agustín; Álvarez-Cao, María-Efigenia; Escuder-Rodríguez, Juan-José; González-Siso, María-Isabel; Cerdán, M. Esperanza; Becerra, Manuel (2017): Rational mutagenesis by engineering disulphide bonds improves *Kluyveromyces lactis* beta-galactosidase

for high-temperature industrial applications. In *Sci. Rep.* 7, p. 45535. DOI: 10.1038/srep45535.

Rodríguez Patino, Juan M.; Carrera Sánchez, Cecilio; Rodríguez Niño, Ma Rosario (2008): Implications of interfacial characteristics of food foaming agents in foam formulations. In *Adv. Colloid. Interface Sci.* 140 (2), pp. 95–113. DOI: 10.1016/j.cis.2007.12.007.

Roebuck, B. D.; Goldblith, S. A.; Westphal, W. B. (1972): Dielectric Properties of Carbohydrate-Water Mixtures at Microwave Frequencies. In *J. Food Sci.* 37 (2), pp. 199–204. DOI: 10.1111/j.1365-2621.1972.tb05816.x.

Romano, Vittorio Raffaele; Marra, Francesco; Tammara, Umberto (2005): Modelling of microwave heating of foodstuff: study on the influence of sample dimensions with a FEM approach. In *J. Food Eng.* 71 (3), pp. 233–241. DOI: 10.1016/j.jfoodeng.2004.11.036.

Roser, B. (1991): Trehalose, a new approach to premium dried foods. In *Trends Food Sci. Technol.* 2, pp. 166–169. DOI: 10.1016/0924-2244(91)90671-5.

Rowe, R. C.; Shesky, P. J.; Quinn, M. E. (2009): Handbook of pharmaceutical excipients. 6th ed. London: RPS Publishing, checked on 10/17/2018.

Ruíz-Henestrosa, V. P.; Sánchez, C. C.; Rodríguez Patino, J. M. (2008): Effect of sucrose on functional properties of soy globulins. Adsorption and foam characteristics. In *J. Agric. Food Chem.* 56 (7), pp. 2512–2521. DOI: 10.1021/jf0731245.

Sadahira, M. S.; Akhtar, M.; Murray, B. S.; Netto, F. M. (2018): Influence of pH on foaming and rheological properties of aerated high sugar system with egg white protein and hydroxypropylmethylcellulose. In *LWT--Food Sci. Technol.* 89, pp. 350–357. DOI: 10.1016/j.lwt.2017.10.058.

Saint-Jalmes, A.; Peugeot, M.-L.; Ferraz, H.; Langevin, D. (2005): Differences between protein and surfactant foams: Microscopic properties, stability and coarsening. In *Colloids Surf., A* 263 (1-3), pp. 219–225. DOI: 10.1016/j.colsurfa.2005.02.002.

Salahi, M. R.; Mohebbi, M.; Taghizadeh, M. (2015): Foam-Mat Drying of Cantaloupe (Cucumis melo). Optimization of Foaming Parameters and Investigating Drying Characteristics. In *J. Food Process. Preserv.* 39 (6), pp. 1798–1808. DOI: 10.1111/jfpp.12414.

Samanta, Sayantan; Ghosh, Pallab (2011): Coalescence of bubbles and stability of foams in aqueous solutions of Tween surfactants. In *Chem. Eng. Res. Des.* 89 (11), pp. 2344–2355. DOI: 10.1016/j.cherd.2011.04.006.

Sangamithra, A.; Sivakumar, V.; Swamy, J. G.; Kannan, K. (2015): Foam Mat Drying of Food Materials. A Review. In *J. Food Process. Preserv.* 39 (6), pp. 3165–3174. DOI: 10.1111/jfpp.12421.

- Sankat, C. K.; Castaigne, F. (2004): Foaming and drying behaviour of ripe bananas. In *LWT-- Food Sci. Technol.* 37 (5), pp. 517–525. DOI: 10.1016/S0023-6438(03)00132-4.
- Santander-Ortega, M. J.; Jódar-Reyes, A. B.; Csaba, N.; Bastos-González, D.; Ortega-Vinuesa, J. L. (2006): Colloidal stability of pluronic F68-coated PLGA nanoparticles. A variety of stabilisation mechanisms. In *J. Colloid Interface Sci.* 302 (2), pp. 522–529. DOI: 10.1016/j.jcis.2006.07.031.
- Santivarangkna, C.; Higl, B.; Foerst, P. (2008): Protection mechanisms of sugars during different stages of preparation process of dried lactic acid starter cultures. In *Food Microbiol.* 25 (3), pp. 429–441. DOI: 10.1016/j.fm.2007.12.004.
- Santivarangkna, C.; Wenning, M.; Foerst, P.; Kulozik, U. (2007a): Damage of cell envelope of *Lactobacillus helveticus* during vacuum drying. In *J. Appl. Microbiol.* 102 (3), pp. 748–756. DOI: 10.1111/j.1365-2672.2006.03123.x.
- Santivarangkna, Chalut; Kulozik, Ulrich; Foerst, Petra (2007b): Alternative drying processes for the industrial preservation of lactic acid starter cultures. In *Biotechnol. Prog.*, pp. 302–315. DOI: 10.1021/bp060268f.
- Saqib, Shaima; Akram, Attiya; Halim, Sobia Ahsan; Tassaduq, Raazia (2017): Sources of β -galactosidase and its applications in food industry. In *3 Biotech* 7 (1), p. 79. DOI: 10.1007/s13205-017-0645-5.
- Sawyer, Lindsay; Kontopidis, George; Wu, Su-Ying (1999): beta-Lactoglobulin - a three-dimensional perspective. In *Int. J. Food Sci. Technol.* 34 (5-6), pp. 409–418. DOI: 10.1046/j.1365-2621.1999.00320.x.
- Scaman, C. H.; Timothy, Durance, T. D.; Drummond, L.; Sun, D.-W. (2015): Chapter 23 - Combined Microwave Vacuum Drying. In Da-Wen Sun (Ed.): *Emerging Technologies for Food Processing*. 2nd ed. Burlington: Elsevier Science (Food science and technology), pp. 427–445.
- Schersch, K.; Betz, O.; Garidel, P.; Muehlau, S.; Bassarab, S.; Winter, G. (2010): Systematic investigation of the effect of lyophilizate collapse on pharmaceutically relevant proteins I. Stability after freeze-drying. In *J. Pharm. Sci.* 99 (5), pp. 2256–2278. DOI: 10.1002/jps.22000.
- Schersch, Kathrin; Betz, Ortrud; Garidel, Patrick; Muehlau, Silke; Bassarab, Stefan; Winter, Gerhard (2012): Systematic investigation of the effect of lyophilizate collapse on pharmaceutically relevant proteins, part 2. Stability during storage at elevated temperatures. In *J. Pharm. Sci.* 101 (7), pp. 2288–2306. DOI: 10.1002/jps.23121.

- Schiffmann, R. (2016): Packaging for microwave foods. In Marc Regier, Kai Knoerzer, Helmar Schubert (Eds.): *Microwave Processing of Foods*. 2nd ed. Cambridge: Elsevier Science & Technology (Woodhead Publishing Series in Food Science, Technology and Nutrition), pp. 273–299.
- Schmitt, S. (2012): The Freeze Drying Challenge. In *Pharm. Technol. Eur.* 24 (4). Available online at <http://www.pharmtech.com/freeze-drying-challenge>.
- Searles, J. A.; Carpenter, J. F.; Randolph, T. W. (2001): Annealing to optimize the primary drying rate, reduce freezing-induced drying rate heterogeneity, and determine T(g)' in pharmaceutical lyophilization. In *J. Pharm. Sci.* 90 (7), pp. 872–887. DOI: 10.1002/jps.1040.
- Semenova, M.; Belyakovam, L.; Antipova, A.; Polikarpov, Y.; Klouda, L.; Markovic, A.; Il'in, M. (2003): Effect of maltodextrins on the surface activity of small-molecule surfactants. In *Colloids Surf., B* 31, pp. 47–54.
- Severo, M. G.; Zeferino, A. S.; Soccol, C. R. (2017): Development of a Rabies Vaccine in Cell Culture for Veterinary Use in the Lyophilized Form. In : *Current Developments in Biotechnology and Bioengineering*: Elsevier, pp. 523–560.
- Sharma, K. S.; Rakshit, A. K. (2004): Investigation of the properties of decaoxyethylene n-dodecyl ether, C12E10, in the aqueous sugar-rich region. In *JSD* 7 (3), 305–316. DOI: 10.1007/s11743-004-0316-8.
- Shinoda, Kozo.; Kobayashi, Makoto.; Yamaguchi, Nobuyoshi. (1987): Effect of "Iceberg" formation of water on the enthalpy and entropy of solution of paraffin chain compounds. The effect of temperature on the critical micelle concentration of lithium perfluorooctane sulfonate. In *J. Phys. Chem.* 91 (20), pp. 5292–5294. DOI: 10.1021/j100304a031.
- Shogren, Randal; Biresaw, Girma (2007): Surface properties of water soluble maltodextrin, starch acetates and starch acetates/alkenylsuccinates. In *Colloids Surf., A* 298 (3), pp. 170–176. DOI: 10.1016/j.colsurfa.2006.10.070.
- Simon, S.; Krause, H. J.; Weber, C.; Peukert, W. (2011): Physical degradation of proteins in well-defined fluid flows studied within a four-roll apparatus. In *Biotechnol. Bioeng.* 108 (12), pp. 2914–2922. DOI: 10.1002/bit.23257.
- Sochanski, J. S.; Goyette, J.; Bose, T. K.; Akyel, C.; Bosisio, R. (1990): Freeze dehydration of foamed milk by microwaves. In *Drying Technol.* 8 (5), pp. 1017–1037. DOI: 10.1080/07373939008959933.

- Song, Xian-ju; Zhang, Min; Mujumdar, Arun S.; Fan, Liuping (2009): Drying Characteristics and Kinetics of Vacuum Microwave–Dried Potato Slices. In *Drying Technol.* 27 (9), pp. 969–974. DOI: 10.1080/07373930902902099.
- Sosa-Morales, M. E.; Valerio-Junco, L.; López-Malo, A.; García, H. S. (2010): Dielectric properties of foods. Reported data in the 21st Century and their potential applications. In *LWT–Food Sci. Technol.* 43 (8), pp. 1169–1179. DOI: 10.1016/j.lwt.2010.03.017.
- Sosulski, Frank W.; Imafidon, Gilbert I. (1990): Amino acid composition and nitrogen-to-protein conversion factors for animal and plant foods. In *J. Agric. Food Chem.* 38 (6), pp. 1351–1356. DOI: 10.1021/jf00096a011.
- Staples, E.; Thompson, L.; Tucker, I.; Penfold, J.; Thomas, R. K.; Lu, J. R. (1996): The Influence of Sorbitol on the Adsorption of Surfactants at the Air–Liquid Interface. In *J. Colloid Interface Sci.* 184 (2), pp. 391–398. DOI: 10.1006/jcis.1996.0633.
- Stubenrauch, Cosima; Klitzing, Regine von (2003): Disjoining pressure in thin liquid foam and emulsion films—new concepts and perspectives. In *J. Phys.: Condens. Matter* 15 (27), R1197–R1232. DOI: 10.1088/0953-8984/15/27/201.
- Tanaka, Y.; Kagamiishi, A.; Kiuchi, A.; Horiuchi, T. (1975): Purification and properties of beta-galactosidase from *Aspergillus oryzae*. In *J. Biochem.* 77 (1), pp. 241–247.
- Tang, Juming; Hao, Feng; Lau, Ming (2002): Microwave heating in food processing. In Xiusheng Harrison Yang, Juming Tang (Eds.): *Advances In Bioprocessing Engineering*, vol. 1: WORLD SCIENTIFIC (Advances in Agricultural Science & Technology), pp. 1–44.
- Thomas, L. C. (2017): Thermal Analysis. In S. Suzanne Nielsen (Ed.): *Food Analysis*. Cham: Springer International Publishing, pp. 529–544.
- Thuwapanichayanan, R.; Prachayawarakorn, S.; Soponronnarit, S. (2012): Effects of foaming agents and foam density on drying characteristics and textural property of banana foams. In *LWT–Food Sci. Technol.* 47 (2), pp. 348–357. DOI: 10.1016/j.lwt.2012.01.030.
- Timasheff, S. N. (1992): Water as ligand. Preferential binding and exclusion of denaturants in protein unfolding. In *Biochemistry* 31 (41), pp. 9857–9864. DOI: 10.1021/bi00156a001.
- Timasheff, S. N. (1993): The Control of Protein Stability and Association by Weak Interactions with Water: How Do Solvents Affect These Processes? In *Annu. rev. biophys. biomol. struct.* 22, pp. 67–97.
- Tonnis, W. F.; Mensink, M. A.; Jager, A. de; van der Voort Maarschalk, K.; Frijlink, H. W.; Hinrichs, W. L. J. (2015): Size and molecular flexibility of sugars determine the storage stability of freeze-dried proteins. In *Mol. Pharm.* 12 (3), pp. 684–694. DOI: 10.1021/mp500423z.

- Töpel, Alfred (2016): Chemie und Physik der Milch. Naturstoff, Rohstoff, Lebensmittel. 4. überarbeitete Auflage. Hamburg: Behr's Verlag. Available online at <http://www.behrs.de>.
- Toro-Sierra, José; Tolkach, Alexander; Kulozik, Ulrich (2013): Fractionation of α -Lactalbumin and β -Lactoglobulin from Whey Protein Isolate Using Selective Thermal Aggregation, an Optimized Membrane Separation Procedure and Resolubilization Techniques at Pilot Plant Scale. In *Food Bioprocess Technol.* 6 (4), pp. 1032–1043. DOI: 10.1007/s11947-011-0732-2.
- Trelea, I. C.; Passot, S.; Marin, M.; Fonseca, F. (2009): Model for Heat and Mass Transfer in Freeze-Drying of Pellets. In *J. Biomech. Eng.* 131 (7), p. 1301. DOI: 10.1115/1.3142975.
- Tsapkina, E. N.; Semenova, M. G.; Pavlovskaya, G. E.; Leontiev, A. L.; Tolstoguzov, V. B. (1992): The influence of incompatibility on the formation of adsorbing layers and dispersion of n-decane emulsion droplets in aqueous solution containing a mixture of 11S globulin from *Vicia faba* and dextran. In *Food Hydrocolloids* 6 (3), pp. 237–251. DOI: 10.1016/S0268-005X(09)80092-1.
- Tsourouflis, Spyros; Flink, James M.; Karel, Marcus (1976): Loss of structure in freeze-dried carbohydrates solutions. Effect of temperature, moisture content and composition. In *J. Sci. Food Agric.* 27 (6), pp. 509–519. DOI: 10.1002/jsfa.2740270604.
- Tulasidas, T. N.; Raghavan, G. S.; van de Voort, F.; Girard, R. (1995): Dielectric properties of grapes and sugar solutions at 2.45 GHz. In *J. Microw. Power Electromagn. Energy* 30 (2), pp. 117–123. DOI: 10.1080/08327823.1995.11688266.
- Tutuncu, M. A.; Labuza, T. P. (1996): Effect of Geometry on the Effective Moisture Transfer Diffusion Coefficient. In *J. Food Eng.* 30, pp. 443–447.
- Uniprot (2021): UniProtKB - P00723 (BGAL_KLULA). Available online at <https://www.uniprot.org/uniprot/P00723#structure>, updated on 4/7/2021, checked on 5/20/2021.
- van Remmen, H. H. J.; Ponne, C. T.; Nijhuis, H. H.; Bartels, P. V.; Kerkhof, P. J. A. M. (1996): Microwave Heating Distributions in Slabs, Spheres and Cylinders with Relation to Food Processing. In *J. Food Sci.* 61 (6), pp. 1105–1114. DOI: 10.1111/j.1365-2621.1996.tb10941.x.
- Walstra, P. (1989): Principles of Foam Formation and Stability. In A. J. Wilson (Ed.): *Foams. Physics, Chemistry and Structure*. Berlin Heidelberg New York: Springer-Verlag, pp. 11–17.
- Walstra, Pieter (1999): Dairy technology. Principles of milk properties and processes. New York: Marcel Dekker (Food science and technology, 90). Available online at

<http://search.ebscohost.com/login.aspx?direct=true&scope=site&db=nlebk&db=nlabk&AN=11513>.

- Walters, R. H.; Bhatnagar, B.; Tchessalov, S.; Izutsu, K.-I.; Tsumoto, K.; Ohtake, S. (2014): Next generation drying technologies for pharmaceutical applications. In *J. Pharm. Sci.* 103 (9), pp. 2673–2695. DOI: 10.1002/jps.23998.
- Wan, L. S.; Lee, P. F. (1974): CMC of polysorbates. In *J. Pharm. Sci.* 63 (1), pp. 136–137. DOI: 10.1002/jps.2600630136.
- Wang, B.; Pikal, M. J. (2012): Stabilization of Lyophilized Pharmaceuticals by Process Optimization: Challenges and Opportunities. In *Am. Pharm. Rev.* 15, pp. 82–89.
- Wang, D. Q.; Hey, J. M.; Nail, S. L. (2004): Effect of collapse on the stability of freeze-dried recombinant factor VIII and alpha-amylase. In *J. Pharm. Sci.* 93 (5), pp. 1253–1263. DOI: 10.1002/jps.20065.
- Wang, Rui; Zhang, Min; Mujumdar, Arun S.; Sun, Jin-Cai (2009): Microwave Freeze–Drying Characteristics and Sensory Quality of Instant Vegetable Soup. In *Drying Technol.* 27 (9), pp. 962–968. DOI: 10.1080/07373930902902040.
- Wang, W.; Hu, D.; Pan Y.; Z., Y.; Chen, G. (2015): Freeze-drying of aqueous solution frozen with prebuilt pores. In *AIChE J.* 61 (6), pp. 2048–2057.
- Wang, Wei; Zhang, Shuo; Pan, Yanqiu; Tang, Yujia; Chen, Guohua (2020): Wave-absorbing material aided microwave freeze-drying of vitamin C solution frozen with preformed pores. In *Drying Technol.*, pp. 1–14. DOI: 10.1080/07373937.2020.1752229.
- Wang, Yifen; Wig, Timothy D.; Tang, Juming; Hallberg, Linnea M. (2003): Dielectric properties of foods relevant to RF and microwave pasteurization and sterilization. In *J. Food Eng.* 57 (3), pp. 257–268. DOI: 10.1016/S0260-8774(02)00306-0.
- Wang, Z.; Narsimhan, G. (2005): Interfacial dilatational elasticity and viscosity of beta-lactoglobulin at air-water interface using pulsating bubble tensiometry. In *Langmuir : the ACS journal of surfaces and colloids* 21 (10), pp. 4482–4489. DOI: 10.1021/la047374g.
- Wang, Zhao Hui; Shi, Ming Heng (1998): The Effects of Sublimation-Condensation Region on Heat and Mass Transfer During Microwave Freeze Drying. In *J. Heat Transfer* 120 (3), pp. 654–660. DOI: 10.1115/1.2824333.
- Wangsakan, Apiradee; Chinachoti, Pavinee; McClements, David J. (2004): Effect of surfactant type on surfactant-maltodextrin interactions. Isothermal titration calorimetry, surface tensiometry, and ultrasonic velocimetry study. In *Langmuir : the ACS journal of surfaces and colloids* 20 (10), pp. 3913–3919. DOI: 10.1021/la0361619.

- Weaire, D. L.; Hutzler, S. (2001): The physics of foams. 1. publ. as paperback. Oxford: Clarendon Press.
- Wertheim, J. H.; Mishkin, A. R.: "Freeze drying a frozen foam of coffee concentrate." U.S. Patent No. 4,565,706. 21 Jan. 1986. (4,565,706).
- Wilde, Peter; Mackie, Alan; Husband, Fiona; Gunning, Patrick; Morris, Victor (2004): Proteins and emulsifiers at liquid interfaces. In *Adv. Colloid. Interface Sci.* 108-109, pp. 63–71. DOI: 10.1016/j.cis.2003.10.011.
- Wilson, A. (1989): Foams. Physics, Chemistry and Structure. London, UK: Springer London.
- Wojdyło, Aneta; Figiel, Adam; Lech, Krzysztof; Nowicka, Paulina; Oszmiański, Jan (2014): Effect of Convective and Vacuum–Microwave Drying on the Bioactive Compounds, Color, and Antioxidant Capacity of Sour Cherries. In *Food Bioprocess Technol.* 7 (3), pp. 829–841. DOI: 10.1007/s11947-013-1130-8.
- Xu, Hui; Li, Pei Xun; Ma, Kun; Thomas, Robert K.; Penfold, Jeffrey; Lu, Jian Ren (2013): Limitations in the application of the Gibbs equation to anionic surfactants at the air/water surface: sodium dodecylsulfate and sodium dodecylmonooxyethylenesulfate above and below the CMC. In *Langmuir : the ACS journal of surfaces and colloids* 29 (30), pp. 9335–9351. DOI: 10.1021/la401835d.
- Yadav, Jay Kant (2013): Macromolecular Crowding Enhances Catalytic Efficiency and Stability of α -Amylase. In *ISRN Biotechnol.* 2013, p. 737805. DOI: 10.5402/2013/737805.
- Yaghmaee, P.; Durance, T. D. (2002): Predictive Equations for Dielectric Properties of NaCl, D-sorbitol and Sucrose Solutions and Surimi at 2450 MHz. In *J. Food Sci.* 67 (6), pp. 2207–2211. DOI: 10.1111/j.1365-2621.2002.tb09528.x.
- Yam, K. L.; Lai, C. C. (2004): Microwavable frozen food or meals. In Y. H. Hui, Paul Cornillon, Isabel Guerrero Legarreta (Eds.): Handbook of Frozen Foods. Hoboken: Marcel Dekker Inc (Food science and technology, 133).
- Yang, Geer; Gilstrap, Kyle; Zhang, Aili; Xu, Lisa X.; He, Xiaoming (2010): Collapse temperature of solutions important for lyopreservation of living cells at ambient temperature. In *Biotechnol. Bioeng.* 106 (2), pp. 247–259. DOI: 10.1002/bit.22690.
- Yang, X.; Foegeding, E. A. (2010): Effects of sucrose on egg white protein and whey protein isolate foams. Factors determining properties of wet and dry foams (cakes). In *Food Hydrocolloids* 24 (2-3), pp. 227–238. DOI: 10.1016/j.foodhyd.2009.09.011.
- Yu, Z.; Yahsi, U.; McGervey, J. D.; Jamieson, A. M.; Simha, R. (1994): Molecular weight-dependence of free volume in polystyrene studied by positron annihilation measurements.

- In *J. Polym. Sci. B Polym. Phys.* 32 (16), pp. 2637–2644. DOI: 10.1002/polb.1994.090321609.
- Zeeb, Benjamin; Jost, Theresa; McClements, David Julian; Weiss, Jochen (2019): Segregation Behavior of Polysaccharide–Polysaccharide Mixtures-A Feasibility Study. In *Gels*. DOI: 10.3390/gels5020026.
- Zhang, M.; Tang, J.; Mujumdar, A. S.; Wang, S. (2006): Trends in microwave-related drying of fruits and vegetables. In *Trends Food Sci. Technol.* 17 (10), pp. 524–534. DOI: 10.1016/j.tifs.2006.04.011.
- Zhang, Xingyun; Ruan, Cunjun; Haq, Tanveer Ul; Chen, Kanglong (2019): High-Sensitivity Microwave Sensor for Liquid Characterization Using a Complementary Circular Spiral Resonator. In *Sensors (Basel)* 19 (4). DOI: 10.3390/s19040787.
- Zhang, Yi; Huang, Yi; Zhang, Tengfei; Chang, Huicong; Xiao, Peishuang; Chen, Honghui et al. (2015): Broadband and tunable high-performance microwave absorption of an ultralight and highly compressible graphene foam. In *Adv. Mater.* 27 (12), pp. 2049–2053. DOI: 10.1002/adma.201405788.
- Zheng, Xian-Zhe; Liu, Cheng-Hai; Zhou, He (2011): Optimization of Parameters for Microwave-Assisted Foam Mat Drying of Blackcurrant Pulp. In *Drying Technol.* 29 (2), pp. 230–238. DOI: 10.1080/07373937.2010.484112.
- Zhou, Quinn Z.K; Chen, Xiao Dong (2001): Effects of temperature and pH on the catalytic activity of the immobilized β -galactosidase from *Kluyveromyces lactis*. In *Biochem. Eng. J.* 9 (1), pp. 33–40. DOI: 10.1016/S1369-703X(01)00118-8.